Mass Spectrometry-Based Analysis of Urinary Metabolites of 1,3-Butadiene (BD) in Humans and Influence of BD-DNA Adducts on DNA Replication

A DISSERTATION
SUBMITTED TO THE FACULTY OF THE GRADUATE SCHOOL
OF THE UNIVERSITY OF MINNESOTA
BY

Srikanth Kotapati

IN PARTIAL FULFILLMENT OF THE REQUIREMENTS
FOR THE DEGREE OF
DOCTOR OF PHILOSOPHY

Dr. Natalia Y. Tretyakova, Adviser

October 2013

Acknowledgements

First and foremost, I would like to express my sincere gratitude to my advisor, Dr. Natalia Tretyakova, for her support, guidance, and encouragement over the last five years. I am also thankful to Dr. Stephen Hecht, for being my mentor and constant source of inspiration and support throughout my graduate studies. I would also like to thank my committee members Drs. Rory Remmel, and Mark Distefano for their valuable feedback and suggestions over the years. I would also like to acknowledge Dr. Rodney Johnson for his support and encouragement. The majority of the work in my thesis would not have been possible without the help and support of our collaborators Dr. Loic Le Marchand and Dr. Lani Park (University of Hawaii-Honolulu, HI), Dr. Vernon Walker (University of Vermont-Burlington, VT), Dr. James Swenberg (University of North Carolina-Chapel Hill, NC), Drs. F. Peter Guengerich, Lawrence Marnett, Michael Stone, Matthew Pence, Leena Maddukuri, and Ewa Kowal (Vanderbilt University-Nashville, TN). I would also like to thank the NIH and the UMN graduate school for financial support.

I am grateful to all my lab members (current and past) for their valuable discussions and suggestions that played a key role in development of this thesis. I am especially thankful to Amanda Esades, Dewakar Sangaraju, Susith Wickramaratne, Emily Boldry, Amy Grant, Dr. Melissa Goggin and Dr. Uthpala Seneviratne for making significant contributions to my thesis. I am also thankful to Dr. Delshanee Kotandeniya, Xun Ming, Dr. Bhaskar Malayappan, Arnie Groehler, Chris Seiler, Dr. Teshome Gherezghiher and Dr. Jung-Eun Yeo for their helpful insights and technical discussions.

I am very thankful to Brock Matter for training me in HPLC and MS instrumentation as well as for his advice and help during method development and troubleshooting throughout my graduate studies. I am also thankful to Dr. Peter Villalta for his help with the new LTQ Orbitrap instrumentation. I would also like to thank Steve Carmella for his valuable discussions and insights during the HPLC-MS/MS method development. Thanks to Bob Carlson for his valuable help in preparing graphics for this thesis and other publications. I am also thankful to members of Hecht lab, Murphy lab and Peterson

lab for graciously allowing me to use instrumentation from time to time. I am grateful to Tammy Argentine (Waters), Gerald Nagatani (Phenomenex), Martin Cherrier (Biotage) and Cullin Bachmeier (Chromtech/Agilent) for their technical assistance during SPE and HPLC-MS/MS method development.

Last but not least, I could not have accomplished this work without the support of my family and friends, especially my parents, Peddanna and Rama Devi, and wife Divya. I would also like to thank my in-laws, Malleswara Rao and Rama Devi and sister-in-law Mounika Alla. Special thanks to all my friends in US and India for their continuous support and encouragement.

Dedication

In loving memory of my sister, Deepthi (1986-2002)

Abstract

Cigarette smoking is a known risk factor for the development of lung cancer: approximately 1 out of 5 heavy smokers will develop the disease. However, there are significant differences in risk of lung cancer among smokers from different ethnic/racial groups. African American and Native Hawaiian smokers are at a higher risk of lung cancer than European American, Japanese American or Latin American smokers. Cigarette smoke has more than 70 known carcinogens. Following metabolic activation to electrophilic species, these carcinogens can form covalent DNA adducts, which are capable of inducing heritable mutations ultimately resulting in lung cancer. It has been hypothesized that the observed ethnic/racial differences in lung cancer risk in smokers are due to different frequencies of specific polymorphisms in drug metabolizing genes, leading to a different degree of carcinogen bioactivation to DNA-reactive intermediates.

1,3-Butadiene (BD) is among the most abundant and potent carcinogens present in cigarette smoke. BD is metabolically activated primarily by CYP2E1 to form 3,4-epoxy-1-butene (EB), hydroxymethyl vinylketone (HMVK), 3,4-epoxy-1,2-butanediol (EBD), and 1,2,3,4-diepoxybutane (DEB). EB, HMVK, EBD, and DEB have been shown to modify DNA bases to form promutagenic adducts. Alternatively, EB, EBD, and DEB can undergo detoxification via epoxide hydrolysis (the main pathway in humans) or glutathione conjugation and further metabolic conversion into urinary mercapturic acids, 1-hydroxy 2-(N-acetylcysteinyl)-3-butene (MHBMA), 1,2-dihydroxy-4-(N-acetyl cysteinyl)-butane (DHBMA), 1,2,3-trihydroxy-4-(N-acetylcysteinyl)-butane (THBMA), and 1,4-*bis*-(*N*-acetylcysteinyl)butane-2,3-diol (*bis*-BDMA), respectively.

The research presented in this thesis focuses on revealing any ethnic/racial differences in metabolism of BD in smokers and examining the ability of BD-DNA adducts to cause mutations. In the first part of the thesis, we have identified two novel metabolites of BD which have not been previously detected *in vivo*: 1,2,3-trihydroxy-4-(*N*-acetylcysteinyl)-butane (THBMA), and 1,4-*bis*-(*N*-acetylcysteinyl)butane-2,3-diol (*bis*-BDMA). To enable their detection in smokers, sensitive and specific HPLC-ESI$^-$-MS/MS methods were developed for both metabolites in human urine. We observed

significant amounts of THBMA in samples from smokers, non-smokers and occupationally exposed workers. In contrast, *bis*-BDMA amounts in urine of smokers and occupationally exposed workers were below the method's limit of detection, although it was found in urine of F344 rats exposed to 62.5 or 200 ppm BD. Additionally we found significant interspecies differences in BD metabolism between laboratory rats and humans. DHBMA accounted for only 47% of BD urinary mercapturic acids in rats while the corresponding percentage in humans is 93%.

We further developed a high throughput HPLC-ESI$^-$-MS/MS method for the quantification of MHBMA and DHBMA in humans and applied this method to quantify urinary BD-mercapturic acids metabolites in workers from a BD and styrene butadiene rubber (SBR) manufacturing facility and smokers belonging to different ethnic groups in two separate multi-ethnic cohort studies. Workers occupationally exposed to BD excreted significantly more BD-mercapturic acids than administrative workers at the same plant. In a small multi-ethnic study of smokers belonging to European American, Native Hawaiian and Japanese American (N = 200 per group), mean urinary MHBMA and MHBMA/DHBMA+MHBMA metabolic ratio were highest in European American and lowest in Japanese American smokers. Similar results were obtained in the larger study (N = 450 per group) composed of European American and African American smokers. Urine of European American smokers contained higher concentrations of MHBMA than that of African Americans. Genome-wide association study (GWAS) analysis conducted for the larger multi-ethnic group has revealed significant associations between single-nucleotide polymorphisms (SNPs) in chromosome 22 (22564172bp – 22735492 bp, nearby genes GSTT1, GSTT2, DDT and MIF) and urinary BD-mercapturic acid levels in smokers, providing the first evidence for genetic and ethnic/racial differences in metabolism of BD.

The second part of my thesis work has focused on evaluating the mutagenic ability of three recently discovered BD-dA lesions: N^6-(2-hydroxy-3-buten-1-yl)-adenine (N^6-HB-dA), N^6,N^6-(2,3-dihydroxybutan-1,4-diyl)-2′-deoxyadenosine (N^6,N^6-DHB-dA), and 1,N^6-(2-hydroxy-3-hydroxymethylpropan-1,3-diyl)-2′-deoxyadenosine (1,N^6-γHMHP-dA). *In vitro* translesion synthesis experiments were performed on synthetic

oligonucleotides containing each of the three lesions at a site-specific position by gel electrophoresis and HPLC-MS/MS. We found that human translesion synthesis (TLS) polymerases hPols *η, κ, ι* and human polymerase *β* were able to bypass (*S*)-N^6-HB-dA in an error-free manner because of the conserved Watson-Crick base pairing with dT. However, replication past both *(R,R)*-N^6,N^6-DHB-dA and *(R,S)*-1,N^6-γHMHP-dA lesions by TLS polymerases hPols *η* and *κ* was highly error-prone, resulting in A→T, A→C mutations and frameshift deletions. This is the first study that identifies *(R,R)*-N^6,N^6-DHB-dA and *(R,S)*-1,N^6-γHMHP-dA as BD-DNA adducts potentially responsible for the induction of A→T mutations by BD.

TABLE OF CONTENTS

LIST OF TABLES

LIST OF FIGURES

LIST OF ABBREVIATIONS

1,N^6-α-HMHP-dA	1,N^6-(1-hydroxymethyl-2-hydroxypropan-1,3-diyl)-2′-deoxyadenosine
1,N^6-γ-HMHP-dA	1,N^6-(2-hydroxy-3-hydroxymethylpropan-1,3-diyl)-2′-deoxyadenosine
A	Adenine
ADH	alcohol dehydrogenase
APCI	atmospheric pressure chemical ionization
BD	1,3-butadiene
bis-BDMA	1,4-*bis*-(*N*-acetylcysteinyl)butane-2,3-diol
bis-N7G-BD	1,4-*bis*-(guan-7-yl)-2,3,-butanediol
C	Cytosine
CID	collision induced dissociation
CYP 450	cytochrome P450 monooxygenase
DEB	1,2,3,4-diepoxybutane
DHBMA	dihydroxybutyl mercapturic acid [4-(*N*-acetyl-L-cystein-S-yl)-1,2-dihydroxybutane]
DNA	deoxyribonucleic acid
dNTP	deoxynucleotide triphosphate
Dpo4	*Sulfolobus solfataricus* S2 DNA polymerase IV
EB	3,4-epoxy-1-butene
EBD	3,4-epoxy-1,2-diol
EH	epoxide hydrolase
ESI	electro spray ionization
FTMS	fourier transform mass spectrometry
G	Guanine
GST	glutathione S-transferase
GWAS	genome-wide association study
Hb	Hemoglobin

HB-Val	*N*-(2-hydroxy-3-butenyl)–valine
HEB	2-hydroxy-3,4-epoxybut-1-yl
HILIC	hydrophilic interaction liquid chromatography
HMVK	Hydroxymethylvinylketone
HPLC	high performance liquid chromatography
HPLC-ESI$^-$-MS/MS	high performance liquid chromatography-electrospray ionization tandem mass spectrometry
hPol	human polymerase
HRMS	high resolution mass spectrometry
LOD	limit of detection
LOQ	limit of quantification
MHBMA	monohydroxybutenyl mercapturic acid [2-(*N*-acetyl-L-cystein-S-yl)-1-hydroxybut-3-ene + 1-(*N*-acetyl-L-cystein-S-yl)-2-hydroxybut-3-ene]
MS/MS	tandem mass spectrometry
N^6,N^6-DHB-dA	N^6,N^6-(2,3-dihydroxybutan-1,4-diyl)-2□-deoxyadenosine
N^6-HB-dA	N^6-(2-hydroxy-3-buten-1-yl)-adenine
N^6-HEB-dA	N^6-(2-hydroxy-3,4-epoxybut-1-yl) adenine
NMR	nuclear magnetic resonance
ppm	parts per million
pyr-Val	*N*,*N*-(2,3-dihydroxy-1,4-butadiyl)-valine
SBR	styrene-butadiene rubber
SNP	single-nucleotide polymorphism
SPE	solid phase extraction
SRM	selected reaction monitoring
T	Thymine
THBMA	trihydroxybutyl mercapturic acid [4-(*N*-acetyl-L-cystein-S-yl)-1,2,3-trihydroxybutane]

THB-Val	1,2,3-trihydroxybutyl-valine
TLS polymerase	translesion synthesis polymerase
U	Uracil
UDG	uracil DNA glycosylase
TOF	time of flight
TSQ	triple stage quadrupole

I. LITERATURE REVIEW

1.1 Lung Cancer

1.1.1 Smoking associated lung cancer

According to the International Agency for Research on Cancer (IARC), worldwide mortality due to cancer in 2008 was 7.6 million. The annual mortality is predicted to increase to 13.1 million by 2030 *(1)*. Lung cancer accounts for approximately 14% of all cancer deaths worldwide *(1)* and 27% of all cancer deaths in the US *(1)*. According to the American Cancer Society, an estimated 159,480 lung cancer deaths are expected to occur in the US in 2013. Approximately 228,190 new cases of lung cancer are expected to be diagnosed in the US in 2013 *(2)*. Cigarette smoking is the major risk factor accounting for 87% of lung cancer deaths and 30% of all cancer deaths. Other risk factors include exposure to radon, secondhand smoke, asbestos, chromium, cadmium, arsenic, radiation, air pollution, diesel exhaust, and paint *(2)*. In 2011, approximately 21.6% of men and 16.5% of women, a grand total of 43.8 million adults were current cigarette smokers in the US *(3)*. According to the study conducted by the Center for Disease Control (CDC) regarding tobacco use among US high school students, 28% of male students and 18% of female students admitted to have used tobacco in the past month. 5% of adult men and less than 1 of adult women used smokeless tobacco in 2011 *(3)*.

Cigarette smoke consists of more than 70 known carcinogens, including polycyclic aromatic hydrocarbons (PAHs), heterocyclic compounds, *N*-nitrosamines, aromatic amines, heterocyclic aromatic amines, phenolic compounds, volatile hydrocarbons, nitrohydrocarbons, metals, inorganic compounds, and other miscellaneous compounds (Table 1.1 and Chart 1.1) *(4;5)*. The mechanism of induction of

carcinogenesis by cigarette smoke has been a subject of multiple investigations (Figure 1.1). Many tobacco carcinogens require metabolic activation by cytochrome P450 monooxygeneses (CYP 450) 1A1, 1A2, 1B1, 2A13, 2E1, and 3A4 to form electrophilic metabolites *(6)*. These electrophilic metabolites can be detoxified by glutathione-S-transferases, epoxide hydrolases and UDP-glucuronosyl transferases *(6)*. If not detoxified, the electrophilic metabolites of tobacco carcinogens can react with the nucleophilic positions in DNA nucleobases to form DNA adducts *(7)*. These DNA adducts may be repaired by alkyltransferases, base excision repair, nucleotide excision repair, and mismatch repair *(8)*. If DNA adducts escape repair and persist *in vivo*, they can lead to miscoding during the DNA replication process, leading to permanent mutations (Figure 1.1) *(7)*. If these mutations are in critical regions of oncogenes such as *ras* and *myc* or in tumor-suppressor genes such as *p53*, they can lead to activation of the oncogenes and deactivation of tumor suppressor genes ultimately resulting in uncontrolled cellular growth and cancer (Figure 1.1) *(5;7)*.

Table 1.1 Known Carcinogens present in cigarette smoke *(4)*

Chemical Class	**No. of carcinogens**	**Examples**
Polycyclic aromatic hydrocarbons (PAHs) and their heterocyclic analogues	15	Benzo[*a*]pyrene (BaP) Dibenz[a,h]anthracene
N-Nitrosamines	8	4-(Methylnitrosamino)-1-(3-pyridyl)-1-butanone (NNK) *N′*-Nitrosonornicotine (NNN)
Aromatic amines	12	4-Aminobiphenyl 2-Naphthylamine
Aldehydes	2	Formaldehyde Acetaldehyde
Phenols	2	Catechol Caffeic acid
Volatile hydrocarbons	3	Benzene 1,3-Butadiene Isoprene
Other organics	12	Ethylene oxide Acrylonitrile
Inorganic compounds	8	Cadmium Polonium-210

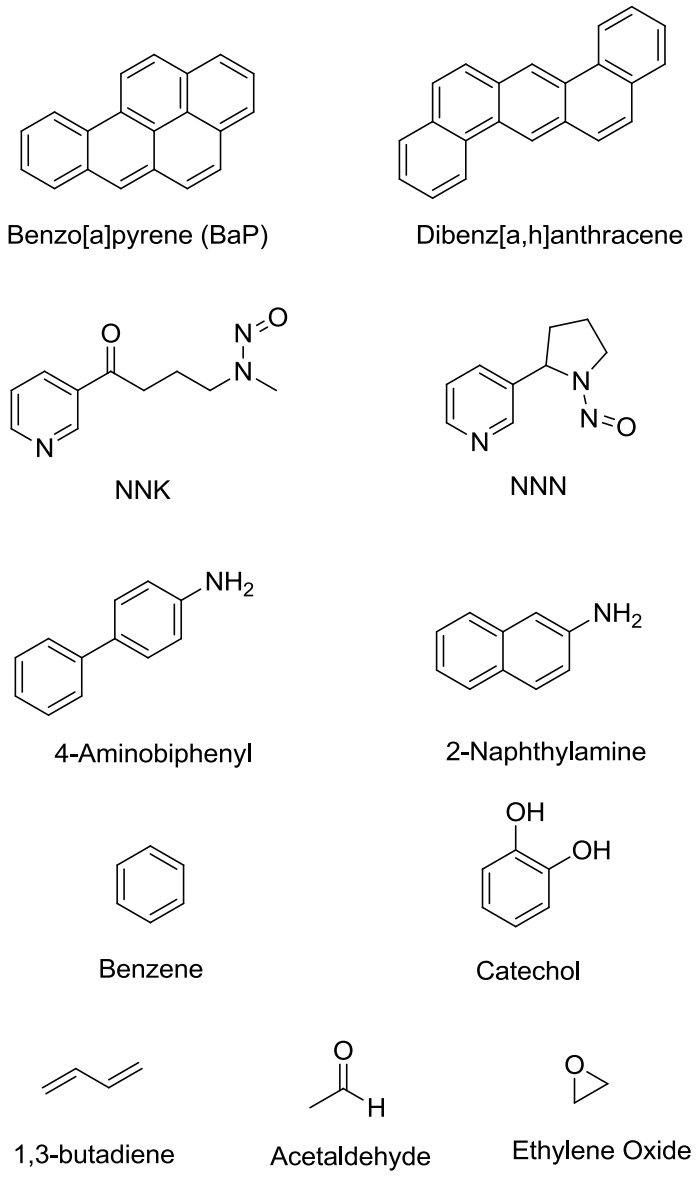

Chart 1.1 Examples of carcinogens present in cigarette smoke

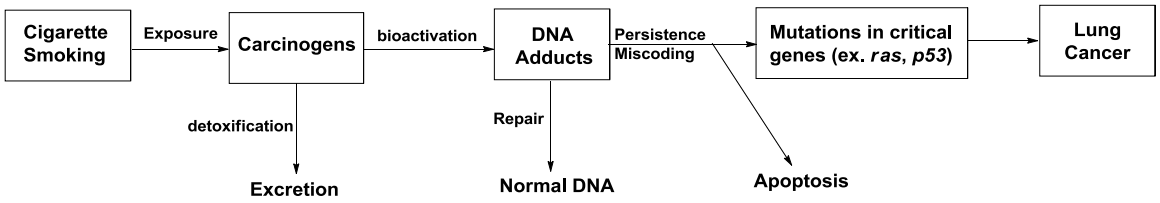

Figure 1.1 Proposed mechanism of chemical carcinogenesis induced by cigarette smoking *(7)*

1.1.2 Ethnic differences in smoking induced lung cancer risk

While smoking is recognized as a known risk factor for lung cancer, the incidence and mortality rates of lung cancer differ among ethnic groups in the United States. Le Marchand and co-workers conducted two case-control studies involving 740 lung cancer patients and 1616 controls between 1979 and 1985 in Oahu, Hawaii to identify ethnic differences in lung cancer risk *(9)*. Among the five ethnic groups included in the study, the age adjusted lung cancer incidence rates in males were found to be Hawaiian > Caucasian > Chinese > Japanese > Filipino *(9)*. The corresponding lung cancer incidence rates in females were Hawaiian > Caucasian > Chinese > Filipino > Japanese *(9)*. Le Marchand et al. hypothesized that the observed differences in lung cancer risk might be due to differences in diet or metabolic differences in activation and detoxification of carcinogens as a result of genetic polymorphisms *(9)*. Hinds and co-workers conducted a multi-ethnic cohort study involving 375 cases and 2404 controls in Japanese, Chinese and Hawaiian women from Hawaii *(10)*. They found that the trend of lung cancer risk to be Hawaiian > Japanese > Chinese women *(10)*. Schwartz et al. conducted similar studies to identify ethnic differences in lung cancer risk among African American and European Americans *(11)*. The study included 5588 lung cancer cases and 3692 controls *(11)*. They found that even after adjustments for smoking habits, African Americans have 2-4 times higher risk of lung cancer than European American smokers in the 40-54 age group *(11)*. In a similar study conducted by Stellman et al. in men from the United States and Japan, it was observed that lung cancer risk was at least 10 times higher in Americans than Japanese *(12)*. Stellman and co-workers conducted another study in European American

and African American smokers but surprisingly did not find any ethnic differences in lung cancer risk among the two groups *(13)*.

Haiman et al. completed a comprehensive multi-ethnic cohort study involving 183,813 smokers belonging to African-American, Japanese-American, Latino, Native Hawaiian, and European American ethnicity to identify ethnic and racial differences in smoking-related lung cancer risk (Table 1.2) *(14)*. In smokers who smoked less than or equal to 10 cigarettes/day, the relative risk of lung cancer among African-American, Japanese-American, Latino, Native Hawaiian, and European American smokers was found to be 1.00, 0.25, 0.21, 0.88 and 0.45, respectively. However, at smoking level greater than 30 cigarettes/day the relative risks were 1.00, 0.75, 0.79, 0.95 and 0.82, respectively *(14)*. The age-adjusted incidence rates and relative risks of lung cancer among different ethnic groups by gender are presented in Table 1.2. The study did not find any association between socio-economic status or diet with ethnic differences, but concluded that these ethnic differences might be due to differences in metabolism of tobacco carcinogens *(14)*. According to the recent statistics from the National Cancer Institute, the five year (2006-2010) lung cancer incidence rates among different ethnic groups were African American > European American > American Indian > Asian > Hispanic in males (Table 1.3) *(15)*. In females the corresponding lung cancer incidence rates were European American > African American > American Indian > Asian > Hispanic (Table 1.3) *(15)*.

Table 1.2 Age-adjusted incidence rates and relative risks of lung cancer among different ethnic groups by gender *(14)*

Variable	African American	Native Hawaiian	Latino	Japanese American	European American
Men					
No. of Men	11,186	5,803	19,487	24,970	21,012
Lung Cancer cases	304	103	142	301	285
Incidence/100,000	263.9	263.9	79.2	121.4	158.3
Relative Risk	1.00	1.00	0.30	0.46	0.60
Women					
No. of Women	19,894	7,545	20,992	28,188	24,736
Lung Cancer cases	299	63	84	129	269
Incidence/100,000	161.2	129.0	46.7	50.0	133.8
Relative Risk	1.00	0.80	0.29	0.31	0.83

Table 1.3 Lung Cancer incidence rates in US by ethnic groups (2006-2010) *(15)*

Race/Ethnicity	**Male (per 100,000)**	**Female (per 100,000)**
European American	74.5	54.6
African American	95.8	52.2
Asian/Pacific Islander	50.7	28.1
American Indian	51.2	35.7
Hispanic	40.6	26.3

1.2 1,3-butadiene: Overview

1,3-butadiene (BD) is a colorless and volatile gas generated as a byproduct of ethylene production in steam cracking process *(16)*. Global industrial production of BD was estimated to be more than 9 million metric tons per year *(17)*. BD is primarily used as a monomer in the synthetic rubber industry for the production of styrene-butadiene rubber, polybutadiene rubber, adiponitrile, styrene-butadiene latex, neoprene rubber, acrylonitrile-butadiene-styrene resins, and nitrile rubber *(16)*. BD is also used as a chemical intermediate in the production of industrial chemicals including Captan and Captafol *(18)*. Workers involved in the production or usage of BD are exposed to the chemical by inhalation *(18)*. However, the general population can also be exposed to BD because it is an environmental pollutant present in gasoline, automobile exhaust and cigarette smoke *(16)*. BD is present in relatively high quantities in cigarette smoke (20-75 µg and 205-360 µg in mainstream and sidestream smoke, respectively per cigarette) *(19)*. Additionally, average concentrations of BD in urban air are reported to be 1-10 ppb *(16)*. Studies in laboratory rodents have reported that BD induces tumors at multiple sites *(20;21)*. Epidemiological studies in workers in the synthetic rubber industry have shown an association between BD exposure and increased risk of lymphatic and hemopoietic cancer *(22-24)*. BD has the highest cancer risk index among several other carcinogens present in tobacco smoke *(25)*. Based on inhalation studies in laboratory animals and epidemiological evidence, BD is classified as a "known to be a human carcinogen" by the US National Toxicology program (NTP) and "human carcinogen" by the US EPA and IARC *(26)*.

1.2.1 Metabolism of 1,3-butadiene

As shown in Scheme 1.1, BD is metabolically activated by cytochrome P450 monoxygenases CYP 2E1 (major) and CYP 2A6 to form R- and S- enantiomers of 3,4-epoxy-1-butene (EB) *(27;28)*. EB can undergo a second oxidation by CYP 2E1 to form 1, 2, 3, 4-diepoxy butane (DEB) *(27;29)*. Alternatively, EB can be detoxified either by microsomal epoxide hydrolase (EH) to form 1-butene-3,4-diol (EB-diol) (Scheme 1.1) *(30)* or conjugation with glutathione (via glutathione *S*-transferase, GSTT1). The glutathione conjugate of EB can further undergo metabolic conversion via the mercapturic acid pathway and be excreted in urine as 2-(*N*-acetyl-L-cystein-S-yl)-1-hydroxybut-3-ene and 1-(*N*-acetyl-L-cystein-S-yl)-2-hydroxybut-3-ene, together referred to as mono hydroxybutyl mercapturic acid (MHBMA) (Scheme 1.1) *(31)*. The other detoxification product from EB, EB-diol can either undergo metabolic activation by CYP 2E1 to form 3,4-epoxy-1,2-butanediol (EBD) or oxidation by alcohol dehydrogenase (ADH) to form hydroxymethyl vinyl ketone (HMVK) (Scheme 1.1) *(32)*. HMVK can then undergo GSH conjugation and conversion to the mercapturic acid 4-(*N*-acetyl-l-cystein-*S*-yl)-1-hydroxy-2-butanone, which is further reduced by carbonyl reductase to form *N*-acetyl-*S*-(3,4-dihydroxybutyl)-L-cysteine, also referred to as dihydroxybutyl mercapturic acid (DHBMA) (Scheme 1.1) *(33)*. Apart from its formation from EB-diol, EBD can also be produced by hydrolysis of one of the epoxide groups of DEB by epoxide hydrolase. EBD and DEB can be further detoxified by glutathione conjugation and mercapturic acid pathways to be excreted in urine as 4-(*N*-acetyl-L-cystein-S-yl)-1,2,3-trihydroxybutane (THBMA) and 1,4-*bis*-(*N*-acetyl-L-cystein-S-yl)butane-2,3-diol (*bis*-BDMA), respectively (Scheme 1.1).

Scheme 1.1 *in vivo* metabolism of 1,3-butadiene

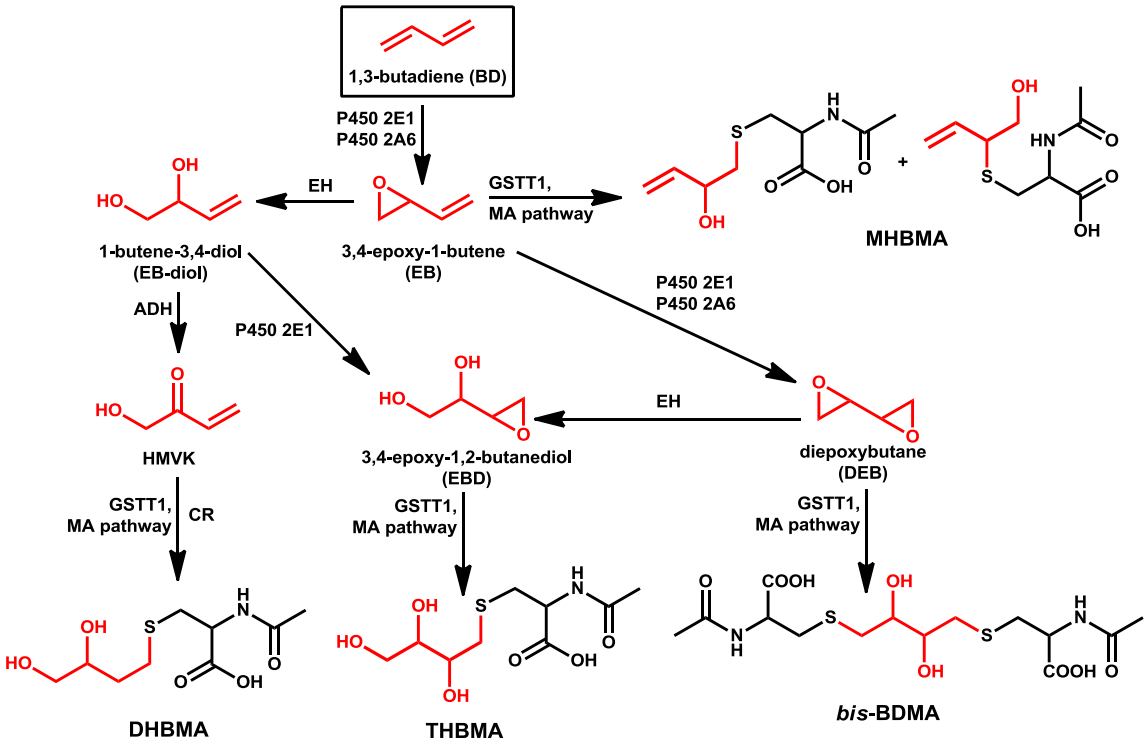

1.2.2 Toxicity and mutagenicity of 1,3-butadiene

A long term study in Sprague Dawley rats (N=110 per sex) exposed to 0, 1,000, or 8,000 ppm of 1,3-butadiene 6 h/day, 5 days/week, for 105 weeks (females) and 111 weeks (males) revealed that BD induces tumors at multiple tissue sites including mammary gland, brain, Zymbal gland, uterus, pancreas, testis, and thyroid gland *(21)*. The national toxicology program (NTP) conducted similar chronic inhalation studies in B6C3F1 mice *(20)*. B6C3F1 mice (N=70 per sex) were exposed to 0, 6.25, 20, 62.5, 200 or 200 ppm BD 6 h/day, 5 days/week, for 103 weeks. Mice exposed to 6.25-625 ppm BD developed lymphocytic lymphoma and tumors of the heart, lung, forestomach, Harderian gland, preputial gland, liver, mammary gland, and ovary *(20)*.

Extensive *in vitro* and *in vivo* evidence indicates that the genotoxic effects of BD are mainly caused by its DNA-reactive epoxides, EB, DEB and EBD. Among the three epoxides, DEB is regarded as the ultimate carcinogenic metabolite of BD because it is 100-200 fold more mutagenic than EB and EBD. Studies in TK6 human lymphoblastoid cells have shown that DEB is mutagenic in human cells at concentration levels of 1–5 µM. In comparison, EB and EBD were mutagenic at concentration levels of 100–800 µM *(34)*. A comparison of mutational spectra at *hprt* of TK6 lymphoblasts exposed to DEB (4 µM for 24h) and EB (400 µM for 24h) revealed that DEB induced AT→TA transversions and partial deletions, while EB induced GC→AT point mutations and AT→TA transversions (Table 1.4) *(35)*. BD increased the frequency of AT→GC transitions and AT→TA transversions in the spleen and bone marrow in B6C3F1 *laci* transgenic mice exposed to 62.5 ppm, 625 ppm or 1250 ppm of BD for 6 h/day, 5 days/week for 4 weeks. In addition, GC→AT point mutations were also observed in spleen *(35)*. Some studies investigating the mutagenic ability of BD in humans found

increased *hprt* mutation frequencies in blood lymphocytes of exposed workers as compared to controls but these results are not consistent. Ma et al. *(36)* and Liu et al. *(37)* have reported that there was significant increase in frequency of exon deletions in *hprt* gene in workers occupationally exposed to BD. Ma et al. have also observed that BD-induced AT→TA transversions and frame shift mutations were increased in exposed workers *(36)*. In contrast, studies by Hayes et al. *(38)* and Tates et al. *(39)* didn't find statistically significant differences in *hprt* mutant frequencies between exposed and control workers.

Table 1.4 *hprt* mutational spectra of EB and DEB in human TK6 cells *(35)*

Mutation Class	**No. Mutations (%)**		
	Control	**EB (400 µM for 24 h)**	**DEB (4 µM for 24 h)**
GC → AT	10 (23)	15 (30)*	3 (6)
GC → CG	1 (2)	2 (4)	2 (4)
GC → TA	3 (7)	2 (4)	2 (4)
AT → GC	3 (7)	6 (12)	1 (2)
AT → CG	3 (7)	2 (4)	1 (2)
AT → TA	2 (5)	12 (24)*	9 (18)*
Other alterations	1 (2)	12 (24)	40 (59)
Partial deletions	1 (2)	0 (<2)	7 (14)*

*Statistically significant compared to control

1.3 Biomarkers of BD exposure

Given the high carcinogenicity of BD, it is critical to develop biomarkers of BD metabolites for biomonitoring of BD exposure in humans and also to study its *in vivo* effects. DNA adducts, protein adducts, and urinary metabolites have been used as biomarkers of exposure to BD, while genetic and chromosomal changes have been employed as biomarkers of effect.

1.3.1 DNA adducts

The N7-position of guanine, the N3-position of thymidine and the N1-, N3- and N^6-positions of adenine are the most common sites of DNA adduct formation by BD and its metabolites *(40)*. EB can react with DNA bases to form N7-(2-hydroxy-3-buten-1-yl)guanine (EB-Gua I), N7-(1-hydroxy-3-buten-2-yl)guanine (EB-Gua II), N1-(2-hydroxy-3-buten-1-yl)adenine (EB-Ade I) and N1-(1-hydroxy-3-buten-2-yl)adenine (EB-Ade II) (Chart 1.2) *(41-43)*. Similarly, EBD and DEB can form N7-(2',3',4'-trihydroxybut-1'-yl)guanine (THB-Gua), N^6-(2',3',4'-trihydroxybut-1'-yl)adenine (N^6-THB-Ade), and N3-(2',3',4'-trihydroxybut-1'-yl)adenine (N3-THB-Ade) (Chart 1.2) *(43;44)*. DEB is a bis electrophile which can sequentially react with two DNA bases to form inter-strand and intra-strand DNA-DNA cross links such as 1,4-*bis*-(guan-7-yl)-2,3-butanediol (*bis*-N7G-BD), 1-(guan-7-yl)-4-(aden-1-yl)-2,3-butanediol (N7G-N1A-BD), 1-(guan-7-yl)-4-(aden-3-yl)-2,3-butanediol (N7G-N3A-BD), 1-(guan-7-yl)-4-(aden-7-yl)-2,3-butanediol (N7G-N7A-BD) and 1-(guan-7-yl)-4-(aden-N^6-yl)-2,3-butanediol (N7G-N^6A-BD) cross-links (Chart 1.2) *(45-47)*. Alternatively, DEB can react with two sites on the same base to form exocyclic DNA adducts such as *1*,N^6-(2-hydroxy-3-hydroxymethylpropan-1,3-diyl)-2'-deoxyadenosine (*1*,N^6-γ-HMHP-dA) and *1*,N^6-(1-

hydroxymethyl-2-hydroxypropan-1,3-diyl)-2'-deoxyadenosine (*1,N*^{6}-α-HMHP-dA) (Chart 1.2) *(48-51)*. Since DNA adducts are responsible for the mutagenicity of BD and subsequently carcinogenesis, they can be used as reliable biomarkers of risk.

Koivisto et al. and Zhao et al. employed ^{32}P-post labeling methodology to quantify several DNA adducts induced by BD and its metabolites. Koivisto et al. have reported the formation of EB-Gua I, EB-Gua II, *N*^{6}-EB-Ade, and THB-Gua in several tissues of mice and rats exposed to BD *(52-56)*. Zhao et al. observed significantly higher amounts of N1-THB-Ade adducts in human lymphocytes of BD-exposed workers as compared to non exposed workers or controls *(57;58)*. Tretyakova et al. detected the formation of EB-Gua I, EB-Gua II and THB-Gua in liver tissues of mice and rats exposed to 1250 ppm BD for 10 days by isotope dilution mass spectrometry *(59)*. Koc et al. expanded this study further to construct dose-response curves in liver, lung and kidney tissues of mice and rats exposed to 20, 62.5 or 625 ppm of BD *(60)*. THB-Gua adducts were also found to be persistent *in vivo* with half lives of greater than 4 days in laboratory animals *(61)*. These three adducts, along with another regio-isomer of THB-Gua, N7-(1-hydroxymethyl-2,3-dihydroxypropyl)-guanine, were found in liver, lung and testis DNA of mice and rats exposed to [2,3-^{14}C]-1,3-butadiene by HPLC with on-line UV and radioactivity detection methodology *(62;63)*.

Our laboratory has developed sensitive HPLC-ESI$^+$-MS/MS methods for quantification of DEB-specific DNA adducts *in vivo*. Significant levels of racemic *bis*-N7G-BD adducts were detected in the liver (3.2 ± 0.4 adducts per 10^6 dG) and lung (1.8 ± 0.5 adducts per 10^6 dG) tissues of C57BL/6 mice exposed to 625 ppm BD for 7h/day for 5 days *(64)*. N7G-N1A-BD adducts (quantified as N7G-N^{6}A-BD following forced

Dimroth rearrangement) were also found in liver DNA of B6C3F1 mice exposed to 625 ppm BD for 2 weeks *(65)*. The levels of *bis*-N7G-BD, N7G-N1A-BD adducts in laboratory mice exposed by inhalation increased linearly with BD exposure (0-625 ppm) *(66)*. In contrast, the adduct levels in tissues of rats reached a plateau at 62.5 ppm indicating metabolic saturation in this species *(66)*. Tissue distribution studies of *bis*-N7G-BD adducts in mice and rats revealed that the highest adduct levels were found in liver *(66)*. By a highly sensitive column switching HPLC-ESI^+-MS/MS method, *1*,N^6-HMHP-dA adducts (0.44 ± 0.08 adducts per 10^8 nucleotides) were detected in liver DNA of B6C3F1 mice exposed to 625 ppm BD *(67)*. More recently, an accurate and sensitive nanoHPLC-nanoESI^+-MS/MS method was successfully developed in our laboratory for the quantification of *bis*-N7G-BD adducts in liver tissue of rats exposed to low level BD exposure (0-1.5 ppm) *(68)*.

While the majority of the BD-DNA adducts have been detected and quantified in laboratory animals exposed to BD, human data for these DNA adducts is missing. Since humans are exposed to low amounts of BD (< 2 ppm), the levels of these adducts will be very low, requiring extremely sensitive methods for detection. N7-THBG has been recently detected in human lymphocytes in our laboratory by HPLC-HRMS/MS methodology on an LTQ Orbitrap Velos instrument *(69)*. BD-DNA adducts, if detected in humans, can serve as specific biomarkers; however further research needs to be done.

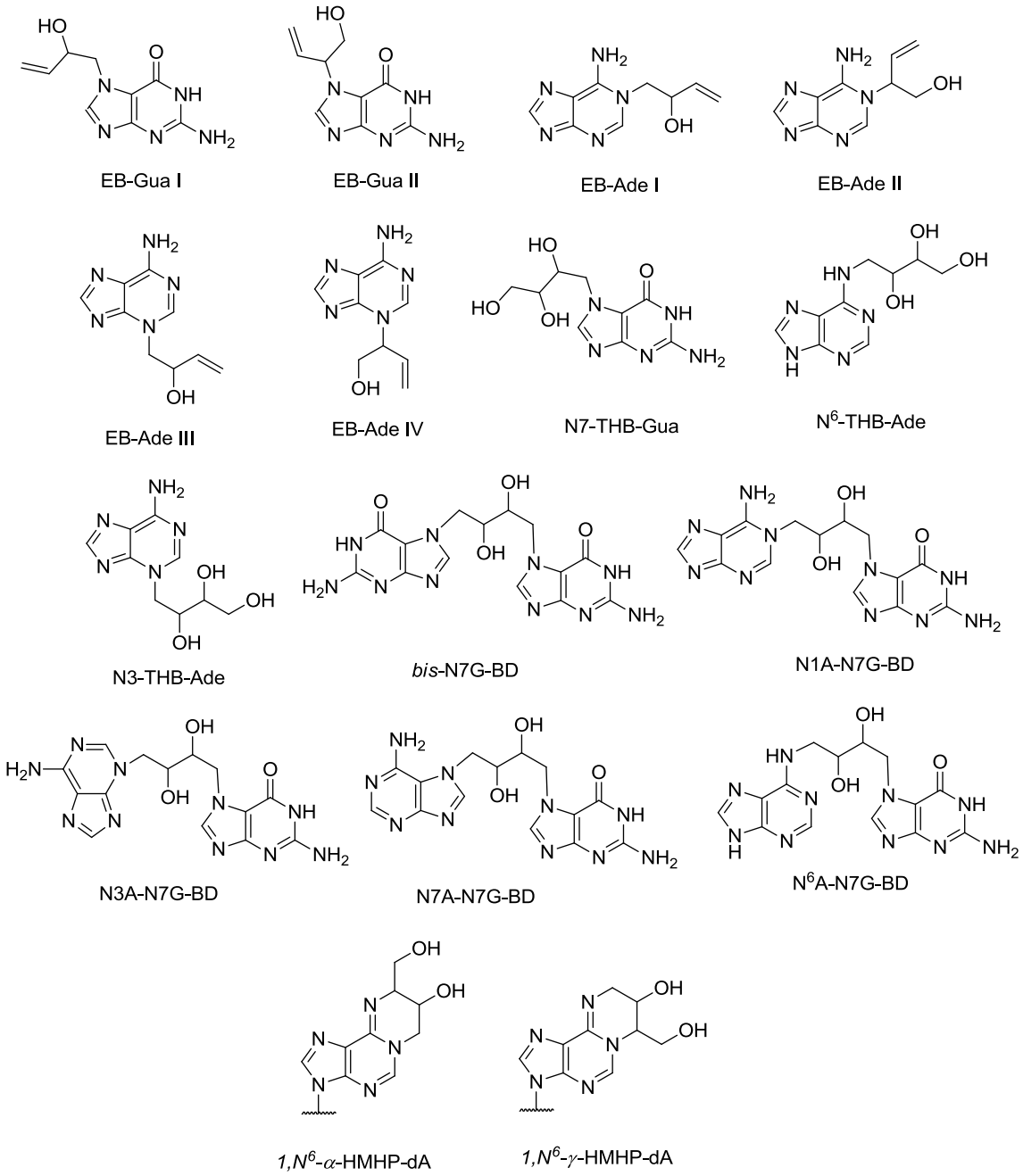

Chart 1.2 Structures of BD-DNA adducts

1.3.2 Hemoglobin adducts

The electrophilic epoxide metabolites of BD can also react with proteins to form adducts. For example, EB, DEB or EBD can react at multiple sites on hemoglobin or serum albumin to form adducts *(70-72)*. These adducts can be used as surrogate biomarkers to understand BD metabolism *in vivo* and mechanisms of carcinogenesis *(26)*. Additionally, unlike DNA adducts which can be repaired, protein adducts accumulate over lifetime of red blood cells, and hemoglobin is more abundant and easily obtained compared to DNA for human studies *(40)*. Most of the *in vivo* work is focused on N-terminal valine adducts of hemoglobin as they are the most abundant adducts formed by BD epoxides *(73)*. EB can react with N-terminal valine in hemoglobin to form *N*-(2-hydroxy-3-butenyl)–valine (HB-Val) adducts (Scheme 1.2) *(74)*. Similarly, EBD and DEB generate *N*-(2,3,4-trihydroxybutyl)–valine (THB-Val) *(75)* and *N*,*N*-(2,3-dihydroxy-1,4-butadiyl)–valine (*pyr*-Val) (Scheme 1.2) *(76)* adducts, respectively. All three N-terminal valine adducts were quantified in hemoglobin isolated from blood erythrocytes of laboratory animals and humans. HB-Val and THB-Val were quantified by a modified Edman degradation, followed by derivatization to pentaflurophenyl thiohydantoins and analysis by GC-MS/MS by stable isotope dilution with labeled internal standards *(74;75)*. *Pyr*-Val on the other hand was quantified as a 7- or 11-mer peptide generated by proteolytic digestion of hemoglobin with trypsin, followed by HPLC or immunoaffinity enrichment and stable isotope dilution LC-MS/MS analysis *(76;77)*.

Osterman-Golker and co-workers were the first researchers who reported the detection of HB-Val and THB-Val *in vivo*. A linear dose response relationship was observed with HB-Val adduct levels and BD exposure in Wistar rats exposed to 0, 250, 500 or 1000 ppm BD 6 h/day for 2 weeks *(74)*. The mean HB-Val amount in the 1000

ppm BD exposure group was 3 nmol/g Hb *(74)*. This study was further extended to the other BD-Hb adduct, THB-Val. THB-Val was detected in several strains of mice and rats exposed to 0, 2, 10 or 200 ppm BD and also in workers occupationally exposed to BD (1 ppm). The researchers reported detection of 1-3 pmol HB-Val/g Hb and 10-14 pmol THB-Val/g Hb adducts in blood of occupationally exposed workers *(75;78)*. Tornqvist et al. were the first researchers to observe the formation of the DEB-specific hemoglobin adduct *pyr*-Val in mice and rats injected with high concentrations of DEB *(76;79)*.

Swenberg and co-workers have done pioneering work in detection and quantification of BD specific hemoglobin adducts in mice, rats and humans to understand inter-species, inter-individual and gender differences in metabolism of BD. Swenberg et al. *(80)* successfully quantified HB-Val and THB-Val in mice and rats B6C3F1 mice and Sprague-Dawley rats (1,000 ppm BD for 13 weeks at 6 hours/day, 5 days/week). They reported that THB-Val adducts in blood increased with exposure in a time course study in B6C3F1 female mice. In the same study, they reported statistically significant differences in THB-Val amounts between Chinese workers not occupationally exposed to BD (39 ± 13 pmol/g Hb) and occupationally exposed workers (88 ± 59 pmol/g Hb) *(80)*. These results were subsequently confirmed by another study involving butadiene-polymer production workers and controls from China *(81)*.

Albertini et al. compared the amounts of HB-Val and THB-Val adducts in male workers working in administration, monomer production, or polymer production in a BD and SBR production facility in the Czech Republic. Statistically significant differences were observed in levels of both adducts in the three groups (K-W, $P<0.001$). The adduct levels were found to be in the order of polymer production > monomer production >

administration workers *(82)*. This comprehensive study also looked at several other biomarkers including urinary metabolites, T-cell mutations, *hprt* gene mutation frequencies, and sister chromatid exchanges *(83)*. This study was later expanded to include female workers to understand gender differences in BD metabolism in humans. THB-Val adduct levels were found to be significantly higher in males as compared to females and the rate of increase of THB-Val adduct with BD exposure was lower in females which led to the observation that females absorb or metabolize less BD than males per unit exposure *(84;85)*. There were no significant differences in smoking status between males and females and hence these gender differences were due to differences in metabolism *(85)*. However, no differences were found in THB-Val adduct levels between exposed and control workers in an epidemiological study involving Italian workers *(86;87)*.

Boysen et al. quantified *pyr*-Val adducts and compared them with HB-Val and THB-Val in B6C3F1 mice and F344 rats exposed to 3, 62.5, 1250 ppm BD (6 h/day for 2 weeks) and found that THB-Val was the major adduct in both species. Also, mice formed much higher amounts of *pyr*-Val as compared to rats *(77)*. A highly sensitive nanoUPLC-MS/MS method was developed to quantify *pyr*-Val in mice and rats exposed to 0, 0.5, 1, 1.5, 6.25, 62.5, 200 or 625 ppm BD. By this method, *pyr*-Val was detected in lower level exposed animals (<1 ppm BD) *(88)*. More recently, Boysen et al. applied the nanoUPLC-MS/MS method to human samples and found background levels of *pyr*-Val (0.11 ± 0.07 pmol/g Hb) in control workers not exposed to BD. As expected, *pyr*-Val levels were much higher in BD occupationally exposed workers (0.11 ± 0.07 pmol/g Hb) *(89)*.

Scheme 1.2 Structures of BD-hemoglobin adducts

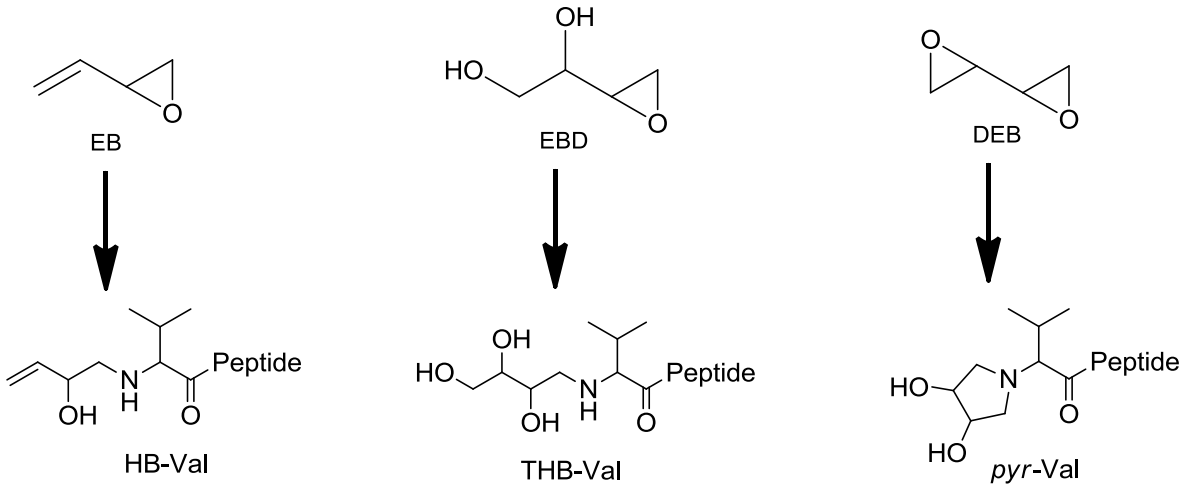

1.3.3 Urinary bio-markers of exposure to BD

Quantification of DNA and hemoglobin adducts of BD in humans requires access to blood samples. In contrast, urine collection is non-invasive and human urine is readily available. Urinary metabolites can be used as biomarkers of exposure to BD as they represent the detoxification metabolites of BD epoxides. Furthermore, in human studies where the concentrations of DNA adducts are extremely low (<1 per 10^9 nucleotides) and their detection requires ultra-sensitive methodologies, urinary biomarkers are a suitable alternative. As discussed above, EB, HMVK, EBD, DEB can be conjugated with glutathione and excreted in urine as the corresponding mercapturic acids, MHBMA, DHBMA, THBMA and *bis*-BDMA, respectively (Scheme 1.1).

Several studies have focused on quantification of BD-mercapturic acids *in vivo*. In a study by Sabourin et al. *(90)*, Sprague-Dawley rats, B6C3F1 mice, Syrian hamsters, and cynomolgus monkeys were exposed to 8000 ppm of ^{14}C-BD, and the BD urinary metabolites were analyzed. This study revealed that all four species excreted primarily 2-(*N*-acetyl-L-cystein-S-yl)-1-hydroxybut-3-ene/1-(*N*-acetyl-L-cystein-S-yl)-2-hydroxybut-3-ene (MHBMA or M-II) and *N*-acetyl-*S*-(3,4-dihydroxybutyl)-L-cysteine (DHBMA or M1) *(90)*. Bechtold et al. observed higher concentration of DHBMA in urine of workers exposed to BD (3200 ng/ml) as compared to controls not exposed to BD (320 ng/ml). However, MHBMA levels were below the LOD (100 ng/ml) even in exposed workers suggesting that it is a relatively minor metabolite of BD in humans *(91)*. Nauhaus et al. conducted a comprehensive study of urinary metabolites of BD in laboratory rodents exposed to 800 ppm ^{13}C-BD. MHBMA and DHBMA together accounted for 87% and 73% of total urinary metabolites in rats and mice, respectively. Other urinary metabolites detected in mouse urine included *S*-(1-(hydroxymethyl)-2-propenyl)-L-cysteine (4%). *N*-

Acetyl-*S*-(1-hydroxy-3-butenyl)-L-cysteine (4%), *N*-acetyl-*S*-(3-hydroxypropyl)-L-cysteine (5%), *N*-acetyl-*S*-(2-carboxyethyl)-L-cysteine (5%) and *N*-acetyl-*S*-(1-(hydroxymethyl)-3,4-dihydroxypropyl)-L-cysteine (5%) *(92)*.

4-(*N*-acetyl-L-cystein-S-yl)-1,2,3-trihydroxybutane (THBMA) and its regio-isomer 3-(*N*-acetyl-L-cystein-S-yl)-1,2,4-trihydroxybutane were discovered for the first time in the urine of rats and mice exposed to 200 ppm ^{14}C-BD for 6 hours by Richardson and co-workers *(93)*. Together, these urinary metabolites accounted for 10% of the total urinary radioactivity in laboratory animals. The formation of these metabolites was not surprising given a previous *in vitro* observation for the formation of *S*-(1-(hydroxymethyl)-2,3-dihydroxypropyl) glutathione and *S*-(2,3,4-dihydroxybutyl) glutathione upon incubation of DEB and ^{3}H-GSH in liver and lung cytosol from B6C3F1 mice and Sprague–Dawley rats and human liver cytosol from six volunteers *(94)*. Another interesting observation in that study by Boogaard et al. was the evidence for the formation of bis glutathione conjugate of DEB *(94)*. Further, Booth et al. confirmed the formation of MHBMA, DHBMA and THBMA at a more relevant BD exposure level (1-20 ppm) using ^{14}C-BD inhalation studies in rats and mice *(62)*.

Van Sittert et al. developed a sensitive GC-MS/MS method (LOD: 0.1 ng/ml) for the quantification of MHBMA and DHBMA in the urine of workers in the rubber industry from the Netherlands or the Czech Republic. Background levels of MHBMA and DHBMA in control workers with no known exposure to BD were detected by this sensitive method. Overall, the median values of MHBMA and DHBMA in polymer workers> monomer workers> controls. The median MHBMA and DHBMA concentrations in control workers were 2 and 524 ng/ml, respectively. Although they

attempted to quantify THBMA, they were not successful due to high interferences *(31)*. This study was later expanded to compare the urinary metabolite levels in humans with rat, mice and monkeys exposed to BD. The mean concentrations of MHBMA and DHBMA in exposed workers were 39 and 2213 ng/ml, respectively. Additionally, the DHBMA/(MHBMA+DHBMA) ratio in humans was determined to be 0.98. In comparison, the DHBMA/(MHBMA+DHBMA) ratio in rats and mice were 0.5 and 0.3, respectively. The conclusions from this second study were that humans are most efficient at hydrolysis of BD epoxides than rats and mice and hence have the least cancer risk associated with BD among all the species *(95)*.

Albertini et al. *(83)* further expanded the above two studies to find correlations between urinary metabolites and other parameters including BD exposures, hemoglobin adducts, metabolic genotypes, hprt mutations and cytogenetic end points. MHBMA and DHBMA levels generally correlated with BD exposure (Spearman correlation coefficient, $r>0.5$). The correlations between urinary metabolites (MHBMA and DHBMA) and hemoglobin adducts (HB-Val and THB-Val) were also positive. No association was found between either of the urinary metabolites and *CYP2E1*, *EH*, and *ADH* polymorphisms. Also, no significant correlations were observed between urinary metabolites and *hprt* mutations and cytogenetic end points *(83)*. The above study was an all-male study and hence, the same researchers conducted another study which included both female and male workers to understand the gender differences in metabolism of BD. MHBMA and DHBMA along with several other biomarkers were evaluated in that study *(85)*. The study found that males excreted significantly higher concentrations of MHBMA and DHBMA per unit BD exposure compared to females *(85)*.

Urban and co-workers developed a novel stable isotope dilution HPLC-APCI-MS/MS method for rapid quantification (run time of 10 minutes) of MHBMA and DHBMA in urine of smokers and non-smokers (N=10 per group). The analytes present in urine samples (5 ml) were enriched by SPE with Strata-X cartridges. It was found that MHBMA concentrations in smokers (86.4 ± 14.0 µg/24 hr) were significantly higher than non-smokers (12.5 ± 1.0 µg/24 hr) *(96)*. McDonald et al. reported a comprehensively validated LC-MS/MS method with turbo spray ion source for the quantification of MHBMA and DHBMA in 1 ml of human urine. The LOQ of the method was 1.4 and 4.1 ng/ml for MHBMA and DHBMA, respectively (Table 1.5) *(97)*. Fustinoni et al. conducted similar studies in workers working in an Italian petrochemical company. By using a strong anion exchange (SAX) SPE method and HPLC-MS/MS on an ion trap, they found that there were no statistically significant differences between control and BD-exposed workers with respect to either of the urinary metabolites MHBMA or DHBMA *(98)*. Sapkota et al. developed a rapid and sensitive HPLC-ESI-MS/MS method for the simultaneous quantification of MHBMA and DHBMA in urine of three general population exposure groups: suburban-weekend exposure, urban-weekday exposure and toll collectors workday exposure. The LODs of the method were reported to be 0.4 and 3.7 ng/ml for MHBMA and DHBMA, respectively (Table 1.5). However, there were no significant differences in urinary metabolite levels in the three groups *(99)*. Navasumrit et al. used LC-APCI-MS/MS to quantify urinary MHBMA and found that temple workers exposed to BD from incense smoke had much higher amounts of MHBMA as compared to control workers *(100)*. Later, they also observed that MHBMA levels were not different among traffic policemen and policemen who worked in an office *(101)*.

Schettgen et al. developed a column switching LC-ESI$^-$-MS/MS method for the simultaneous quantification of urinary biomarkers of 1,3-butadiene (MHBMA, DHBMA) and acrylonitrile (CEMA). However, the LOQ of the method for MHBMA was 2 ng/ml (Table 1.5) and hence it could not be detected in the majority of the urine samples (80%) of the general population exposed passively or actively to cigarette smoke. Smokers excreted significantly higher amounts of MHBMA as compared to non-smokers *(102)*. Carmella et al. have developed a novel LC-APCI-MS/MS method for simultaneous quantification of MHBMA, DHBMA, HPMA (from acrolein), HBMA (from crotonaldehyde) and HEMA (from ethylene oxide). They applied this method to look at the effect of smoking cessation on the urinary biomarker levels of carcinogens present in cigarette smoke. MHBMA levels decreased significantly (>80%) 3 days after smokers quit smoking and >95% after 56 days post smoking cessation. DHBMA levels on the other hand remained constant after smoking cessation *(33)*. This method was later applied to study differences in MHBMA levels between smokers who developed lung cancer (cases) and those who remained cancer free (controls) in a Shanghai cohort study. Mean MHBMA concentrations were significantly ($P<0.001$) greater in cases (11.3 pmol/mg Cr) as compared to controls (8.3 pmol/mg Cr) *(103)*.

Ding et al. developed a novel LC-ESI-MS/MS method for simultaneous quantification of MHBMA, DHBMA, CEMA, HEMA, HPMA, PMA in urine of smokers and non-smokers. The advantages of this method were minimal sample preparation (direct injection of diluted urine sample) and high sensitivity (LOD of MHBMA and DHBMA were 0.05, 0.14 ng/ml, respectively) (Table 1.5). DHBMA but not MHBMA concentrations were significantly higher in smokers than non-smokers, contradictory to

earlier reported results. Also, the median concentrations of MHBMA in non-smokers (21.3 ng/mg creatinine) were higher than in smokers (10.2 ng/mg creatinine) *(104)*. Roethig and co-workers developed two separate HPLC-ESI-MS/MS methods for quantification of MHBMA and DHBMA in urine. The sample preparation for MHBMA involved SPE enrichment, while DHBMA analysis was performed by direct injection of diluted urine *(105)*. Their method was extremely sensitive with LOQs of 0.1 and 10.1 ng/ml for MHBMA and DHBMA, respectively (Table 1.5). This method was applied to a stratified, cross-sectional, multicenter study involving 3,585 adult cigarette smokers and 1,077 nonsmokers. MHBMA amounts were 12-fold higher in smokers as compared to non-smokers. The study also found statistically greater amounts of MHBMA and DHBMA in males as compared to females. Higher amounts of BD-mercapturic acids were excreted by European-American smokers as compared to African-American smokers *(105)*. This method was recently applied to compare the MHBMA levels in 3 spot urine samples vs 24 hours urine collection. It was found that spot urine samples are a good alternative for 24 hour urine sample *(106)*.

Eckert et al. developed a HILIC-ESI-MS/MS method for the simultaneous quantification of six hydroxyalkyl mercapturic acids in human urine including MHBMA and DHBMA. The method was relatively less sensitive with LODs of 5 and 4.5 ng/ml for MHBMA and DHBMA, respectively (Table 1.5) *(107)*. This method was slightly modified and applied to smokers and non-smokers from Germany. MHBMA couldn't be detected in 90% of the human urine samples *(108)*. More recently, the method was further modified to improve the sensitivity of MHBMA analysis (0.5 ng/ml). MHBMA was detected in more than 60% of workers with known or unknown exposure to

chloroprene; MHBMA and DHBMA concentrations were significantly higher in exposed workers as compared to controls *(109)*. Most recently Sterz et al. reported for the first time detection of the other regio-isomer of MHBMA, 2-(*N*-acetyl-L-cystein-S-yl)-1-hydroxybut-3-ene in human urine with a novel UPLC-HILIC-MS/MS method. Only 100 µl of the urine was used for analysis without any SPE and the LOD of the method was <0.25 ng/ml which highlights the extremely good sensitivity of this method (Table 1.5) *(110)*.

In summary, many research groups developed methods for quantification of MHBMA and DHBMA in human urine (Table 1.5). Most of the studies observed higher amounts of the urinary metabolites in smokers and exposed workers as compared to non-smokers or controls. MHBMA is a better biomarker of exposure to BD in the general population because of its relatively low background levels in non-smokers. However, to our knowledge, no studies have successfully detected or quantified THBMA and *bis*-BDMA in the urine of either rodents or humans exposed to BD. Development of quantitative methods for these biomarkers is critical in understanding the complex mechanisms of carcinogenesis of BD.

Table 1.5 Summary of previous HPLC-MS/MS methods for quantification of MHBMA and DHBMA

Method	Urine volume	SPE cartridge	HPLC column and ionization source	Run time (min)	LOD(ng/ml)	LOQ(ng/ml)
Urban *(96)* (2003)	5 ml	Strata X	Synergi Luna (4.6 X 100 mm, 5 µ); APCI	10	0.9 (MHBMA) 23 (DHBMA)	2.7 (MHBMA) 76 (DHBMA)
McDonald *(97)* (2004)	1 ml	Waters C18	Phenomenex C18 Aqua; Turbo Spray	7.5	< 1 (MHBMA) < 1 (DHBMA)	1.4 (MHBMA) 4.1 (DHBMA)
Sapkota *(99)* (2006)	1 ml	Oasis HLB	Alltech custom Mixed mode (C8/anion) (2.1 x 100 mm, 7 µ); ESI	6	0.4 (MHBMA) 3.7 (DHBMA)	NA
Schettgen *(102)* (2009)	0.5 ml	None (column switching)	Trap: LiChrospher RP-8 ADS (4 X 100 mm, 25 µ) Analytical: Luna C8(2) (4.6 X 50 mm, 3 µ); ESI	25	1 (MHBMA) 5 (DHBMA)	2 (MHBMA) 10 (DHBMA)
Carmella *(33)* (2009)	2 ml	Oasis MAX	Synergi MAX-RP (4.6 X 250 mm, 4 µ); APCI	27	0.75 (MHBMA) 3 (DHBMA)	NA
Ding *(104)* (2009)	0.1 ml	None (Dilution and injection)	Waters Xterra C18 MS column (4.6 mm × 50 mm, 5 µ); ESI	12	0.05 (MHBMA) 0.14 (DHBMA)	NA
Roethig* *(105)* (2009)	0.5 ml (M) 0.2 ml (D)	Oasis HLB (M) Dilution and injection (D)	Hypersil-Keystone BioBasic AX column (150 × 4.6 mm, 5 µ); ESI	NA	NA	0.1 (MHBMA) 10.1 (DHBMA)
Eckert *(107)* (2010)	2 ml	Isolute ENV+	XBridge HILIC (2.1 × 150 mm, 3.5 µ); ESI	22	5 (MHBMA) 4.5 (DHBMA)	NA
Sterz[#] *(110)* (2012)	0.1 ml	Evaporation and dilution	BEH HILIC column (3 x 150 mm, 1.7 µ); Turbo spray	21	0.05 (1-MHBMA) 0.24 (2-MHBMA)	0.15 (1-MHBMA) 0.72 (2-MHBMA)

**(M): MHBMA, (D):DHBMA. Two separate methods were used for quantification of MHBMA and DHBMA*

[#] 1-MHBMA and 2-MHBMA are the two regioisomers of MHBMA

NA: Not available

1.4 Species and gender differences in BD metabolism

Differences in BD metabolism among different species are well studied. Earlier studies reported that mice developed tumors even at 6.25 ppm BD exposure while rats developed small number of tumors even at exposures as high as 1000 ppm *(20;21)*. Lung and liver tumors were observed at exposure concentrations of 6.25 and 20 ppm BD, respectively in female mice. The corresponding exposure levels that induced lung and liver tumors in male mice were 62.5 and 200 ppm *(26)*. Also, the *in vitro* oxidation rates of BD to EB in several tissues were higher in mice than rats *(27;111)*. *In vitro* experiments which estimated the V_{max}/K_m values for the conversion of EB to DEB in mice, rat and human liver microsomes revealed that in mice the rates of conversion were 3.5 fold faster than rats, and 3-60 fold greater than humans *(29;112)*. Also, the rates of epoxide hydrolase-mediated detoxification of EB to EB-diol were higher is humans followed by rats and least in mice *(27;30)*. Similarly, the rates of detoxification by GST are higher in rats as compared to mice *(27)*.

Henderson et al. observed that the tissue concentrations of EB were 3-10 fold higher in mice than rats and DEB were 30-50 fold higher in mice than rats *(113)*. Blood concentrations of EB and DEB were at least 5 fold higher in mice as compared to rats *(114;115)*. These researchers also reported that concentrations of DEB in blood, femur, lung and fat tissues were greater in female rats as compared to male rats *(115)*. However no such gender differences were observed with respect to EB *(116)*. Similar differences in EB, DEB concentrations between mice and rats were also obtained by Filser et al. *(117)*. These researchers also reported that the blood concentrations of EB-diol were

similar in rats and mice and the concentrations of EBD were higher in mice than rats *(117)*.

DHBMA/(DHBMA +MHBMA) ratio is an indication of whether EB is metabolized by EH or GST. Bechtold et al. observed that this ratio was 0.20, 0.52 and 0.98 in mice, rats and humans, respectively *(91)*. Also the ratio of *in vivo* kinetic rate constants for the metabolism of EB by EH or GST were found to be 0.04, 0.08, 1.8 in mice, rats, and humans, respectively which clearly showed that the metabolism of BD is different among the three species *(91)*. Henderson et al. reported similar results for DHBMA/(DHBMA +MHBMA) ratio among mice, rats and humans *(113)*. MHBMA and DHBMA concentrations in male control and male exposed workers were significantly higher than female control and female exposed workers, respectively *(85)*. Also, the MHBMA/(MHBMA+DHBMA) ratio was significantly higher in male exposed workers as compared to female exposed workers.

Comparison of the levels of BD-hemoglobin adducts between B6C3F1 mice and F344 rats showed 4-10 fold higher concentrations of HB-Val and *pyr*-Val in mice as compared to rats at 0-62.5 ppm BD exposure. The ratio of THB-Val to total BD-hemoglobin adduct formation in rodents were 2-6 while in humans that ratio was >500 *(26;73)*. Interestingly, THB-Val adduct levels were significantly higher in male control and male exposed workers than female control and female exposed workers, respectively *(84)*. Among mice, rats and humans exposed to 1 ppm BD, HB-Val and *pyr*-Val adducts were the highest in mice. Also, % THB-Val was highest in humans (99.6%) proving that metabolism of BD is different among the three species (Table 1.6) *(26;89)*. The

concentrations of *pyr*-Val are much higher in mice compared to rats or humans (Table 1.6) which suggest that mice produce higher concentrations of DEB. *bis*-N7G-BD adduct levels in several tissues were also higher in mice as compared to rats exposed to the same concentration of BD (Table 1.7) *(66)*. Additionally, female mice were observed to have significantly higher levels of *bis*-N7G-BD adducts as compared to their male counterparts. These gender differences were not observed in rats. In the same study, N7G-N^6A-BD adducts were found to be significantly higher in mice as compared to rats *(66)*. THB-Gua adducts were also significantly higher in liver, lung and kidney tissues of mice as compared to rats exposed to 625 ppm BD *(60)*.

In summary, significant inter-species and gender differences in metabolism of BD have been observed. Among the species examined, laboratory mice convert a relatively high fraction of BD to DEB, followed by rats and humans. Since DEB is the most genotoxic metabolite of BD believed to be responsible for its adverse health effects, this may suggest that mice are most susceptible to BD associated cancer while humans are least susceptible. Although gender differences in BD hemoglobin adduct formation were observed at relatively high exposure of BD in rodents, there is less evidence for such differences at low BD exposures *(88)*. These differences in BD metabolism makes BD risk assessment complex.

Table 1.6 Comparison of BD-hemoglobin adducts (pmol/g globin) in mice, rats and humans exposed to ~1 ppm BD

	HB-Val	***pyr*-Val**	**THB-Val**
B6C3F1 Mice	21.5 ± 4.0	66.8 ± 5.9	525 ± 307
F344 Rats	1.6 ± 0.5	1.4 ± 0.2	29 ± 3
Human Workers	2.2 ± 1.4	0.3 ± 0.2	716 ± 426

Table 1.7 Differences in *bis*-N7G-BD adduct levels (per 10^7 nucleotides) between female B6C3F1 mice and female F344 rats exposed to 625 ppm BD *(66)*

Tissue (N=4)	B6C3F1 mice	F344 rats
Liver	3.95 ± 0.89	0.36 ± 0.23
Lung	1.35 ± 0.12	0.30 ± 0.01
Kidney	1.10 ± 0.13	0.14 ± 0.05
Brain	0.38 ± 0.15	0.24 ± 0.06
Thymus	1.15 ± 0.26	0.21 ± 0.06

1.5 Mutagenicity of BD-DNA adducts

1.5.1 Translesion synthesis polymerases

The DNA damage induced by endogenous or exogenous factors can be repaired by one of the several mechanisms including direct reversal, base excision repair (BER), nucleotide excision repair (NER), mismatch repair (MMS), and double-strand break (DSB) repair *(118;119)*. Some of the adducts either escape repair *(120)* or can be temporarily tolerated by specialized cellular mechanisms *(121)*. These adducts block DNA replication since they cannot be accommodated in the active site of replicative DNA polymerases *(122)*. The cellular mechanisms that can tolerate these lesions include translesion synthesis by a specialized group of polymerases called the translesion synthesis (TLS) polymerases *(122)*. The major TLS polymerases in mammalian cells are hPol *η*, hPol *ι,* hPol *κ*, Rev1 from the Y family and hPol ζ from the B family *(121;122)*. The Y family polymerases have a thumb, palm and finger domains similar to the replicative polymerases (A and B family) and play the same roles in DNA replication *(123;124)*. However, the thumb and finger domains are significantly smaller in the Y-family polymerases as compared to the replicative polymerases *(124)*. As a result of this, the active site in the palm domain of the Y-family polymerases is more open and solvent accessible *(123)*. The presence of an open and larger active site enables Y-family polymerases to accommodate bulky lesions *(121)*.

The Y family polymerases also have a unique and conserved domain which extends from the finger domain called the little finger (LF) domain *(125)* or polymerase-associate domain (PAD) *(126)*. This LF domain is responsible for making additional

contacts with DNA *(121)*. Another important difference between the Y-family polymerases and the replicative polymerases is the conformational change of finger domain in the latter during the replication process *(123)*. When a regular Watson-crick base pairing is being formed in the replicative polymerases, a conformational change (induced fit) in the finger domain allows the base pair to be placed in a closed active site *(123)*. However, when the replicative polymerases encounter a damaged DNA adduct, such a conformational change doesn't occur thereby leading to reduced catalytic rate *(123)*. On the other hand, Y family polymerases don't adopt an "induced fit" mode of replication as their active site is open and "preformed" and hence can catalyze base pairing opposite a DNA lesion *(123)*. Another important difference is the lack of intrinsic 3' to 5'exonuclease domain responsible for proofreading in the Y family polymerases as compared to the replicative polymerases *(127)*.

The human replicative polymerases belonging to the A and B families have high replication fidelity since they have proofreading activity and replicate via an "induced fit" model. The error rates for replicative polymerase are one incorrect nucleotide for every 10^6 to 10^8 bases replicated *(121;128)*. In contrast, the Y family polymerases have extremely low fidelity with very high error rates ranging from one incorrect nucleotide for every 10 to 10,000 bases *(121)*. Since the replication by TLS polymerases is highly error-prone, they can be potentially mutagenic *(121)*. The mechanism of translesion synthesis involves multiple "polymerase switching" events (Figure 1.2) *(129)*. When the DNA replication machinery encounters a DNA adduct, the replicative polymerase is blocked and the replication is stalled (Figure 1.2) *(122)*. The replicative polymerase is

then switched with a TLS polymerase which can incorporate a correct or incorrect nucleotide opposite the lesion and carries out replication past it (Figure 1.2) *(130)*. Once the lesion is bypassed by the TLS polymerase, another "polymerase switching" event occurs and the regular replicative polymerase is recruited to carry out further DNA synthesis (Figure 1.2) *(130)*.

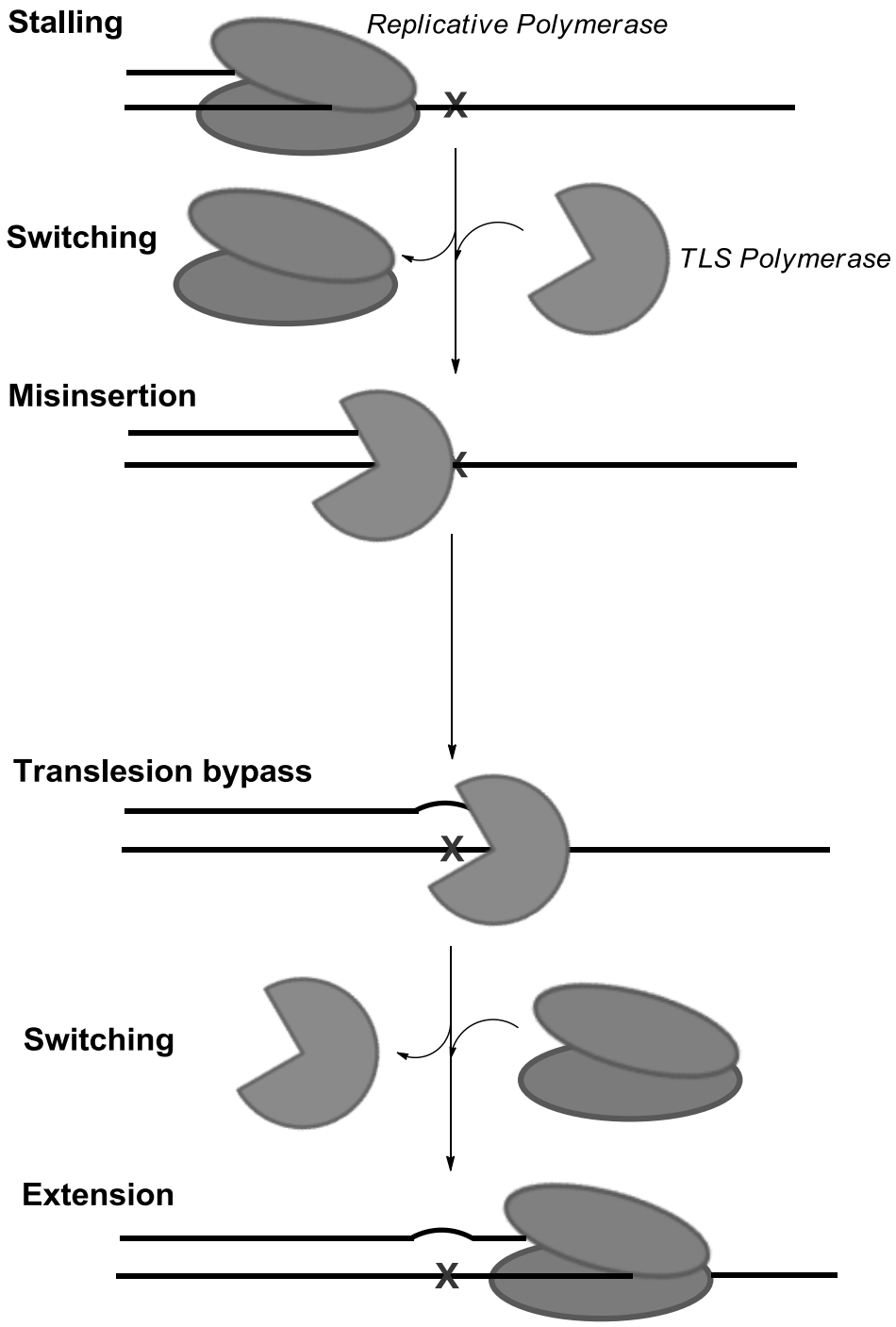

Figure 1.2 Mechanism of translesion synthesis *(129)*

1.5.2 DNA sequencing by tandem mass spectrometry

Tandem mass spectrometry (MS/MS) has been extensively used in sequencing native (unmodified) oligonucleotides. Initial efforts in this area employed fast atom bombardment (FAB) *(131;132)* and plasma desorption (PD) *(133;134)* coupled with single stage mass spectrometry to achieve "bi-directional" sequencing of oligonucleotides. These techniques resulted in the cleavage of phosphodiester bonds, thereby leading to the formation of fragment ions (5'-P and 3'-P sequence ions) which can be used to determine the sequence *(131)*. However, matrix interferences and surface fragmentation interfered with accurate sequencing by FAB-MS, a problem solved by employing tandem mass spectrometry *(135)*. Cerny et al. were among the first to sequence a short oligonucleotide (less than 6 bases in length) by fast atom bombardment (FAB) coupled with tandem mass spectrometry (FAB-MS/MS) *(135;136)*. FAB-MS/MS sequencing of oligonucleotides soon fell out of favor due to its high detection limit (10 nmol for oligonucleotides of MW>1200) *(137)*. Instead, MALDI-MS methods using a variety of matrices have been developed and successfully applied to oligonucleotide sequencing *(138-141)*. The use of a delayed extraction (DE) methodology *(142)* has improved the resolution of MALDI-MS, while post source decay (PSD) *(137;143;144)* provided useful fragmentation information during oligonucleotide sequencing. Recently, the use of 1,5-diaminonapthalene as a matrix has been reported to improve in-source dissociation (ISD) of oligonucleotides during MALDI-MS *(145)*. More spectral fragment ions have been observed with this technique which is useful for accurate sequencing *(145)*.

McLuckey et al. *(146)* employed ESI-MS/MS to determine the sequence of short oligonucleotides (4-8 nucleotides in length) and proposed a comprehensive nomenclature for fragment ions, which is analogous to the nomenclature of peptide fragments (Figure 1.3). Under most CID conditions, the phosphodiester bond can be cleaved at four different positions, giving rise to several types of 5'-terminus containing fragments (*a*, *b*, *c*, and *d)* and several types of 3'-terminus group containing fragments *(w*, *x*, *y*, and *z)* (Figure 1.3) *(146)*. Each of these ions is assigned a numerical subscript (a_n, z_n etc.), where *n* represents the cleavage position from the respective termini (Figure 1.3). In addition, "*a"* series of ions that underwent the neutral loss of a DNA base are commonly observed due to the facile cleavage of N-glycosydic bonds. The corresponding ions are designated as a_n-B_n, where upper case B denotes the cleaved base, and subscript n stands for the position of the base from the 5' terminus. Finally, *d* and *w* series ions can lose water molecules to form ions with the same *m/z* as fragment ions *c* (*d*-H_2O) and *x* (*w*-H_2O), respectively. Structurally modified oligomers exhibit similar fragmentation patterns, and the characteristic mass shifts observed for modification-containing fragments can be used to determine the positions of structurally altered bases within the sequence *(147)*.

Negative ion ESI-MS/MS is especially suitable to oligonucleotide sequencing due to its high sensitivity and the production of multiply charged ions *(146;148-152)*. However, CID spectra of oligonucleotides can be quite complex, especially for longer oligonucleotides (> 10-mers), making data interpretation challenging *(150;152;153)*. Manual interpretation of this data can be cumbersome, but can be facilitated by computational interpretation. Several useful computer algorithms have been developed in

the last 10 years for interpreting the MS/MS spectra. McCloskey and coworkers developed a program called Mongo oligo mass calculator *(154)*. When the user inputs a known oligonucleotide sequence, the program can perform multiple functionalities including molecular mass calculations, predicting electrospray series, potential MS/MS fragments obtained by collision-induced dissociation (CID), and fragments of enzymatic digests by endonuclease and exonuclease. Simple oligonucleotide sequencer (SOS) was the first automated sequencing algorithm launched in 2002 by Rozenski and McCloskey *(155)*. This algorithm could be successfully used for *de novo* sequencing of oligonucleotides 20 bases long or less but can't be used for base or sugar modified oligonucleotides of greater than 10 bases *(155).* The program identifies the 5′ (a–B-ions)- and 3′ (w-ions)-end ion series and extends the series by addition of masses of one of the four bases to derive different combinations of *m/z* values which will be compared with the experimental spectra *(155)*.

Oberascher et al. started with comparative *s*equencing algorithm (COMPAS) *(156)* for sequencing oligonucleotides and later developed a global *de novo* sequencing algorithm that starts with a known nucleotide composition and generates a theoretical mass spectra by extending it with different base combinations leading to increased run times *(157)*. More recently, Oberascher et al. improved their previous global *de novo* sequencing algorithm by usage of simulated annealing for stochastic optimization *(158).* Briefly, the nucleotide composition of a given oligonucleotide is determined from accurate molecular mass measurements to yield an initial sequence. The algorithm predicts the fragmentation spectra for this reference sequence and compares it with the

experimental fragmentation spectra and a parameter called fitness (FS) which measures the difference between the predicted and observed m/z *(158)*. If the FS value is smaller, a simulated annealing algorithm is applied wherein two bases of the initially predicted oligonucleotide sequence are randomly changed and again the FS value is calculated. If the FS value is greater than the first iteration, the new sequence will become the reference sequence and this process continues until the optimal sequence is predicted.

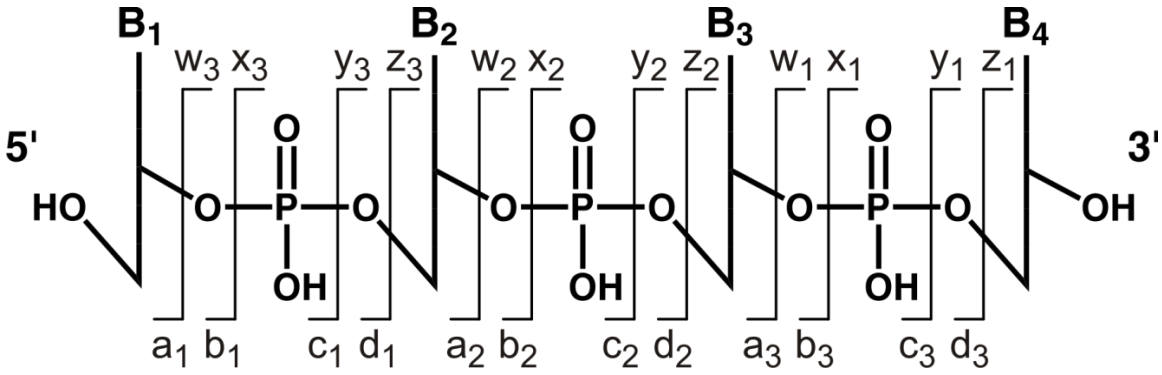

Figure 1.3 CID fragmentation of DNA oligonucleotides *(159)*

1.5.3 Primer extension studies

Mass spectrometry along with gel electrophoresis is an important tool employed in studying the mutagenic ability of structurally defined DNA adducts *in vitro (160-164).* These *in vitro* translesion synthesis experiments are generally performed by annealing a DNA template strand containing a site specific DNA adduct to a complementary DNA strand (primer). The length of the primer strand is shorter than the template, so that the 3' terminus of the primer is positioned prior to the lesion *(162;164)*. The template-primer duplexes are incubated in the presence of a TLS polymerase and all four dNTPs allowing for primer extension. The primer extension products have been traditionally visualized by gel electrophoresis using a ^{32}P-end labeled primer *(165-167)*. However, the exact sequence of primer extension products cannot be determined by gel electrophoresis, and multiple time consuming experiments involving individual dNTPs must be conducted to evaluate each incorporation step *(164)*. More importantly, gel electrophoresis fails to detect deletion products occurring when a polymerase skips the modified base, resulting in frameshift mutations. HPLC-ESI-MS/MS can be used to accurately sequence primer extension products in a single experiment, without the use of radioactivity *(164)*.

Because of size limitations for sequencing oligonucleotides by MS/MS, Zang et al have developed a methodology in which the primer is engineered to contain a uracil residue close to its 3' terminus (Scheme 1.3) *(164)*. Following primer extension, the extension products are cleaved with uracil DNA glycosylase (UDG) and hot piperidine (95 ^{0}C) to generate shorter oligonucleotides which can be readily sequenced by tandem mass spectrometry (Scheme 1.3).

For the specific template-primer complex shown in Scheme 1.3, 7-mer products are generated when the primer extension is complete. Depending on the specific base incorporated opposite the adduct (**X**) and assuming the enzyme does not make any additional errors while copying beyond the adduct, the sequence of the extension product can be any of the following: 5'p-TC**A**ATGA-3', 5'p-TC**G**ATGA-3', 5'p-TC**C**ATGA-3', or 5'p-TC**T**ATGA-3'. The preliminary identity of the product can be obtained by determining the *m/z* values of the observed oligonucleotide products with full scan HPLC-ESI$^-$ MS. MS/MS spectra of each product are then obtained on an ion trap or triple quadrupole, and are compared to the predicted spectra (Mongo Oligo Mass Calculator v2.06).

The methodology developed by Zang et al. has been successfully used in translesion synthesis studies of several important DNA adducts including 1,N^2-etheno guanine *(160;164)*, malondialdehyde-deoxyguanosine (M1-dG) *(162;168)*, 7-8-dihydro-8-oxodeoxyguanosine *(169;170)*, O^6-benzylguanine *(171;172)*, O^6-methylguanine *(172;173)*, O^6-[4-oxo-4-(3-pyridyl)butyl]guanine (O^6-Pob-G) *(172)*, N^2-alkyl guanine adducts *(174)*, C8- and N^2-deoxyguanosine adducts of the dietary mutagen 2-amino-3-methylimidazo[4,5-f]quinolone *(163)*, N^6-deoxyadenosine-BPDE adducts *(175)*, 2,6-diamino-4-hydroxy-N^5-(methyl)-formamidopyrimidine (MeFapy-dGuo) *(176)*, and 7-(2-oxoheptyl)-1,N^2-etheno-2′-deoxyguanosine *(161)*.

Scheme 1.3 Workflow of primer extension studies using HPLC-MS/MS *(159)*

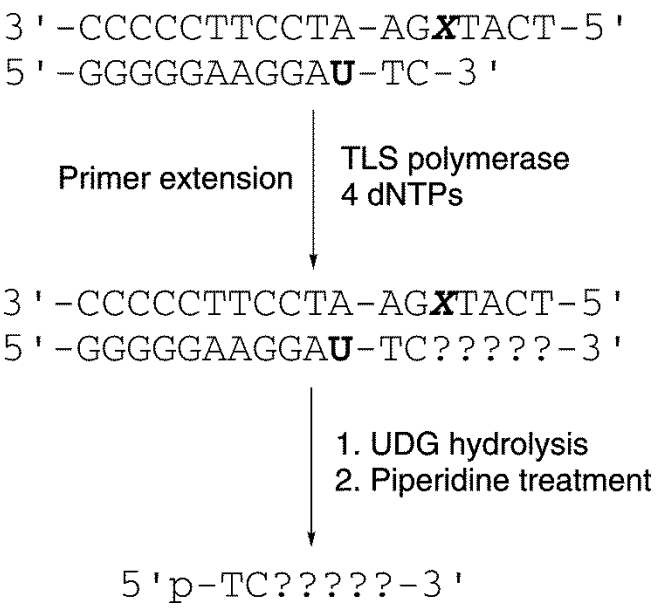

1.5.4 *In vitro* and *in vivo* translesion synthesis past BD-DNA adducts

As already discussed in the previous sections, EB induces GC→AT point mutations and AT→TA transversions while DEB induces AT→TA transversions and partial deletions *(35)*. Lloyd et al. investigated the mutagenic potential of four BD-DNA adducts, *R* and *S* stereoisomers of N^6-(1-hydroxy-3-buten-2-yl)- 2′-deoxyadenosine (N^6-HB-dA II) (formed from EB) and *(R,R)* and *(S,S)* stereoisomers of N^6-THB-dA adduct (formed from DEB) *(177)*. These adducts were site-specifically incorporated onto an 11-mer oligonucleotide strand representing human N-ras codon 61. These 11 mer oligonucleotide strands were further ligated into a single stranded vector M13mp7L2 (*in vivo* studies) or 85-mer oligonucleotide strands (*in-vitro* studies). *In vitro* translesion synthesis experiments were conducted on 85-mer oligonucleotide strands containing one of the four lesions annealed to one of the three γ^{32}P-labeled -5, -2 or +5 primers. The duplexes were then added to the appropriate buffer and further incubated in the presence of *E.Coli* DNA polymerases and dNTPs for specified time points *(177)*. The reaction mixture was quenched and products were separated on 15% sequencing gel and visualized by autoradiography *(177)*. None of the lesions affected DNA replication and were bypassed by *E.Coli* DNA polymerases as evident by the extension of all three primers *(177)*. For *in vivo* studies, M13mp7L2 vector containing the modified adducts were transfected into *E.Coli*. *R* and *S* stereoisomers of N^6-(1-hydroxy-3-buten-2-yl)-2′-deoxyadenosine were not mutagenic (Chart 1.3) but the N^6-THB-dA adducts induced mutations albeit at low frequency. *(R,R)* N^6-THB-dA adducts induced A→G mutations (0.14%), while their stereoisomers *(S,S)* N^6-THB-dA induced A→T mutations (0.25%) (Chart 1.3) *(177)*.

Similar *in vitro* and *in vivo* experiments were also performed by Lloyd et al. to understand the mutagenic ability of *R* and *S* stereoisomers of N^2-(1-hydroxy-3-buten-2-yl)- 2′-deoxyguanosine and *(R,R)* and *(S,S)* stereoisomers of the N^2-THB-dG adduct *(178)*. All four N^2-dG adducts primarily blocked DNA replication by *E.Coli* polymerases and were weakly mutagenic (1%) as they induced G→T, G→A and G→ C mutations (Chart 1.3) *(178)*. In contrast, the N1-deoxyinosine adducts (formed from EB) were highly mutagenic *(179)*. It was observed that the *(S)*- N^6-(1-hydroxy-3-buten-2-yl)- 2′-deoxyinosine adducts induced A→G (80%), A→C (10%) and A→T (8%) mutations (Chart 1.3) *(179)*. *(R)*- N^6-(1-hydroxy-3-buten-2-yl)-2′-deoxyinosine adducts also induced the same mutations but with frequencies of 48, 7 and 4%, respectively *(179)*. N3-(2-hydroxy-3-buten-1-yl)-deoxyuridine adducts formed from alkylytation of Cytosine by EB followed by deamination, were reported to be highly mutagenic (97%) *in vivo (180)*. These adducts induced C→T > C→A > C→G mutations (Chart 1.3) *(180)*.

Lloyd et al. also performed studies with intrastrand 1,4-*bis*-N^2-guanine-2,3-butanediol (N^2G-N^2G) cross-links formed from DEB *(181)*. It was found that these intra strand cross links mostly blocked DNA replication *in vitro* and *in vivo* (Chart 1.3). However, it was also reported that N^2G-N^2G cross links induced a small frequency of G→A transitions, G→T and G→C transversion mutations. Interestingly, the *S,S* steroisomer was observed to be more mutagenic than the *R,R* stereoisomer *(181)*. Additional studies with N^6,N^6-deoxyadenosine intrastrand cross-links formed from DEB revealed that they induced A→G > A→C > A→T mutations (Chart 1.3) *(179)*. The mutation frequency was higher for *R,R* (54%) as compared to *S,S* stereoisomer (20%)

(179). While significant research has been conducted to understand the mutagenic ability of several BD-DNA adducts, the identity of the specific BD-DNA adduct responsible for primarily A→T mutations still needs to be established.

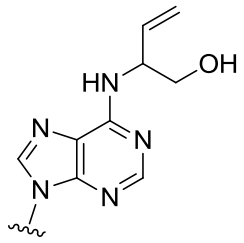

N^6-(1-hydroxy-3-buten-2-yl)-dA

Non-Mutagenic

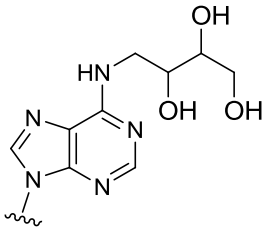

N^6-THB-dA

Weakly mutagenic (A→G, A→T)

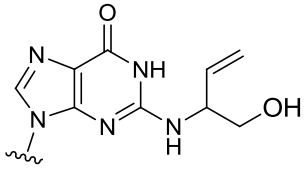

N^2-(1-hydroxy-3-buten-2-yl)-dG

Strongly blocking

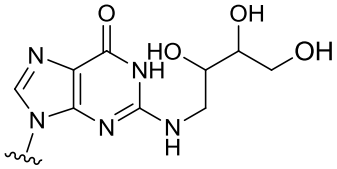

N^2-THB-dG

Strongly blocking

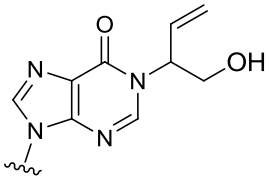

N^6-(1-hydroxy-3-buten-2-yl)-dI

Highly mutagenic (A→G, A→C, A→T)

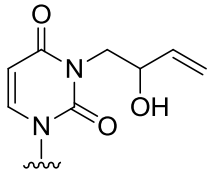

N3-(2-hydroxy-3-buten-1-yl)-dU

Highly mutagenic (C→T, C→A, C→G)

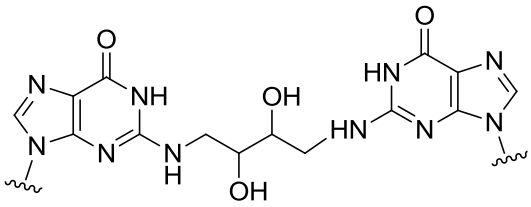

1,4-*bis*-N^2-Guanine-2,3-butanediol

Strongly blocking

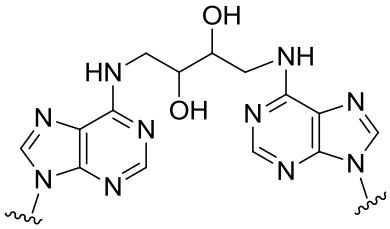

1,4-*bis*-N^6-Adenine-2,3-butanediol

Highly mutagenic (A→G, A→C, A→T)

Chart 1.3 Mutations induced by BD-DNA adducts

1.5.5 Potentially mutagenic BD-dA adducts

EB can alkylate the exocylic N^6 position of adenine to form two different adducts, N^6-(2-hydroxy-3-buten-1-yl)-2′-deoxyadenosine (N^6-HB-dA I) and N^6-(1-hydroxy-3-buten-2-yl)-2′-deoxyadenosine (N^6-HB-dA II) (Scheme 1.4) *(182)*. It is also hypothesized that N^6-HB-dA adducts can be formed by Dimroth rearrangement of N1-EB-dA adducts *(42)*. Koivisto and co-workers observed N^6-HB-dA adducts upon treatment of calf thymus DNA with EB *(52)*. Additionally a linear dose response relationship was observed between N^6-HB-dA adducts and BD exposure in lung DNA of mice and rats exposed to BD *(52)*. Koivisto and coworkers also determined the relative percentages of *in vivo* formation of the two regioisomers N^6-HB-dA I and N^6-HB-dA II to be 31 and 69%, respectively *(183)*. While the N^6-HB-dA II was found to be non mutagenic in *in vitro* and *in vivo* translesion synthesis experiments *(177)*, the mutagenic ability of N^6-HB-dA I was not previously determined *(184)*.

Our laboratory has recently discovered two novel exocyclic BD-dA adducts formed by alkylation of the exocylic N^6 position of adenine by DEB *(48)*. DEB reacts with the exocyclic amine group of adenine to form N^6-2-hydroxy-3,4-epoxybut-1-yl-dA (N^6-HEB-dA) lesions (Scheme 1.4) *(48)*. The epoxy group in the N^6-HEB-dA is highly electrophilic and can undergo nucleophilic attack by another site in the same lesion to form fused ring structures such as N^6,N^6-(2,3-dihydroxybutan-1,4-diyl)-2′-deoxyadenosine (N^6,N^6-DHB-dA) and 1,N^6-(2-hydroxy-3-hydroxymethylpropan-1,3-diyl)-2′-deoxyadenosine (1,N^6-γ-HMHP-dA) (Scheme 1.4) *(48)*. Another BD-dA exocyclic adduct, 1,N^6-(1-hydroxymethyl-2-hydroxypropan-1,3-diyl)-2′-deoxyadenosine

(1,N^6-α-HMHP-dA) can be formed by the alkylation of the N-1 position of adenine to form N1-(2-hydroxy-3,4-epoxybut-1-yl)-adenine adducts followed by spontaneous cyclization *(48)*. 1,N^6-α-HMHP-dA and 1,N^6-γ-HMHP-dA adducts can interconvert under physiological conditions with the former adduct being thermodynamically stable (Scheme 1.4) *(48)*. N^6,N^6-DHB-dA adducts were found in smaller quantities upon treatment of calf thymus DNA with 200 fold excess DEB but they were not detected *in vivo (48)*. 1,N^6-α-HMHP-dA and 1,N^6-γ-HMHP-dA adducts were found in significant quantities *in vitro* and in liver DNA of mice exposed to BD *(48)*. A linear dose response relationship was observed between 1,N^6-HMHP-dA adducts in mouse liver DNA and BD exposure *(67)*. Additionally, it was found that the *in vivo* half life of 1,N^6-HMHP-dA adducts in mouse liver and kidney tissues was 38-42 days *(185)*. N^6,N^6-DHB-dA and 1,N^6-HMHP-dA cannot form the regular Watson Crick base pairing with dT as the N^6 position is blocked and therefore can be promutagenic *(48)*. Since 1,N^6-HMHP-dA adducts persist *in vivo* and are not repaired, and based on structural similarity to 1,N^6-etheno-dA and 1,N^6-ethano-dA, they were hypothesized to be potentially mutagenic *(186)*. Studies focusing on determining the mutagenic ability of N^6,N^6-DHB-dA and 1,N^6-HMHP-dA will be interesting.

Scheme 1.4 Mechanism of formation of exocyclic BD-dA adducts from EB and DEB

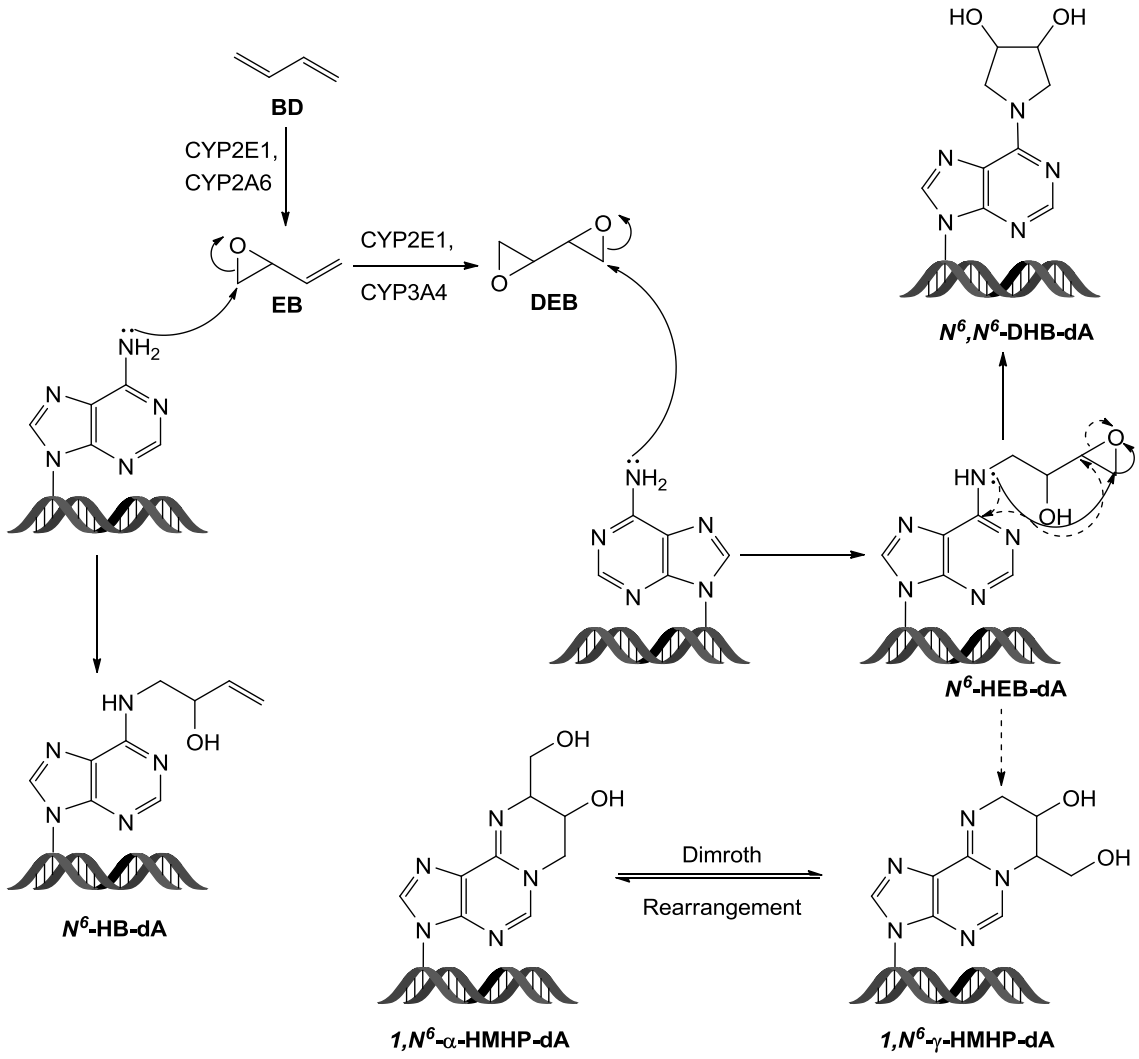

1.6 Summary and thesis goals

BD is a high volume industrial chemical used as a monomer in the production of rubber and plastics. The general population is exposed to BD because of its presence in cigarette smoke and automobile exhaust. Based on studies in laboratory animals and epidemiological studies in workers in the rubber industry, BD is classified as a known human carcinogen. BD is metabolically activated to EB, HMVK, EBD and DEB (Scheme 1.1). These electrophilic metabolites can be detoxified by glutathione conjugation and further metabolic conversion into urinary mercapturic acids: MHBMA, DHBMA, THBMA and *bis*-BDMA, respectively (Scheme 1.1). These BD-urinary metabolites can be used as biomarkers of exposure to BD in human biomonitoring studies. MHBMA and DHBMA have been previously detected in urine of rats exposed to BD, workers occupationally exposed to BD and smokers. However, neither THBMA (formed from EBD, the most abundant BD epoxide) nor *bis*-BDMA (formed from DEB, the most genotoxic BD epoxide) has been detected before. Hence the initial goals of this thesis work were to develop HPLC-MS/MS methods for the quantification of these two novel urinary metabolites of BD *in vivo*.

It is also known that there are significant ethnic/racial differences in susceptibility to smoking associated lung cancer (Tables 1.2 and 1.3). It has been hypothesized that these differences might be due to genetic polymorphisms contributing to differences in metabolic activation and deactivation of carcinogens. Since BD is one of the most abundant and potent carcinogens present in cigarette smoke, it will be interesting to study whether there are any differences in metabolism of BD. Our second goal of this thesis

work was to develop a high throughput HPLC-MS/MS method for quantification of MHBMA and DHBMA in human urine and apply this method to urine samples of smokers belonging to two different multi-ethnic cohort studies to identify ethnic differences in BD metabolism.

EB and DEB induce a large number of A→T mutations. However, the identity of the BD-dA lesions responsible for these mutations remains to be established. The mutagenic ability of N^6-HB-dA formed from EB, N^6,N^6-DHB-dA and 1,N^6-HMHP-dA formed from DEB (Scheme 1.4) has not been evaluated before. Hence the final goal of this research was to conduct *in vitro* translesion synthesis studies on synthetic oligonucleotide strands containing these lesions at a site-specific position in the presence of human TLS polymerases.

II. QUANTITATIVE ANALYSIS OF TRIHYDROXYBUTYL MERCAPTURIC ACID, A URINARY METABOLITE OF 1,3-BUTADIENE, IN HUMANS

Reprinted with permission from: Srikanth Kotapati, Brock A. Matter, Amy L. Grant, and Natalia Y. Tretyakova. *Chem. Res. Toxicol.* (2011) 24, 1516-1526.

2.1 Introduction

1,3-Butadiene (BD) is a colorless gas with a gasoline-like odor that is widely used in the polymer industry for the production of rubber and plastics *(18)*. BD is a multi-site carcinogen in laboratory animals, capable of inducing lymphocytic lymphoma and neoplasms of the heart, forestomach, Harderian gland, mammary gland, ovary, liver, and the lung *(16)*. Based on epidemiological evidence for an increased risk of leukemia in occupationally exposed workers *(23;24;187)*, BD is classified as a "known human carcinogen" in the Ninth Report on Carcinogens (2000) by the US National Toxicology Program *(18)* and is categorized as a "human carcinogen" by the US EPA and IARC *(26)*. BD is also present in automobile exhaust, urban air, and is abundant in cigarette smoke (16-75 μg in main- stream smoke and 205-361 μg in side-stream smoke) *(19)*, leading to widespread exposure of the general population. Toxicological risk analysis suggests that BD has the highest cancer risk index among all tobacco constituents *(25)*, necessitating further studies of its mechanism of action.

The genotoxic effects of BD are attributed to its epoxide metabolites *(16;188)*. Cytochrome P450 monooxygenases P450 2E1 and P450 2A6 catalyze the initial epoxidation of BD to yield *(R)*- and *(S)*-3,4-epoxy-1-butene (EB) (Scheme 1.1) *(27;28)*. EB can be hydrolyzed to 1-butene-3,4-diol (EB-diol) *(30)*, which can be further oxidized to form 3,4-epoxy-1,2-butanediol (EBD) *(189)* or can undergo further metabolism to

hydroxymethyl vinylketone (HMVK) *(32)*. Alternatively, EB can be subject to second oxidation catalyzed by cytochrome P450 2E1 and 3A to yield *S,S, R,R,* and *meso*-diepoxybutane (DEB) *(27;29)*.

All three epoxides of BD, e.g. EB, DEB, and EBD, are direct-acting mutagens, with DEB exhibiting the most potent genotoxicity *(34;188)*. If not detoxified by epoxide hydrolysis or glutathione conjugation, they can react with nucleophilic sites in DNA and proteins to form covalent adducts *(41;44;47;190)*. DNA adducts induced by BD exposure include N-7-(2-hydroxy-3-buten-1-yl)guanine, N-7-(1-hydroxy-3-buten-2-yl)guanine, N-7-(2,3,4-trihydroxy-3-buten-2-yl)guanine *(191)*, 1,4-*bis*-(guan-7-yl)-2,3,-butanediol (*bis*-N7G-BD) *(46;64)*, 1-(guan-7-yl)-4-(aden-1-yl)-2,3-butanediol (N7G-N1A-BD), 1-(guan-7-yl)-4-(aden-3-yl)-2,3-butanediol(N7G-N3A-BD), and 1-(guan-7-yl)-4-(aden-7-yl)-2,3-butanediol (N7G-N7A-BD) *(46)*. Several BD-induced hemoglobin adducts have been identified, e.g. *N*-(2-hydroxy-3-buten-1-yl)-valine (HB-Val), 1,2,3-trihydroxybutyl-valine (THB-Val), and *N,N*-(2,3-dihydroxy-1,4-butadiyl)-valine (*pyr*-Val) *(80;84)*. DEB also induces DNA-protein cross-links that are hypothesized to interfere with DNA replication, transcription, and repair *(192;193)*.

BD is a potent carcinogen in mice *(20)*, but is only a weak carcinogen in rats, requiring 300-fold higher concentrations to achieve the same tumor numbers *(21)*. This can be explained by more efficient metabolic activation of butadiene to EB, DEB, and EBD, and an inefficient detoxification of butadiene epoxides in the mouse *(113;194;195)*. Indeed, the concentrations of butadiene-induced DNA and protein

adducts are greater in tissues of mice than in rats exposed to the same butadiene concentration *(60;66;77;196;197)*.

BD metabolites are excreted in urine as mercapturic acids. Glutathione conjugates of EB are processed *via* the mercapturic acid pathway to yield 2-(*N*-acetyl-L-cystein-S-yl)-1-hydroxybut-3-ene and 1-(*N*-acetyl-L-cystein-S-yl)-2-hydroxybut-3-ene, collectively called MHBMA (Scheme 1.1) *(31;95)*. HMVK undergoes glutathione conjugation followed by reduction and is excreted as 4-(*N*-acetyl-L-cystein-S-yl)-1,2-dihydroxybutane (DHBMA) *(32;33)*. EBD undergoes similar glutathione conjugation and metabolic conversion to form another mercapturic acid, 4-(*N*-acetyl-L-cystein-S-yl)-1,2,3-trihydroxybutane (THBMA) *(31;93)*. *N*-acetylcysteine conjugates of EB (MHBMA in Scheme 1.1), HMVK (DHBMA), and EBD (THBMA) can serve as useful indicators of BD exposure and genotoxicity in smokers and occupationally exposed individuals, allowing for human bio-monitoring and risk assessment from BD exposure *(31;33;95;99;105)*.

While MHBMA and DHBMA have been found in smokers and non-smokers, to our knowledge, THBMA has not been previously detected in humans. THBMA has been found in urine of rats and mice exposed to 200 ppm of radiolabeled ^{14}C-1,3-BD for 6 hours. THBMA accounted for about 4.1% and 6.7% of the total BD dose in the rat and in mice, respectively *(93)*. Van Sittert et al. *(31)* have attempted to quantify the amounts of THBMA in human urine by a GC-NECI-MS/MS method. In their approach, THBMA was isolated from smoker's urine (1 mL) by strong anion exchange SPE and derivatized

with pentafluorobenzyl bromide, followed by GC-NECI-MS/MS analysis. However, THBMA could not be quantified due to high interferences from sample matrix *(31)*.

The goal of the present study was to develop a sensitive, accurate and reliable isotope dilution HPLC-ESI$^-$-MS/MS method for quantification of THBMA in human urine and evaluate its potential as a biomarker of exposure to BD in cigarette smoke and its metabolism to DNA-reactive species. The novel method was employed to determine the concentrations of THBMA in urine of current smokers and non-smokers and to analyze the effects of smoking cessation on THBMA levels.

2.2 Materials and Methods

Materials. HPLC-MS grade acetic acid, methanol, acetonitrile, and *d,l* DEB were purchased from Sigma Aldrich (St. Louis, MO). HPLC grade acetonitrile and methanol were obtained from Fisher Scientific (Pittsburgh, PA). THBMA and its deuterated analog, d_3-THBMA, were synthesized in our laboratory as described below. d_3-*N*-acetyl-L- cysteine was purchased from Toronto Research Chemicals (Ontario, Canada). Isolute ENV+ 50 mg/1 mL SPE cartridges were purchased from Biotage (Charlotte, NC). All other materials and solvents were from Sigma-Aldrich (St. Louis, MO)

Synthesis of 4-(N-acetyl-L-cystein-S-yl)-1,2,3-trihydroxybutane (THBMA) and its deuterated analogue (d_3-THBMA). THBMA and d_3-THBMA were prepared as shown in Scheme 2.1. *N*-acetyl-L-cysteine (338 mg, 2 mmol) was dissolved in 1 mL of water. Racemic DEB (155 µL, 2 mmol) was added, followed by mixing and incubation at 65°C for 72 h. THBMA was isolated by semi-preparative HPLC. HPLC purification was performed on an Agilent 1100 HPLC system equipped with a DAD UV detector

(Agilent Technologies, Santa Clara, CA) on an Agilent Eclipse XDB C18 column (10 mm x 250 mm; 5 µm). The buffer system consisted of 5 mM *N, N,* dimethylhexylamine adjusted to pH 9.2 with acetic acid (A) and 25:56.25:18.75 5 mM *N, N,* dimethylhexylamine (pH 9.2):methanol:acetonitrile. The flow rate was 3 mL/min, and the solvent composition was changed linearly from 1 to 13% (B) in the first 12 min. The gradient was ramped up to 50% (B) in the next 2 minutes and held at that composition for 3 minutes. The solvent composition was brought back to the initial composition of 1% (B) in the next three minutes and equilibrated at those conditions for 12 minutes. THBMA eluted as a broad peak at 14 minutes.

HPLC fractions containing THBMA were collected, concentrated under vacuum, and re-purified with the same column and solvent system with a slower gradient. For the second round of purification, the flow rate was 3 mL/min, and the solvent composition was linearly changed from 8 to 30% (B) in 20 minutes. The system was brought back to 8% (B) in 1 min and equilibrated at these conditions for 11 min. Under these conditions, THBMA eluted at 10.5 min. HPLC peaks corresponding to THBMA were collected and concentrated under vacuum (estimated reaction yield, 1%). d_3-THBMA was synthesized analogously starting with *N*-acetyl- d_3- L- cysteine (Scheme 2.1). The isotopic purity of d_3-THBMA as determined by HPLC-ESI-MS/MS was 99.7%.

Scheme 2.1 Synthesis of THBMA and d_3-THBMA

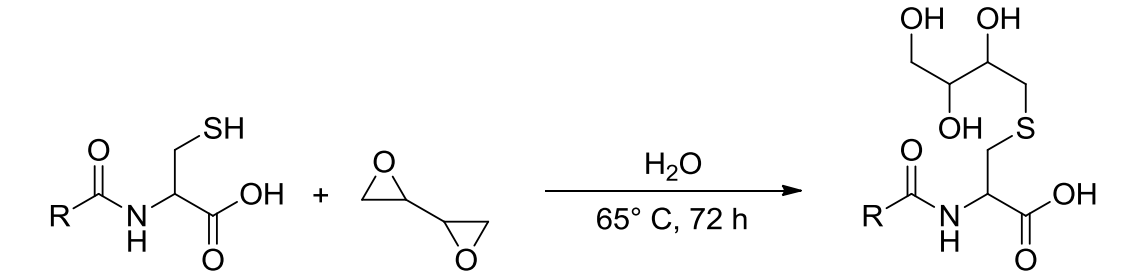

N-acetyl-L-cysteine or
d_3-*N*-acetyl-L-cysteine

DEB

R= CH_3 or CD_3

THBMA or d_3-THBMA

THBMA and d_3-THBMA (Scheme 2.1) were structurally characterized by high resolution tandem mass spectrometry on Waters Acquity UPLC/Synapt G2 QTOF mass spectrometer and NMR. The HPLC conditions for accurate mass measurements included a Waters Acquity UPLC HSS T3 column (2.1 x 100, 1.8µ) eluted at a flow rate of 0.4 ml/min using 97:3 0.1% formic acid in water: 0.1% formic in ACN as the mobile phase. The sample was introduced into the mass spectrometer using "Lockspray" dual electrospray ion source (leucine-enkephalin as calibrant) and analyzed in the negative ionization mode with a *m/z* scan range of 50-1500. MS/MS fragmentation patterns were as follows: THBMA (ESI-MS : 266.0698 $[M-H]^-$, MS/MS: 137.0348, 128.0423 and 119.0233); d_3-THBMA (ESI-MS : 269.0882 $[M-H]^-$, MS/MS: 137.0342, 131.0602, 119.0228) (Figure 2.1). ^{1}H NMR of THBMA: δ 7.9 (1H, s, cys-NH), 4.2 (1H, m, αC-cys), 3.5-3.3 (4H, m, OCH_2, OCH), 2.9-2.5 (4H, m, SCH_2), 1.8 (3H, s, $COCH_3$) (Figure 2.2).

THBMA stock solution concentrations were determined by proton NMR. Toluene (1.12 µmol) was added to THBMA standard dissolved in DMSO (Figure 2.2). The ratio of ^{1}H NMR integrations corresponding to aromatic protons of toluene (5H, 7.2 ppm) and a C-H proton of THBMA (1H, 4.2 ppm) was used to determine THBMA concentration (Figure 2.2). d_3-THBMA concentrations were determined by capillary HPLC-UV using THBMA as an external standard and confirmed by HPLC-ESI-MS/MS analysis of solutions spiked with known amounts of unlabeled THBMA.

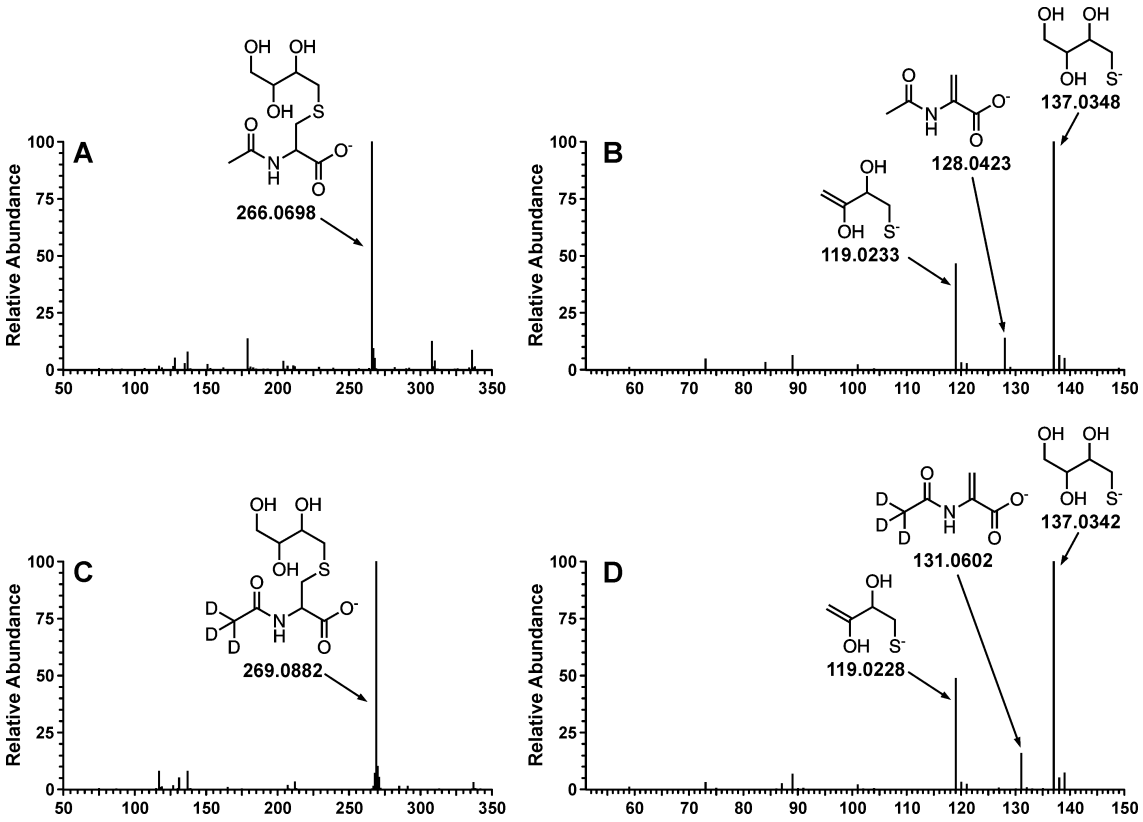

Figure 2.1 UPLC-ESI$^-$-TOF-MS/MS spectra of THBMA and d_3-THBMA (B)

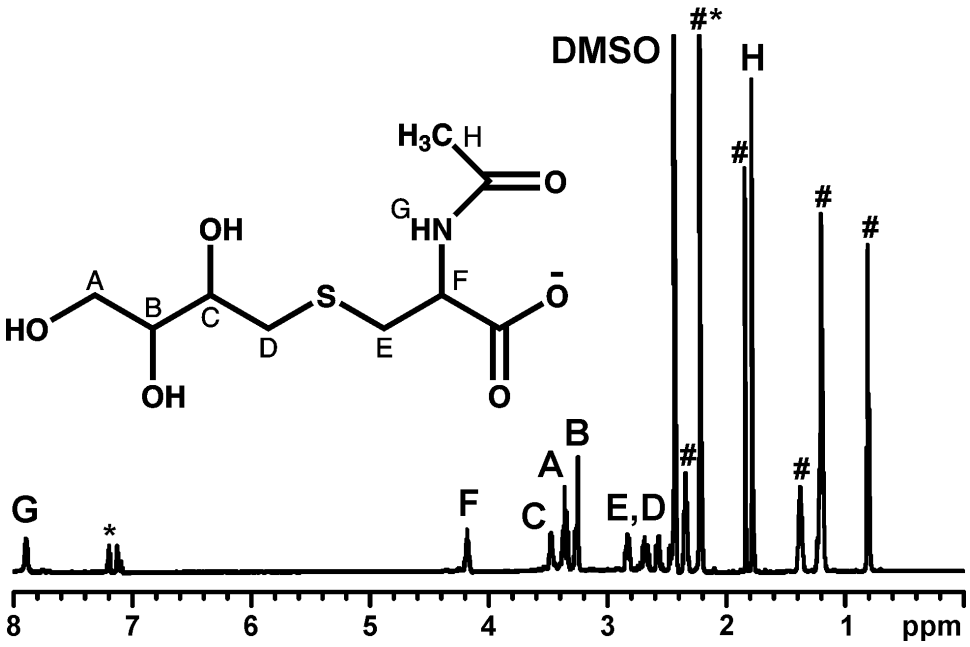

Figure 2.2 ^{1}H NMR spectrum of THBMA

Toluene* was added as an internal standard for quantification. (Residual *N, N*-dimethylhexylamine$^{\#}$ from HPLC purification is observed).

Sample Preparation. Solid phase extraction (SPE) was performed using Isolute ENV+ cartridges (1 mL / 50 mg) obtained from Biotage (Charlotte, NC, USA). Human urine (100 µL) was mixed with 100 µL of 50 mM ammonium formate buffer (pH 2.5), 10 µL of formic acid (98%), and 60 ng of d_3-THBMA. Samples were vortexed repeatedly and centrifuged at 13,000 rpm for 15 minutes. The supernatant was loaded onto SPE cartridges pre-conditioned with methanol and 0.3% formic acid (3 ml each). The cartridges were sequentially washed with 1.5 mL of 0.3% formic acid and 0.75 mL of 5% aqueous methanol containing 0.3% formic acid and allowed to dry completely under vacuum for 20 minutes. THBMA and d_3-THBMA were eluted with 1.2 mL of 2% formic acid in methanol, dried under vacuum, and reconstituted with 20 µL of 0.2% acetic acid for HPLC-ESI-MS/MS analysis.

Liquid chromatography-Tandem Mass spectrometry. HPLC-ESI$^-$-MS/MS analysis was conducted on an Agilent 1100 HPLC system (Agilent Technologies, Santa Clara, CA) coupled with a Thermo-Finnigan TSQ Quantum Discovery mass spectrometer (Thermo Scientific Corp., Waltham, MA). A SIELC Primesep B2 column (5 µm, 2.1 x 50 mm) was equipped with a guard column of the same packing (5 µm, 2.1 x 10 mm). The column was maintained at 50° C and eluted with a gradient of 0.2% acetic acid (A) and acetonitrile (B) at a flow rate of 150 µl/min. The solvent composition was maintained at 1% B for the first six minutes and then increased to 50% B in the next three minutes. The column was eluted with 50% B for three more minutes, and the solvent composition was brought back to the initial conditions of 1% B in the next three minutes. The column was equilibrated at 1% B for 10 minutes before a new injection was made. Under these

conditions, THBMA and d_3-THBMA eluted at 5.12 and 5.18 minutes, respectively. The total HPLC-ESI$^-$-MS/MS run time was 25 minutes.

The mass spectrometer was operated in the ESI$^-$ mode, and typical MS settings were as follows: spray voltage, - 3500 V; sheath gas pressure, 50 psi; capillary temperature, 250° C; collision energy, 16; source CID, -9 V; collision gas pressure, 1.0 mTorr; Q1 (FWHM), 0.4; Q3 (FWHM), 0.7; scan width , 0.4 *m/z*; and scan time, 0.4 s. The mass spectrometer settings were optimized upon direct infusion of authentic standards and may vary slightly between analyses. Quantification of THBMA was performed in the selected reaction monitoring (SRM) mode by isotope dilution with d_3-THBMA. The SRM transitions used for quantitation were: *m/z* 266.1 → 137.1 (THBMA) and *m/z* 269.1 → 137.1 (d_3-THBMA). An additional SRM transition (*m/z* 266.1 → 128.1 for THBMA and 269.1→131.1 for d_3-THBMA) was used to confirm the identity of the THBMA peak.

Calibration curves were constructed by injecting standard solutions containing fixed amount of d_3-THBMA (25 ng) and varying amounts of THBMA (0.05, 0.25, 0.5, 1, 1.5, 2.5, 5 and 12.5 ng), in triplicate (on column). Regression analyses were conducted to determine the correlation between the theoretical molar ratio and the HPLC-ESI$^-$-MS/MS response ratio (ratio of THBMA and d_3-THBMA peak areas).

Method Validation. Eight validation standards were prepared by spiking non-smoker urine (100 μL) with increasing amounts of THBMA (0.1, 0.5, 1, 2, 3, 5, 10 and 25 ng) and a fixed amount of d_3-THBMA (50 ng), in triplicate. These samples were

processed by SPE and analyzed by HPLC-ESI$^-$-MS/MS as described above. Regression analysis was conducted to compare the measured and the theoretical THBMA amounts.

Determination of LOD/LOQ. Artificial urine (100 μL) was spiked with 100, 50, 25 or 10 pg of THBMA and 60 ng of d_3-THBMA, and the samples were processed by SPE and analyzed by HPLC-ESI$^-$-MS/MS as described above. The limit of quantification (LOQ) was estimated as the amount of analyte which gave the signal to noise ratio (S/N) greater than 10 (Thermo Xcalibur, ICIS algorithm) and % CV < 15%. Limit of Detection (LOD) was determined as the amount of analyte which produced the signal to noise ratio > 3.

Precision and Accuracy. To determine the intraday and interday precision and accuracy of the new method, artificial urine (100 μL) was spiked with 1, 3, or 6 ng of THBMA and 60 ng of d_3-THBMA. The samples were subjected to SPE as described above and analyzed by HPLC-ESI$^-$-MS/MS three times per day on three consecutive days.

Extraction Recovery. Extraction recovery was determined by analyzing blank urine samples spiked with 2 ng of THBMA prior to SPE and 60 ng of internal standard post-extraction (n = 3) and the same urine sample spiked with both the analyte and the internal standard post SPE (n = 3).

Freeze-thaw stability. Stock solutions containing either 5 ng/ml or 30 ng/ml of THBMA were analyzed before and after three freeze-thaw cycles. The solutions were stored at - 20^0 C for 23 hours and thawed for 1 hour at room temperature, after which a

fixed amount of internal standard (60 ng) was added, and the mixture was analyzed by HPLC-ESI$^-$-MS/MS using standard methods. This procedure was repeated for 3 days.

A similar procedure was used to assess analyte stability in urine. Blank human urine sample (1 ml) was spiked with 5 ng or 30 ng of THBMA standard. The spiked urine samples were stored at -20^0 C for 23 hours and thawed for 1 hour at room temperature. Three 100 μL aliquots from each of the tubes were drawn and following the addition of d_3-THBMA internal standard and SPE cleanup, HPLC-ESI$^-$-MS/MS was used to quantify THBMA. The procedure was repeated for 3 consecutive days.

Matrix effects. Urine samples from a confirmed non-smoker and a confirmed smoker (100 μl each) were processed by SPE and spiked with THBMA (2 ng) and d_3-THBMA (60 ng), followed by HPLC-ESI$^-$-MS/MS analysis. HPLC-ESI$^-$-MS/MS peak areas were compared for spiked samples and pure standard mixtures containing 2 ng of THBMA and 60 ng of internal standard to identify any potential analyte suppression by the biological matrix.

Human Urine Samples. Urine samples from confirmed smokers (N = 27) and non-smokers (N = 19) were obtained from the University of Minnesota Tobacco Research Programs and stored at - 20° C. Urine samples (100 μL) were processed by SPE and analyzed by HPLC-ESI$^-$-MS/MS methods as described above. THBMA amounts were normalized to creatinine, which was determined with the VITROS CREA kit and VITROS 350 system (Ortho-clinical Diagnostics, Rochester, New York).

Smoking cessation samples were obtained from the previously described study.[40] In brief, 5 smokers from Minneapolis were asked to continue smoking for 2 weeks

(baseline) and 24 hour urine samples were collected 14 and 7 days *prior* to smoking cessation. Following a two-week baseline period, the smokers were asked to quit smoking. Urine samples were collected on days 3, 28 and 56 post smoking cessation and analyzed by HPLC-ESI$^-$-MS/MS as described above.

Statistical Analysis. Method calibration and validation curves were constructed in Microsoft Excel. Linear regression analysis was performed and residual plots were constructed to determine the homogeneity of the error. An unpaired t test was compiled to look at the differences in levels of THBMA between smokers and non-smokers. A *p*-value < 0.01 was considered statistically significant.

2.3 Results

2.3.1 Synthesis and structural characterization of THBMA

Authentic THBMA and its deuterated internal standard (d_3-THBMA) were synthesized by reacting *N*-acetyl-L- cysteine and d_3-*N*-acetyl-L-cysteine, respectively, with commercial *d,l* DEB (Scheme 2.1). Although multiple stereoisomers of THBMA are possible, they were not resolved by our HPLC methods, and both standards were isolated as racemic mixtures.

The structural identities of THBMA and d_3-THBMA were confirmed by high resolution mass spectrometry, tandem mass spectrometry, and proton NMR spectroscopy (Figures 2.1, 2.2). Accurate masses of THBMA and d_3-THBMA as determined by Q-TOF MS (*m/z* 266.0698 and 269.0882; M-H) (Figures 2.1A, 2.1C) were consistent with the theoretical values (*m/z* 266.0698 and 269.0887, respectively). Tandem mass spectrometry analysis of THBMA (*m/z* 266.0827 $(M-H)^-$) generated product ions at

137.0348 (2,3,4-trihydroxybutane-1-thiolate formed following the C-S bond cleavage), 128.0423 (2-acetamidoacrylate, the other fragment formed as a result of C-S bond cleavage) and 119.0233 (the loss of water from 2,3,4-trihydroxybutane-1-thiolate) (Figure 2.1B). The corresponding ions for d_3-THBMA were observed at *m/z* 269.0997 $(M-H)^-$, 137.0342, 131.0602 and 119.0228 (Figure 2.1D) and were consistent with theoretical values. The isotopic purity of d_3-THBMA standard was 99.7%.

2.3.2 SPE Method Development for THBMA

THBMA is a highly polar metabolite that is not well retained on reverse phase HPLC stationary phases, complicating SPE method development. Due to the presence of a carboxylic acid functionality in its structure (pKa = 3.5), THBMA can potentially be retained *via* the anion exchange mechanism. Several types of SPE packing have been tested for solid phase extraction of THBMA from human urine, including reversed phase (Strata X, Bond Elut C18), weak anion exchange (Strata X-AW), strong anion exchange (Isolute SAX, Baker SAX, Agilent SAX), and mixed mode reversed phase/anion exchange (Oasis MAX, Oasis HLB), but the recoveries were insufficient (below 5%). The best results were achieved with ENV+ cartridges (Biotage), which are packed with a stationary phase composed of highly cross-linked hydroxylated polystyrene divinylbenzene copolymer. Since analyte retention on this packing is primarily due to hydrophobic interactions between the analyte and the stationary phase, samples were loaded under acidic conditions (formic acid) to neutralize the carboxylate group of THBMA, resulting in stronger binding of the analyte to the stationary phase. ENV+ cartridges have been previously employed by Eckert et al. for solid phase extraction of

six hydroxylalkyl mercapturic acids, including MHBMA and DHBMA, from human urine *(107)*. The published method *(107)* was modified to enable the isolation of THBMA, which has a greater polarity than the other two BD-mercapturic acids due to the presence of an additional hydroxyl group (Scheme 1.1). Small SPE cartridges (1 mL, 50 mg) were employed for processing 100 μL urine samples. Our optimized SPE method has an estimated recovery of 54.5% (Table 2.1).

2.3.3 HPLC-ESI-MS/MS Method Development

As discussed above, the ESI^- MS/MS spectrum of THBMA is characterized by the main product ion at *m/z* 137.0348 corresponding to C-S bond cleavage and the formation of trihydroxybutyl thiolate anion (Figure 2.1A). The second most abundant fragment (*m/z* 128.0423) corresponds to other half of the molecule following C-S bond cleavage and negative charge retention on the carboxylate functionality. The d_3-THBMA internal standard produces analogous fragments at *m/z* 137.0342 and 131.0602 (Figure 2.1B). Similar fragments are observed with a triple quadrupole mass spectrometer (results not shown). Our selected reaction monitoring method is therefore based on the transitions 266.1 → 137.1 (THBMA) and 269.1 → 137.1 (d_3-THBMA). The secondary fragmentation pathway 266.1 → 128.1 (THBMA) and 269.1 → 131.1 (d_3-THBMA) was used for confirmation purposes (see below).

HPLC-ESI-MS/MS method development for THBMA was complicated by its poor retention on standard HPLC columns and ESI^- signal suppression due to the presence of other polar compounds in human urine samples. Our initial method employed a capillary Thermo Hypercarb column. Although excellent sensitivity was achieved for

pure standards, this method was not robust when analyzing multiple urine samples due to a sample-dependent retention time shift, complicating peak identification (results not shown). Therefore, a different HPLC method was sought.

Multiple HPLC columns were evaluated, including Thermo BetaMax Acid (2.1 x 50 mm), Waters Xterra MS C18 (4.6 x 50 mm), and Synergi Hydro RP (2.1 x 100 mm). The best results were achieved with the Primesep B2 column (SIELC), a mixed mode column containing C12 alkyl chains and weak anion exchange groups. Various solvent combinations, flow rates, and temperatures were evaluated in an effort to achieve good analyte retention, baseline resolution of the THBMA peaks from matrix components, and improved HPLC peak shape. Solvent composition consisting of 0.2% acetic acid (A) and acetonitrile (B) proved to be very efficient, and a temperature of 50° C was necessary to successfully resolve THBMA from the interfering matrix peaks (see below). THBMA was eluted at 1% of acetonitrile. This is not uncommon as many of the researchers including Boettcher et al. *(198)* reported the use of low percentages of organic solvents to achieve efficient separation of polar metabolites. Under our optimized conditions, THBMA and d_3-THBMA have a similar retention time (5.0-5.2 min) and are resolved from the impurities present in human urine (see below). The total HPLC-ESI$^-$-MS/MS run time is 25 minutes to allow for efficient column cleaning and equilibration prior to the next injection.

2.3.4 Method Validation

Calibration curves covering a broad THBMA concentration range were constructed by analyzing standard solutions containing fixed amounts of d_3-THBMA (50

ng) and increasing amounts of THBMA (0.1-25 ng) (8 points) and plotting the ratios of the observed HPLC-ESI-MS/MS peak areas against the theoretical THBMA/ d_3-THBMA molar ratios. A linear curve with a slope of 1 and an R^2 value > 0.99 was obtained (Figure 2.3). The LOQ value for pure THBMA standard was less than 1 pg (on column).

The HPLC-ESI$^-$-MS/MS method was validated by analyzing non-smoker urine (100 μL) spiked with known amounts of THBMA (8 concentrations, 0.1-25 ng) and d_3-THBMA (50 ng). Spiked samples were processed by SPE and analyzed by HPLC-ESI$^-$-MS/MS as described above. The results were plotted as the amount of THBMA spiked versus the amount measured by HPLC-ESI$^-$-MS/MS. The resulting method validation curve (Figure 2.4) has a slope of 0.98 and an R^2 > 0.99, confirming that THBMA can be accurately quantified in human urine. The y-intercept of the validation curve is 1.54, corresponding to ~15.4 ng/mL of THBMA present in non-smoker urine (see below). Linear regression analysis *(199)* showed that the error was homogenous (homoscedasticity), and hence no weighing factor was applied for plotting the validation curve.

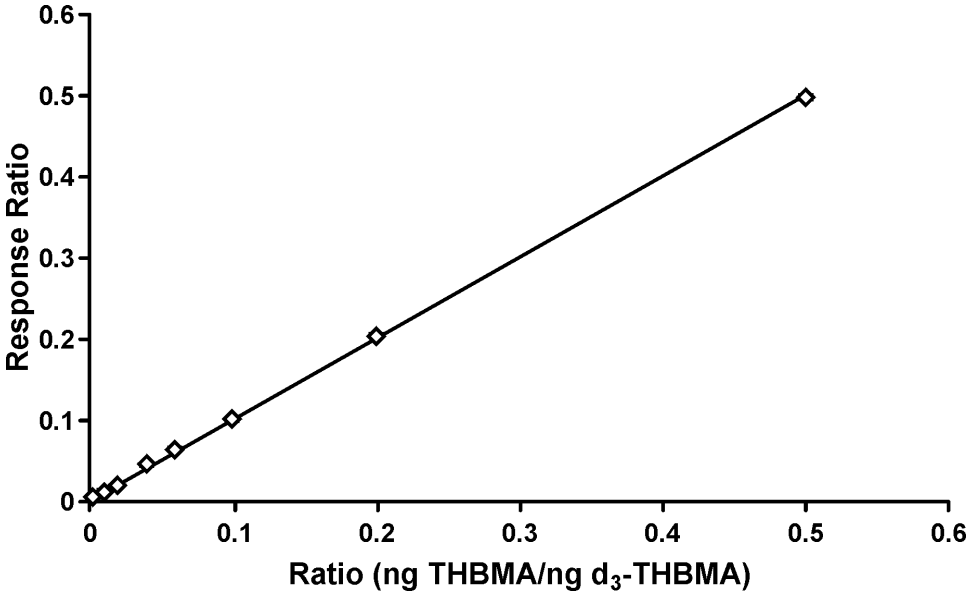

Figure 2.3 Standard curve for HPLC-ESI$^-$-MS/MS analysis of THBMA

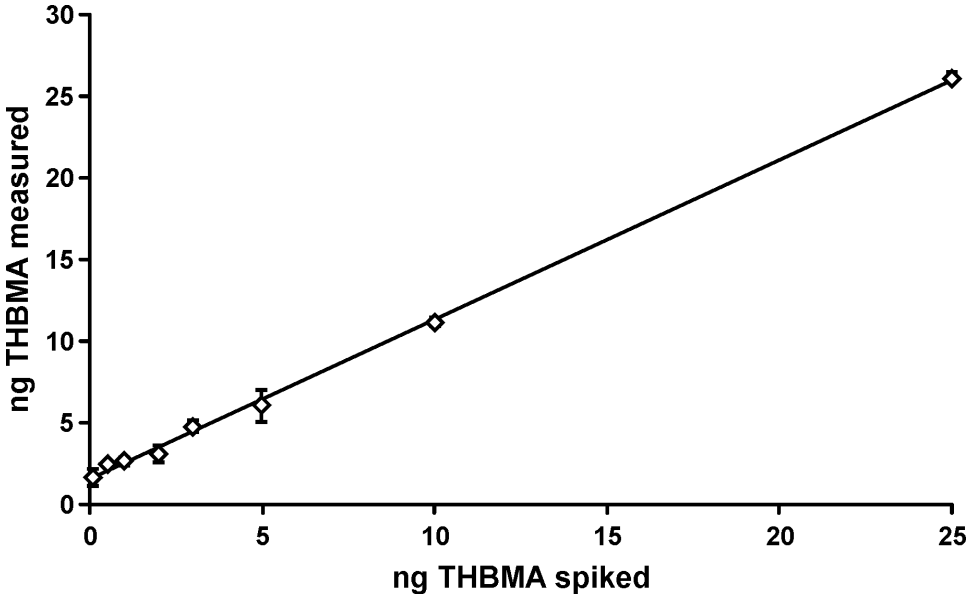

Figure 2.4 Method validation curve for THBMA spiked in non-smoker urine

2.3.5 Linearity, limits of detection, and extraction recovery

The linearity of the HPLC-ESI$^-$-MS/MS method for THBMA has been demonstrated over a broad range of concentrations (1 to 250 ng/ml) (Figure 2.4). To determine the sensitivity of the method, artificial urine (100 μL) was spiked with 10-100 pg of THBMA. Artificial urine was used due to the presence of THBMA in urine of both smokers and non-smokers (see above). The spiked samples were processed by standard methods and analyzed by HPLC- ESI$^-$-MS/MS. Based on the signal to noise ratio > 10 and % CV < 15%, the LOQ was found to be 1 ng/mL urine (Table 2.1). The LOD for the HPLC- ESI$^-$-MS/MS assay was estimated to be as 0.1 ng/mL urine (S/N > 3). The optimized extraction recovery was determined to be ~ 54.5% due to the polar nature of the analyte (Table 2.1).

2.3.6 Precision and Accuracy

The precision and accuracy of our HPLC-ESI$^-$-MS/MS assay were determined using artificial urine (100 μL) spiked with 1, 3, or 6 ng of THBMA. The samples were analyzed in triplicate on three consecutive days. The mean accuracy for THBMA was 85-115% at all the three concentration levels, while the intra-day and inter-day precision was < 15%. The precision and accuracy data for THBMA are reported in Table 2.2

Table 2.1 Analytical detection limits and extraction recovery for HPLC-ESI⁻-MS/MS analysis of THBMA

Analyte	Range (ng/mL)	LOD (ng/mL)	LOQ (ng/mL)	Extraction Recovery (%)
THBMA	1.0-250	< 0.1	1.0	54.5

Table 2.2 Precision and accuracy data for HPLC-ESI$^-$-MS/MS analysis of THBMA

Concentration (ng/ml)	Intraday Precision RSD (%)	Interday Precision RSD (%)	Accuracy (%)
10	4.58	4.87	101.73 ± 4.75
30	6.55	7.85	106.67 ± 6.16
60	0.88	1.63	102.42 ± 1.67

2.3.7 Freeze-thaw Stability and matrix effects

Stability experiments determined that THBMA concentrations were essentially unchanged upon several freeze-thaw cycles, both in stock solutions and in spiked human urine. Analyte losses were < 3% over three freeze-thaw cycles at concentration levels of 5 ng/ml and 30 ng/ml.

A direct comparison of HPLC-ESI$^-$-MS/MS peak areas corresponding to pure THBMA in buffer and THBMA mixed with SPE-processed human urine (smoker or non-smoker, 100 µl) revealed no significant signal suppression by the matrix, with peak areas remaining within 5% of the original value.

2.3.8 Quantification of THBMA in urine from smokers and nonsmokers

To determine the relationship between smoking and urinary THBMA concentrations, urine samples from 27 confirmed smokers and 19 non-smokers (100 µL) were analyzed. Representative HPLC-ESI$^-$-MS/MS extracted ion chromatograms are shown in Figure 2.5 Interestingly, the HPLC-ESI-MS/MS retention time of THBMA was reproducibly 0.05-0.06 minutes shorter than that of the d_3-internal standard. This is unusual since the non-deuterated compound is expected to have the same retention time as its non-deuterated analog or elute slightly later due to stronger van der Waals interactions between the C-H bonds and the stationary phase as compared to the C-D bonds *(200)*. To confirm that the peak of interest indeed corresponded to THBMA, sample was spiked with 6 ng/mL of authentic THBMA and re-analyzed. HPLC-ESI-MS/MS analysis confirmed that authentic THBMA co-eluted with the peak observed in

human samples, which was accompanied by proportional increase in the HPLC-ESI-MS/MS peak area corresponding to concentration increase by 6 ng/mL.

To obtain additional evidence for the presence of THBMA in human urine, the same sample was re-analyzed on a different HPLC column, Primesep D (2.1 x 100 mm) using a pH gradient method comprising of 0.5% acetic acid and 15 mM ammonium acetate in methanol. Similar results were obtained, with THBMA peak eluting 0.05 min before its deuterated standard. The calculated amounts of THBMA were the same for the sample analyzed by two different HPLC-ESI-MS/MS methods.

Finally, a sample obtained from a larger volume of urine (500 μL) was analyzed in the product ion scan mode to reveal additional MS/MS fragments. These experiments revealed that the THBMA peak present in human samples produced fragment ions at *m/z* 137.1, 128.1, and 119.1, which are consistent with the structure of THBMA (Figure 2.1). SRM analysis with two transitions (266.1→137.1 and 266.1→128.1) revealed HPLC-ESI-MS/MS peaks in both ion channels. THBMA amounts calculated with the two SRM transitions were identical, further confirming the identity of the peak observed in human urine sample.

The new method was then employed to determine the effects of smoking on urinary THBMA concentrations. A box plot showing the creatinine-corrected THBMA concentrations in urine of non-smokers (N = 19) and smokers (N = 27) is shown in Figure 2.6. Smokers contained significantly higher concentrations of THBMA than non-smokers (21.6 ± 10.2 versus 13.7 ± 7.9 ng THBMA/mg creatinine; $p < 0.01$ using unpaired two-sample t-test). Importantly, THBMA concentration varied widely within

each group (11.3 to 47.2 ng/mg creatinine in smokers, and 2.9 -31.0 ng/mg creatinine in non-smokers), revealing significant inter-individual differences.

The presence of THBMA in samples from non-smokers suggests that sources other than smoking contribute to its formation in human urine. For example, environmental exposures to BD from automobile exhaust and urban air may contribute to THBMA formation. Furthermore, the metabolic precursor of THBMA, EB-diol, has been hypothesized to form endogenously as a product of catabolism of carbohydrates *(87)*.

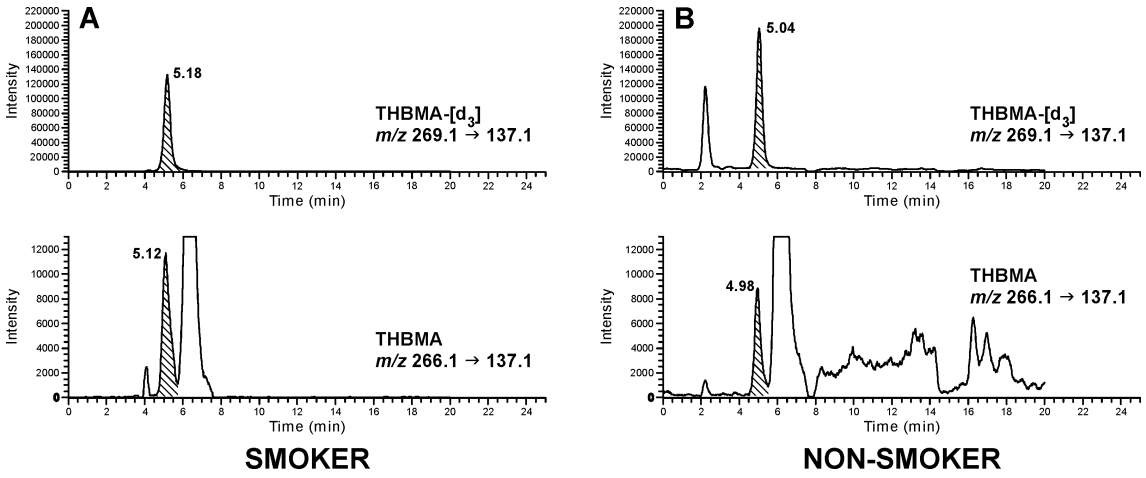

Figure 2.5 HPLC-ESI-MS/MS analysis of THBMA in urine of a smoker and non-smoker

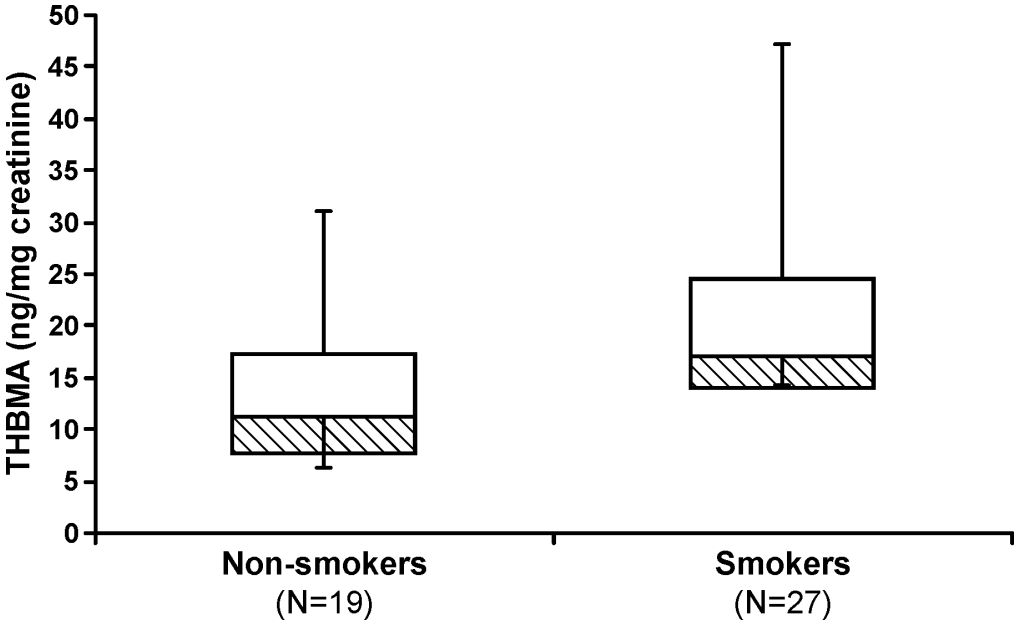

Figure 2.6 Comparison of THBMA concentrations (ng/mg creatinine) between smokers and non-smokers

*boxes represent 25th and 50th percentiles and lines represent the minimum and maximum concentrations.

2.3.9 Smoking cessation study

To investigate the effect of smoking on THBMA concentrations in human urine, samples were obtained from five individuals participating in a smoking cessation study. Five urine samples from each smoker were considered: the first two represented baseline values (-14th day and –7th day) prior to smoking cessation, and an additional three samples were obtained following termination of smoking (3, 28, and 56 days post cessation). Urine samples (100 µl) were processed by SPE and analyzed by HPLC-ESI$^-$-MS/MS as described above. THBMA concentrations measured post smoking cessation were normalized to the baseline value to reveal any changes in urinary THBMA levels following the termination of smoking (Figure 2.7). As shown in Figure 2.7, the mean urinary THBMA levels decreased by 25-50% following smoking cessation, confirming that a significant portion of human exposure to BD can be attributed to exposure to cigarette smoke.

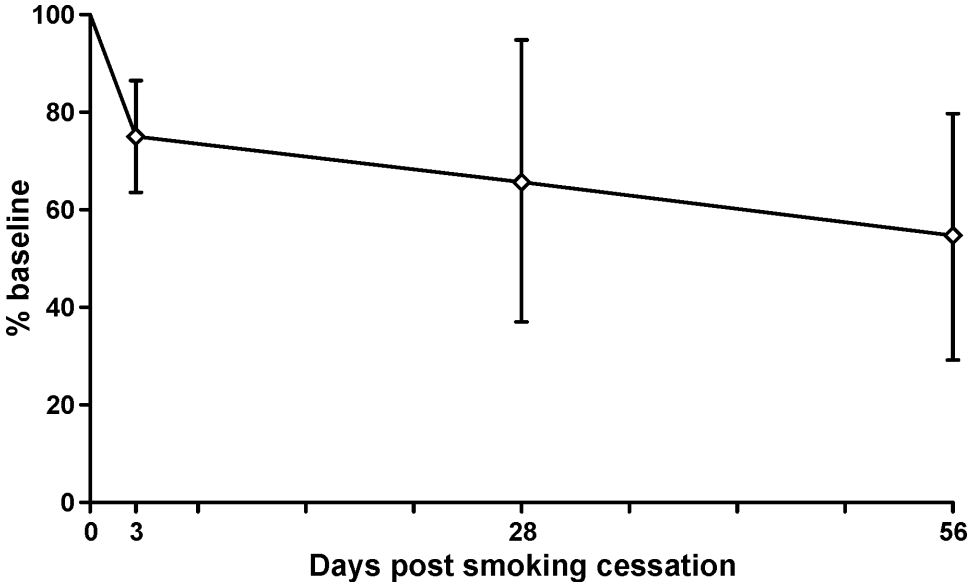

Figure 2.7 Percent reduction in urinary THBMA concentrations in smokers after smoking cessation

2.4 Discussion

A recognized critical step in BD-mediated carcinogenesis is the chemical modification of DNA by its epoxy metabolites to form covalent nucleobase adducts *(41;44;47;190)*. Because of the requirement for metabolic activation of BD to DNA-reactive epoxides, enzymes that are involved in the formation and detoxification of butadiene epoxides largely determine the individual sensitivity to BD-mediated mutagenesis and carcinogenesis. Therefore, quantitative analysis of butadiene metabolites in human samples may provide important information in regard to BD exposure and metabolic activation in a given individual.

Several laboratories previously quantified MHBMA and DHBMA (Scheme 1.1 and Table 1.5) in human urine by liquid chromatography-tandem mass spectrometry *(33;96-99;104)* and gas chromatography-tandem mass spectrometry techniques *(31;95)*. The concentrations of MHBMA have been reported as 1 -132 ng/mL (smokers) and 1-73.4 ng/mL (non-smokers), while the corresponding values for DHBMA are 16-1,959 ng/mL (smokers) and 20-1000 (non-smokers) *(33;96-99;104)*. Following smoking cessation, the levels of MHBMA in human urine decreased from 66.1 ± 69.4 nmol/24 h (baseline) to 3.66 ± 2.41 nmol/24 h (56 days post cessation); while the concentrations of DHBMA dropped from 1038 ± 514 nmol/24 h (baseline) to 662 ± 248 nmol/24 h (56 days post cessation) *(33)*. In contrast, little is known about THBMA excretion in urine of smokers and non-smokers, despite the fact that it is produced from EBD, the most abundant epoxide metabolite of BD in humans *(26)*.

Scheme 2.2 Work flow for HPLC-ESI$^-$-MS/MS analysis of THBMA in human urine

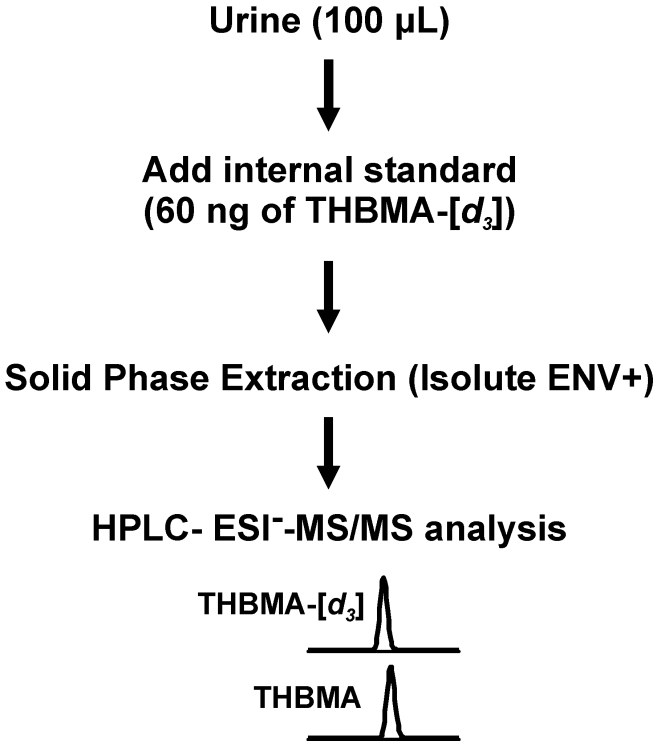

In the present study, a highly sensitive and specific HPLC-ESI$^-$-MS/MS method was developed for quantitative analyses of THBMA in human urine (LOQ, 1 ng/mL). Our methodology (Scheme 2.2) incorporates isotope dilution with d_3-THBMA, sample processing *via* SPE on ENV+ cartridges, and HPLC-ESI$^-$-MS/MS analysis using a Primesep B2 column. The new method is reproducible (Table 2.2) and reasonably fast, with an average analysis time of 25 minutes. We also found out that the analyte concentrations in urine are essentially unchanged upon multiple freeze-thaw cycles.

Several laboratories previously employed ENV+ solid phase extraction for isolation of mercapturic acids from human urine *(107;198;201-203)*. However, lower SPE recoveries have been reported as analyte polarity increased *(107;198;201-203)*. While percent recoveries for SPE of MHBMA and DHBMA using ENV+ cartridges have been reported as 81 and 67%, respectively *(107)*, THBMA is significantly more polar than MHBMA and DHBMA due to the presence of an additional hydroxyl group in its structure (Scheme 1.1). To maximize THBMA recovery from small urine samples (100 μL), samples were loaded onto ENV+ cartridges (50 mg) under acidic conditions and eluted with 2% formic acid in methanol following several washing steps to remove impurities. We found that THBMA recovery decreased and interferences increased when stronger solvents such as acetonitrile were employed.

Our HPLC-ESI-MS/MS method development for THBMA was complicated by its high polarity, leading to poor analyte retention on typical reverse phase HPLC columns. Previous researchers have employed reversed phase HPLC with polar embedded groups to improve the retention of mercapturic acids and took advantage of

reduced-length bonded phase chains (C8 and C12) to prevent stationary phase collapse under highly aqueous conditions required for their separation. For example, Carmella et al. utilized Synergi MAX-RP column with a C12 bonded phase for the analysis of a series of mercapturic acids including MHBMA and DHBMA in human urine *(33)*. Boettcher et al. *(198)* and Schettgen et al. *(102)* used a Luna C8(2) column for the analysis of BD mercapturic acids. Eckert et al. employed hydrophilic interaction liquid chromatography (HILIC) for analyses of various mercapturic acids *(107)*. We have selected a mixed mode Primesep B2 column with C12 bonded phase length and embedded basic ion pairing groups, which in our hands provided the best separation of THBMA from other sample components (Figure 2.5).

The optimized HPLC-ESI-MS/MS method was applied to quantify THBMA in urine samples from 27 smokers and 19 non-smokers (Figure 2.6). We found that THBMA concentrations in urine of smokers (30.7 ng/mL) were significantly greater than in samples from non-smokers (16.3 ng/mL, ~ 45% difference, $p < 0.001$). This difference was less pronounced when THBMA amounts were normalized to urinary creatinine (36%) due to the higher creatinine levels in urine of smokers as compared to non-smokers. However, the differences between creatinine-adjusted concentrations of THBMA in smokers and non-smokers were still statistically significant ($p < 0.01$).

To our knowledge, THBMA had not been previously quantified in human urine. However, the corresponding N-terminal valine hemoglobin adducts, THB-Val, have been quantified in humans *(80;84)*. Most recently, Vacek et al. *(84)* compared the levels of BD-hemoglobin adducts in males and females with different smoking status. The mean

concentrations of THB-Val adducts in male smokers were reported as 501.9 pmol/g hemoglobin (N = 7) and 179.1 pmol/g hemoglobin in male non-smokers (N = 15). THB-Val concentrations in smoking females were 189.2 pmol/g hemoglobin (N = 6) as compared 180.2 pmol/g hemoglobin in non-smoking females (N = 19) *(84)*. Since both THBMA and THB-Val are produced from the same metabolite of BD (EBD, Scheme 1.1), these results are consistent with our data (Figure 2.6), which reveal that both smokers and non-smokers excrete significant amounts of THBMA.

The urinary concentrations of THBMA observed in the present study are 2-3 fold higher than the published concentrations of MHBMA in smokers and 20-30 fold lower than previously observed concentrations of DHBMA. For example, Urban et al. *(96)* reported that the mean MHBMA levels in smokers were 86.4 µg/24 h (N = 10) while the corresponding levels in non-smokers were 12.5 µg/ 24 h (N = 10). DHBMA levels in smokers and non-smokers were 644 and 459 µg/ 24h (N = 10), respectively *(96)*. Several studies, including the most recent one by Carmella et al. *(33)* concluded that MHBMA is a better biomarker of exposure to BD as compared to DHBMA. Existence of alternate source of exposure to the precursors to DHBMA other than BD has been speculated *(33)*. Similar to THBMA, MHBMA and DHBMA are present in significant levels in the urine of non-smokers, which may be a result of background exposure to BD due to passive smoking and environmental exposure to BD *(102)*.

Richardson et al. previously employed HPLC with radioflow detection to analyze THBMA in urine of rats and mice exposed to radiolabeled ^{14}C-1,3-butadiene (200 ppm of for 6 hours) *(93)*. Their analyses revealed 2 peaks corresponding to THBMA. The main

peak was identified as 4-(*N*-acetyl-L-cystein-S-yl)-1,2,3-trihydroxybutane based on co-chromatography with a synthetic standard. The authors inferred that the second peak was the other regioisomer of THBMA, 3-(*N*-acetyl-L-cystein-S-yl)-1,2,4-trihydroxybutane, which would form *via* glutathione conjugation to an internal carbon of EBD *(93)*. However, synthetic standard for 3-(*N*-acetyl-L-cystein-S-yl)-1,2,4-trihydroxybutane was not available to validate this result *(93)*. An attempt to synthesize all possible isomers of THBMA yielded only the diastereoisomers of 4-(*N*-acetyl-L-cystein-S-yl)-1,2,3-trihydroxybutane, but no 3-(*N*-acetyl-L-cystein-S-yl)-1,2,4-trihydroxybutane *(204)*. In the current study, only 4-(*N*-acetyl-L-cystein-S-yl)-1,2,3-trihydroxybutane was observed both in reactions of N-acetylcysteine with *d,l* DEB and in human samples. However, it is possible that our HPLC-MS methods cannot resolve the THBMA regioisomers, therefore the potential formation of 3-(*N*-acetyl-L-cystein-S-yl)-1,2,4-trihydroxybutane cannot be excluded.

In summary, we have successfully developed and validated a sensitive and reproducible HPLC-ESI$^-$-MS/MS method for quantification of THBMA in human urine. Our results provide evidence for the presence of THBMA in urine of smokers and non-smokers, with smokers excreting significantly higher concentrations of this metabolite. Smoking cessation results indicated that a significant portion of THBMA found in human urine is due to exposure of BD in cigarette smoke. However, the presence of any other endogenous and exogenous sources of THBMA in humans requires further investigation.

III. DISCOVERY OF A DEB SPECIFIC BIOMARKER, *BIS*-BDMA AND INTERSPECIES DIFFERENCES IN METABOLISM OF BUTADIENE TO ITS ULTIMATE CARCINOGENIC SPECIES

3.1 Introduction

1,3-butadiene (BD) is a high volume industrial chemical extensively used in the production of synthetic rubber, resins, and polymers *(16;18)*. BD is also an environmental chemical present in automobile exhaust, automotive fuel, forest fires, and cigarette smoke *(16;18)*. C57BL/6 x C3H F1 mice exposed to relatively low doses of BD (6.25-200 ppm) by inhalation developed lymphocytic lymphoma and tumors of the heart, lung, forestomach, Harderian gland, preputial gland, liver, mammary gland, and ovary *(20)*. Sprague-Dawley rats exposed to 1000 - 8000 ppm BD exhibited neoplasms in the mammary gland, brain, Zymbal gland, uterus, pancreas, testis, and thyroid gland *(21)*. Occupational exposure of humans to BD is associated with an increased risk of leukemia, lymphatic, and hematopoietic cancer *(23;24)*. Based on the above evidence, BD has been classified as a known human carcinogen in the Twelfth Annual Report on Carcinogens published by the National Toxicology Program (2011) *(18)*.

Although the exact mechanisms of BD-mediated cancer are unknown, metabolic activation of BD to DNA-reactive intermediates is required for its genotoxic and carcinogenic activity *(26)*. BD is initially metabolized by CYP 2E1 to *(R,S)*-3,4-epoxy-1-butene (EB), which can be further oxidized to form 1,2,3,4-diepoxybutane (DEB) (Scheme 1.1) or hydrolyzed by EH to 1-butene-3,4-diol (EB-diol) *(16)*. EB-diol can in turn undergo another CYP 2E1-mediated oxidation to 3,4-epoxy-1,2-butanediol (EBD)

(16) or alcohol dehydrogenase-mediated conversion to hydroxymethyl vinyl ketone (HMVK)*(32)* (Scheme 1.1). While all the three BD-derived epoxides are mutagenic *(16)*, DEB is 30-fold more genotoxic than EB and 100-fold more mutagenic than EB-diol *(34)*, probably due to its bifunctional nature that enables DEB to cross-link cellular biomolecules. Epoxide hydrolase-mediated hydrolysis appears to be the predominant pathway of metabolic deactivation of EB, DEB, and EBD in rats and humans *(30)*.

If not inactivated, BD-derived electrophilic metabolites can modify DNA nucleobases to give a wide range of adducts, including N-7-(2-hydroxy-3-buten-1-yl)guanine (HB-Gua I), N-7-(1-hydroxy-3-buten-2-yl)guanine (HB-Gua II), and N-7-(2,3,4-trihydroxy-3-buten-2-yl)guanine (THB-G) (Chart 1.2) *(26)*. DNA alkylation by DEB initially produces 2-hydroxy-3,4-epoxybut-1-yl monoadducts *(205)*, which can further react with another nucleophilic site to form exocyclic deoxyadenosine lesions such as 1, N^6-(2-hydroxy-3,4-epoxybut-1-yl)-2'-deoxyadenosine *(67;185)*, DNA-DNA cross links *(46;47;64;68)* (Chart 1.2), and DNA-protein cross links *(192;193)*.

Previous studies in laboratory animals have revealed significant species and gender differences in susceptibility to BD, which have been attributed to profound differences in metabolism. Specifically, laboratory mice developed tumors at ~ 200-fold lower BD concentrations than rats, supposedly a result of higher BD bioactivation/detoxification ratio in the mouse *(21)*. Epoxide hydrolase-mediated hydrolysis of DEB was more efficient in human liver microsomes than in rat microsomes, while no hydrolysis was detected in mouse microsomes *(30)*. Female mice were more susceptible to BD-mediated cancer than males exposed at the same conditions and

exhibited greater numbers of DNA-DNA cross-links *(66)*. In contrast, hemoglobin adduct measurements in BD-exposed Czech workers suggested that females absorbed or metabolized BD to a lesser extent than males *(84)*. If present, any interspecies and gender differences in metabolism of BD are critically important for human cancer risk assessment.

Urinary metabolites can provide a sensitive, non-invasive measure of carcinogen metabolism to their ultimate tumorigenic species. As shown in Scheme 1.1, EB, EB-diol, and HMVK are excreted in urine as MHBMA, THBMA, and DHBMA, respectively (Scheme 1.1) *(33;82;96;97;105;107;206)*. By analogy, DEB is expected to react with two molecules of glutathione and be excreted in urine as the corresponding *bis*-mercapturic acid, 1,4-*bis*-(*N*-acetyl-L-cystein-S-yl)butane-2,3-diol (*bis*-BDMA, Scheme 1.1). However, to our knowledge, such conjugates had not been previously detected. We hypothesized that *bis*-BDMA, if formed *in vivo*, can serve as a non-invasive biomarker of BD metabolism to its ultimate carcinogenic species, DEB. To test this hypothesis, we prepared synthetic *bis*-BDMA and developed an accurate isotope dilution HPLC-ESI$^-$-MS/MS method for its analysis *in vivo*. The new methodology was used to quantify *bis*-BDMA and other BD-mercapturic acids (MHBMA, DHBMA, and THBMA) in urine of F344 rats exposed to 0-200 ppm BD, workers occupationally exposed to BD, and confirmed smokers. We also quantified DEB-induced DNA-DNA cross-links in liver tissues of the same BD-treated rats. Our results reveal pronounced interspecies and gender differences in the metabolic pathways of BD in rats and humans.

3.2 Materials and Methods

Materials. *N*-acetyl-L-cysteine and HPLC-MS grade formic acid were purchased from Sigma Aldrich (St. Louis, MO). HPLC-MS grade acetonitrile was obtained from Fisher Scientific (Pittsburgh, PA). Isolute ENV+ 50 mg/1 mL SPE cartridges were purchased from Biotage (Charlotte, NC). *R, R*-Diepoxybutane was synthesized as reported previously *(47)*. MHBMA, DHBMA, $^{2}H_{6}$-MHBMA, $^{2}H_{7}$-DHBMA, and $^{2}H_{3}$-N-acetyl-L-cysteine were obtained from Toronto Research Chemicals (Ontario, Canada). THBMA and $^{2}H_{3}$-THBMA standards were available from a previous study (Chapter II) *(206)*. *Bis*-BDMA and $^{2}H_{6}$-*bis*-BDMA were synthesized in our laboratory as described below.

Synthesis of 1,4-*bis*-(N-acetyl-L-cystein-S-yl)butane-2,3-diol (*bis*-BDMA) and its deuterated analogue ($^{2}H_{6}$-*bis*-BDMA). *N*-acetyl-L-cysteine (280 mg, 1.70 mmol) was dissolved in 8 mL of water, and the pH was adjusted to 10 with 1N NaOH. *R, R*-Diepoxybutane *(47)* (75 mg, 0.85 mmol) was added, and the reaction mixture was stirred at room temperature for 4 hours. At the end of the reaction, sodium ions were removed by the addition of Bio-Rad AG 50W-X8 cation exchange resin, followed by filtration. *Bis*-BDMA was isolated by semi preparative HPLC on an Agilent 1100 HPLC system interfaced to a DAD UV detector (Agilent Technologies, Santa Clara, CA). HPLC separation was achieved with a Synergi HydroRP column (250 mm × 10.00 mm; 4 µ) (Phenomenex, Torrance, CA) by isocratic elution with 6% acetonitrile in 0.1% trifluoroacetic acid/water. Under these conditions, *bis*-BDMA eluted as sharp peak at 19.6 min. HPLC fractions containing *bis*-BDMA (19.0-20.2 min) were manually

collected and concentrated under vacuum to yield a white powder. $^{2}H_{6}$-*bis*-BDMA was similarly synthesized starting with $^{2}H_{3}$-*N*-acetyl-L-cysteine.

Bis-BDMA and $^{2}H_{6}$-*bis*-BDMA were structurally characterized by NMR and high resolution mass spectrometry. ^{1}H NMR of *bis*-BDMA (Figure 3.1): δ 8.3 (2H, s, cys-NH), 4.4 (2H, m, αC-cys), 3.7 (2H, s, internal OH), 3.6 (2H, m, CHOH), 3.0-2.8 (4H, m, βC-cys), 2.7-2.5 (4H, m, SCH_2), 1.9 (6H, s, $COCH_3$). HRMS results (Figure 3.2): *bis*-BDMA (ESI^--MS : 411.0905 $[M-H]^-$, MS/MS: 282.0468, 153.0042, and 128.0348); $^{2}H_{6}$-*bis*-BDMA (ESI^--MS : 417.1275 $[M-H]^-$, MS/MS: 285.0668, 153.0045, and 131.0544). Stock solutions of *bis*-BDMA and $^{2}H_{6}$-*bis*-BDMA were prepared in water and stored at -20 °C.

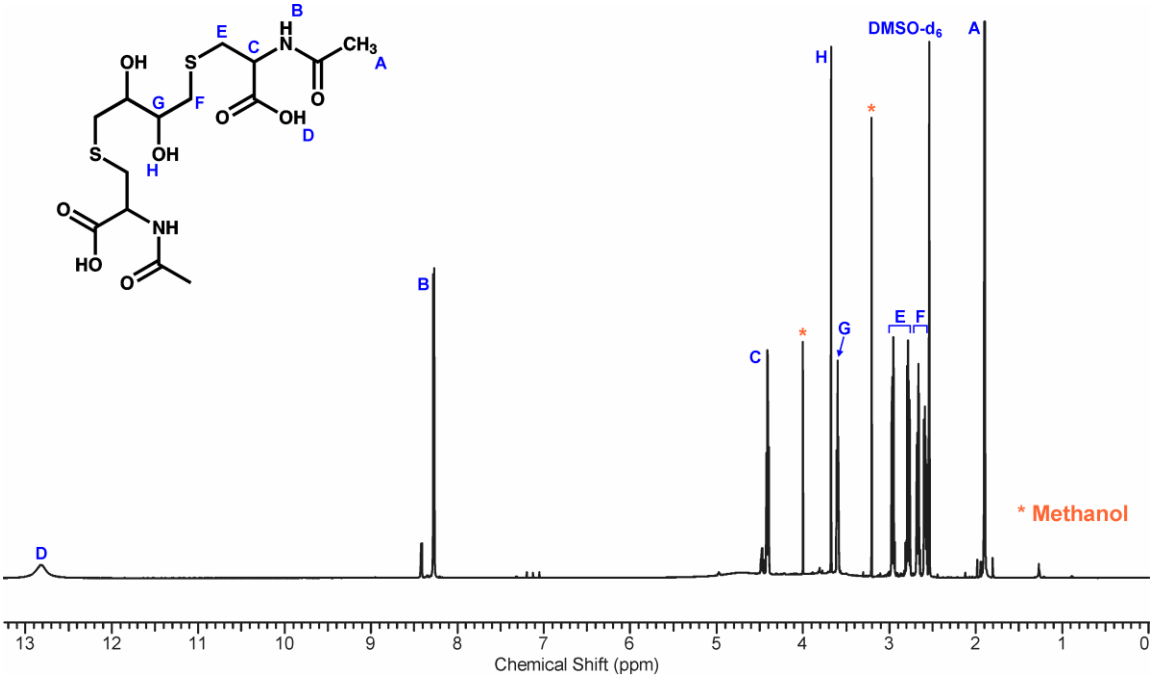

Figure 3.1 ^{1}H NMR spectra of *bis*-BDMA

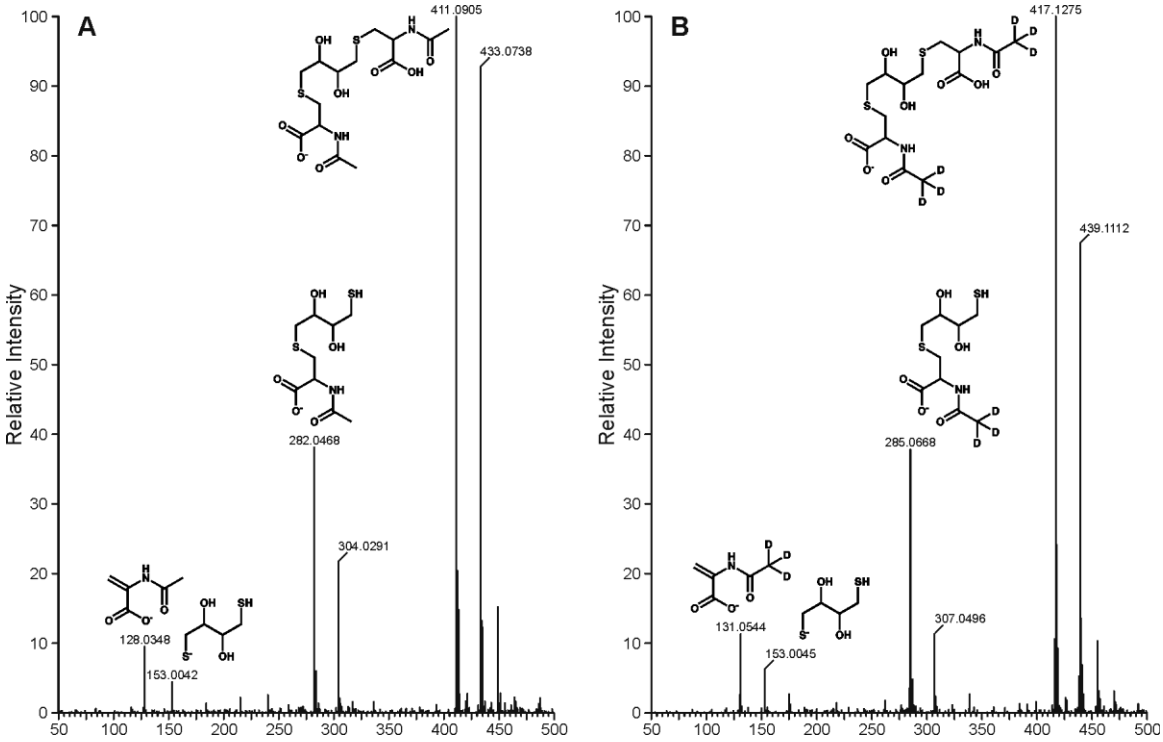

Figure 3.2 UPLC-ESI⁻-TOF-MS/MS spectrum of *bis*-BDMA (A) and $^{2}H_{6}$-*bis*-BDMA (B)

Animals and treatment. Male and female F344 rats (aged 27-29 days) were purchased from Charles River Breeding Laboratories (Raleigh, NC) and housed in cages with animal chow and water in temperature (72 ± 4°F) and humidity (50 ± 10%) controlled rooms with a 12-h light/dark cycle (NIH Publication 86-23, 1985) at the Environmental Exposure and Inhalation Health facility (EEIH, at the University of Texas Medical Branch at Galveston). After a 7 day acclimation period, the animals were randomly separated into air-control and exposure groups by weight. All procedures involving the use of animals were approved by the Institutional Animal Care and Use Committee. Rats were exposed whole-body to nominal 62.5 ppm or 200 ppm BD in air for 2 weeks (6 h/day, 5 days/week) in Hinnar exposure chambers. Rats in the third chamber received filtered air only as a control group. Stock BD (99+ %; from Air Gas Southwest, Texas City, Texas) was metered with a mass flow valve and diluted with HEPA filtered room air and then pumped into the exposure chambers. Fresh animal chow and water were provided to the rats during the exposure period. Following exposures, the left-over food and water were discarded, and animals were returned to their appropriate housing box until the next exposure. Monitoring of exposure atmosphere was achieved using a Shimadzu GC-17A gas chromatograph equipped with a DB-1 column and a FID detector.

Groups of female and male rats (N = 4 per exposure level and sex) were randomly selected and transferred from exposure chambers into metabolic cages at the end of a 6 h exposure period on days 7 or 8 of BD exposure. Rats were held in metabolic cages, with access to food and water, until the next exposure period, when they were returned to

Hinnar exposure chambers. Urine excreted by individual rats during overnight housing in metabolic cages was placed in Eppendorf tubes, snap frozen, and stored at – 80 °C. At the end of the final exposure period, animals were euthanized via cardiac puncture. Liver and lung tissues were collected and immediately flash frozen in liquid nitrogen and stored at -80 °C. Frozen rat urine samples and liver tissues were shipped on dry ice to the University of Minnesota, where they were stored at -80 °C until analysis. A total of 24 rat urine samples (N = 8 per exposure level; exposed to 0, 62.5ppm, 200 ppm BD for 2 weeks) were analyzed.

Human subjects. The formation of *bis*-BDMA was investigated in urine samples of smokers and occupationally exposed individuals. For occupational exposure study, 72 subjects working in a BD production facility were included. Of these, 40 were controls (administrative workers) and 32 were BD production workers. BD exposures in workers were determined by personal monitoring tubes for 8 h work shifts on 10 separate occasions over a 4-month interval for each study subject. Ambient air samples were also analyzed for BD concentrations. Details of the occupational exposure study have been reported previously *(85)*. The experimental protocol was approved by the Institutional Review Boards at Regional Institute of Hygiene of Central Bohemia and the University of Vermont. Archived urine samples were shipped to the University of Minnesota on dry ice and stored at – 80 °C.

Smoker urine samples (N = 36) were obtained from the University of Minnesota Tobacco Research Programs and University of Hawaii Cancer Center and stored at – 80

°C. Smoking status was confirmed by cotinine analysis. These samples were blinded since they are part of an ongoing large epidemiological study.

Quantitation of *bis*-BDMA. Urine samples (100 μL) were vortexed and diluted with 100 μL of 50 mM ammonium formate buffer (pH 2.5) and 10 μL of formic acid. $^{2}H_{6}$-*bis*-BDMA (internal standard, 60 ng) was added, and the samples were mixed and centrifuged at 13,000 rpm for 15 minutes. The supernatant was loaded onto Isolute ENV+ cartridges (1 mL/50 mg) pre-conditioned with methanol (3 ml) and 0.3% formic acid (3 ml). The cartridges were then washed with 1.5 mL of 0.3% formic acid, followed by 0.75 mL of 5% methanol in 0.3% formic acid, and allowed to dry completely under vacuum for 20 minutes. *Bis*-BDMA and its internal standard were eluted with 1.2 mL of 2% formic acid in methanol. SPE eluates were dried under vacuum and reconstituted with 30 μL of water. Typically, 3 μL of this solution was injected onto the HPLC column for HPLC-ESI^{-}-MS/MS analysis.

HPLC-ESI^{-}-MS/MS analysis of *bis*-BDMA was conducted with an Agilent 1100 HPLC system (Agilent Technologies, Santa Clara, CA) coupled to a Thermo-Finnigan TSQ Quantum Discovery mass spectrometer (Thermo Scientific Corp., Waltham, MA). HPLC separations were carried out on a SIELC Primesep D column (2.1 x 100 mm, 5 μm particle size) equipped with a guard column (Primesep D; 2.1 x 10 mm). The column was maintained at 50 °C and eluted with a gradient of water (Solvent A) and 1% formic acid in 50% acetonitrile (Solvent B), at a flow rate of 200 μl/min. Gradient program was as follows (Time, % of solvent B): 0-8 min, 40 to 48% B; 8-10 min, 48 to 75% B; 10-13 min, isocratic at 75% B; 13-15 min, 75 to 40% B; 15-25 min, finally maintained at 40%

B. The flow was directed into the MS detector only during 4.5-10 min of the chromatographic run.

The TSQ Vantage triple quadrupole instrument (Thermo Scientific), was operated in the negative electrospray ionization (ESI^-) mode. Typical MS parameters were as follows: spray voltage, - 3500 V; sheath gas pressure, 50 psi; capillary temperature, 250° C; collision energy, 16; source CID, -9 V; collision gas pressure, 1.0 mTorr; Q1(FWHM), 0.4; Q3 (FWHM), 0.7; scan width , 0.4 *m/z*; and scan time, 0.4 s. The MS parameters we optimized by direct infusion of authentic standards and may differ between runs. The mass spectrometer was operated in the selected reaction monitoring (SRM) mode. The SRM transitions used for quantification of *bis*-BDMA were: *m/z* 411.1 → 282.1 (*bis*-BDMA) and *m/z* 417.1 → 285.1 ($^2H_6$-*bis*-BDMA). For confirmation purposes, additional SRM transitions were also monitored (*m/z* 411.1 → 153.1, 411.1 → 128.1 for *bis*-BDMA and *m/z* 417.1 → 153.1, 417.1 → 131.1 for $^2H_6$-*bis*-BDMA).

HPLC-ESI-MS/MS Method validation for *bis*-BDMA. The standard curves for HPLC-ESI-MS/MS analysis of *bis*-BDMA were constructed by analyzing standard solutions containing 0.05-160 ng of *bis*-BDMA and 6 ng of $^2H_6$-*bis*-BDMA, in triplicate. The amounts of *bis*-BDMA observed were calculated by comparing the peak area ratios between the analyte and the internal standard. Regression analyses were conducted to determine the correlation between the expected and experimentally observed *bis*-BDMA amounts. Method calibration curves were constructed by spiking control rat urine samples (100 µl) with 0.5 - 1600 ng of *bis*-BDMA and 60 ng of $^2H_6$-*bis*-BDMA in

triplicate, followed by SPE and HPLC-ESI-MS/MS analysis. The observed *bis*-BDMA amounts were plotted against the theoretical values (ng/ml).

The limit of detection (LOD) and the limit of quantification (LOQ) of the HPLC-ESI-MS/MS method for *bis*-BDMA were determined by addition of 10-500 pg of *bis*-BDMA and 60 ng of $^{2}H_{6}$-*bis*-BDMA to 100 µl of control rat urine. These fortified urine samples were processed by SPE and analyzed by the validated HPLC-ESI-MS/MS method as described below. The lowest concentration of *bis*-BDMA which gave a S/N > 10 and % CV < 15% was reported as the LOQ, while the lowest concentration of *bis*-BDMA which gave S/N > 3 was reported as the LOD.

In order to determine the precision and accuracy of the analytical method, control rat urine (100 µL) was spiked with 100 ng of *bis*-BDMA and 60 ng of $^{2}H_{6}$-*bis*-BDMA, followed by SPE and analysis by HPLC-ESI^{-}-MS/MS three times per day on three consecutive days. The relative standard deviations between these measurements were calculated and reported as intra-day and inter-day precision, while the accuracy range was determined from the equation $(100 \times C_m)/C_s$ by comparing each of the nine concentration measurements (C_m) to the actual concentration spiked (C_s).

Extraction recovery of the SPE method was determined from the equation: $R_b/R_a \times 100\%$ where R_b is the relative response ratio calculated from HPLC-ESI^{-}-MS/MS peak areas of analyte and the internal standard obtained upon analyzing control rat urine samples spiked with 100 ng of analyte prior to SPE and 60 ng of internal standard post-extraction (n = 3) and R_a is the corresponding relative response ratio obtained from the analysis of same control rat urine sample spiked with same amounts of analyte and the

internal standard mentioned above post SPE (n = 3). Analyte signal suppression in the presence of urine matrix was evaluated from the equation (100-(100 x A_m)/A_s) where A_m is the peak area of the analyte or internal standard obtained by SPE and HPLC-ESI$^-$-MS/MS analysis of control rat urine spiked with 100 ng of analyte and 60 ng of internal standard and A_s is the corresponding peak area of the analyte or internal standard obtained by HPLC-ESI-MS/MS analysis of a pure standard mix containing 100 ng of analyte and 60 ng of internal standard.

Quantitative analysis of MHBMA, DHBMA and THBMA. Urine samples (200 μL) were spiked with 60 ng of each $^2H_6$-MHBMA and $^2H_7$-DHBMA and processed by SPE on Waters HLB cartridges. The SPE eluates were dried, reconstituted in 30 μL of 0.1% formic acid, and analyzed by HPLC-ESI$^-$-MS/MS with a Pursuit 3 Diphenyl (2.1 x 150 mm, 3 μm) column eluted with a gradient of 0.1% formic acid and acetonitrile (*Kotapati and Tretyakova, manuscript in preparation)*. For THBMA analysis, urine aliquots (100 μL) were spiked with $^2H_3$-THBMA and processed by Isolute ENV+ SPE as described previously *(206)*. The gradient program was modified as follows (Time, % of solvent B): 0-6 min, 15 to 21% B; 8-10 min, 21 to 75% B; 10-13 min, isocratic at 75% B; 13-15 min, 75 to 15% B; 15-25 min, finally maintained at 15% B.

Determination of *bis*-N7G-BD in rat liver DNA. NanoHPLC-NSI$^+$-MS/MS methodology developed in our laboratory *(68)* was used to quantify DEB-induced *bis*-N7G-BD crosslinks in liver DNA of rats exposed to 0, 62.5 or 200 ppm BD by inhalation. In brief, DNA was extracted with NucleoBond AXG500 anion exchange cartridges (Machery-Nagel, Düren, Germany). DNA concentrations and purity were

determined by HPLC-UV analysis of dG in enzymatic digests. DNA (100 μg) was spiked with 50 fmol of racemic $^{15}N_{10}$-*bis*-N7G-BD (internal standard) and subjected to neutral thermal hydrolysis at 70 °C for 1 hour to release N7-guanine adducts as free bases. Partially depurinated DNA was removed by ultrafiltration. *Bis*-N7G-BD and its internal standard were enriched by offline HPLC and reconstituted in 0.01% aqueous acetic acid. Samples (8 μl) were injected onto a trap column (Symmetry C18 nanoAcquity, 0.18 × 20 mm, Waters Corp., Millford, MA) connected to a manually packed Zorbax SB-C18 nano HPLC column (75 μm x 200 mm, 5μ), which was eluted with 0.01% acetic acid in 1:1 methanol:acetonitrile at a flow rate of 0.4 μl/min. *Bis*-N7G-BD adducts were quantified by isotope dilution HPLC-ESI$^+$-MS/MS. The SRM transitions for *bis*-N7G-BD and $^{15}N_{10}$-*bis*-N7G-BD were *m/z* 389.1 $[M + H]^+ \rightarrow$ *m/z* 238.1 $[M + H - Gua]^+$) and *m/z* 399.1 $[^{15}N_{10}\text{-}M+H]^+ \rightarrow$ *m/z* 243.1 $[M + H - [^{15}N_5]Gua]^+$, respectively. Accurate quantitation of *bis*-N7G-BD was achieved by comparing the areas of nanoHPLC-NSI$^+$-MS/MS peaks corresponding to the analyte and its internal standard using standard curves *(68)*.

3.3 Results

3.3.1 Development of HPLC-MS/MS methodology for *bis*-BDMA

It has been proposed that susceptibility of a given organism towards BD-induced cancer can be determined from the extent of metabolic activation of BD to its ultimate carcinogenic metabolite, DEB *(113)*. In support of this notion, we have previously observed that DNA of laboratory mice (more sensitive species) contained 5-10-fold greater numbers of DEB-specific *bis*-N7G-BD adducts than rats (less sensitive species)

exposed at the same conditions *(66)*. However, human tissue and blood samples are not readily available. We therefore examined the feasibility of using urinary *bis*-BDMA as a novel, non-invasive biomarker of BD bioactivation to DEB.

Authentic standards of *bis*-BDMA and its deuterated analogue were prepared by reacting DEB with N-acetyl-L-cysteine and $^{2}H_{3}$-N-acetyl-L-cysteine, respectively. Both standards were characterized by high resolution mass spectrometry and proton NMR (Figures 3.1 and 3.2) and were used for the development of a sensitive and specific isotope dilution HPLC-ESI-MS/MS method for *bis*-BDMA in urine. In our approach, *bis*-BDMA is isolated by solid phase extraction (SPE) and quantified by negative ion HPLC-ESI-MS/MS using isotope dilution with the corresponding deuterated internal standard ($^{2}H_{6}$-*bis*-BDMA).

Our HPLC-MS/MS method for *bis*-BDMA is based on selected reaction monitoring of MS/MS transitions corresponding to C-S bond cleavage (*m/z* 411 → 281.1 for the analyte and *m/z* 417 → 285.1 for the deuterated internal standard, respectively, see Figure 3.2). Analysis of standard solutions containing a fixed amount of $^{2}H_{6}$-*bis*-BDMA internal standard and increasing amounts of *bis*-BDMA confirmed that HPLC-ESI^{-}-MS/MS responses were linear between 0.05-160 ng of *bis*-BDMA (on column) (Figure 3.3 A). Further method validation was conducted by spiking control rat urine sample (100 µl) with 60 ng of $^{2}H_{6}$-*bis*-BDMA and 0.5-1600 ng of *bis*-BDMA, followed by SPE and HPLC-ESI^{-}-MS/MS analysis (Figure 3.3 B). Excellent correlation between the measured and expected concentrations of *bis*-BDMA was observed (Figure 3.3 B) (R^2 = 0.9999). The limit of detection (LOD) and the limit of quantification (LOQ) for *bis*-BDMA in

urine were determined to be 1 and 5 ng/ml, respectively (Table 3.1). The intra-day and inter-day precision (% RSD) determined by repeated analysis of *bis*-BDMA (100 ng) spiked into control rat urine sample (100 µl) were 0.88 and 1.17%, respectively. Comparison of analyte or internal standard peak areas in buffer and analyte/internal standard spiked into control urine matrix (post SPE) revealed very moderate (< 2%) signal suppression of the analyte by the sample matrix. Method accuracy was observed to be 96.2-100.5%. Complete HPLC-ESI$^-$-MS/MS method validation parameters are compiled in Table 3.1.

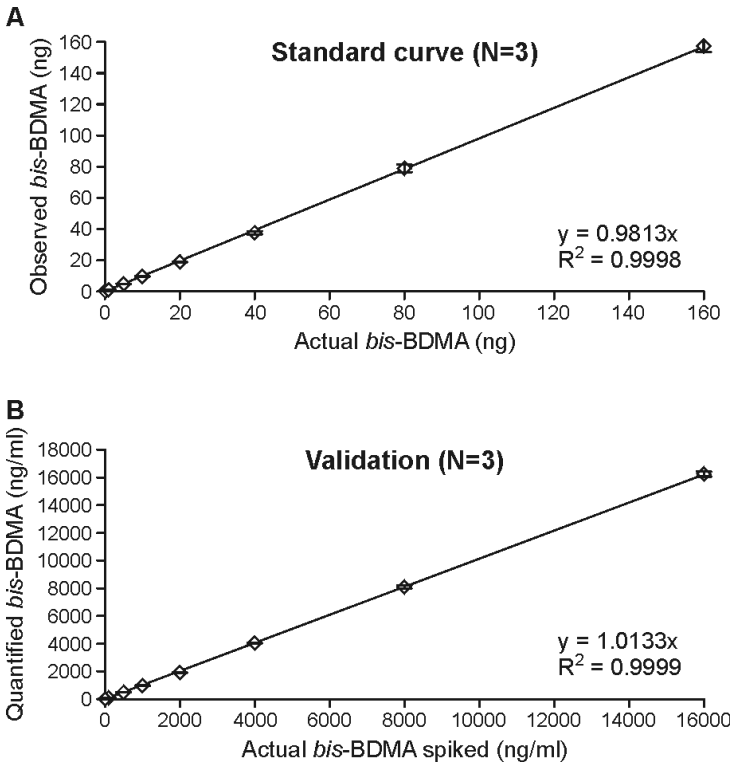

Figure 3.3 Standard and method validation curves for *bis*-BDMA

Table 3.1 Validation parameters for HPLC-ESI-MS/MS analysis of *bis*-BDMA

Range (ng/ml)	LOD (ng/ml)	LOQ (ng/ml)	Intra-day precision (%)	Inter-day Precision (%)	Accuracy (%)	Extraction Recovery (%)
5-16,000	1.0	5.0	0.88	1.17	98.04	46

3.3.2 Quantification of BD-mercapturic acids in urine of F344 rats exposed to BD by inhalation

The new HPLC-ESI-MS/MS methodology described above was used to quantify *bis*-BDMA in urine of male and female F344 rats (N = 4 per exposure level and sex) treated with 0, 62.5, or 200 ppm BD by inhalation for 2 weeks (6 h/day, 5 days/week). Other BD-mercapturic acids were also determined in the same samples. No *bis*-BDMA was detected in urine of control rats exposed to air (Figure 3.4 A), and a concentration-dependent increase in *bis*-BDMA amounts was observed in animals exposed to 62.5 ppm and 200 ppm BD (Figures 3.4 B and 3.5 A). The identity of *bis*-BDMA observed in rat urine was further confirmed by examining two additional MS/MS transitions and by re-analyzing the samples on a different HPLC column (Synergi Hydro-RP). Mean urinary concentration of *bis*-BDMA following exposure to 200 ppm BD was 4.8 ± 2.9 µg/ml urine, while the concentrations of MHBMA, DHBMA and THBMA in the same samples were 77.9 ± 37.8 µg/ml, 209.5 ± 85.1 µg/ml, and 150.3 ± 59.9 µg/ml, respectively (Figures 3.5 B-D). Urinary BD-mercapturic acid concentrations correlated with BD exposure, with 2-3 fold higher amounts observed in 200 ppm BD exposure group as compared to 62.5 ppm exposure group (Figure 3.5). Urine of unexposed rats contained background levels of MHBMA (68.5 ± 17.1 ng/ml), DHBMA (3192.7 ± 533.2 ng/ml) and THBMA (561.7 ± 81.7 ng/ml), but no *bis*-BDMA. This is consistent with previous studies that have revealed the presence of these metabolites in unexposed animals and human subjects due to an unidentified endogenous source *(96;97;206)*.

Urinary *bis*-BDMA concentrations tended to be 2-3 fold higher in female rats as compared to the male animals exposed under the same conditions but the difference was only marginally significant (Figure 3.5A, $p = 0.06$). In contrast, female rats excreted slightly lower levels of MHBMA, DHBMA and THBMA as compared to males, although these differences were not statistically significant ($p > 0.3$, Figures 3.5B-D). These results suggest that the metabolic pathways of BD are distinct in female vs male animals, supposedly a result of hormonal effects on xenobiotic metabolizing enzymes.

The relative concentrations of the four BD-mercapturic acids in urine of BD-exposed rats were DHBMA (47%) > THBMA (37%) > MHBMA (15%) > *bis*-BDMA (1 %) (Figure 3.6A). These results are consistent with previous studies that examined BD-induced hemoglobin adducts in blood of rats exposed by inhalation *(88).* Similar DHBMA/THBMA/MHBMA/ *bis*-BDMA metabolic ratios were observed in animals treated with 62.5 and 200 ppm BD, but the contribution of *bis*-BDMA were consistently higher in females (1.6-2%) as compared to males (0.6 %).

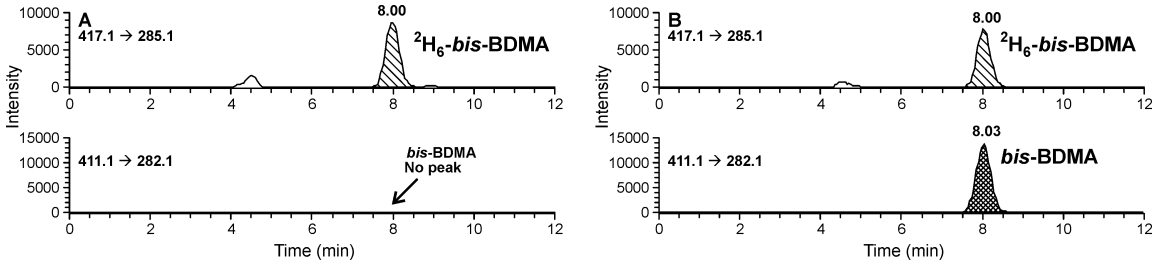

Figure 3.4 HPLC-ESI$^-$-MS/MS analysis of *bis*-BDMA in urine of control (A) and BD exposed (B) F344 rats

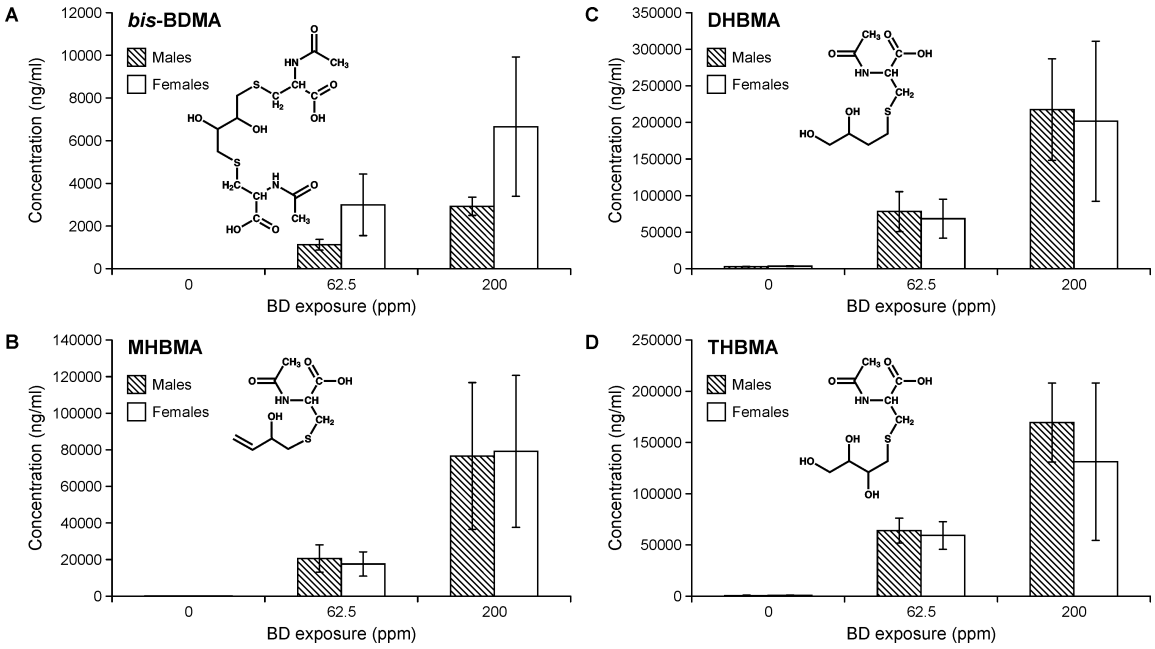

Figure 3.5 Dose response relationships for *bis*-BDMA, MHBMA, DHBMA and THBMA in urine of F344 rats exposed to 0-200 ppm BD

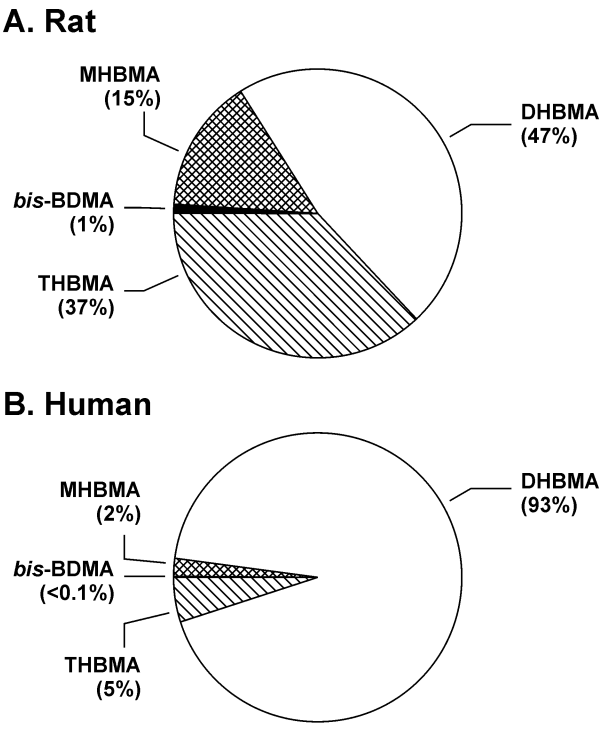

Figure 3.6 Inter-species differences in BD metabolism between rats and humans

3.3.3 Quantification of BD-mercapturic acids in urine of smokers and occupationally exposed workers

To examine the possibility of DEB and *bis*-BDMA formation in humans, two populations chronically exposed to BD were examined: smokers and occupationally exposed individuals. Workers at a BD polymer production plants (N = 32) were exposed to 0.1 - 2 ppm BD, while the corresponding controls (office workers, N = 40) were exposed to < 0.02 ppm BD. Current smokers (N = 36) were exposed to BD due to its presence in cigarette smoke (~ 46 μg/ cigarette in main-stream smoke and 283 μg/cigarette in side-stream smoke). For comparison, the other three urinary BD-mercapturic acids (MHBMA, DHBMA and THBMA) were also analyzed. The high sensitivity and specificity of our HPLC-ESI-MS/MS method has enabled us to use small volumes of urine (100-200 μl) for these analyses. *Bis*-BDMA concentrations in both groups were below the limit of detection of our method (1 ng/ml) (Figure 3.7A); it was not detectable even when a more sensitive capillary HPLC-ESI-MS/MS method was employed (LOD, 0.1 ng/ml), (Figure 3.7B) or when larger urine samples were analyzed (up to 1 ml). Relative contributions of MHBMA, DHBMA, THBMA and *bis*-BDMA to the total urinary BD- mercapturic acids excreted by smokers were 2, 93, 5 and <0.1%, respectively (Figure 3.6B). DHBMA was the major BD metabolite excreted in human urine (93%), followed by THBMA and MHBMA. These results are consistent with previous studies in liver microsomes and hemoglobin adduct measurements that suggested that BD metabolism to DEB is less efficient in humans than in rats and mice *(26;89)*. These results indicate that the metabolic pathways of BD in humans are distinct from those in laboratory mice and rats.

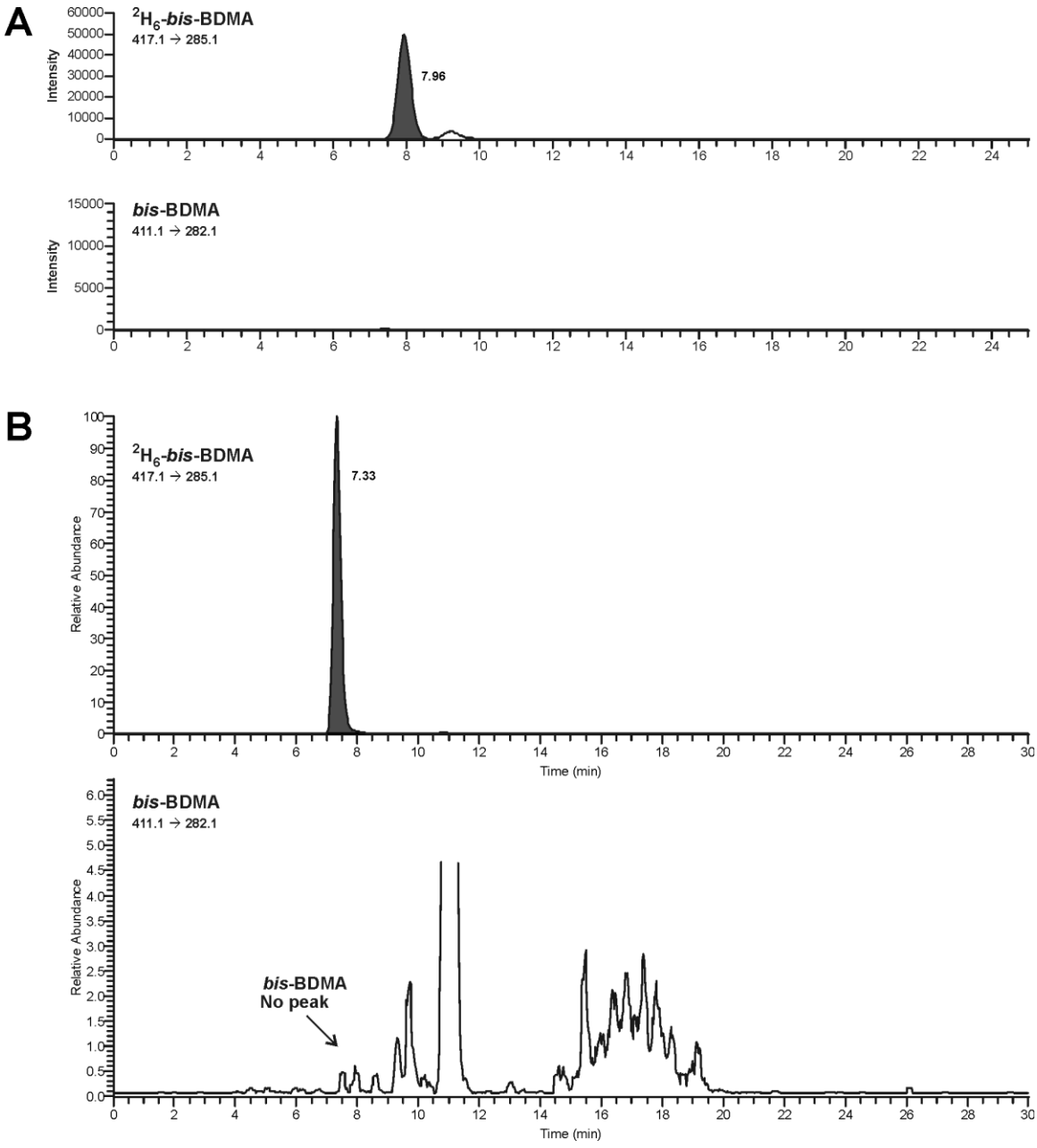

Figure 3.7 HPLC-ESI$^-$-MS/MS analysis of *bis*-BDMA in human urine using narrow bore (A) and capillary (B) HPLC methods

3.3.4 Dose response studies of DEB-derived *bis*-N7G-BD adducts in rat liver DNA

In order to examine the correlation between urinary metabolite and DNA-bound DEB, DEB-specific *bis*-N7G-BD adducts were quantified in liver DNA of laboratory rats exposed to BD by inhalation. Ultra-sensitive nanoHPLC-nanoESI^{+}-MS/MS methodology recently reported by our group was employed *(68)*. In brief, DNA was spiked with $^{15}N_{10}$-*bis*-N7G-BD internal standard and subjected to neutral thermal hydrolysis to release *bis*-N7G-BD as a free base conjugates, which were enriched by off-line HPLC *(68)*. As expected, no *bis*-N7G-BD was detected in control animals (Figure 3.8A), while BD-exposed animals contained significant amounts of the cross-link (Figure 3.8B). Interestingly, dose-response relationships for *bis*-N7G-BD adducts in rat liver were not linear, with highest levels of the cross-links observed following exposure to 62.5 ppm BD (1.4 adducts/10^8 nucleotides) (Figure 3.8C). As was the case with *bis*-BDMA, female rats had higher numbers of *bis*-N7G-BD adducts (1.6 adducts/10^8 nucleotides) as compared to males (1.2 adducts/10^8 nucleotides) at 62.5 ppm BD exposure, but this difference was not statistically significant (Figure 3.8).

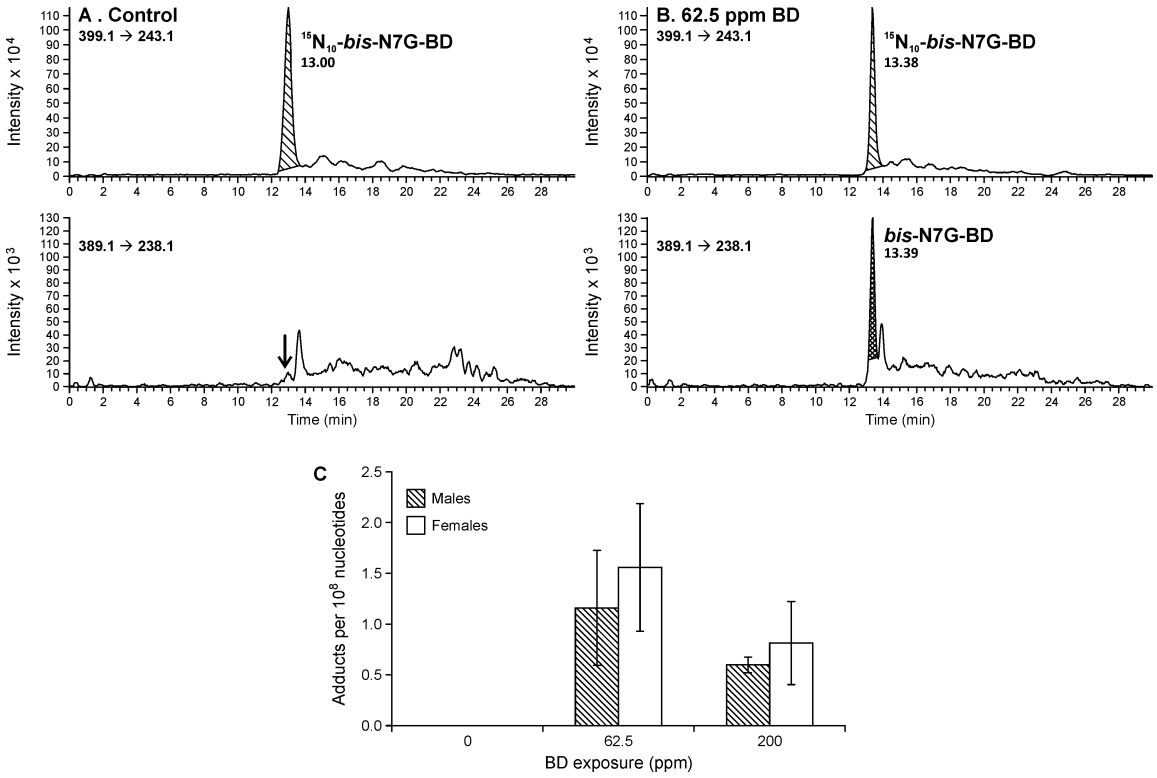

Figure 3.8 nanoHPLC-NSI$^+$-MS/MS analysis of *bis*-N7G-BD in liver DNA of control (A) and BD exposed (B) F344 rats and dose-response relationship (C)

3.4 Discussion

A potent human and animal carcinogen, BD is metabolically activated to four electrophilic species: EB, HMVK, EBD, and DEB (Scheme 1.1) *(16;32)*. Among these, DEB displays the greatest genotoxicity *in vitro* and has been hypothesized to be the ultimate carcinogenic metabolite of BD *(16)*. DEB is 50-fold more effective at inducing sister chromatid exchanges and chromosomal aberrations in human lymphocytes than EB *(207;208) in vitro* and is two orders of magnitude more mutagenic than EB and EBD in TK6 lymphoblasts (Table 1.4) *(34)*. More efficient DEB formation from BD in laboratory mice is thought to be responsible for their increased sensitivity to BD-induced lung and liver cancer as compared to laboratory rats *(66;196)*. Previous studies of DEB formation in humans are limited, although experiments with human liver microsomes suggest that any DEB produced in humans is rapidly detoxified via epoxide hydrolase-catalyzed hydrolysis *(29)*.

Urinary mercapturic acids are commonly used as biomarkers of exposure to carcinogens and as a measure of their metabolic activation to DNA-reactive intermediates *(209)*. In the present work, *bis*-BDMA was employed as a novel urinary biomarker for DEB formation form BD. To our knowledge, *bis*-BDMA has not been previously reported *in vivo*, although Boogaard et al. detected the formation of a conjugation product of DEB with two molecules of glutathione following *in vitro* incubation of DEB with radiolabeled glutathione in human liver cytosolic tissue fractions *(94)*. Analogous *bis*-glutathione conjugates have been also reported for other *bis*-electrophiles such as hexachloro-1,3-butadiene *(210)*, vinyledene chloride *(211)*, and 1,2-dibromoethane *(212)*.

Such conjugates are formed via consecutive reactions of the two electrophilic groups with two molecules of glutathione. While the first reaction is catalyzed by glutathione S-transferases, the second conjugation step may be either spontaneous or enzymatic *(212)*. The resulting *bis*-glutathion-*S*-yl conjugates undergo further processing by glutamyltransferases, cysteinyl-glycinases, and acetylases in the kidney (mercapturic acid pathway) and are excreted in urine as the corresponding *bis*-N-acetylcysteine conjugates.

The availability of specific urinary biomarkers for DEB, EB, HMVK, and EBD (*bis*-BDMA, MHBMA, DHBMA, and THBMA, respectively, Scheme 1.1), has enabled us to evaluate the formation of all four electrophilic metabolites of BD *in vivo* (BD-exposed rats and humans exposed to BD in the workplace or via smoking). While MHBMA, DHBMA, and THBMA were observed in both species, *bis*-BDMA was detected only in BD-treated rats, but not in BD-exposed humans. Furthermore, the metabolic ratios differed dramatically between the two species. In humans, DHBMA accounted for 93% of total urinary BD-mercapturic acids (Figure 3.6B), while the other three BD-mercapturic acids were much less abundant, with THBMA at 5%, MHBMA at 2%, and *bis*-BDMA at < 0.1% (Figure 3.6B). In contrast, in the rat, DHBMA accounted for only 47% of metabolites, closely followed by THBMA (37%). In the latter species, MHBMA comprised for 15% and *bis*-BDMA for 1% of BD-mercapturic acids excreted (Figure 3.6A). Although in the present study, humans were exposed to lower concentrations of BD that rats, the sensitivity of our HPLC-ESI-MS/MS methodology (LOD, 0.1 ng/ml urine for the capillary method) should have been more than sufficient to detect *bis*-BDMA if it was produced in human urine similar to rats. By comparison, EB,

EBD, and DEB in blood of rats exposed to 62.5 ppm or 200 ppm BD followed a similar order EB-diol (DHBMA) > EBD (THBMA) > EB (MHBMA) > DEB (*bis*-BDMA). Furthermore, the relative abundance of the corresponding hemoglobin adducts in blood of BD-exposed rats was THB-Val (from EBD) > HB-Val (from EB) > *pyr*-Val (from DEB) *(26)*. Overall, results from these studies are consistent with significant interspecies differences in BD metabolism between humans and laboratory rats, which are commonly used as a model organism for human risk assessment from exposure to BD.

Background amounts of MHBMA (68.5 ± 17.1 ng/ml), DHBMA (3192.7 ± 533.2 ng/ml) and THBMA (561.7 ± 81.7 ng/ml) were observed in urine of control animals exposed to filtered air only. This finding is consistent with a previous report by Mcdonald et al. who detected MHBMA and DHBMA in urine of control F344 rats (10 and 1,500 ng/ml, respectively) *(97)*. Georgieva et al. also observed significant background levels of the corresponding hemoglobin adducts (HB-Val and THB-Val) in F344 control rats *(73;88)*, suggesting that there is a significant endogenous source of these metabolites in mammals. In our recent paper *(206)*, we observed significant amounts of THBMA in urine of non-smokers (16.3 ng/ml), although smokers excreted higher amounts of this metabolite (30.7 ng/ml). In contrast, DEB-specific biomarker adducts *bis*-N7G-BD (Figure 3.8) and *pyr*-Val were not detected in control animals *(73;88)*.

Our results reveal that female F344 rats excrete higher concentrations of DEB-specific metabolite than males (Figure 3.5A). Consistent with this observation, liver DNA of female animals contained higher concentrations of DEB-specific *bis*-N7G-BD cross-links as compared to males (Figure 3.8C). We have previously reported that *bis*-N7G-BD

formation was influenced by gender in a larger study that examined dose-dependent DNA adduct formation in BD-exposed mice and rats *(66)*. Furthermore, Boysen et al. reported that the concentrations of DEB-specific hemoglobin adducts (*pyr*-Val) were 2-4 fold higher in female rats as compared to males following exposure to 1000 ppm BD *(77)*, although no gender differences were observed following 200 ppm BD exposure *(66;88)*. Increased formation of DEB in females may be responsible for their enhanced susceptibility towards BD-induced cancer as revealed in animal inhalation studies *(20)*. Therefore, future studies are needed to evaluate gender differences in metabolism of BD.

To evaluate the correlation between urinary metabolites of DEB and the amounts of diepoxide bound to genomic DNA, DEB-specific DNA-DNA cross-links (*bis*-N7G-BD) were quantified in liver DNA of the same BD-exposed rats (Figure 3.8). Unlike linear curve observed for *bis*-BDMA, *bis*-N7G-BD followed a more complex dose-response relationship, with the highest adduct numbers observed at a medium exposure levels (62.5 ppm BD, see Figure 3.8C).

It has been previously hypothesized that the metabolic activation of EB to DEB in the rat is saturated at high BD concentrations (> 62.5 ppm)*(66;213)*. Our data for urinary *bis*-BDMA in the same animals is not consistent with this hypothesis, since *bis*-BDMA amounts continue to increase following inhalation exposure to 62.5 and 200 ppm BD (Figure 3.5A).

An alternative explanation for *bis*-N7G-BD adduct levels decrease in the high exposure group includes the induction of DNA damage response and oxidative stress pathways. These cellular stress responses could include cell cycle arrest, senescence, and

cell death *(214;215)*. Such dose-related apoptosis is expected to reduce measurable DNA adduct levels by removing affected cells from the population. In addition, cell cycle arrest induced by BD-DNA damage could induce DNA repair by influencing the levels of gene expression *(216)*. Indeed, Rusyn et al. have observed significant epigenetic changes in rats exposed to BD *(217)*. For example, such changes could involve the *p53* gene that codes for a transcription factor for the DNA damage response pathway and mediates apoptosis in DEB-exposed cells *(218)*. These possibilities should be investigated in further studies.

In summary, the current study for the first time establishes *bis*-BDMA as a novel urinary biomarker of BD bioactivation to DEB in the rat. Unlike other BD-mercapturic acids, *bis*-BDMA is not present in urine of unexposed animals, suggesting that it is a specific biomarker of exposure to BD. Furthermore, since *bis*-BDMA was detected in rats exposed to BD by inhalation, but not in occupationally exposed workers or smokers, humans appear to be less efficient than rats in respect to metabolizing BD to DEB, revealing interspecies differences in metabolism of BD that may be relevant to human risk assessment.

IV. DEVELOPMENT OF A HIGH THROUGHPUT HPLC-ESI⁻-MS/MS METHOD FOR QUANTIFICATION OF URINARY METABOLITES OF BD IN HUMANS AND DISCOVERY OF ETHNIC/RACIAL DIFFERENCES IN METABOLISM OF BD

4.1 Introduction

1,3-butadiene (BD) is a high volume industrial chemical widely used as a monomer in the production of synthetic rubber and plastics *(18)*. BD is also an intermediate for the manufacture of other industrial chemicals *(18)*. The primary sources of exposure of general population to BD include automobile exhaust, forest fires, urban air, and cigarette smoke *(18)*. Among these, cigarette smoke contains relatively high quantities of BD (16-75 μg/cigarette in main-stream smoke and 205-361 μg/cigarette in side- stream smoke *(19)*. Inhalation studies in laboratory mice and rats have shown that BD induces tumors in multiple tissues including lung, heart, liver and mammary gland *(20;21)*. Epidemiological studies in rubber industry and BD production workers have revealed a strong association between BD exposure and the development of leukemia, lymphatic, and hematopoietic cancers *(22-24)*. Based on this evidence, BD has been classified as a human carcinogen by the National Toxicology Program, EPA and IARC *(18;26)*.

BD requires metabolic activation to electrophilic epoxides for its mutagenic activity *(16;206)*. CYP2E1 and CYP2A6 monoxygenase-mediated oxidation of BD produces *(R)*- and *(S)*-3,4-epoxy-1-butene (EB), which can be hydrolyzed to 3,4-epoxy-1,2-butanediol (EBD). EB can undergo further oxidation to 1,2,3,4-diepoxybutane (DEB) or epoxide hydrolysis and oxidation to hydroxymethyl vinylketone (HMVK) (Scheme 1.1) *(27;29;32)*. If not detoxified by epoxide hydrolase (EH) or glutathione S-transferase

(GST), BD-derived epoxides EB, EBD and DEB can alkylate DNA to form mutagenic covalent DNA adducts *(16;26;30)*. The glutathione conjugates of EB, HMVK, EBD and DEB are further modified by γ-glutamyltranspeptidase, cysteinylglycine dipeptidase, and cysteine S-conjugate N-acetyltransferase *(110)*, and are ultimately excreted in urine as 2-(*N*-acetyl-L-cystein-S-yl)-1-hydroxybut-3-ene/1-(*N*-acetyl-L-cystein-S-yl)-2-hydroxybut-3-ene (MHBMA), 4-(*N*-acetyl-L-cystein-S-yl)-1,2-dihydroxybutane (DHBMA), 4-(*N*-acetyl-L-cystein-S-yl)-1,2,3-trihydroxybutane (THBMA), and 1,4-*bis*-(*N*-acetyl-L-cystein-S-yl)butane-2,3-diol (*bis*-BDMA), respectively (Scheme 1.1) *(31;110;206)*.

Because they are derived from toxic and carcinogenic metabolites of BD, urinary mercapturic acids are useful biomarkers of BD exposure and bioactivation *(82;85;99)*. Among the four BD mercapturic acids, MHBMA is regarded as a specific biomarker of BD exposure because urinary MHBMA concentrations decrease by more than 90% upon smoking cessation *(33)*. In contrast, DHBMA and THBMA were present in urine of both smokers and non-smokers, suggesting that they are at least partially formed from an unknown endogenous source *(33;96;206)*. *bis*-BDMA, a specific biomarker of DEB, is not detectable in urine of smokers and workers occupationally exposed to BD, probably because of the inefficient formation of DEB in humans (Chapter III). The MHBMA/(MHBMA+DHBMA) metabolic ratio has been previously used as relative measure of BD activation because it reflects the portion of EB that is not detoxified via epoxide hydrolysis and is available for binding to biomolecules *(85;96)*. Several mass spectrometry-based methods have been developed for quantification of MHBMA and DHBMA in human urine *(31;33;96;97;99;102;104;105;107)*. However, many of these

methods (Table 1.5) require a large sample volume (> 1 ml) and are not amenable to high throughput analyses.

As discussed in section 1.1.2, there are significant differences in lung cancer risk among ethnic groups *(9;14)*. Haiman et al. reported the lung cancer risk among five different ethnic groups as: African American > Native Hawaiian > European American > Japanese American > Latin American smokers *(14)*. It has been proposed that these differences in risk are because of differences in metabolic activation and detoxification of tobacco carcinogens *(9;14)*. Hence, it is important to determine whether there are differences in metabolism of BD in smokers belonging to different ethnic groups. Ethnic differences in BD metabolism would manifest in variation of MHBMA, DHBMA concentrations and their metabolic ratio among different ethnic/racial groups.

In the present study, a sensitive HPLC-ESI$^-$-MS/MS method for simultaneous quantification of MHBMA and DHBMA in human urine was developed. The method requires only 150-200 µl of urine and employs a 96 well plate high throughput SPE cleanup amenable for processing multiple samples at the same time. The new method has high sensitivity, with LOQ values of 0.5 and 10 ng/ml for MHBMA and DHBMA, respectively. The intra-day and inter-day precision (%RSD) was < 5% for both analytes, confirming the reproducibility of our method. This method was applied to urine samples from workers employed at a BD and styrene-butadiene rubber manufacturing facility in Czech Republic *(85)*. THBMA concentrations were also determined in the same urine samples by a previously published method by our laboratory *(206)*. We found that the concentrations of MHBMA, DHBMA, and THBMA were significantly higher in

workers occupationally exposed to BD as compared to the controls, suggesting that BD-mercapturic acids can be used as sensitive biomarkers of BD exposure and bioactivation. Furthermore, the concentrations of MHBMA and DHBMA were also determined in smokers belonging to different ethnic groups in two separate multi-ethnic cohort studies. Significant differences in MHBMA concentrations were observed, suggesting that the metabolism of BD is different among ethnic/racial groups.

4.2 Materials and Methods

Materials. MHBMA, DHBMA, $^{2}H_{6}$-MHBMA and $^{2}H_{7}$-DHBMA were purchased from Toronto Research Chemicals (Toronto, Canada). THBMA and $^{2}H_{3}$-THBMA were synthesized in our laboratory as described previously *(206)*. HPLC grade methanol, LC-MS grade formic acid and acetonitrile were obtained from Fisher Scientific (Pittsburgh, PA). All other reagents and chemicals were obtained from Sigma Aldrich (St. Louis, MO). Oasis HLB SPE 96 well plates (30 mg) were purchased from Waters Corporation (Milford, MA) and Isolute ENV+ 96 well plates (50 mg) were obtained from Biotage (Charlotte, NC).

Sample preparation. Urine samples (200 µl) were diluted with 200 µl of water and acidified with 20 µl of 1 N hydrochloric acid. $^{2}H_{6}$-MHBMA and $^{2}H_{7}$-DHBMA internal standards (60 ng each) were added, and the spiked samples were vortexed and centrifuged. The supernatant was loaded onto an Oasis HLB 96 well plate (30 mg) pre-conditioned with 1 ml methanol and 1 ml of water. The SPE wells were washed with 1 ml of 5% methanol. MHBMA, DHBMA, $^{2}H_{6}$-MHBMA and $^{2}H_{7}$-DHBMA were eluted into a 96 well elution plate with 75% methanol. The eluates were completely dried under

vacuum and reconstituted with 30 µl of 0.1% formic acid for analysis by HPLC-ESI$^-$-MS/MS methodology as described below.

For analysis of THBMA, 100 µl aliquots of human urine were processed by Isolute ENV+ 96 well plate (50 mg) by the SPE methodology described previously *(206)*. Briefly, 100 µl aliquots of urine were acidified with 100 µl of 50 mM ammonium formate buffer (pH 2.5) and 10 µL of formic acid. $^2H_3$-THBMA internal standard (60 ng) was added to the acidified sample, followed by thorough mixing by vortexing. The samples were centrifugated, and the supernatants were loaded onto an Isolute ENV+ 96 well plate pre-conditioned with 3 ml each of methanol and 0.3% formic acid. The well plates were washed with 1.5 mL of 0.3% formic acid and further with 0.75 mL of 5% aqueous methanol containing 0.3% formic acid. The well plates were dried completely under vacuum, and the analyte and its internal standard were eluted with 1.2 ml of 2% formic acid in methanol into a 96 well elution plate. The elution plate was dried under vacuum, and the eluates were reconstituted in 30 µl of water. THBMA concentrations were determined by isotope dilution HPLC-ESI$^-$-MS/MS as described below.

HPLC-ESI$^-$-MS/MS method for quantification of MHBMA and DHBMA. The HPLC-ESI$^-$-MS/MS system consisted of an Agilent 1100 HPLC system (Agilent Technologies, Santa Clara, CA) equipped with a 96 well plate autosampler and interfaced to Thermo TSQ Vantage mass spectrometer (Thermo Scientific Corp., Waltham, MA). Samples (10 µl) were injected onto an Agilent Pursuit 3 Diphenyl column (2.0 x 150 mm, 3 µm) connected to an Agilent Metaguard Pursuit 3 DP guard column. The column was eluted with a gradient of aqueous 0.1% formic acid (A) and 0.1% formic acid in

acetonitrile (B) at a flow rate of 150 µl/min and 5 ^{0}C. The analytes were resolved with the following linear gradient program (time, % of solvent B): 0-12 min, 3 to 9% B; 12-14 min, 9 to 50% B; 14-16 min, isocratic at 50% B; 16-18 min, 50 to 3% B; 18-30 min, conditioning at 3% B.

The mass spectrometer was operated in the ESI^{-} mode, at the following MS settings: spray voltage, -3000 V; sheath gas pressure, 65 psi; capillary temperature, 250 ^{0}C; collision energy, 14 (MHBMA), 24 (DHBMA); S-lens, 75; source CID, 8 V; collision gas pressure, 1.1 mTorr; Q1 (fwhm), 0.4; Q3 (fwhm), 0.7; scan width, 0.4 *m/z*; and scan time, 0.3 s. MHBMA and DHBMA were quantified in the SRM mode by comparing the peak area of analytes with their corresponding internal standards ($^{2}H_{6}$-MHBMA and $^{2}H_{7}$-DHBMA, respectively). The SRM transitions used were *m/z* 238.1 → 109.1 ($^{2}H_{6}$-MHBMA), 232.1 → 103.1 (MHBMA), 257.1 → 78.1 ($^{2}H_{7}$-DHBMA) and 250.1 → 75.1 (DHBMA).

HPLC-ESI^{-}-MS/MS method for quantification of THBMA. THBMA was quantified by the HPLC-ESI^{-}-MS/MS methodology previously reported by our laboratory (Chapter III). Samples (10 µl) were injected onto a SIELC Primesep D column (2.1 x 100 mm, 5 µm particle size) connected to a guard column (Primesep D; 2.1 x 10 mm). The HPLC-MS system consisted of Agilent 1100 HPLC system (Agilent Technologies, Santa Clara, CA) interfaced to a Thermo-Finnigan TSQ Quantum Discovery mass spectrometer (Thermo Scientific Corp., Waltham, MA). The column was eluted with a gradient of water (A) and 49.5:49.5:1 water: ACN: formic acid (B) as reported previously (Section 3.2) THBMA concentrations were determined by isotope dilution with the

corresponding internal standard ($^2H_3$-THBMA). The mass spectrometer was operated in the selected reaction monitoring (SRM) mode by monitoring the transitions *m/z* 269.1 → 137.1 ($^2H_3$-THBMA) and 266.1 → 137.1 (THBMA).

Calibration Curves. Non-smoker urine samples (200 µl) were spiked with 9 different amounts of MHBMA (0.1–40 ng), DHBMA (2.0–1000 ng) and 60 ng each of $^2H_6$-MHBMA and $^2H_7$-DHBMA, in triplicate. The samples were processed by Oasis HLB 96 well plate (30 mg) SPE method and the analyte concentrations were determined by the new HPLC-ESI$^-$-MS/MS method described above. Calibration curves were constructed separately for MHBMA and DHBMA to determine the correlation between the analyte/internal standard amount ratio and the corresponding MS peak area ratios.

LOD and LOQ determination. Synthetic urine (200 µl) was spiked with MHBMA (20–100 pg) and DHBMA (0.2–2.0 ng) and 60 ng each of $^2H_6$-MHBMA and $^2H_7$-DHBMA (internal standards for quantitation). These spiked samples were subjected to SPE enrichment on Oasis HLB 96 well plates (30 mg) and subsequently analyzed by HPLC-ESI$^-$-MS/MS as described above. Analyte amounts at which the signal-to-noise ratio (S/N) was greater than 10 and % CV < 15% was designated as the method's limit of quantification (LOQ). Similarly, the lowest analyte amount at which the signal-to-noise ratio (S/N) was greater than 3 was defined as the limit of detection (LOD).

Intra-day and Inter-day Precision. Nine 200 µL urine aliquots from a confirmed smoker were processed by SPE as described above. The reconstituted SPE eluates were pooled into a single sample, and the pooled sample was injected three times

per day on three consecutive days. Intra-day and Inter-day precision were determined by calculating the relative standard deviations (%RSD) between these 9 measurements.

Method Accuracy. Aliquots of non-smoker urine (N = 5) were spiked with 10 ng/ml of MHBMA, 250 ng/ml of DHBMA and 60 ng each of $^{2}H_{6}$-MHBMA and $^{2}H_{7}$-DHBMA. The aliquots were processed by SPE and subsequently analyzed by HPLC-MS/MS as described above. Background concentrations of MHBMA and DHBMA in the non-smoker urine sample were determined by analyzing 200 µl aliquots of the non-spiked nonsmoker urine by HPLC-MS/MS in triplicate and subtracted from the observed concentration for determination of method accuracy.

Analyte Recovery. Three aliquots of non-smoker urine (200 µl each) were spiked with MHBMA (10 ng/ml), DHBMA (250 ng/ml), and 60 ng each of $^{2}H_{6}$-MHBMA and $^{2}H_{7}$-DHBMA, followed by SPE as described above. Three additional urine aliquots from the same sample were processed by the same method as above, with the exception that $^{2}H_{6}$-MHBMA and $^{2}H_{7}$-DHBMA internal standards were added following SPE purification. All six samples were analyzed by HPLC-ESI-MS/MS as described above, and SPE recoveries of MHBMA and DHBMA were determined by comparing the relative (analyte/internal standard) response ratios between the two sets of samples.

Quantification of BD urinary metabolites in workers in a BD production facility. Urine samples from 72 workers were obtained from workers employed at a BD monomer and SBR production facility near Prague, Czech Republic *(83;85)*. Out of 72 subjects, 40 were administrative workers (21 male and 19 female) not occupationally exposed to BD (< 0.03 mg/m^{3}) while 32 were workers in the production unit (16 male

and 16 female; BD exposure, 0.05-1.5 mg/m^3). Complete details of the study population have been published previously *(83;85)*. The present study was conducted in a blind fashion, e.g. subject information was not revealed until the urinary BD mercapturic acid concentrations of all the subjects were determined. After the analyses were completed, the information about BD exposure, age, gender, protein biomarkers, mutation frequencies, and smoking status of each subject were made available.

Quantification of MHBMA and DHBMA in smokers belonging to different ethnic groups. The newly developed HPLC-MS/MS method for MHBMA and DHBMA quantification (described above) was employed to study inter-ethnic/racial differences in BD metabolism in two different multi-ethnic cohort studies (blinded). The first study (Study # 1) involved smokers belonging to three different ethnic groups: Native Hawaiians, European Americans and Japanese American (N = 200 per group). Additionally, thirty-five blind duplicates were included for quality control measures. Study # 2 included smokers of European American and African American ethnicity (N = 450 per group). MHBMA and DHBMA concentrations were determined for all the smoker urine samples in both studies and metabolic ratios were calculated later.

Statistical Analysis. Multiple regression analyses were conducted to determine the associations between urinary BD-mercapturic acids and gender, BD exposure, and smoking status. Additionally, Pearson partial correlation coefficients were computed to determine the correlation between MHBMA, DHBMA, THBMA, THB-Val, *pyr*-Val and hprt mutation frequencies. A two-way ANOVA test was also performed to identify any

differences in urinary MHBMA, DHBMA, THBMA concentrations between the control and occupationally exposed groups.

For the multi-ethnic cohort studies, MHBMA and DHBMA concentrations were normalized to urinary creatinine to account for differing dilution. To examine ethnic/racial differences in study # 1, least square means were computed for each ethnic/racial group using multi variable linear regression model. For the study # 2, a Wilcoxon non-paramateric test was performed and p-values were calculated to observe any differences in urinary MHBMA, DHBMA, and their metabolic ratio between the European American and African American smokers. Additionally, genome wide association study (GWAS) was also completed to identify any correlation between the genetic polymorphisms and BD urinary metabolites.

4.3 Results

4.3.1 SPE and HPLC-MS/MS method development for MHBMA and DHBMA

While multiple methods exist in the literature for quantitative analysis of BD-mercapturic acids (MHBMA and DHBMA) in human urine (Table 1.5) *(33;96;97;99;102;104;105;107),* most of them require large sample sizes and are not amenable for high throughput analyses. The goal of the present study was to develop an HPLC-ESI-MS/MS method for MHBMA/DHBMA that is sensitive enough to quantify urinary BD-mercapturic acids in small volumes of human urine (< 200 µl) and that could be applied to large numbers of samples typical for molecular epidemiology studies.

Because urinary concentrations of MHBMA in smokers are 50-100 fold lower than that of DHBMA based on previous reports *(102;105),* our method development efforts have focused on maximizing analyte recovery for MHBMA. We chose solid phase extraction (SPE) for analyte cleanup step because of its ability to remove the bulk of interferences from urine with minimal analyte losses. Multiple SPE stationary phases have been tested, including reversed phase, anion exchange, weak anion exchange, and mixed modes. Among these, Oasis HLB (Waters Corporation, Milford, MA) which is a hydrophilic-lipophilic balanced stationary phase with high reversed-phase retention provided the highest MHBMA recoveries and therefore was chosen for final SPE method development. Our SPE method for MHBMA and DHBMA is based on the previously published procedure *(99),* which was modified by incorporating an additional 5% methanol wash (to remove additional interferences) and a final elution step with 75% methanol to maximize analyte recoveries of MHBMA and DHBMA. SPE recoveries for MHBMA and DHBMA by our method were determined to be 92 and 18%, respectively. Low recovery for DHBMA did not interfere with the analysis due to the use of an isotopically labeled internal standard and because of the relatively high concentrations of DHBMA in human urine *(33;105).*

HPLC-ESI-MS/MS method development for MHBMA and DHBMA was complicated by their poor retention on reverse phase columns. Both BD-mercapturic acids are highly polar metabolites with hydroxyl and carboxylic acid functionalities in their structure (Scheme 1.1). Furthermore, MHBMA is a mixture of four isomers (Scheme 4.1), which complicates its HPLC separation. Multiple HPLC stationary phases

were evaluated in an attempt to find a stationary phase that makes it possible to resolve MHBMA and $^{2}H_{6}$-MHBMA isomers from any co-eluting interferences present in the human urine matrix.

Scheme 4.1 Structures of the four isomers of MHBMA

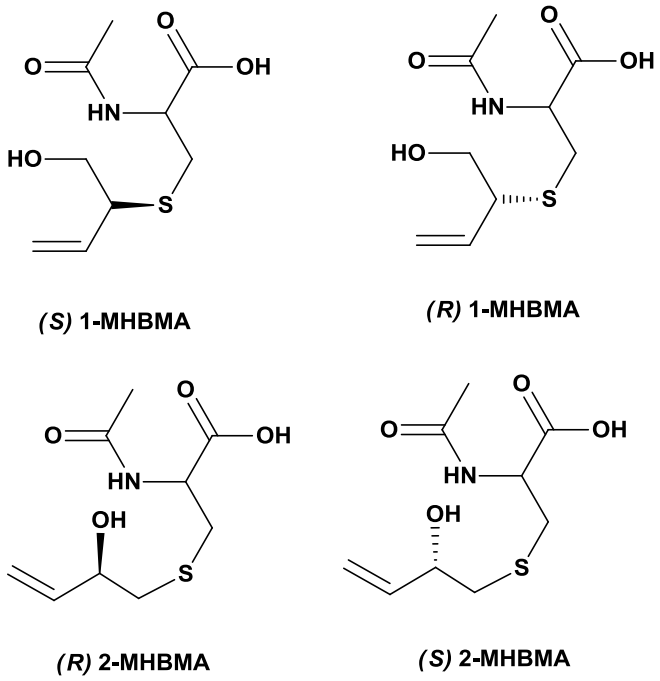

In the initial stages of method development, we attempted to employ capillary HPLC columns (0.5 mm i.d.) for improved HPLC-ESI-MS/MS sensitivity. Despite promising results for pure standards, poor results were obtained for actual urine samples due to the complexity and the variability of human urine matrix, which has led to sample-dependent retention time shifts. To minimize retention time shifts, we turned our attention to narrow bore (2.1 mm i.d.) columns. The use of ion pairing reagents such as *N*,*N*-dimethyl hexylamine and triethylamine increased analyte retention, but required longer equilibration times and resulted in a severe ion suppression for subsequent users. Therefore, we focused on specialized HPLC phases capable of retaining polar analytes in the absence of ion pairing agents.

While good analyte retention in the absence of ion-pairing agents was achieved on a number of columns, including Synergi MAX-RP (Phenomenex), Luna C18 (Phenomenex), Xterra MS-C18 (Waters), Primesep B2 (Sielc), Primesep D (Sielc), Zorbax SB-C18 (Agilent) and Hypersil Gold (Thermo), these columns were unable to resolve MHBMA from a co-eluting interference present in most human urine samples. The best results in terms of analyte retention and separation from the matrix was achieved with an Agilent Pursuit Diphenyl column (2.1 x 150 mm, 3 µ) (Agilent Technologies). In order to maximize analyte retention, the carboxylate group of the analyte (pKa ~4.5) was protonated by employing acidic mobile phase (0.1% formic acid, pH ~2.5). While higher sensitivity was achieved with 0.5% acetic acid, MHBMA separation from a co-eluting peak was not satisfactory with this mobile phase. A linear gradient of acetonitrile in 0.1% aqueous formic acid has afforded good HPLC resolution and MS sensitivity for

MHBMA. The HPLC column was maintained at 5 °C to maximize the separation of MHBMA analyte peaks from an interfering matrix peak.

For HPLC-ESI-MS/MS detection of MHBMA/DHBMA, the best sensitivity was achieved in the negative ion mode. The major ESI^- MS/MS fragmentation pathway for MHBMA and DHBMA corresponds to the cleavage of the C-S bond. Therefore, the main MS/MS transitions of MHBMA and DHBMA and their deuterated analogs used as internal standards are 238.1 → 109.1 ($^2H_6$-MHBMA), 232.1 → 103.1 (MHBMA), 257.1 → 128.1 ($^2H_7$-DHBMA) and 250.1 → 121.1 (DHBMA). Because of a co-eluting peak in the major SRM transition for DHBMA and $^2H_7$-DHBMA (results not shown), an alternative MS/MS transition was selected for quantification of this analyte: 257.1 → 78.1 ($^2H_7$-DHBMA) and 250.1 → 75.1 (DHBMA). As shown in Figure 4.1 for a representative sample from a BD-exposed worker, MHBMA isomers elute as two HPLC-ESI^--MS/MS peaks at 13.2 and 14.1 min (Figure 4.1A, second panel), while the corresponding isomers of $^2H_6$-MHBMA internal standard elute at 12.8 and 13.8 min, respectively (Figure 4.1A, top panel). The first peak contains (*R*) and (*S*) 2-MHBMA as well as one of the stereoisomers of 1-MHBMA, while the second peak corresponds to the other stereoisomer of 1-MHBMA. In the same samples, DHBMA signal is observed at 8-8.2 min, while $^2H_7$-DHBMA internal standard elutes slightly earlier at 7.9-8.1 min (Figure 4.1, bottom panels). THMBA was analyzed by a similar HPLC-ESI^--MS/MS approach as described previously (Chapter 4, Figure 4.2). Our optimized methodology for quantification of BD-mercapturic acids in human urine is summarized in Scheme 4.2.

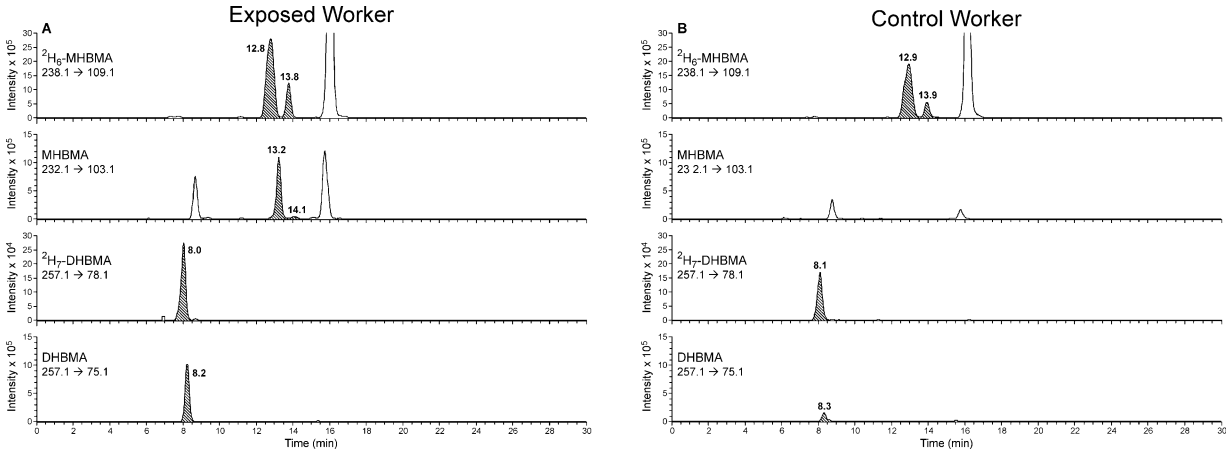

Figure 4.1 Representative traces for HPLC-ESΙ-MS/MS analysis of MHBMA and DHBMA in urine of a BD-exposed worker and a control worker

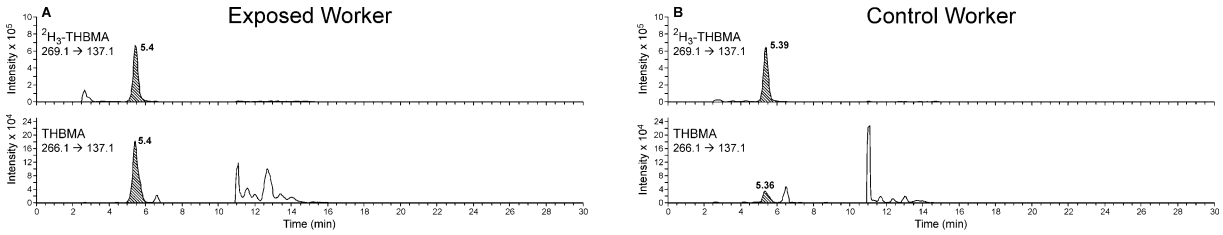

Figure 4.2 Representative traces for HPLC-ESI$^-$-MS/MS analysis of THBMA in urine of a BD-exposed worker and a control worker

Scheme 4.2 Workflow for quantification of MHBMA, DHBMA and THBMA in human urine

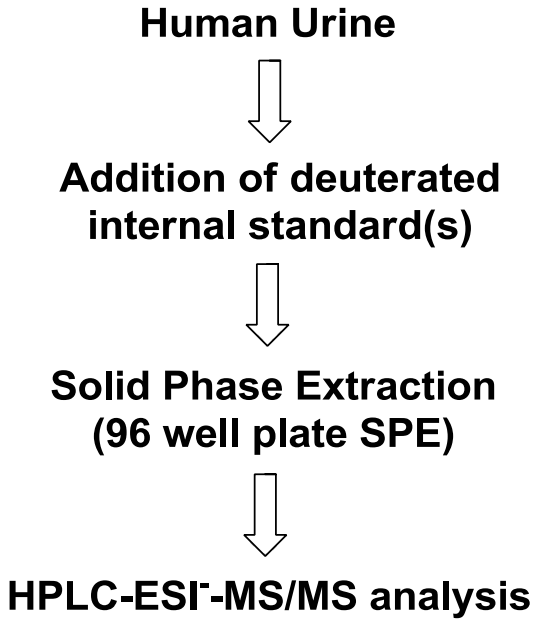

4.3.2 Method Validation

The new HPLC-ESI$^-$-MS/MS method for MHBMA and DHBMA was validated by analyzing non-smoker urine spiked with increasing concentrations of MHBMA and DHBMA and constant amount of the corresponding internal standards. As shown in Figure 4.3, linear correlation curves were obtained for both analytes ($R^2 > 0.9998$). The HPLC-ESI$^-$-MS/MS method was linear between 0.5-200 ng/ml for MHBMA and 10-5000 ng/ml for DHBMA (Table 4.1). The y-intercepts in the correlation curves were above zero (Figure 4.3) due to background concentrations of MHBMA and DHBMA in non-smoker urine (MHBMA, 3.8 ng/ml; DHBMA, 229 ng/ml). The LOD and LOQ values for MHBMA were 0.2 and 0.5 ng/ml, respectively, while the corresponding values for DHBMA were 5 and 10 ng/ml (Table 4.1). The LOD and LOQ values for DHBMA were higher because minor SRM transitions were chosen for quantification of this analyte (see above). However, this did not prevent accurate analysis of DHBMA due to relatively high concentrations of this analyte in human urine. Intra-day and inter-day precision was determined by repeated analysis of a smoker urine sample (three times per day on three consecutive days). The calculated % RSD values for both analytes were below 5% (Table 4.1), demonstrating the reproducibility of our HPLC-ESI$^-$-MS/MS method. The accuracy of the HPLC-ESI$^-$-MS/MS method for MHBMA and DHBMA was determined by spiking known amounts of each analyte (MHBMA, 10 ng/ml and DHBMA, 250 ng/ml) into a non-smoker urine sample. We found that the accuracy range for MHBMA was 100.5 ± 5.1, while the corresponding value for DHBMA was 102.7 ± 3.2. Complete validation parameters for both analytes are presented in Table 4.1.

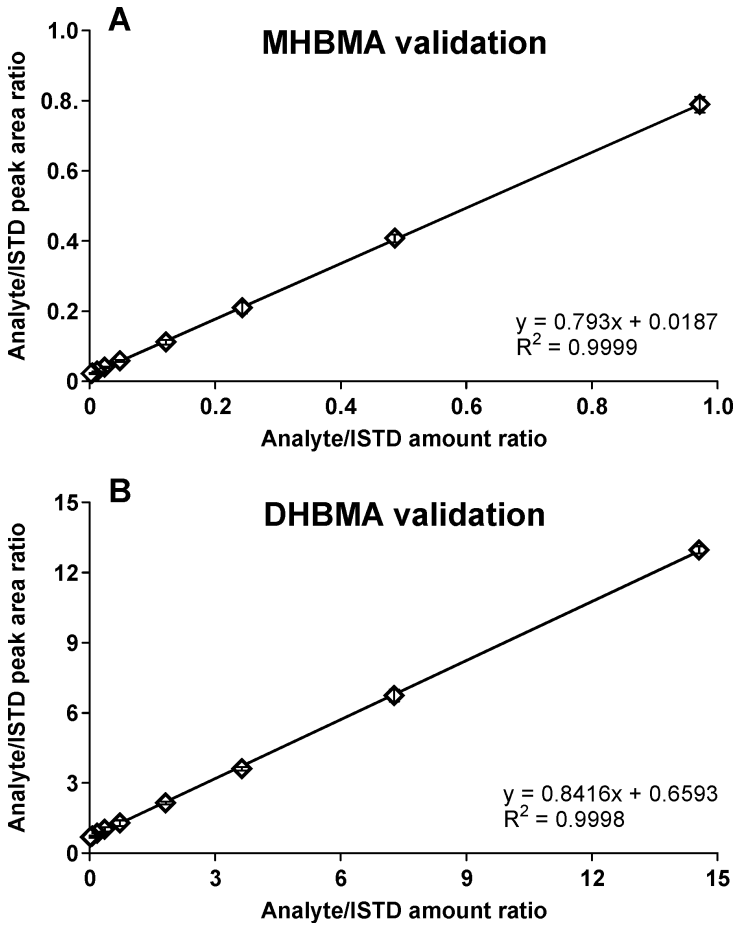

Figure 4.3 Method validation curves for MHBMA and DHBMA spiked into non-smoker urine (200 µl).

Table 4.1 HPLC-ESI⁻-MS/MS method validation parameters for quantification of MHBMA and DHBMA in human urine.

Analyte	Range (ng/ml)	LOD (ng/ml)	LOQ (ng/ml)	Precision (% RSD)		Accuracy (%)	Recovery (%)
				intra-day	inter-day		
MHBMA	0.5-200	0.2	0.5	4.1	4.5	100.5 ± 5.1	92
DHBMA	10.0-5000	5	10	2.4	3.0	102.7 ± 3.2	18

4.3.3 Urinary BD concentrations in occupationally exposed workers and the corresponding controls.

In order to test the applicability of the new method to human bio-monitoring, the concentrations of MHBMA, DHBMA and THBMA were determined in after-work urine samples of 72 workers in a BD and SBR production facility in Czech Republic. Among 72 workers, 40 were administrative workers (21 male and 19 female) with minimal exposure to BD (<0.03 mg/m^3) and 32 were workers in BD production unit (16 male and 16 female, 0.05-1.5 mg/m^3). Each worker's individual exposure to BD was monitored separately during their work shifts with diffusive solid sorbent tubes *(85)*. This procedure was repeated on 10 different days over a 4-month interval, and the average BD exposure concentrations were determined. Average BD exposure concentration was 0.007 ± 0.005 mg/m^3 in control workers and 0.55 ± 0.50 mg/m^3 in exposed workers.

Urinary BD-mercapturic acids (MHBMA, DHBMA and THBMA) were detected in both control and exposed groups, but their concentrations were significantly greater in samples from occupationally exposed individuals as compared to controls (Figures 4.1, 4.2 and Table 4.2). For example, as demonstrated in Figure 4.1, HPLC-ESI^--MS/MS peak areas corresponding to MHBMA and DHBMA were much higher in exposed workers (Figure 4.1A) than in controls (Figure 4.1B). Similarly higher concentrations of THBMA were found in exposed workers as compared to controls (compare Figures 4.2A and 4.2B). A summary of urinary concentrations of MHBMA, DHBMA and THBMA and their metabolic ratio in control and exposed workers are given in Table 4.2.

Table 4.2 Mean urinary MHBMA, DHBMA, THBMA concentrations and metabolic ratios in exposed and control workers by sex

			Concentrations (ng/ml)			
	N	**BD exposure (mg/m^3)**	**MHBMA***	**DHBMA***	**THBMA***	**Metabolic Ratio***
Males						
Controls	21	0.007 ± 0.005^{a}	$9.9 \pm 11.2^{a,b}$	$1480.6 \pm 968.5^{a,b}$	$57.1 \pm 33.5^{a,b}$	0.007 ± 0.008^{a}
Exposed	16	$0.68 \pm 0.41^{a,c}$	$95.9 \pm 111.4^{a,c}$ (176.5 ± 228.3)^{e}	$3136.1 \pm 2560.3^{a,c}$ (5922.7 ± 4737.5)	$139.3 \pm 104.7^{a,c}$ (254.1 ± 152.1)	0.027 ± 0.026^{a} (0.07 ± 0.10)
Females						
Controls	19	0.007 ± 0.005^{d}	$3.1 \pm 4.8^{b,d}$	561.2 ± 531.5^{b}	24.2 ± 16.6^{b}	0.006 ± 0.007^{d}
Exposed	16	$0.32 \pm 0.34^{c,d}$	$8.3 \pm 8.1^{c,d}$ (44.3 ± 45.4)^{e}	716.1 ± 830.7^{c} (3251.3 ± 2907.5)	47.4 ± 70.9^{c} (232.2 ± 243.2)	0.017 ± 0.012^{d} (0.11 ± 0.14)

*Values in parenthesis ( ) are per unit dose of BD

[a]Male exposed significantly greater than male controls (Two way ANOVA test, p-value <0.01)
[b]Male controls significantly greater than Female controls (Two way ANOVA test, p-value <0.01)
[c]Male exposed significantly greater than Female exposed (Two way ANOVA test, p-value <0.01)
[d]Female exposed significantly greater than Female controls (Two way ANOVA test, p-value <0.05)
[e]Male exposed significantly greater than Female exposed (Two way ANOVA test, p-value <0.01)

Mean MHBMA concentrations in urine of BD-exposed female workers (8.3 ± 8.1 ng/ml) were significantly higher than those in control female workers (3.1 ± 4.8 ng/ml) ($p < 0.05$) (Table 4.2). An even greater difference was seen in male workers, with mean MHBMA concentrations of 95.9 ± 111.4 ng/ml (exposed) and 9.9 ± 11.2 ng/ml (controls) ($p = 0.001$). Interestingly, urinary MHBMA concentrations in males were significantly greater than in females for both groups ($p < 0.05$ for controls and $p = 0.005$ for occupationally exposed). This difference remained when the metabolite values were normalized to BD exposure concentrations (Table 4.2, numbers in parentheses). Taken together, these results indicate that occupational exposure to BD is reflected in significantly increased levels of MHBMA in human urine, with males excreting higher amounts of the metabolite than females.

Urinary concentrations of DHBMA (561.2 ± 531.5 ng/ml in control female workers and 716.1 ± 830.7 ng/ml in occupationally exposed females) were 20-30 times greater than MHBMA in the same samples (Table 4.2). Although DHBMA concentrations were higher in the female BD exposed workers as compared to the control group, the difference was not statistically significant ($p > 0.05$). Mean DHBMA concentrations in exposed males (3136.1 ± 2560.3 ng/ml) were significantly higher than in control males (1480.6 ± 968.5 ng/ml) ($p = 0.01$). Similar to our results for MHBMA, urinary DHBMA concentrations in males were higher than in females for both the controls ($p < 0.001$) and the occupationally exposed group ($p = 0.001$).

Mean THBMA concentrations in control and BD exposed females were 24.2 ± 16.6 ng/ml and 47.4 ± 70.9 ng/ml, respectively (Table 4.2). The corresponding values in

males were 57.1 ± 33.5 ng/ml (control males) and 139.3 ± 104.7 ng/ml (BD exposed males). No significant difference was seen between THBMA concentrations between exposed and control groups in females. However, in males, the urinary THBMA concentrations were significantly higher in exposed group as compared to the controls ($p = 0.001$). Furthermore, THBMA concentrations in males were higher than females in control ($p < 0.001$) as well as the exposed group ($p < 0.01$).

Metabolic ratio calculated as MHBMA/(MHBMA+DHBMA+THBMA) can be used as an indicator of fraction of BD undergoing bioactivation via the CYP450 pathway. As shown in Table 4.2, the metabolic ratio was significantly higher in BD exposed group than in control group in both females and males ($p < 0.005$). However, there were no gender differences in the BD metabolic ratio. Overall, urinary concentrations of all three BD urinary metabolites were present in significantly higher concentrations in urine of exposed workers as compared to controls.

4.3.4 Correlation studies

Multiple regression analyses were conducted to reveal any associations of urinary biomarkers with gender, BD exposure concentration, cigarette pack years, and current smoking status. Among the four factors, significant correlation was found between BD urinary metabolites (MHBMA, DHBMA and THBMA) and BD exposure ($p < 0.005$). Additionally, MHBMA and DHBMA concentrations were associated with current smoking status ($p < 0.05$). Linear regression analyses were conducted to further understand the association between BD mercapturic acids concentrations/metabolic ratio and BD exposure. We found that urinary MHBMA concentrations and metabolic ratio in

individual workers significantly correlated with BD exposure (Figure 4.4). Additionally, DHBMA and THBMA concentrations were significantly associated with BD exposure, suggesting that occupational exposure to BD leads to the increased formation of EB, HMVK and EBD, which are excreted in urine as MHBMA, DHBMA and THBMA.

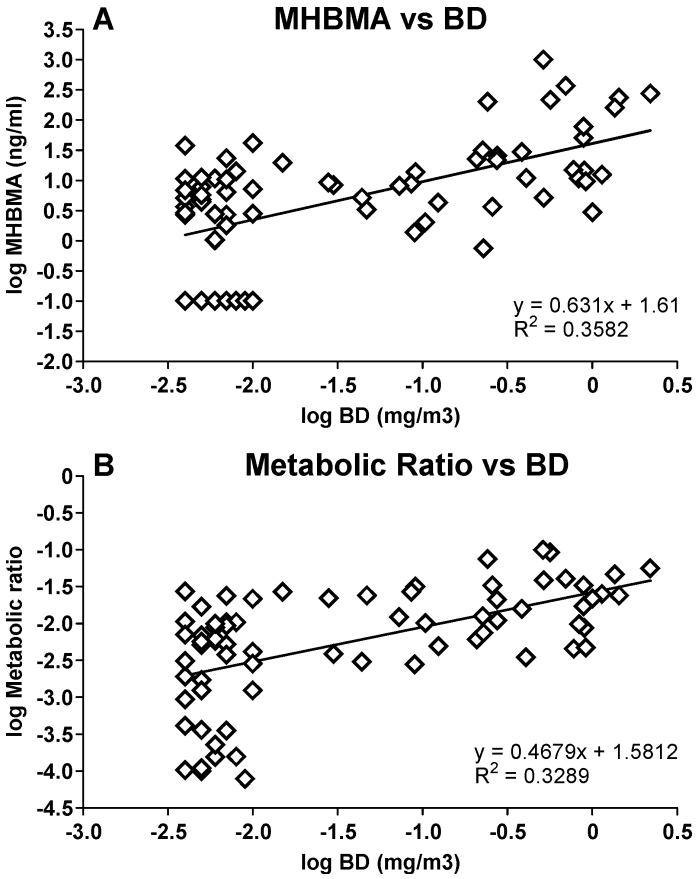

Figure 4.4 Associations between urinary MHBMA/metabolic ratio and BD exposure

Pearson correlation coefficients were computed to determine the correlation between BD mercapturic acids (MHBMA, DHBMA and THBMA), BD-hemoglobin adducts (THB-Val, *pyr*-Val) and *hprt* mutation frequencies (Table 4.3, Figure 4.5). Significant correlation was found between MHBMA and DHBMA ($r = 0.742$, $p < 0.001$), MHBMA and THBMA ($r = 0.419$, $p < 0.001$) (Table 4.3, Figure 4.5), and DHBMA and THBMA ($r=0.594$, $p<0.001$) (Table 4.3). These results are consistent with the fact that all three metabolites originate from BD exposure. MHBMA and DHBMA concentrations were also significantly correlated with both THB-Val and *pyr*-Val concentrations (Table 4.3). As predicted, THBMA was strongly associated with THB-Val (Table 4.3), since both originate from EB-diol (Scheme 1.1 and Scheme 1.2). In contrast, the correlation between THBMA and *pyr*-Val was not significant ($p=0.07$), probably because THBMA originates from EB-diol, while *pyr*-Val in formed from DEB (Scheme 1.1 and Scheme 1.2, Table 4.3). The Pearson correlation coefficient for all these associations were between 0.45-0.75, with a p-value <0.001. These observations reveal a correlation between and among the three BD-mercapturic acids and also between BD-mercapturic acids and BD-DNA adducts. In contrast, no correlation was found between BD-urinary mercapturic acids and *hprt* mutation frequencies (Table 4.3).

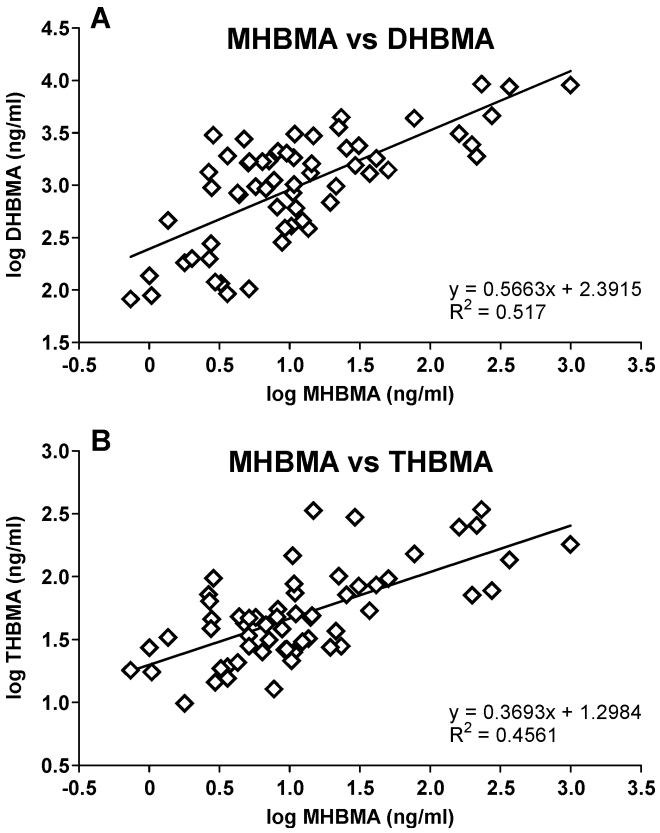

Figure 4.5 Associations between MHBMA and DHBMA/THBMA

Table 4.3 Association between and among all BD biomarkers determined by Pearson correlation analysis (p-values)

	MHBMA	**DHBMA**	**THBMA**	**THB-Val**	***pyr*-Val**	***hprt* mutation Frequency**
MHBMA	NA	<0.001	<0.001	0.007	<0.001	None
DHBMA	<0.001	NA	<0.001	<0.001	<0.001	None
THBMA	<0.001	<0.001	NA	<0.001	*0.07*	None

NA: Not Applicable
None: No significant association observed

4.3.5 Ethnic differences in BD metabolism (Multi-ethnic Study # 1)

In our first multi-ethnic study, MHBMA and DHBMA concentrations were determined in urine of smokers belonging to European American, Native Hawaiian and Japanese American ethnic groups (N=200 group). Urinary MHBMA and DHBMA concentrations (g/ml) were normalized to creatinine. Additionally, the BD metabolic ratios (MHBMA/MHBMA+DHBMA) were also determined. Mean urinary MHBMA concentrations in European American, Native Hawaiian and Japanese American smokers were 6.7, 5.3 and 4.4 ng/mg creatinine, respectively (Table 4.4). MHBMA concentrations differed significantly by race/ethnicity ($p = 0.0002$). This ethnic difference was observed in both sexes (males: $p = 0.006$ and females: $p = 0.03$). Mean DHBMA concentrations in European American, Native Hawaiian and Japanese American smokers were 552.8, 488.5 and 506.9 ng/mg creatinine (Table 4.4). No differences in DHBMA were observed among the three different ethnic groups in either sex ($p > 0.05$).

The mean values of BD metabolic ratio in samples from European American, Native Hawaiian and Japanese American smokers were 0.012, 0.011 and 0.009, respectively. Similar to MHBMA, the metabolic ratio also differed by race/ethnicity ($p = 0.005$) (Table 4.4). However, when stratified by sex, the metabolic ratios were only significantly different among the three ethnic groups in females ($p < 0.05$). The observed differences were not due to differences in age or smoking status as all the means were adjusted to age, BMI, nicotine equivalents.

Table 4.4 Geometric means of MHBMA, DHBMA and metabolic ratio, stratified by race/ethnicity and sex (Multi-ethnic study # 1)

		MHBMA (ng/mg Cr)		DHBMA (ng/mg Cr)		metabolic ratio	
	N	geometric means (95% CI)*		geometric means (95% CI)*		geometric means (95% CI)*	
All**							
Japanese Americans	196	4.4	(3.8-5.1)	506.9	(462.1-556.0)	0.009	(0.007-0.010)
Native Hawaiian	193	5.3	(4.6-6.2)	488.5	(444.7-536.7)	0.011	(0.009-0.012)
European Americans	195	6.7	(5.8-7.8)	552.8	(504.3-606.0)	0.012	(0.011-0.014)
p-value[†]			**0.0002**		0.17		**0.005**
Men							
Japanese Americans	96	4.4	(3.6-5.4)	456.9	(392.2-532.4)	0.01	(0.008-0.012)
Native Hawaiian	93	5.1	(4.2-6.3)	471.6	(402.4-552.7)	0.011	(0.009-0.013)
European Americans	95	6.9	(5.7-8.4)	525.5	(451.1-612.3)	0.013	(0.011-0.016)
p-value[†]			**0.006**		0.41		0.14
Females							
Japanese Americans	100	4.4	(3.6-5.4)	561.1	(503.8-625.0)	0.008	(0.006-0.009)
Native Hawaiian	100	5.4	(4.4-6.7)	509.4	(457.5-567.3)	0.01	(0.009-0.013)
European Americans	100	6.6	(5.4-8.2)	579.2	(520.7-644.2)	0.011	(0.009-0.014)
p-value[†]			**0.03**		0.23		**0.03**

*Means are adjusted for age at urine collection, BMI (natural log), nicotine equivalents (natural log)

**Also adjusted for sex

[†]P-value is comparing the difference across the three race/ethnicities

4.3.6 Ethnic differences in BD metabolism (Multi-ethnic Study # 2)

In the second multiethnic study, MHBMA and DHBMA concentrations were determined in urine of smokers belonging to African American and European American ethnicity (N = 450 per group). Urinary MHBMA and DHBMA concentrations were normalized to creatinine, and the metabolic ratio was also determined. Among 900 subjects, 107 samples were removed either because of unusually low nicotine equivalents, lack of co-variate data (QC samples) or due to genotype filters. The differences between the two ethnic groups were determined by Wilcoxon parametric test. As shown in Table 4.5, the median MHBMA concentrations in European Americans (11.2 ng/mg creatinine) were significantly higher ($p = 0.0003$) than in African American smokers (8.9 ng/mg creatinine). DHBMA concentrations and metabolic ratios were also higher in the European American smokers, but the difference is not statistically significant.

Preliminary GWAS showed a strong association between MHBMA and 22 single nucleotide polymorphisms (SNPs) on chromosome 22. The genes that might be responsible for the differences in MHBMA among the ethnic groups are GSTT1, GSTT2, D-dopachrome decarboxylase (DDT) and macrophage migration inhibitory factor (MIF). Similar results were observed with metabolic ratio which correlated with 19 SNPs on chromosome 22, potentially with genes GSTT2, DDT and MIF. However, there were no associations between DHBMA and any genetic polymorphisms. These results are preliminary and further investigation needs to be performed.

Table 4.5 Median MHBMA, DHBMA concentrations and metabolic ratio, stratified by race/ethnicity (Multi-ethnic study #2)

	MHBMA (ng/mg Cr)	**DHBMA (ng/mg Cr)**	**Metabolic Ratio**
European American (N=435)	11.2	547.3	0.019
African American (N=358)	8.9	513.4	0.018
p-value	**0.0003**	0.08	0.10

4.4 Discussion

The availability of sensitive, robust, and high throughput methodologies for monitoring human exposure to butadiene (BD) is essential in human risk assessment and molecular epidemiology studies. Although multiple HPLC-ESI-MS/MS methods have been previously described for quantification of BD-mercapturic acids in humans (Table 1.5) *(33;96;97;99;102;105;107)*, many of these methods required at least 0.5 ml of urine, and thus are not applicable to studies where the sample volume is limited.

Roethig et al. analyzed MHBMA and DHBMA in urine of 3,585 smokers and 1,077 non-smokers *(105)*. Unfortunately, the details of sample preparation were not available for that study *(105)*. MHBMA and DHBMA were determined separately with two different HPLC-MS/MS methods *(105)* that employed 0.5 ml and 0.2 ml of urine, respectively. The LOQ of the method was 0.1 ng/ml for MHBMA and 10.1 ng/ml for DHBMA (Table 1.5) *(105)*. The mean MHBMA concentrations in smokers and non-smokers were 3.61 and 0.3 µg/24 hr, respectively. The corresponding DHBMA concentrations were 556 and 391 µg/24 hr, respectively *(105)*.

Ding et al. reported an HPLC-MS/MS method for simultaneous determination of six mercapturic acid metabolites of volatile organic compounds including MHBMA and DHBMA in 100 µl of human urine *(104)*. The sample preparation involved dilution of urine and direct injection onto HPLC-ESI-MS/MS. The LOD of the method for MHBMA was 0.05 ng/ml (Table 1.5) *(104)*. However, MHBMA concentration in urine of non-smokers analyzed by this technique were unusually high (up to 73.2 ng/ml), and no

statistical significant differences were observed in the MHBMA concentrations (normalized to creatinine) between smokers and non-smokers *(104)*.

Most recently, Sterz et al. developed a sensitive UPLC-HILIC-MS/MS method for the quantification of both regioisomers of MHBMA (1-MHBMA and 2-MHBMA) in 100 µL of human urine *(110)* by hydrophilic interaction chromatography (HILIC). The LOQ values for 1-MHBMA and 2-MHBMA were reported 0.15 and 0.72 ng/ml, respectively (Table 1.5) *(110)*. However, DHBMA was not quantified in that study. Furthermore, when we attempted to employ HILIC methodology for BD-mercapturic acids in our laboratory, severe shifts in HPLC retention times were observed (results not shown), suggesting that this method is not suitable for high throughput analysis.

In the present study, we have developed a novel HPLC-ESI$^-$-MS/MS method for simultaneous quantification of two BD-mercapturic acids, MHBMA and DHBMA, in human urine. Some highlights of the current method are that it measures both metabolites simultaneously, requires only 200 µl of urine, and sample preparation is performed in a high throughput format by 96 well plate SPE. The current method has greater or comparable sensitivity than previously reported methods (Table 1.5) *(33;96;97;99;102;105;107)*. The LOD and LOQ of our HPLC-ESI$^-$-MS/MS method for MHBMA are 0.2 and 0.5 ng/ml, respectively, while the corresponding values for DHBMA are 5 and 10 ng/ml. Additionally, our method is highly accurate and reproducible (Table 4.1).

As an example of the method's applicability to human studies, MHBMA and DHBMA concentrations were determined in urine samples from workers at a BD and

SBR plant (40 controls and 32 exposed) available from an earlier study *(85)*. We found that urinary MHBMA concentrations in occupationally exposed workers were significantly higher as compared to controls (Table 4.2). DHBMA concentrations were also increased with BD exposure, but the difference was only statistically significant in males (Table 4.2). These results are consistent with earlier findings by Albertini *(85)*. In addition to MHBMA and DHBMA, we quantified the third BD-mercapturic acid recently discovered in our laboratory (THBMA, Scheme 1.1), which is a novel biomarker of BD formed from EBD. As observed for MHBMA and DHBMA, THBMA concentrations were increased in exposed group as compared to controls (Table 4.2).

Our results (Table 4.2) suggest that males excrete higher concentrations of MHBMA, DHBMA and THBMA in their urine than females. This is only partially explained by the fact that females are exposed to relatively lower BD concentrations (0.32 mg/m^3) as compared to males (0.68 mg/m^3), because gender differences for MHBMA remained after metabolite concentrations were normalized to BD exposure concentrations (Table 4.2). This suggests that females form significantly lower MHBMA per unit BD than males ($p < 0.05$). In contrast, DHBMA and THBMA concentrations per unit of BD were not significantly different among the two genders (Table 4.2). The metabolic ratio (MHBMA/(MHBMA+DHBMA+THBMA) was higher in males, but the difference is not statistically significant (Table 4.2). These results suggest that the relative utilization of detoxification pathways (conjugation vs. hydrolysis) is similar in both males and females. All three urinary BD-mercapturic acids (MHBMA, DHBMA, and THBMA) were strongly associated with BD exposure (Figure 4.4) ($p < 0.001$) Furthermore,

MHBMA, DHBMA, and their metabolic ratio correlated with the smoking status, consistent with previous study *(96;105)*. Additionally, strong correlations were found between MHBMA and other biomarkers of BD exposure, e.g. DHBMA, THBMA, THB-Val and *pyr*-Val (Figure 4.5, Table 4.3) *(84;89;99)*. Since this is the first time THBMA was quantified in urine of occupationally exposed workers, it was an important finding that THBMA concentrations correlated with MHBMA, DHBMA, and THB-Val (Table 4.3, Figure 4.5). Overall, there were strong associations between and among each of BD biomarkers suggesting that all of them reflect BD exposure. In contrast, there was no association between any of the BD mercapturic acids and *hprt* mutation frequency in the same individuals (Table 4.3).

In the first multi-ethnic study that included European American, Japanese, and Hawaiian smokers, significant differences in MHBMA concentrations and metabolic ratio were observed among the three ethnic groups (Table 4.4). Importantly, Japanese Americans, who have the lowest lung cancer risk among the there groups *(14)*, also excrete the lowest amounts of MHBMA and have low metabolic ratio. However, the highest concentrations of MHBMA and metabolic ratio were observed in European American smokers who are in the intermediate risk group *(14)*. These differences in MHBMA and metabolic ratio might be due to differences in frequency of genetic polymorphisms in the genes encoding the BD metabolizing enzymes. For example, the frequency of the *CYP2E1 DraI* variant allele was 6.6%, 33.3% and 15.4% in Caucasians, Japanese and Hawaiians, respectively *(219)*. The frequency of the *CYP2E1 RsaI* allele was 2.0%, 25.6% and 16.2% in Caucasians, Japanese and Hawaiians, respectively *(219)*.

Correlations between genetic polymorphisms and BD urinary metabolites will provide further insights into differences in BD metabolism.

In the second multi-ethnic study, we found significant differences in MHBMA concentrations between the European American and African American smokers, with the highest concentrations found in the former group (Table 4.5). Preliminary GWAS analysis revealed a strong association between MHBMA and 22 SNPs on chromosome 22. This chromosome houses the GSTT1 gene, which along with GSTM1 is involved in the detoxification of EB (precursor to MHBMA) *(220)*. No ethnic/racial differences in DHBMA concentrations were observed in both the studies. This is not surprising given the fact that DHBMA is present endogenously in very high concentrations in non-smokers *(33)*.

In conclusion, we report a robust, sensitive, high throughput HPLC-ESI$^-$-MS/MS method for quantification of MHBMA and DHBMA in human urine. The applicability of the new method was demonstrated in urine samples from workers employed at a BD-SBR production facility. We found that urinary BD-mercapturic acids concentrations were strongly associated with BD exposure. We also observed that MHBMA concentrations (adjusted per unit of BD exposure) were significantly higher in males as compared to females, suggesting that there might be gender differences in metabolism of BD in humans. The novel method was successfully applied to two large multiethnic cohort studies, leading to identification of significant ethnic/racial differences in metabolism of BD. Future studies will focus on identifying any correlations between genetic polymorphisms and BD urinary metabolites.

V. TRANSLESION SYNTHESIS ACROSS 1,N^6-(2-HYDROXY-3-HYDROXY METHYLPROPAN-1,3-DIYL)-2′-DEOXYADENOSINE (1,N^6-γ-HMHP-dA) ADDUCTS BY HUMAN AND ARCHEBACTERIAL DNA POLYMERASES

Reprinted with permission from: Srikanth Kotapati, Leena Maddukuri, Susith Wickramaratne, Uthpala Seneviratne, Melissa Goggin, Matthew G Pence, Peter Villalta, F. Peter Guengerich, Lawrence Marnett and Natalia Y. Tretyakova. *J Biol Chem.* (2012) 287, 38800-38811.

5.1 Introduction

Cellular DNA is constantly damaged by physical and chemical factors, including reactive oxygen species, lipid peroxidation products, UV light, environmental pollutants, and dietary carcinogens *(221)*. If not repaired, the resulting DNA adducts can block the progression of replicative DNA polymerases along the damaged strand *(122;222)*. In this case, a specialized group of polymerases, translesion synthesis polymerases (TLS), are recruited to the damaged site and can carry out DNA polymerization across the lesion (Figure 1.2) *(223;224)*. Five TLS DNA polymerases are primarily involved in translesion synthesis in humans: hPol η, hPol ι, hPol κ, Rev1 from the Y family and hPol ζ from the B family of polymerases *(121;225;226)*. The archebacterial translesion DNA polymerase from *Sulfolobus solfataricus* P2 (Dpo4) has been widely used as a model TLS polymerase for kinetic and structural studies of DNA lesions due its ready availability and its functional similarity to human hPol η *(164;227)*. This damage tolerance mechanism allows the cell to overcome replication blocks induced by bulky lesions such as UV-induced thymine dimers, facilitating cell survival. However, TLS polymerases are less catalytically efficient than replicative DNA polymerases and have a relatively low

fidelity due to an increased size and flexibility of their active sites *(120;123;124;127;228)*.

An important DNA lesion that occurs upon exposure to the human carcinogen 1,3-butadiene (BD) is 1,N^6-(2-hydroxy-3-hydroxymethylpropan-1,3-diyl)-2′-deoxyadenosine (1,N^6-γ-HMHP-dA) and its isomer 1,N^6-(1-hydroxymethyl-2-hydroxypropan-1,3-diyl)-2′-deoxyadenosine (1,N^6-α-HMHP-dA) (Scheme 5.1) *(48)*. BD is an important industrial chemical widely used in the production of synthetic rubber, resins, and polymers; as well as an environmental contaminant present in cigarette smoke, automobile exhaust, and urban air *(26)*. BD is metabolically activated to 1,2,3,4-diepoxybutane (DEB), which can alkylate adenine residues of DNA to give 1,N^6-HMHP-dA *(48)*. HPLC-ESI$^+$-MS/MS analysis of DEB-treated calf thymus DNA revealed a concentration-dependent formation of 1,N^6-α-HMHP-dA and 1,N^6-γ-HMHP-dA adducts *(48)*. Under physiological conditions, the two lesions interconvert *via* a Dimroth rearrangement-like mechanism *(48)*. Both isomers of 1,N^6- HMHP-dA have been detected in liver, lung, and kidney tissues of laboratory mice exposed to 6.25-625 ppm BD *(67)*. Although these lesions are less abundant than guanine monoadducts and guanine-guanine cross-links of DEB, they are persistent in mouse tissues for at least 10 days, suggesting that they may contribute to the biological effects of BD *(185)*.

Since both the N^6 and the N-1 positions of adenine in 1,N^6-HMHP-dA adducts are blocked by the HMHP exocycle, they can no longer be used to form complementary hydrogen bonds with dT. Structurally related *1,*N^6-ethenodeoxyadenosine (*1,*N^6 -εdA) adducts are known to adopt the *syn* conformation about the glycosidic bond, allowing

them to mispair with protonated dC in the active site of human DNA polymerase *ι (229)*. We therefore hypothesized that 1,N^6-HMHP-dA adducts can similarly form Hoogsteen base pairs with dG and protonated dA, potentially leading to A→T and A→C transversions, respectively. Such mispairing could explain the mutational spectra observed upon treatment of cells and laboratory animals with BD and DEB *(35;177;230)*.

The main aim of the present study was to investigate the ability of human TLS polymerases to carry out DNA synthesis past site-specific (*R*,*S*) 1,N^6-*γ*-HMHP-dA lesions. We have determined steady-state kinetic parameters for nucleotide insertion opposite the lesion and identified primer extension products following *in vitro* replication in the presence of polymerases *κ* , *η* , *ι*, and Dpo4. Our results indicate that hPol *κ*, hPol *η*, and Dpo4 are able to bypass (*R*,*S*) 1,N^6-*γ*-HMHP-dA lesions and to extend the primer beyond the damaged site by incorporating either correct (T) or incorrect base (A or G) opposite the adduct, along with introducing -1 and -2 frameshift mutations. In contrast, replicative hPol *β* is completely blocked by the lesion, and hPol *ι* inserts correct nucleotide, but is unable to extend past the lesion site.

Scheme 5.1 Formation of 1,N^6-γ-HMHP-dA and 1,N^6-α-HMHP-dA adducts from 1,2,3,4-diepoxy butane (DEB)

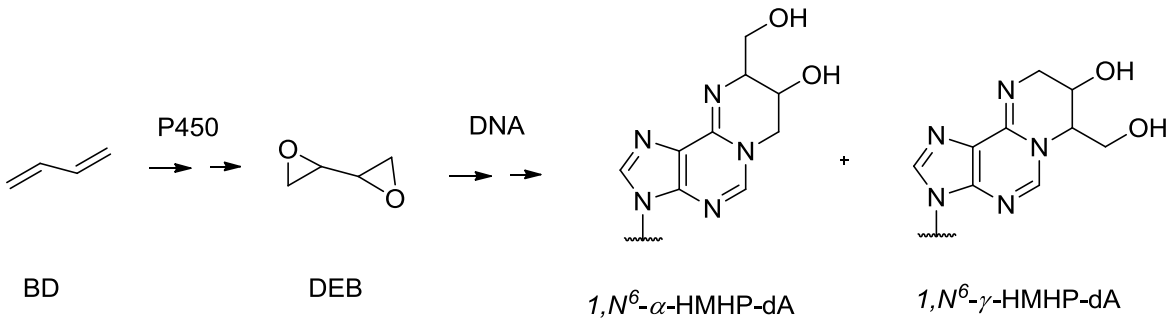

5.2 Experimental Procedures

Materials. Full-length recombinant hPol η, hPol κ, and hPol ι enzymes used for steady-state kinetic experiments were obtained from Enzymax (Lexington, KY). Recombinant human DNA Pol κ (amino acids 19-526), recombinant human DNA Pol ι (amino acids 1-420), and recombinant human Pol η (amino acids 1-437) employed in full length primer extension and mass spectrometry experiments were expressed and purified as described previously *(231-233)*. Dpo4 polymerase was expressed and purified by Professor Michael Stone (Vanderbilt University) as per the previously published methodology *(164)*. hPol β was purchased from Trevigen (Gaithersburg, MD). T4 polynucleotide kinase and *E.coli* uracil DNA glycosylase (UDG) were obtained from New England Biolabs (Beverly, MA). [γ-^{32}P]ATP was purchased from Perkin-Elmer Life Sciences (Boston, MA). The unlabeled dNTPs were obtained from Omega Bio-Tek (Norcross, GA). 40% 19:1 Acrylamide/Bis Solution was purchased from Bio-Rad laboratories (Hercules, CA). All the other chemicals and reagents were obtained from Sigma-Aldrich (St. Louis, MO) and Fisher Scientific (Pittsburgh, PA). Urea, Sigmacote, Tris, boric acid, ammonium acetate, formamide, bovine serum albumin (BSA), dithiothreitol (DTT), magnesium chloride, and N,N,N′,N′-tetramethylethylenediamine were purchased from Sigma Aldrich. Ammonium persulfate, acetonitrile and EDTA were obtained from Fisher Scientific.

Oligonucleotide synthesis. 18-mer oligodeoxynucleotide templates containing site- and stereospecific (*R,S*) 1,N^6-γ-HMHP-dA lesions at the 5th position (5'-TCATXGAATCCTTCCCCC-3') were synthesized by the post-oligomerization methodology developed in our laboratory *(186)*. Briefly, 18-mer oligodeoxynucleotides containing site-specific 6-chloropurine at position X were coupled with (*R,R*)-*N*-Fmoc-1-amino-2-hydroxy-3,4-epoxybutane to generate the corresponding oligomers containing site- and stereospecific (*R,R*)-N^6-(2-hydroxy-3,4-epoxybut-1-yl) adenine (N^6-HEB-dA) adducts. N^6-HEB-dA-containing oligomers were isolated by HPLC and incubated in water at room temperature to allow the cyclization of (*R,R*)-N^6-HEB-dA to (*R,S*) 1,N^6-γ-HMHP-dA *(186)*. The corresponding unmodified 18-mer (5'-TCATAGAATCCTTCCCCC-3') and 13-mer primers (5'-GGGGGAAGGATTC-3', 5'-GGGGGAAGGAUTC-3') were purchased from Integrated DNA Technologies (Coralville, IA). All DNA strands were purified by HPLC, characterized by HPLC-ESI$^-$-MS/MS, and quantified by UV spectrophotometry.

Generation of Primer-template DNA Substrate for *In Vitro* Assays. The 13-mer oligodeoxynucleotide primer (5'-GGGGGAAGGATTC-3') was 5'-end labeled in the presence of γ^{32}-P-ATP (>6000 Ci/mmol) and T4 polynucleotide kinase in 50 mM Na-MOPS buffer (pH 7.5), 10 mM $MgCl_2$, and 5 mM DTT for 1 h at 37 °C. Excess γ^{32}-P-ATP was removed by gel filtration through Bio-spin 6 filters (Bio-Rad). The ^{32}P – endlabeled primer was annealed to an equimolar amount of 18-mer oligodeoxynucleotide templates containing either dA or 1,N^6-γ-HMHP-dA (1:1 molar ratio) by heating at 95 °C for 3 min in the presence of 40 mM NaCl, followed by slow cooling overnight.

Reaction conditions for Enzyme Assays. Primer extension assays and steady state kinetics experiments were conducted for each of the five DNA polymerases (hPol *β*, hPol *η*, hPol *κ*, hPol *ι* and Dpo4). The assays were conducted at 37 °C in buffered solutions containing 50 mM Na-MOPS (pH 7.5), 50 mM NaCl, 5 mM DTT, 100 µg/ml BSA, 10% glycerol (v/v) with 50 nM radiolabeled primer-template complexes, and 5 nM of polymerase enzymes (except for Dpo4 which was used at 25 nM and hPol *β,* 2 units). The reactions were initiated by the addition of individual nucleotides or a mixture of all four dNTPs and $MgCl_2$ (final concentration, 5 mM). The reactions were stopped after pre-selected time intervals by the addition of 36 µL of stop solution (95% formamide (w/v), 10 mM EDTA, 0.03% bromophenol blue (w/v), 0.03% xylene cyanol (w/v)) to a 4 µl aliquot of the sample.

Primer Extension Assays. ^{32}P-endlabeled primer/template complexes containing either unmodified dA or 1,N^6-*γ*-HMHP-dA at position X of the template strand were incubated with DNA polymerases as described above in the presence of all four dNTPs (500 µM) for 0-60 minutes. The reaction products were separated on a 20% (w/v) denaturing polyacrylamide gel containing 7 M urea at a constant voltage (2500 V) for 3 h. The radioactive products were visualized with a phosphorimager (Bio-Rad).

Steady-state Kinetics Analyses. ^{32}P-endlabeled primer/template complexes were incubated with TLS polymerases in the presence of increasing concentrations of individual dNTPs (0-800 µM) for 0-60 minutes. The resulting oligodeoxynucleotide products were separated by gel electrophoresis as described above and visualized with a phosphorimager. DNA amounts in each band were quantified with Quantity One image

software (Bio-Rad), and the steady-state kinetic values were determined by plotting product formation versus dNTP concentration by nonlinear regression analysis (one-site hyperbolic fits in GraphPad Prism).

HPLC-ESI-MS/MS analysis of primer extension products from DNA polymerase reactions. Oligodeoxynucleotide 18-mers (5'-TCATXGAATCCTTCCCCC-3', where X = dA or (*R,S*) 1,N^6-γ-HMHP-dA) were annealed to the 13-mer primer (5'-GGGGGAAGGAUTC-3') (100 pmol each) in 20 µl 50 mM NaCl to form template-primer complexes. The resulting partial duplexes were incubated with individual DNA polymerases (hPol κ, 40 pmol; hPol η, 40 pmol; or Dpo4, 100 pmol) in 50 mM Tris-HCl (pH 7.8) buffer containing 5% glycerol, 5 mM DTT, 5 mM $MgCl_2$, 100 µg/ml BSA at 37 °C for 4-6 hours. Primer extension reactions were initiated by the addition of all four dNTPs (1 mM each) in a final reaction volume of 75 µl. The reactions were terminated by removing excess dNTPs by size exclusion on a Bio-Spin 6 column (Bio-Rad). Tris-HCl, DTT and EDTA were added to the filtrate to restore their concentrations to 50 mM, 5 mM, and 1 mM, respectively.

In order to facilitate MS/MS analyses, oligodeoxynucleotide products were cleaved into smaller fragments by incubation with uracil DNA glycosylase (UDG, 6 units, 37 °C for 6 hours), followed by heating with 0.25 M piperidine at 95 °C for 1 hour *(176)*. The final solution was dried under vacuum, and the residue was reconstituted in 25 µl of water. 14-mer oligonucleotide (5'p-CTTCACGAGCCCCC-3'; 40 pmol) was added as an internal standard for mass spectrometry. The injection volume for mass spectrometric analysis was 8 µl. Primer extension products following reactions catalyzed

by hPol β (10 units) and hPol ι (80 pmol) were not cleaved with UDG/piperidine since only short extension products were observed that could be directly sequenced by MS/MS.

HPLC-ESI$^-$-MS/MS analysis was conducted on an Eksigent HPLC system (Eksigent, Dublin, CA) interfaced to a Thermo LTQ Orbitrap Velos mass spectrometer (Thermo Fisher Scientific, Waltham, MA). The instrument was operated in the negative ion ESI MS/MS mode. Polymerase extension products were separated with an Agilent Zorbax SB 300 C18 (0.5 x 150 mm, 5 µm) column using a gradient of 15 mM ammonium acetate (Buffer A) and acetonitrile (Buffer B). The column was eluted at a flow rate of 15 µl/min. The solvent composition was linearly changed from 1 to 10 % B in 18 min, further to 75% B in 2 min, held at 75% B for 3 min, and brought back to 1% B in 2 min and held at 1% B for 10 min. Under these conditions, all DNA oligodeoxynucleotides, including extension products, eluted between 10 and 13 minutes.

Electrospray ionization conditions were as follows: ESI source voltage, 3.5 kV; source current, 6.7 µA; auxiliary gas flow rate setting, 0; sweep gas flow rate setting, 0; sheath gas flow setting, 30; capillary temperature, 275 °C; and S-lens RF level, 50%. The most abundant ions from the ESI$^-$-FTMS spectra were selected and subjected to collision-induced dissociation (CID) analysis on the linear ion trap. The MS/MS conditions were as follows: normalized collision energy, 35%; activation Q, 0.250; activation time, 10 ms; product ion scan range, *m/z* 300-2000. The amount of each extension product was calculated by comparing peak areas corresponding to each product in extracted ion chromatograms with the peak area of the internal standard. Expected CID fragmentation patterns of oligonucleotides were obtained with the Mongo Oligo mass calculator v2.06

available from the Mass Spectrometry Group of Medicinal Chemistry at the University of Utah (http://library.med.utah.edu/masspec/ mongo.htm).

Scheme 5.2 Sequences of DNA substrates with (*R*,*S*) 1,N^6-γ-HMHP-dA adduct employed in primer extension assays

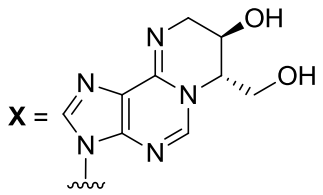

(*R*,*S*)-1,N^6-γ-HMHP-dA

DNA substrates used for gel electrophoresis:

5'-TCA T**X**G AAT CCT TCC CCC-3' (18 mer template)
3'- C TTA GGA AGG GGG-5' (13 mer primer)

5'-TCA T***A***G AAT CCT TCC CCC-3' (18-mer positive control)
3'- C TTA GGA AGG GGG-5' (13 mer primer)

DNA substrates used for LC-MS/MS analysis:

5'-TCA T**X**G AAT CCT TCC CCC-3' (18 mer template)
3'- C T***U***A GGA AGG GGG-5' (13 mer primer with U)

5'-TCA T***A***G AAT CCT TCC CCC-3' (18 mer positive control)
3'- C T***U***A GGA AGG GGG-5' (13 mer primer with U)

5.3 Results

5.3.1 Primer extension studies in the presence of all four dNTPs

Our initial studies investigated the ability of DNA polymerases to bypass 1,N^6-γ-HMHP-dA lesions in the presence of all four dNTPs. 1,N^6-γ-HMHP-dA was site-specifically incorporated into a 18-mer template (5'-TCATXGAATCCT TCCCCC-3', where X = 1,N^6-γ-HMHP-dA), which was annealed to a 13-mer primer (5'-GGGGGAAGGATTC-3'). In the resulting duplex (Scheme 5.2), the primer terminus is positioned immediately prior to the lesion site. The template-primer complexes were subjected to *in vitro* replication in the presence of hPol *β, η, κ, ι,* and Dpo4. Control experiments with template containing only native nucleotides (X = dA) confirmed a complete primer extension by hPol *β*, hPol *κ,* hPol *η*, and Dpo4, to form an 18-mer product (Left panels in Figures 5.1A and 5.2). In addition, some 19-mer products have also been observed with Dpo4 (Figure 5.2C, left panel), which could be attributed to template independent nucleotide incorporation (blunt end addition) as observed previously *(160;234).* hPol *ι* formed primarily a 16-mer product (Figure 5.1B) due to its low processivity as compared to other Y family polymerases *(235-238)*

The presence of 1,N^6-γ-HMHP-dA at position X led to a complete blockage of primer extension by hPol *β,* while hPol *ι* inserted a single nucleotide, but was unable to extend past the lesion site (right panels in Figure 5.1). In contrast, hPol *η* and hPol *κ* were able to extend the primer to the terminus, forming the expected 18-mer products (right panels in Figure 5.2). The efficiency of primer extension was markedly reduced in the presence of 1,N^6-γ-HMHP-dA as compared to unmodified dA, as evident by the presence

of incomplete extension products (15-mers, 16-mers, and 17-mers). No primer extension was observed in Dpo4 reactions with 1,N^6-γ-HMHP-dA-containing DNA template until the enzyme:DNA ratio was increased to 1:2.

To determine whether the incomplete extension products generated by hPol ι (which is stalled after the insertion of dTMP opposite the 1,N^6-γ-HMHP-dA adduct, Figure 5.1B) can be extended by hPol η or κ, ^{32}P-endlabeled primer/template complexes were first incubated in the presence of hPol ι, resulting in the extension of primer by one base to form a 14-mer product. Upon subsequent addition of hPol κ to the above reaction mixture, the 14-mer product was completely extended to form the expected 18-mer product (Figure 5.3). Similar results were obtained in the presence of hPol η (data not shown). This provides preliminary evidence for possible co-operativity of TLS polymerases during the replication of 1,N^6-γ-HMHP-dA-containing DNA, with hPol ι adding one nucleotide across the damaged base, polymerase switching, and hPol η or κ completing the bypass synthesis.

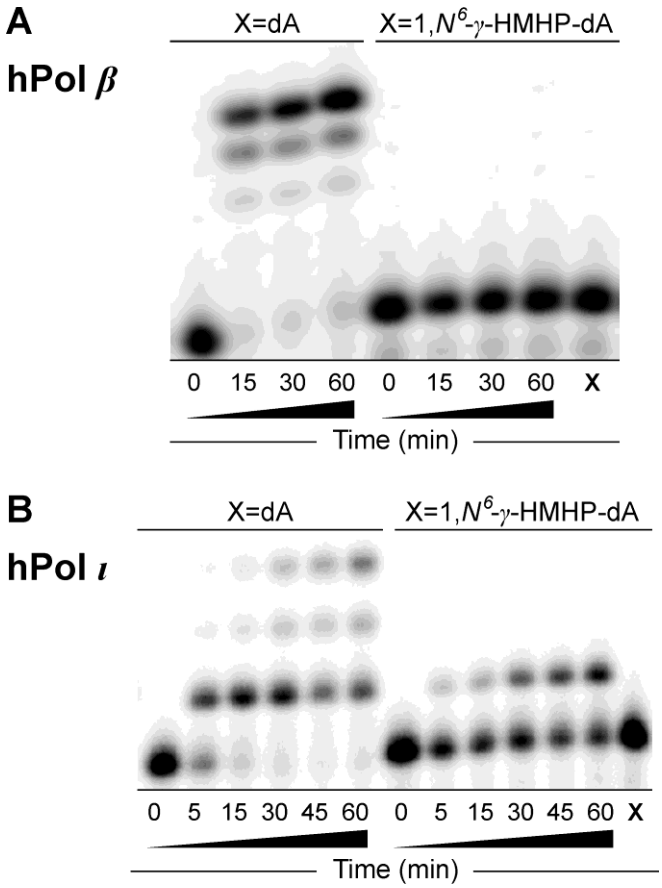

Figure 5.1 Primer extension opposite dA or 1,N6-γ-HMHP-dA adduct by hPol *β* and hPol *ι*

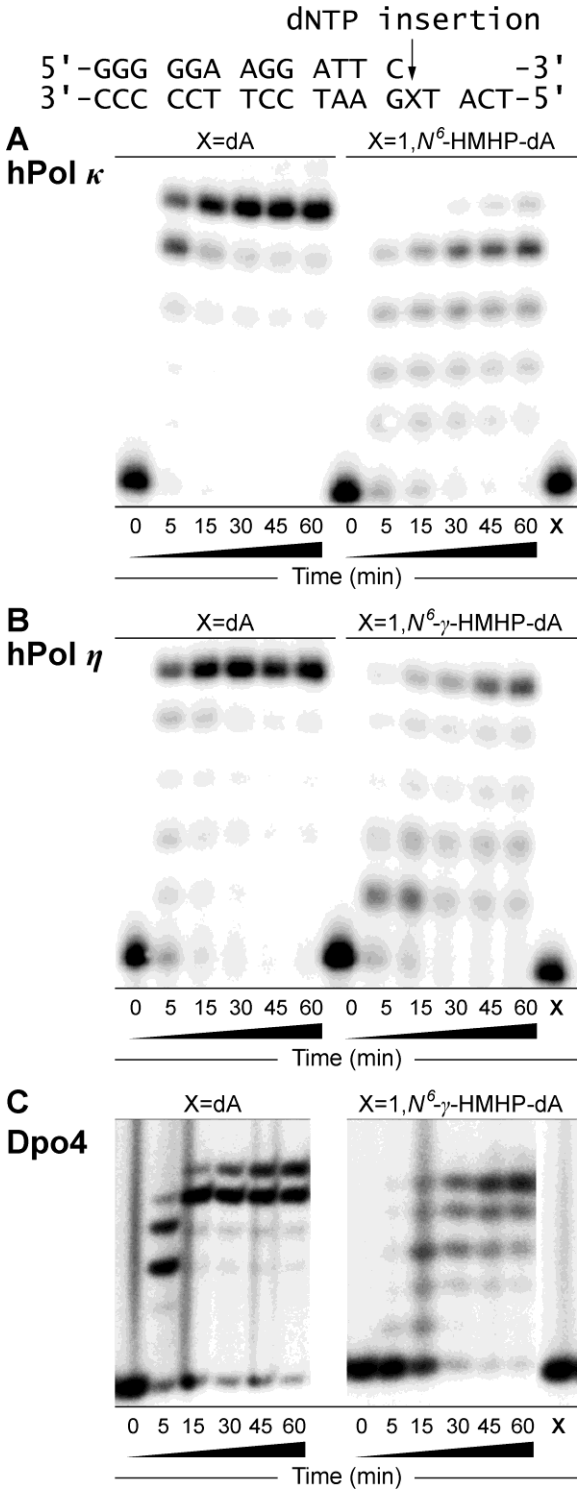

Figure 5.2 Primer extension opposite dA or 1,N^6-γ-HMHP-dA adduct by hPol η, hpol κ and Dpo4

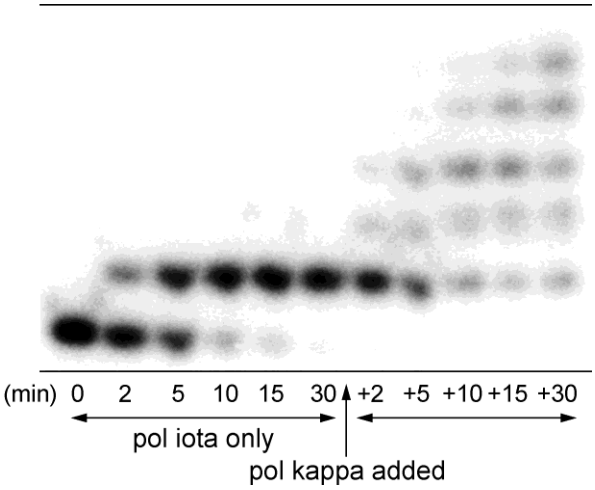

Figure 5.3 Cooperativity of human TLS polymerases ι and κ during the bypass of 1,N^6-γ-HMHP-dA adduct

5.3.2 Steady state kinetic analysis of dNTP incorporation opposite 1,N^6-γ-HMHP-dA adducts

Single nucleotide insertion assays were conducted in order to compare the rates of incorporation of each nucleotide opposite 1,N^6-γ-HMHP-dA lesion by individual TLS DNA polymerases. Template-primer complexes containing 1,N^6-γ-HMHP-dA or unmodified dA (control) were incubated with polymerase enzymes in the presence of each of the four individual dNTPs. Our pilot experiments have revealed that hPol η, hPol κ and Dpo4 incorporate dTMP, dAMP, and dGMP, but not dCMP, opposite the 1,N^6-γ-HMHP-dA lesion (Figure 5.4). hPol ι preferentially inserted dTMP opposite the lesion. Subsequently, the rates of incorporation of dAMP, dGMP, and dTMP opposite 1,N^6-γ-HMHP-dA by hPol η, hPol κ, and Dpo4 were determined in kinetic experiments. No kinetic analysis was possible for hPol β, since it was completely blocked by 1,N^6-γ-HMHP-dA (Figure 5.1). In the case of hPol ι, the kinetic experiments were limited to dTMP, since no incorporation of other nucleotides was observed. The insertion rate for each nucleotide was calculated by plotting reaction velocity against dNTP concentration. The kinetic results are summarized in Table 5.1, where the catalytic specificity constant (k_{cat}/K_m) provides a measure of catalytic efficiency for each dNTP insertion, while the misinsertion frequency (f) reflects the probability of insertion of an incorrect dNTP as compared to that of correct one (dTTP) .

Our kinetic data indicate that hPol η, hPol κ, and hPol ι polymerization rates for template-primer complexes containing 1,N^6-γ-HMHP-dA were 3-8 fold slower than for the control templates containing unmodified dA (Table 5.1). In the case of Dpo4, the

efficiency of incorporation of correct base (dTMP) opposite 1,N^6-γ-HMHP-dA was 600 fold lower than dT incorporation opposite unmodified dA. The preference order for the insertion of individual dNTPs opposite the 1,N^6-γ-HMHP-dA adduct by hPol η was T > G > A, with approximately 1.5-fold preference for incorporation of dTMP as compared to dGMP and dAMP (Table 5.1). A similar specificity (T > G > A) was observed for hPol κ, which was 1.5-fold more likely to incorporate dTMP rather than dGMP opposite the lesion and 5-fold more likely to insert dTMP rather than dAMP (Table 5.1). The preference order for Dpo4 was T > A > G, and this polymerase was 2- fold more likely to incorporate dTMP rather than dAMP and 3-fold more likely to incorporate dTMP rather than dGMP (Table 5.1).

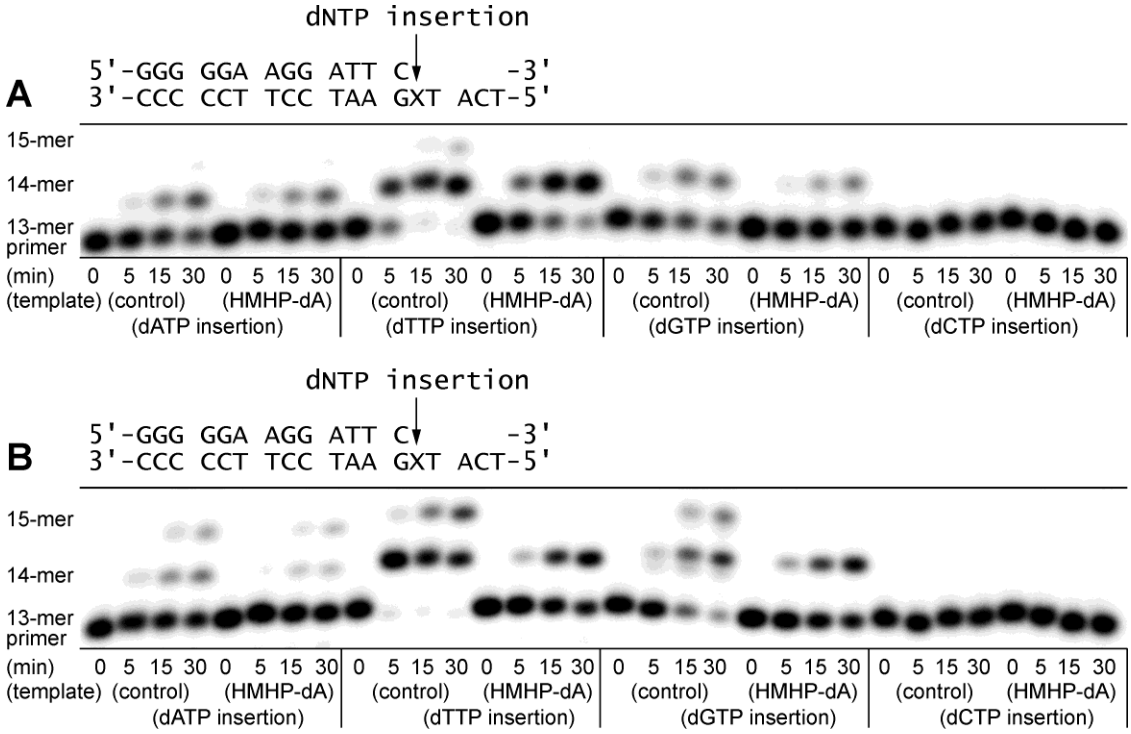

Figure 5.4 Single nucleotide insertion by hPol η (A) and hPol k (B) opposite unmodified dA (control) and 1,N^6-γ-HMHP-dA

Table 5.1 Steady-state kinetic parameters for single nucleotide incorporation opposite dA and 1,N^6-γ-HMHP-dA adduct

Polymerase	Template	incoming nucleotide	k_{cat} (min^{-1})	K_m (μM)	k_{cat}/K_m (μM^{-1} min^{-1})	f
hPol κ	dA	dTTP	0.3 ± 0.01	0.8 ± 0.1	0.38	1
		dATP	0.06 ± 0.005	20 ± 4.6	0.003	0.008
		dGTP	0.27 ± 0.01	73 ± 10.4	0.004	0.01
	1,N^6-γ-HMHP-dA	dTTP	0.3 ± 0.02	4.0 ± 1.0	0.07	1
		dATP	0.2 ± 0.004	13 ± 3.5	0.01	0.2
		dGTP	1.8 ± 0.008	35 ± 7.4	0.05	0.7
hPol η	dA	dTTP	1.6 ± 0.1	3.2 ± 0.9	0.5	1
		dATP	0.04 ± 0.002	5.6 ± 2.3	0.007	0.01
		dGTP	0.09 ± 0.02	35 ± 25	0.002	0.004
	1,N^6-γ-HMHP-dA	dTTP	0.6 ± 0.03	4.4 ± 1.2	0.14	1
		dATP	0.7 ± 0.03	9.2 ± 2.2	0.08	0.57
		dGTP	0.9 ± 0.04	10 ± 2.0	0.09	0.65
Dpo4	dA	dTTP	0.6 ± 0.03	2.8 ± 0.4	0.21	1
		dATP	0.05 ± 0.005	471 ± 112	0.00016	0.0004
	1,N^6-γ-HMHP-dA	dTTP	0.35 ± 0.04	979 ± 194	0.00035	1
		dATP	0.14 ± 0.05	884 ± 272	0.00016	0.45
		dGTP	0.07 ± 0.004	596 ± 77	0.00011	0.31
hPol ι	dA	dTTP	1.6 ± 0.2	21 ± 7	0.08	1
	1,N^6-γ-HMHP-dA	dTTP	0.06 ± 0.004	4.6 ± 1.5	0.01	1

* f is misinsertion frequency

5.3.3 LC-MS/MS Analysis of primer extension products

A mass spectrometry based strategy was employed to confirm the identities of nucleotides incorporated opposite 1,N^6-γ-HMHP-dA adduct by various DNA polymerases and to detect any insertion/deletion events. Synthetic template-primer complexes were incubated with individual polymerases in the presence of all four dNTPs, and the primer extension products were sequenced by capillary HPLC-ESI$^-$-MS/MS using an LTQ Orbitrap Velos instrument. Due to the high sensitivity of this method, 100 pmol of DNA was sufficient to obtain sequence information for the extension products.

Parallel reactions were conducted with unmodified and 1,N^6-γ-HMHP-dA containing template-primer complexes (Scheme 5.2, bottom). To facilitate MS analysis of the products, one of the thymine residues within the primer was substituted for uridine (5'-GGGGGAAGGAUTC-3') to allow for selective cleavage of the extension products with UDG/hot piperidine. This generates oligonucleotides (5-, 6- or 7-mers) that are short enough to be readily sequenced by HPLC-ESI-MS/MS*(164)*. However, the extension products from hPol β and hPol ι-catalyzed reactions were not cleaved since these polymerases generated short products by adding 0-1 nucleotides (Figure 5.1).

Each primer extension reaction mixture was analyzed twice. First, samples were analyzed by full scan HPLC-ESI$^-$-FTMS to detect the molecular ions corresponding to the expected extension products (Figure 5.5). In subsequent analysis, MS/MS spectra of these target ions were obtained (Figure 5.6). Tandem mass spectra of the observed oligodeoxynucleotides (Figures 5.7 and 5.8) were compared to the predicted CID spectra of each extension product to determine their nucleobase sequence.

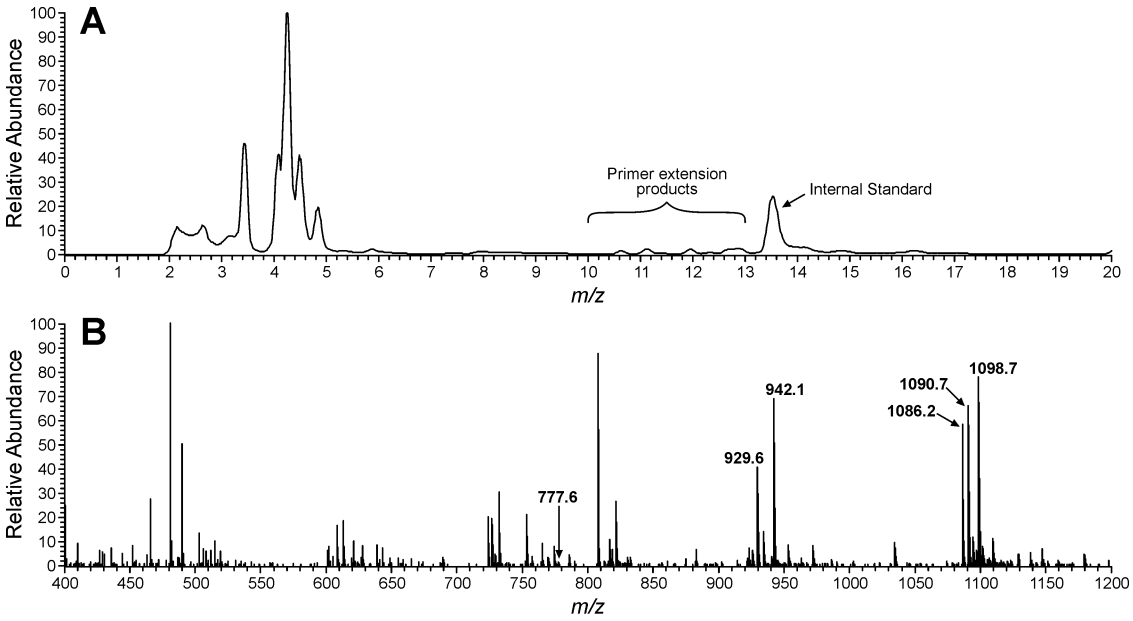

Figure 5.5 HPLC-ESI$^-$-MS/MS analysis of *in vitro* replication opposite 1,N^6-γ-HMHP-dA-adduct containing template by hPol κ

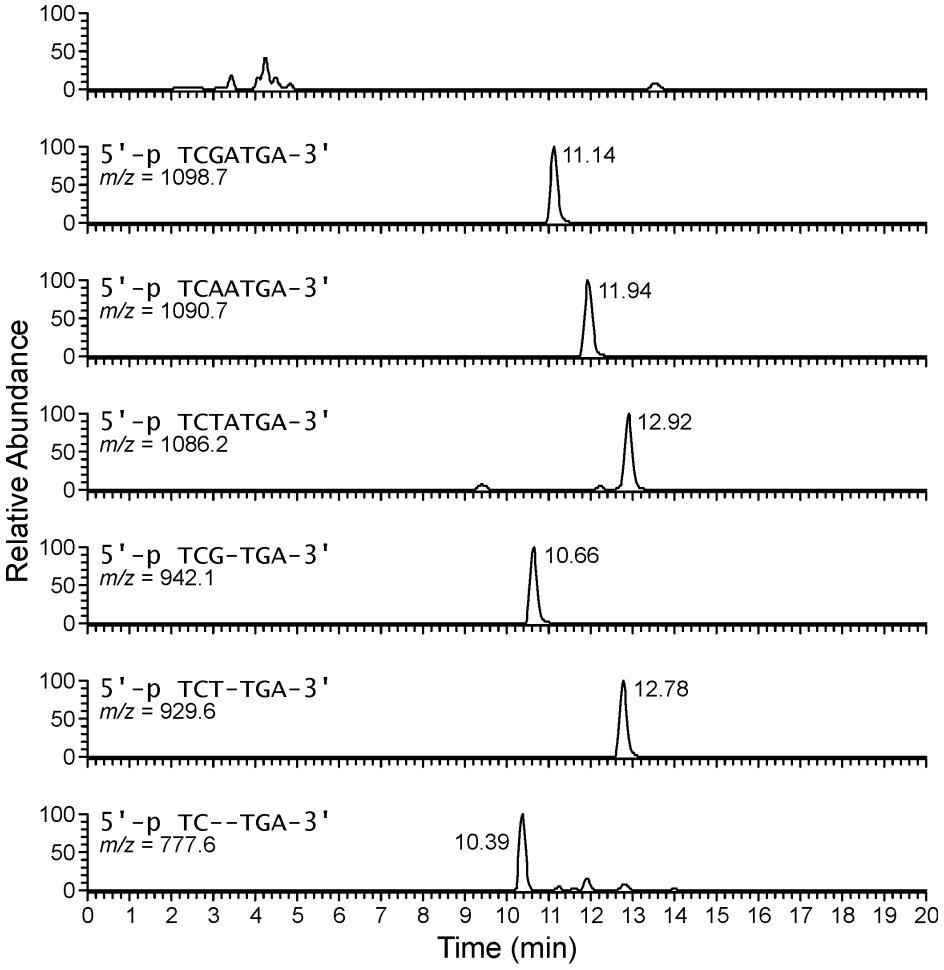

Figure 5.6 Extracted ion chromatograms of primer extension products opposite 1,N^6-γ-HMHP-dA- adduct template by hPol κ

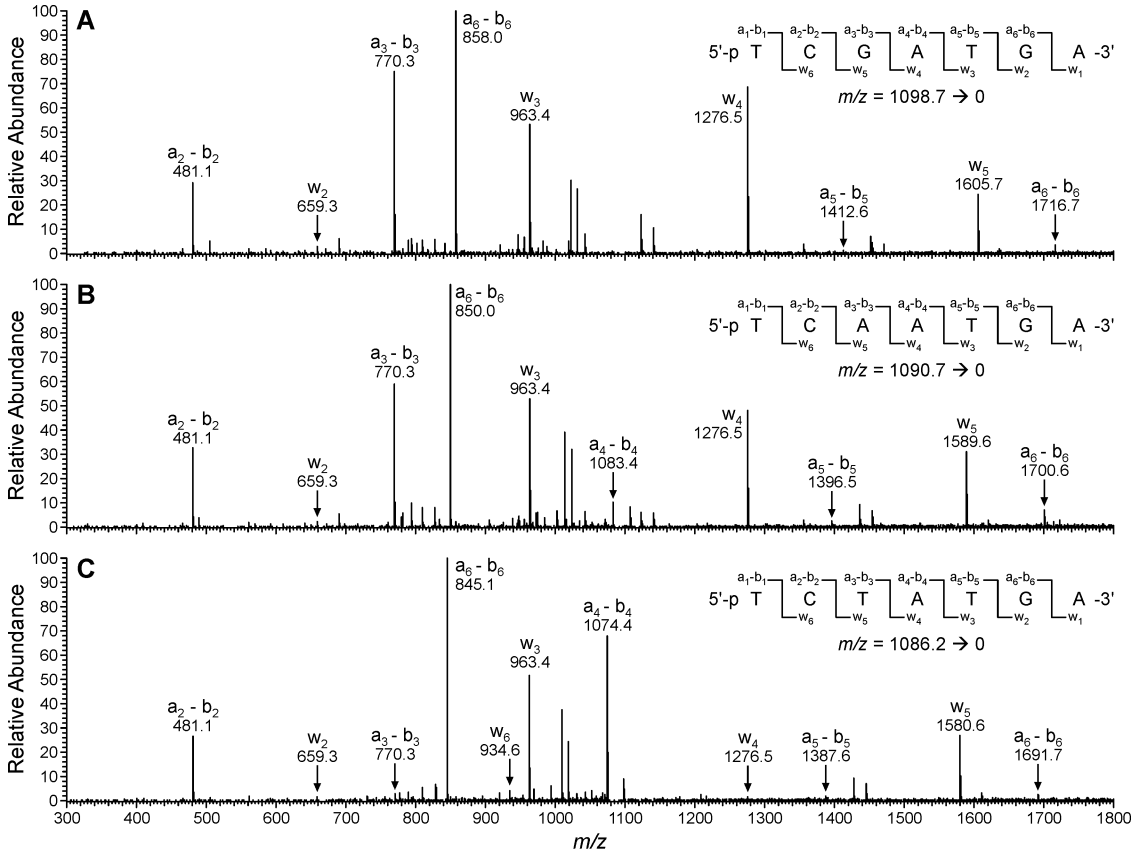

Figure 5.7 MS/MS spectra of full length primer extension products observed following *in vitro* replication of 1,N^6-γ-HMHP-dA-containing template by hPol κ

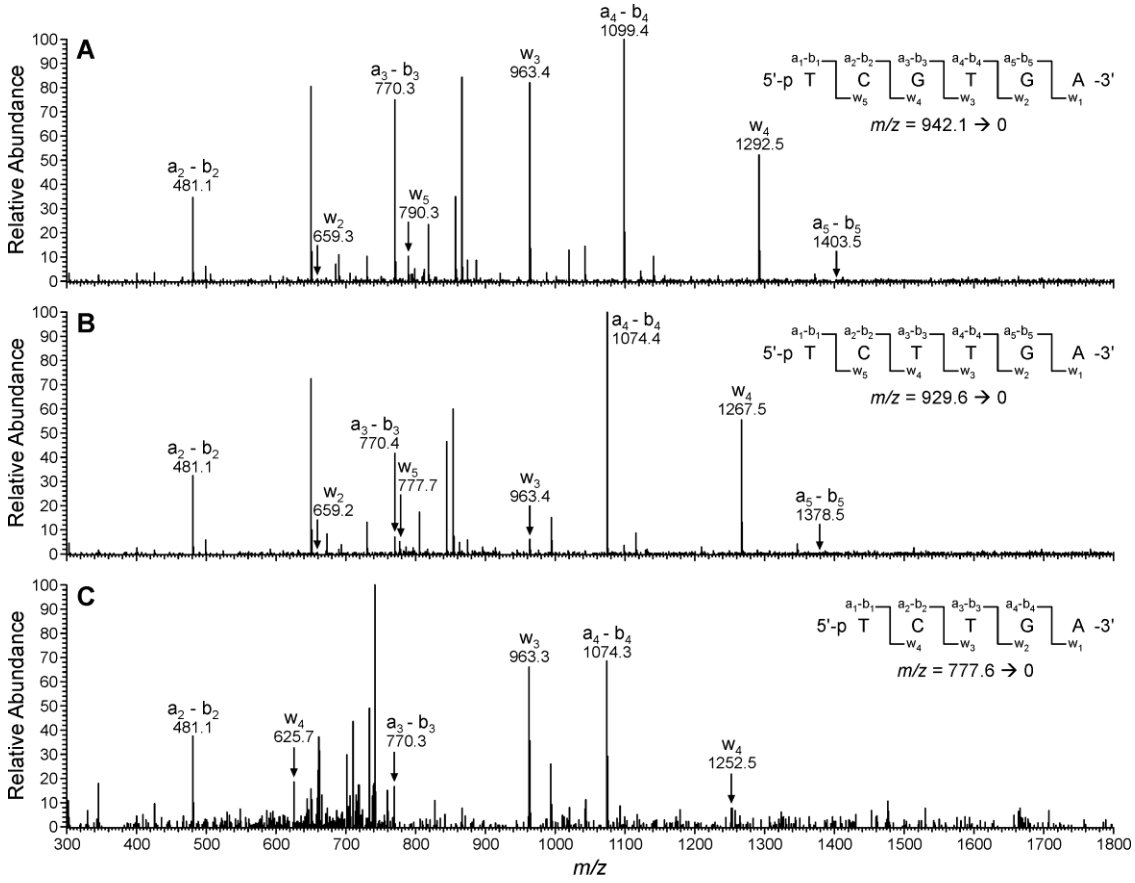

Figure 5.8 MS/MS spectra of -1 and -2 deletion products observed following *in vitro* replication of 1,N^6-γ-HMHP-dA-containing template by hPol κ

HPLC-ESI$^-$-MS/MS analysis of the hPol β reactions with unmodified template-primer complex and all four dNTPs revealed the presence of the fully extended primer (5'-GGGGGAAGGAUTC**TATGA**-3'; *m/z* 1406.23; $[M-4H]^{4-}$) as the major product (> 95%) (not shown). This is consistent with our previous observation (left panel in Figure 5.1A) that in the absence of the lesion, the primer is completely extended by hPol β. In contrast, the corresponding reaction mixtures from hPol β extension of 1,N^6-γ-HMHP-dA containing template:primer complexes contained mainly the unextended primer (5'-GGGGGAAGGAUTC-3'; *m/z* 1015.17; $[M-4H]^{4-}$) (results not shown). These results indicate that primer extension by human Pol β is completely blocked by the 1,N^6-γ-HMHP-dA lesion, in accordance with our previous observation from the gel electrophoresis analysis (right panel in Figure 5.1A).

HPLC-ESI$^-$-MS/MS analysis of the primer extension products produced upon incubation of 1,N^6-γ-HMHP-dA containing template:primer complexes with hPol κ has revealed six major peaks at *m/z*: 777.6, 929.6, 942.1, 1086.2, 1090.7, 1098.7 which correspond to the doubly charged ions of 5'-pTC__TGA-3', 5'-pTC**T**_TGA-3', 5'-pTC**G**_TGA-3', 5'-pTC**TA**TGA-3', 5'-pTC**AA**TGA-3', and 5'-pTC**GA**TGA-3', respectively (Scheme 5.3A, Figure 5.6). CID spectra of each extension product were obtained in order to determine their exact nucleobase sequence (Figures 5.7 and 5.8). This sequence information cannot be obtained from molecular weight only. For instance, the molecular weight of the doubly charged ions at *m/z* 1086.2 (M = 2175.4) is consistent with an oligonucleotide product containing three Ts, two As, one C, and one G. Extension products 5'p-TC**TA**TGA-3' (insertion of T opposite the lesion and A opposite

the next base) and 5'-p TC**A**TTGA-3' (insertion of A opposite the lesion and T opposite the next base) are indistinguishable by gel electrophoresis or MW. By comparing the CID spectra obtained from MS/MS analysis with the predicted CID fragments (a-B and w ions, Figure 5.7C, Table 5.2), the sequence of the product was determined as 5'p-TC**T**ATGA-3', with the correct base (T) inserted opposite the adduct. Detailed MS/MS analysis was conducted for each of the hPol κ extension products detected by HPLC-ESI$^-$-FTMS. According to HPLC-ESI$^-$-FTMS peak areas, 18% of the extension products were error-free, with the incorporation of correct base (T) opposite the lesion (Scheme 5.3A). Approximately 21% and 25% of the extension products were formed by misincorporation of dAMP and dGMP opposite the lesion, respectively. In addition, three deletion products were detected. 5'-pTC**G**_TGA-3' (22%) was formed as a result of misinsertion of G opposite 1,N^6-γ-HMHP-dA and deletion of the next base. 5'-pTC**T**_TGA-3' (13%) was formed upon incorporation of the correct base (T) opposite the lesion and skipping the next base. A minor -2 deletion product, 5'-pTC__TGA-3' (< 1%), was also detected, in which no base was incorporated opposite the lesion or the 3'-neighboring base. These results are summarized in Scheme 5.3A. Overall, our HPLC-ESI$^-$-FTMS results for hPol κ are consistent with the gel electrophoresis data, but revealed several additional products generated upon deletion of one or two bases.

Scheme 5.3 Summary of primer extension products opposite X= (*R*,*S*) 1,N^6-γ-HMHP-dA by hPol κ , hPol η and Dpo4

(A) hPol κ

```
                    TGA 3' <1%
                  T_TGA 3' 13%
                  G_TGA 3' 22%
                  TATGA 3' 18%
                  AATGA 3' 21%
                  GATGA 3' 25%
5' GGGGGAAGGAUTC
3' CCCCCTTCCTAAGXTACT 5'
```

(B) hPol η

```
                    TGA 3' <1%
                  T_TGA 3'  1%
                  G_TGA 3'  3%
                  AATGA 3'  6%
                  GATGA 3'  8%
                  TATGA 3' 81%
5' GGGGGAAGGAUTC
3' CCCCCTTCCTAAGXTACT 5'
```

(C) Dpo4

```
                  A_TGA 3'  2%
                  T_TGA 3'  5%
                  GATGA 3'  4%
                  AATGA 3' 30%
                  TATGA 3' 59%
5' GGGGGAAGGAUTC
3' CCCCCTTCCTAAGXTACT 5'
```

Table 5.2 Expected CID fragments of 5'-pTCTATGA-3'

n	ch	a-B	w	y	d-H2O
1	-1		330.217	250.237	303.189
	-2				151.090
2	-1	**481.274**	**659.427**	579.447	592.374
	-2	240.133	329.209	289.219	295.683
	-3				196.786
3	-1	**770.459**	**963.624**	883.644	896.571
	-2	384.725	481.308	441.318	447.781
	-3	256.147	320.536	293.876	298.185
	-4				223.386
4	-1	**1074.656**	**1276.834**	1196.854	1209.781
	-2	536.824	637.913	597.923	604.386
	-3	357.546	424.939	398.279	402.588
	-4	267.908	318.452	298.457	301.689
	-5				241.149
5	-1	**1387.866**	**1581.031**	1501.051	**1513.978**
	-2	693.429	790.011	750.021	756.485
	-3	461.950	526.338	499.678	503.987
	-4	346.210	394.501	374.506	377.738
	-5	276.766	315.399	299.403	301.989
	-6				251.489
6	-1	**1692.063**	1870.216	1790.236	1843.188
	-2	**845.527**	**934.604**	894.614	921.090
	-3	563.349	622.733	596.073	613.724
	-4	422.259	466.798	446.803	460.041
	-5	337.606	373.236	357.240	367.831
	-6	281.170	310.862	297.532	306.358
	-7				262.448

**Fragments found in the CID spectrum are shown in bold*

HPLC-ESI$^-$-MS/MS analysis of the primer extension products from hPol η -catalyzed reactions revealed the same six major products as observed with hPol κ (5'-pTC__TGA-3', 5'-pTC**T**_TGA-3', 5'-pTC**G**_TGA-3', 5'-pTC**TA**TGA-3', 5'-pTC**AA**TGA-3', and 5'-pTC**GA**TGA-3'), but their relative contributions were entirely different (Scheme 5.3B). Error free replication past the adduct (5'-p TC**TA**TGA-3') accounted for over 80% of the total products. The relative yields of 5'-pTC**GA**TGA-3' and 5'-p TC**AA**TGA-3' corresponding to the incorporation of incorrect bases, G and A, opposite the lesion, accounted for < 10%, while single deletion products, 5'-pTC**G**_TGA-3' and 5'-pTC**T**_TGA-3', accounted for < 5%. The double deletion product (5'-pTC__TGA-3') was also detected, with the relative yield of < 1%. These results are summarized in Scheme 5.3B. Taken together, these results indicate that hPol η makes fewer errors than does hPol κ upon replicating 1,N^6-γ-HMHP-dA containing DNA.

HPLC-ESI-FTMS analysis of hPol ι extension products of 1,N^6-γ-HMHP-dA containing 18-mer oligonucleotide template:primer complexes revealed the formation of a single product with an *m/z* of 1091.20 (not shown). CID fragmentation of *m/z* 1091.20 confirmed that the product was 5'-GGGGGAAGGAUTC**T**-3', which is formed upon incorporation of the correct base (T) opposite the lesion, but no further extension by the enzyme (results not shown). As discussed above, UDG/piperidine cleavage was not employed for hPol ι generated products due to their relatively short length, enabling their direct sequencing by MS/MS. These results confirm that human hPol ι is able to insert the correct base (T) opposite 1,N^6-γ-HMHP-dA, but is unable to extend the primer beyond the damaged site. This result is consistent with our gel electrophoresis results (see above).

HPLC-ESI$^-$-MS/MS analysis of the Dpo4 primer extension mixtures has revealed the presence of five major DNA peaks at *m/z* 929.6, 934.2, 1086.2, 1090.7, and 1098.7 (Scheme 5.3C). The nucleobase sequences of these products were determined by MS/MS as described above. We found that the major products were 5'-pTC**TA**TGA-3' (59%) and 5'-pTC**AA**TGA-3' (30%), corresponding to error-free replication and the misinsertion of A opposite the lesion, respectively. A low abundance product, 5'-pTC**GA**TGA-3' (4%) formed by the misinsertion of G, was also observed. Analogous to our results for hPol *κ*, a single nucleotide deletion product 5'-pTC**T**_TGA-3' (5%) was found. A novel frameshift deletion product, 5'-pTC**A**_TGA-3' (2%), was formed by misinsertion of A opposite the adduct, followed by skipping of the neighboring 3' base. These results are summarized in Scheme 5.3C.

5.4 Discussion

1,2,3,4-Diepoxybutane (DEB) is a key carcinogenic metabolite of 1,3-butadiene (BD), an important industrial and environmental chemical present in urban air and in cigarette smoke. DEB is considered the ultimate carcinogenic metabolite of BD due to its potent genotoxicity *(26)*. Studies in the *hprt* gene have revealed that DEB induces a large number of A → T mutations and deletions, along with smaller numbers of A→G and A→C base substitutions *(230;239)*. Furthermore, exposure of rat2 *laci* transgenic cells and human TK6 lymphoblasts to DEB induced an increased frequency of A → T transversions and partial deletions (Table 1.4) *(35)*.

Despite significant efforts, specific DNA adducts responsible for DEB-induced genetic changes have not been previously identified. DEB-mediated DNA alkylation gives rise to a complex mixture of nucleobase adducts including 2,3,4-trihydroxybut-1-yl (THB) monoadducts, 2,3-dihydroxy-butane-1,4-yl DNA-DNA cross-links, DNA-protein lesions, and exocyclic dG and dA adducts *(177-179;181;193)*. Polymerase bypass studies of synthetic DNA templates containing N^6-THB-adenine monoadducts revealed essentially error-free replication, producing very low levels of A $\rightarrow$ G and A $\rightarrow$ C base substitutions (< 0.3%) *(177)*. N^2-THB-dG lesions completely blocked DNA replication *(178)*. The *N1*-THB-dI lesions originating from deamination of the corresponding *N1*-dA adducts induced high numbers of A $\rightarrow$ G transitions *(179)*. Similar studies conducted with putative N^2-guanine and N^6-adenine intrastrand DNA-DNA cross-links have revealed that *bis*-N^2G-BD crosslinks are not bypassed by DNA polymerases, while *bis*-N^6A-BD lesions induce A $\rightarrow$ G base substitutions at the 3'-base *(179;181)*. It should be noted that *N1*-THB-dI, *bis*-N^6A-BD, and *bis*-N^2G-BD have not been detected in tissues of BD-treated animals and may not be relevant *in vivo*. In summary, studies to date have not uncovered the origins of A $\rightarrow$ T transversions that predominate in DEB-treated cells and tissues.

Previous studies in our laboratory have revealed that DEB can sequentially react with the N1 and the N^6 positions of adenine in DNA to form 1,N^6- α-HMHP-dA adducts (Scheme 5.1) *(48)*. 1,N^6-α-HMHP-dA can undergo a slow, reversible Dimroth-like rearrangement in water at room temperature to 1,N^6-γ-HMHP-dA adducts *(48)*. The concentrations of both exocyclic 1,N^6-HMHP-dA adducts increased linearly when calf

thymus DNA was treated *in vitro* with increasing concentrations of DEB (50 to 1000 μM) *(48)*. Furthermore, 1,N^6-HMHP-dA adducts were formed in a dose-dependent manner in liver, kidney, and lung DNA of B6C3F1 mice exposed to BD by inhalation *(67)*. Importantly, these lesions persisted *in vivo,* with an estimated half-life of > 40 days *(185)*. Based on their stability and their chemical structure that resembles known promutagenic lesions such as 1,N^6-etheno-dA and 1,N^6-ethano-dA, 1,N^6-HMHP-dA adducts have been proposed to contribute to the mutagenicity of BD *(185)*.

In the present study, *in vitro* polymerase bypass experiments were conducted employing synthetic DNA templates containing site specific 1,N^6-γ-HMHP-dA adducts. Human lesion bypass polymerases hPol β, hPol η, hPol κ, hPol ι and archebacterial DNA polymerase Dpo4 were investigated, since these polymerases are known to conduct DNA replication past a variety of DNA lesions. For example, hPol η is capable of bypassing 8-oxoguanine, O^6-methylguanine and *cis-syn* TT dimer *(120)*, while hPol κ efficiently bypasses bulky N^2-guanine adducts *(121;162)*. Additionally, hPol ι has been proven to conduct translesion synthesis across several DNA lesions including N^2-ethylguanine *(235)*. 1,N^2-etheno guanine and M1dG lesions are bypassed by archebacterial polymerase Dpo4 *(164;240)*.

Primer extension experiments combined with gel electrophoresis and HPLC-MS/MS analyses of the products revealed that hPol η, hPol κ, and Dpo4 were able to bypass the lesion and to extend the primer completely to the terminus (Figures 5.1, 5.2, and 5.6). In contrast, hPol β was completely blocked by the lesion, while hPol ι incorporated the correct nucleotide (dTMP) opposite the lesion, but was unable to extend

the primer further (Figure 5.1B). However, incomplete primer extension products generated by hPol ι can be completed either by hPol η or hPol κ (Figure 5.3). Similar co-operativity experiments conducted for N^2-ethylguanine adducts revealed that hPol η can successfully complete the polymerization started by hPol α *(241)*.

Steady state kinetic analysis of the incorporation of single nucleotide opposite the lesion was completed for human Pol η, Pol κ, Pol ι and Dpo4 to determine the specificity constants (k_{cat}/K_m) and to obtain the misinsertion frequencies (*f*). The k_{cat}/K_m values for the incorporation of correct nucleotide (dTMP) opposite 1,N^6-γ-HMHP-dA by hPol η and hPol κ were 0.14 and 0.07 μM^{-1} min^{-1}, respectively, which is comparable to corresponding values for dTMP insertion opposite structurally analogous 1,N^6-εdA lesions (0.004 and 0.001 μM^{-1} min^{-1}, respectively) *(165)*. The efficiency of incorporation of dTMP opposite the lesion by hPol η and hPol κ was 3-8 fold lower than those for the control template containing unmodified dA (Table 5.1). An even greater decrease (600-fold) was observed for archebacterial DNA polymerase Dpo4. Similar decreases in the efficiency of Dpo4 upon replication of damaged templates have been previously reported for the incorporation of dCTP opposite guanine adducts 7,8-dihydro-8-oxodeoxyguanosine *(169)*, O^6-methylguanine *(173)* and *1*,N^2-ethenoguanine *(164)*.

In addition to the correct base (dTMP), hPol η, κ, and Dpo4 also inserted incorrect bases (dGMP and dAMP) opposite 1,N^6-γ-HMHP-dA lesions. The misinsertion frequency was between 0.2-0.7, depending on specific polymerase (Table 5.1). For example, the frequency of dAMP incorporation opposite 1,N^6-γ-HMHP-dA by hPol κ

was 0.7 (Table 5.1). If observed *in vivo*, such mis-incorporation is expected to cause A→T transversion mutations.

An important limitation of gel electrophoresis experiments is that they cannot determine the nucleotide sequence of the primer extension products, potentially yielding misleading or incomplete results. Zang et al. have developed a robust methodology for the analysis of primer extension products by HPLC-ESI-MS/MS *(164)*. In their approach, a uracil residue is introduced into the primer, and the extension products are cleaved with UDG/hot piperidine to facilitate their sequencing by tandem mass spectrometry. This methodology has been previously applied in polymerase bypass studies of several DNA lesions *(160;162;169;173;176)*. We adopted a similar methodology to sequence the *in vitro* replication products of 1,N^6-γ-HMHP-dA containing templates by HPLC-ESI-MS/MS (Figures 5.5-5.7, Schemes 5.3-5.5). To enhance HPLC-ESI$^-$-MS/MS detection sensitivity, a capillary HPLC column was employed instead of the conventional 1.0-2.0 mm i.d. columns used previously *(160;162;169;173;176)*. By this modified HPLC-ESI$^-$-MS/MS methodology, it was possible to characterize primer extension products with only 100 pmol of modified oligonucleotide. In comparison, the previous analytical methods required 1-4 nmol of modified oligonucleotide and large amounts of recombinant polymerases *(160;162;169;173;176)*. The observed CID spectra of the primer extension products were in good agreement with the predicted CID spectra (Figures 5.7, 5.8 and Table 5.2).

HPLC-MS/MS sequencing has revealed that among the three polymerases that are able to conduct DNA synthesis past 1,N^6-γ-HMHP-dA (hPol η, hPol κ, and Dpo4), primer

extension by hPol κ was the most error-prone. hPol κ displayed a greater preference for the incorporation of incorrect nucleotide dGMP opposite the lesion (Scheme 5.3A) as compared to the correct nucleotide dTMP. Only 18% of the total extension products formed corresponded to error-free replication products. In addition, -1 frameshift products accounted for approximately 35% of the total hPol κ extension products (Scheme 5.3A and Figure 5.8). In these cases, dGMP or dTMP were incorporated opposite the lesion, and the next base was skipped, followed by correct primer extension all the way to the terminus (Scheme 5.3A). On the other hand, *in vitro* replication past 1,N^6-γ-HMHP-dA by hPol η and Dpo4 was less error-prone, with a higher production of error-free extension products that accounted for more than 60% of the products and a lower percentage of single nucleotide deletion products (<10%) (Schemes 5.4 and 5.5). For both hPol η and Dpo4, misincorporation of dGMP opposite the lesion accounted for less than 10% of total products. However, Dpo4 reaction mixtures also contained significant amounts of the extension product corresponding to the incorporation of dAMP opposite the lesion (30%). In addition, small amounts of -2 frame shift deletion products were observed in primer extensions catalyzed by Pol κ and η, but not Dpo4.

Taken together, our gel electrophoresis and tandem mass spectrometry results indicate that human TLS polymerases η, κ and Dpo4 are able to bypass DEB-induced 1,N^6-γ-HMHP-dA lesions and to extend the primer to the terminus, but they are potentially error-prone. In addition to correct nucleotide (dTMP), these bypass polymerases incorporate dAMP and dGMP opposite the lesion and produce -1 and -2

deletion products (Schemes 5.3-5.5). In contrast, hPol ι is unable to extend beyond the 1,N^6-γ-HMHP-dA lesion, and hPol β is completely blocked at the modification site.

A possible model for the insertion of dA, dT, dG opposite 1,N^6-γ-HMHP-dA is shown in Scheme 5.4. 1,N^6-γ-HMHP-dA adduct can exist in two tautomeric froms. The *N*1-C6 immonium ion tautomer can be envisioned to adopt a *syn* confirmation and form a stable Hoogsteen base pair with dT or dG. The C6-N^6 imino tautomer could form a Hoogsteen base pair with protonated dA. The ability of 1,N^6-γ-HMHP-dA adduct to adopt a *syn* confirmation and mispair with dG and protonated dA is not unprecedented. For example, 1,N^6-etheno-dA adducts have been shown to adopt the *syn* confirmation in the active site of hPol ι, forming a Hoogsteen base pair with dT or protonated dC *(229)*. Taken together, our results provide a possible mechanism for the induction of A→T and A→C transversions and frame shift mutations by DEB and its metabolic precursor, 1,3-butadiene.

Scheme 5.4 Models for the correct insertion of dT and misinsertion of dG and dA opposite 1,N^6-γ-HMHP-dA

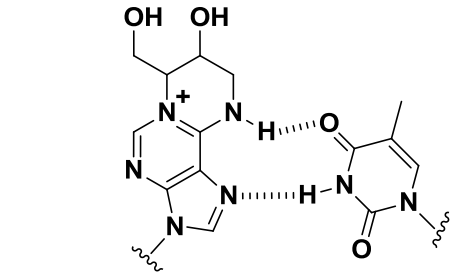

1,N^6-γ-HMHP-dA (*syn*) dT (*anti*)

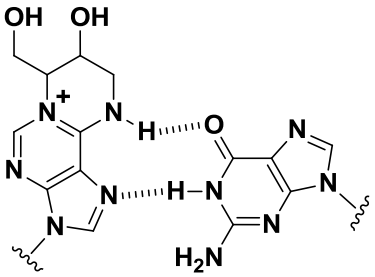

1,N^6-γ-HMHP-dA (*syn*) dG (*anti*)

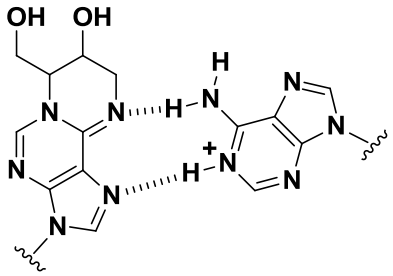

1,N^6-γ-HMHP-dA (*syn*) dA (*anti*)

VI. TRANSLESION SYNTHESIS ACROSS 1,3-BUTADIENE-INDUCED N^6-DEOXYADENOSINE ADDUCTS BY HUMAN DNA POLYMERASES

6.1 Introduction

While the exact mechanisms of smoking-induced lung cancer remain to be established *(7)*, DNA adducts induced by electrophilic metabolites of tobacco carcinogens are thought to induce critical genetic changes required for cancer initiation *(242)*. If not repaired, some tobacco carcinogen-DNA adducts can block DNA replication by normal replicative DNA polymerases *(120;122;243)*. A specialized group of polymerases called translesion synthesis (TLS) polymerases are capable of accommodating damaged DNA bases in their open and flexible active sites, allowing for replication to continue in the presence of nucleobase damage and preventing toxicity *(120;122;123;243)*. hPol η, hpol ι, hpol κ, Rev1 belonging to the Y family and Pol ζ from the B family of polymerases have the ability to carry out translesion DNA synthesis in humans *(120-122;225;226)*. However, TLS polymerases have relatively low fidelity and carry out the replication process with high error rates *(120;128;130)*, potentially contributing to mutations and cancer *(7;242;244;245)*.

1,3-butadiene (BD) is a high volume industrial chemical used in the production of rubber and plastics *(16)*. Exposure of general population to BD is widespread because of its presence in cigarette smoke, forest fires, and automobile exhaust *(16;26)*. Based on inhalation studies in laboratory rodents and epidemiological evidence of an increased risk of leukemia in workers occupationally exposed to BD, BD is classified as a "known human carcinogen" by the National Toxicology Program *(26)*. BD is metabolically

activated by CYP450 2E1 to form 3,4-epoxy-1-butene (EB) *(27)*, which can be further oxidized to the highly mutagenic and genotoxic diepoxide, 1,2,3,4-diepoxybutane (DEB) *(29)*. EB modifies the exocyclic amine groups of adenines in DNA to form N^6-(2-hydroxy-3-buten-1-yl)- 2′-deoxyadenosine (N^6-HB-dA I) and its regioisomer N^6-(1-hydroxy-3-buten-2-yl)- 2′-deoxyadenosine (N^6-HB-dA II) *(42;59;182;246)*. DEB produces exocyclic deoxyadenosine lesions N^6,N^6-(2,3-dihydroxybutan-1,4-diyl)-2′-deoxyadenosine (N^6,N^6-DHB-dA), N^6-(2-hydroxy-3-hydroxymethylpropan-1,3-diyl)-2′-deoxyadenosine (1,N^6-γ HMHP-dA), and 1,N^6-(1-hydroxymethyl-2-hydroxypropan-1,3-diyl)-2′-deoxyadenosine (1,N^6-α HMHP-dA) *(48;67;185)*. The mechanism of formation of N^6-HB-dA I, N^6-HB-dA II and N^6,N^6-DHB-dA from BD is illustrated in Scheme 6.1.

N^6-HB-dA I and N^6-HB-dA II (Scheme 6.1) have been detected *in vitro* (calf thymus DNA treated with EB) *(52;182;246)* and *in vivo* (lung DNA of laboratory mice and rats exposed to BD by inhalation) *(52;183)*. These adducts can be formed directly by alkylation of the N^6 position of adenine or via Dimroth rearrangement of the corresponding N1-HB-dA lesions *(42;246)*. N^6,N^6-DHB-dA adducts are yet to be observed in living cells, probably due to their relatively low abundance. 1,N^6-HMHP-dA adducts were formed *in vitro* upon treatment of calf thymus DNA with DEB *(48)*. Additionally, 1,N^6-HMHP-dA adducts were also detected in DNA extracted from liver, lung and kidney tissues of mice exposed to BD by inhalation *(67)*. Our recent study has revealed that polymerase bypass of 1,N^6-γ-HMHP-dA adducts of DEB leads to A→T and A→C transversions and frameshift mutations (Chapter V) *(247)*. However, the mispairing properties of N^6-HB-dA I and N^6,N^6-DHB-dA lesions have not been

previously evaluated. We hypothesized that the presence of two alkyl groups at the exocyclic N^6 position of adenine of N^6,N^6-DHB-dA interferes with Watson-Crick base pairing, leading to mutations *(48)*. In contrast, the presence of H-bond donor at the N^6 position of N^6-HB-dA I may allow this lesion to form a correct base pair with dT.

The primary goal of the present study is to investigate the influence of N^6-HB-dA I and N^6,N^6-DHB-dA adducts on DNA replication by human lesion bypass polymerases. Primer extension and steady-state kinetics studies for hPol β, hPol κ, hPol η and hPol ι were performed using synthetic DNA templates containing site-specific *(S)*-N^6-HB-dA I or *(R,R)*-N^6,N^6-DHB-dA prepared in our laboratory. Our results reveal significant differences between the biological consequences of replication past N^6-HB-dA I and N^6,N^6-DHB-dA lesions. While the N^6-HB-dA was not mutagenic, N^6,N^6-DHB-dA adduct induced both point mutations and deletions, probably as a result of its inability to form the correct base pair with dT.

Scheme 6.1 Formation of N^6-HB-dA and N^6,N^6-DHB-dA adducts from BD

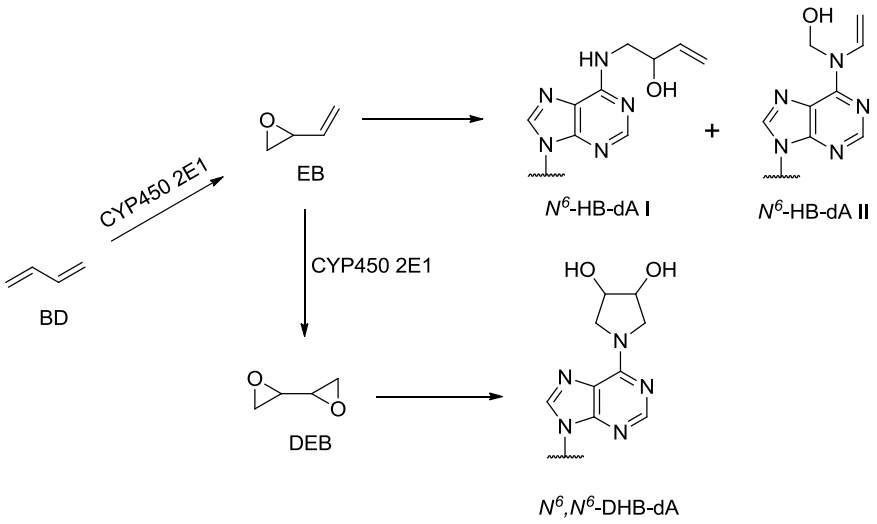

6.2 Experimental Procedures

Materials. Full-length recombinant human polymerase κ (hPol *κ)* used for gel electrophoresis experiments was purchased from Enzymax (Lexington, KY). Human polymerase *β* was obtained from Trevigen (Gaithersburg, MD). Recombinant human DNA polymerases hPol *η* (amino acids 1-437), hPol *ι* (amino acids 1-420) and hPol *κ* (amino acids 19-526) were expressed and purified as per previously published methodologies *(231-233).* T4 polynucleotide kinase (T4-PNK) and *E.coli* uracil DNA glycosylase (UDG) were procured from New England Biolabs (Beverly, MA). [γ-^{32}P]ATP was purchased from Perkin-Elmer Life Sciences (Boston, MA). Ammonium acetate, boric acid, bovine serum albumin (BSA), dithiothreitol (DTT), formamide, magnesium chloride, sigmacote, N,N,N′,N′-tetramethylethylenediamine, trizma base and urea were from Sigma Aldrich (St. Louis, MO), while ammonium persulfate, acetonitrile and EDTA were obtained from Fisher Scientific (Pittsburgh, PA). 40% 19:1 Acrylamide/bis solution and Bio-spin columns were purchased from Bio-Rad laboratories (Hercules, CA).

Oligonucleotides synthesis, labeling and annealing. Synthetic 18-mer oligodeoxynucleotides (5'-TCAT**X**GAATCCTTCCCCC-3') containing 6-chloropurine at position **X** were prepared by standard solid phase synthesis and coupled with *(S)*-N-Fmoc-1-aminobut-3-en-2-ol *(184)* and *(R,R)*-pyrrolidine-3,4-diol *(186)* to yield the corresponding strands containing site- and stereospecific *(S)*-N^6-HB-dA I and *(R,R)*-N^6,N^6-DHB-dA adducts. Detailed methodologies for oligonucleotide synthesis have been previously published *(184;186).* The corresponding unmodified 18-mer template

containing native dA (5'-TCATAGAATCCTTCCCCC-3'), 13-mer primers (5'-GGGGGAAGGATTC-3' and 5'-GGGGGAAGGAUTC-3') and 9-mer primer (5'-GGGGGAAGG-3') were purchased from Integrated DNA Technologies (Coralville, IA). All DNA oligodeoxynucleotides were purified by semi-preparative HPLC, characterized by HPLC-ESI$^-$ MS/MS, and quantified by UV spectrophotometry *(184;186)*. The structures of *(S)*-N^6-HB-dA I, *(R,R)*-N^6,N^6-DHB-dA adducts and the sequences of DNA oligomers used in this study are shown in Scheme 6.2. The 13-mer primer (5'-GGGGGAAGGATTC-3') and the 9-mer primer (5'-GGGGGAAGG-3') were radiolabeled and subsequently annealed to the corresponding 18-mer templates as previously described *(247)* to obtain primer-template complexes for *in vitro* replication studies.

Scheme 6.2 Sequences of DNA substrates containing site specific (*S*)-N^6-HB-dA and *(R,R)*-N^6,N^6-DHB-dA lesions employed in primer extension assays

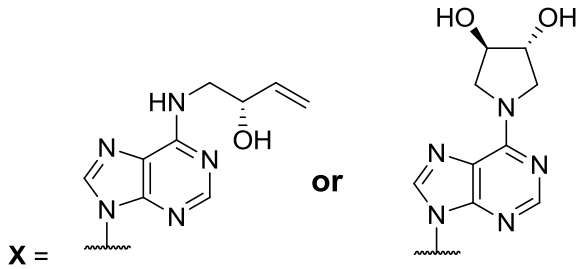

(S)-N^6-HB-dA I *(R,R)*-N^6,N^6-DHB-dA

DNA substrates used for gel electrophoresis

```
5'-TCA TXG AAT CCT TCC CCC-3'  (18 mer template)
3'-      C TTA GGA AGG GGG-5'  (13 mer primer)

5'-TCA TAG AAT CCT TCC CCC-3'  (18 mer positive control)
3'-      C TTA GGA AGG GGG-5'  (13 mer primer)

5'-TCA TXG AAT CCT TCC CCC-3'  (18 mer template)
3'-           GGA AGG GGG-5'  (9 mer running-start primer)

5'-TCA TAG AAT CCT TCC CCC-3'  (18 mer positive control)
3'-           GGA AGG GGG-5'  (9 mer running-start primer)
```

DNA substrates used for LC-MS/MS analysis

```
5'-TCA TXG AAT CCT TCC CCC-3'  (18 mer template)
3'-      C TUA GGA AGG GGG-5'  (13 mer primer with U)

5'-TCA TAG AAT CCT TCC CCC-3'  (18 mer positive control)
3'-      C TUA GGA AGG GGG-5'  (13 mer primer with U)
```

Primer Extension Assays. Primer extension studies were performed using the previously published methods (Section 5.2) *(247)*, with a few modifications. Briefly, ^{32}P-endlabeled 13-mer primer-template duplexes (50 nM, shown in Scheme 6.2) were dissolved in a buffer containing 50 mM Tris-HCl (pH 7.8), 50 mM NaCl, 5 mM DTT, 100 µg/ml BSA, and 10% glycerol (v/v) and incubated at 37 ^{0}C in the presence of individual human DNA polymerases (hPol *β*, 12.5 nM; hPol *η*, 10 nM; hPol *ι*, 20 nM; hPol *κ*, 5 nM). The polymerase reactions were initiated by the addition of dNTP mix (500 µM, all 4 dNTPs) in 5 mM $MgCl_2$. Aliquots of the reaction mixture (4 µl) were taken at 0, 5, 15, 30, 45 and 60 mins and quenched with 36 µl of stop solution (95% formamide (w/v), 10 mM EDTA, 0.03% bromophenol blue (w/v), 0.03% xylene cyanol (w/v)). Similar reactions were performed under running-start conditions with ^{32}P-endlabeled 9-mer primer/template duplexes (shown in Scheme 6.2) in the presence of higher enzyme concentrations (hPol *β*, 25 nM; hPol *η*, 25 nM; hPol *κ*, 12.5 nM). The primer extension products were resolved by gel electrophoresis using a 20% (w/v) denaturing polyacrylamide gel containing 7 M urea. The radioactive primer extension products were visualized on a GE Typhoon FLA 7000 phosphorimager.

Steady-state Kinetics Analyses. The kinetics of incorporation of various nucleotides opposite *(S)*-N^6-HB-dA I or *(R,R)*-N^6,N^6-DHB-dA was evaluated by conducting polymerization reactions in the presence of increasing concentrations of individual dNTPs (0-800 µM) for different time periods (0-180 min). The polymerase concentrations used were same as above, with the exception of hPol *κ* which was used at 2.5 nM, 3.33 nM or 5 nM concentrations. The radioactive product bands visualized on a

GE Typhoon FLA7000 phosphorimager were quantified with ImageQuant software (GE HealthCare). Nonlinear regression analysis (one-site hyperbolic fits in GraphPad Prism) was employed to determine the steady-state kinetic parameters.

HPLC-ESI-MS/MS analysis of primer extension products from DNA polymerase reactions. Uracil-containing 13-mer primer/template complexes (100 pmol) (shown in Scheme 6.2) were incubated with hPol η or hPol κ (40 pmol) in a buffer containing 50 mM Tris-HCl (pH 7.8), 5% glycerol, 5 mM DTT, 5 mM $MgCl_2$, 100 µg/ml BSA and 1 mM each of the four dNTPs at 37 °C for 5 hours. At the end of incubation, excess dNTPs were removed with a size-exclusion chromatography column (Bio-Spin 6 chromatography column; Bio-Rad). The reaction mixture was restored to the concentrations of 50 mM Tris-HCl (pH 7.8), 5 mM DTT and 1 mM EDTA by the addition of appropriate buffers and subjected to UDG hydrolysis and piperidine treatment to reduce the size of primer extension products for sequencing by HPLC-ESI-MS/MS *(247)*. The final reaction mixture was dried under vacuum and reconstituted in 25 µl of water containing 40 pmol of a 14-mer used as an internal standard (5'p-CTTCACGAGCCCCC-3'). Primer extension products were resolved on a Agilent Zorbax SB 300 C18 (0.5 x 150 mm, 5µ) column on an Eksigent HPLC system (Eksigent, Dublin, CA) interfaced to a Thermo LTQ Orbitrap Velos mass spectrometer (Thermo Fisher Scientific, Waltham, MA) *(247)*. The relative quantification and MS/MS sequencing of primer extension products were achieved in the ESI^- MS/MS mode as described previously in Section 5.2 *(247)*.

6.3 Results

6.3.1 Standing-start and Running-Start Primer extension studies with all dNTPs

Our initial experiments were conducted in the presence of all four deoxynucleotides in order to identify DNA polymerases capable of bypassing *(S)*-N^6-HB-dA I and *(R,R)*-N^6,N^6-DHB-dA adducts. Standing-start experiments were conducted with 13-mer primer/18-mer template complexes, where the primer 3' terminus is positioned one base prior to the unmodified dA (control), (*S*)-N^6-HB-dA I, or *(R,R)*-N^6,N^6-DHB-dA on the template (X in Scheme 6.2). Under our experimental conditions, hPol β, hPol κ and hPol η completely extended 13-mer primers annealed to unmodified template (X=dA) to form the corresponding 18-mer products (Figures 6.1A, 6.2A, 6.2B; left panels) while primarily 16-mer (+1) products were formed in the reactions involving hPol ι (Figure 6.1B; left panel). hPol β, hPol κ and hPol η were able to bypass *(S)*-N^6-HB-dA I lesion and completely extend the primer to the terminus to yield 18-mer products (Figures 6.1A, 6.2A, 6.2B; second panels), while hPol ι formed 16-mer products (Figure 6.1B; second panel). The observation of incomplete primer extension products (15, 16, and 17-mers) in reaction mixtures involving *(S)*-N^6-HB-dA I-containing template suggests that the efficiency of DNA synthesis was reduced in the presence of the lesion.

In contrast, standing-start primer extension studies with *(R,R)*-N^6,N^6-DHB-dA template revealed no primer extension in the presence of hPol β at enzyme:DNA ratio of 1:4 (Figure 6.1A; third panel) and an insignificant amount of primer extension (<2%) at enzyme:DNA ratio of 1:2 (Figure 6.1A; fourth panel), suggesting that translesion synthesis by hPol β is blocked by *(R,R)*-N^6,N^6-DHB-dA. hPol ι was able to incorporate a

single base opposite *(R,R)*-N^6,N^6-DHB-dA, but did not extend the primer any further, even at enzyme:DNA concentration of 1:1 (Figure 6.1B; third and fourth panels). Primer extension by hPol κ was stalled after single nucleotide incorporation opposite *(R,R)*-N^6,N^6-DHB-dA to produce 14-mer products (Figure 6.2A; third panel). When the hPol κ:DNA ratio was changed from 1:10 to 1:2, significant amounts of 18-mer products were formed (Figure 6.2A; fourth panel). Similarly, hPol η was able to bypass *(R,R)*-N^6,N^6-DHB-dA to form 18-mer products, but only when the polymerase concentration was increased significantly (hPol η:DNA ratio of 1:2) (Figure 6.2B; third and fourth panels). Overall, DNA synthesis past *(R,R)*-N^6,N^6-DHB-dA by all human polymerases studied was inefficient.

Similar experiments were conducted under running-start conditions with a 9-mer primer/18-mer template duplex (Figure 6.3). We found that hPol β, hPol η, and hPol κ were able to bypass *(S)*-N^6-HB-dA I and extend the primer completely to the terminus (Figures 6.3A-B, middle panel). In contrast, the presence of *(R,R)*-N^6,N^6-DHB-dA in the template has lead to stalling of replication by hPol β at the site of damage and the formation of primarily 13-mer products (Figure 6.3A, right panel). In the presence of polymerases hPol η (data not shown) and hPol κ, primer extension past *(R,R)*-N^6,N^6-DHB-dA primarily yielded 13-mer, 14-mer products and a small amount of 18-mer products (Figure 6.3B, right panel). These results are consistent with our standing-start results (Figure 6.2), confirming that *(R,R)*-N^6,N^6-DHB-dA can be bypassed by hPol η and hPol κ, albeit inefficiently.

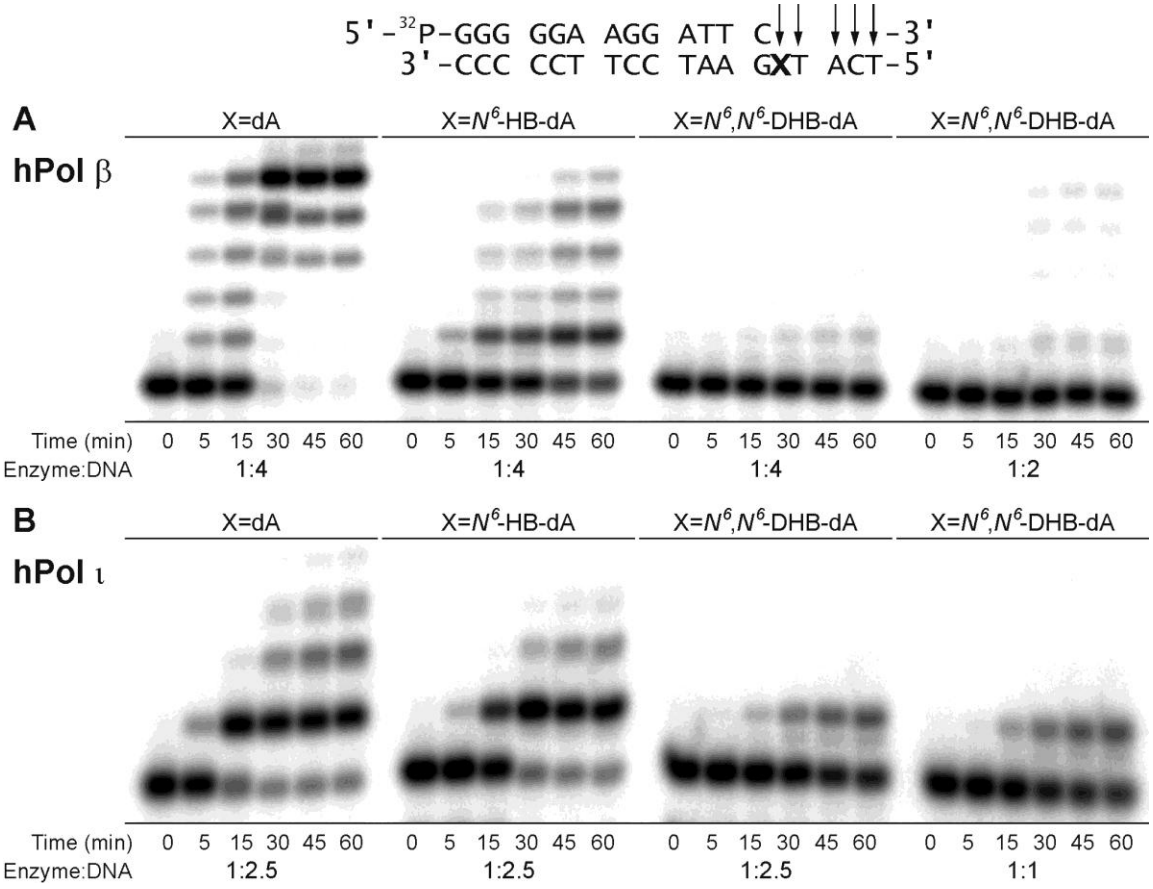

Figure 6.1 Primer extension (standing start) opposite dA, (*S*)-N^6-HB-dA or *(R,R)*-N^6,N^6-DHB-dA adduct by hPol β and hPol ι

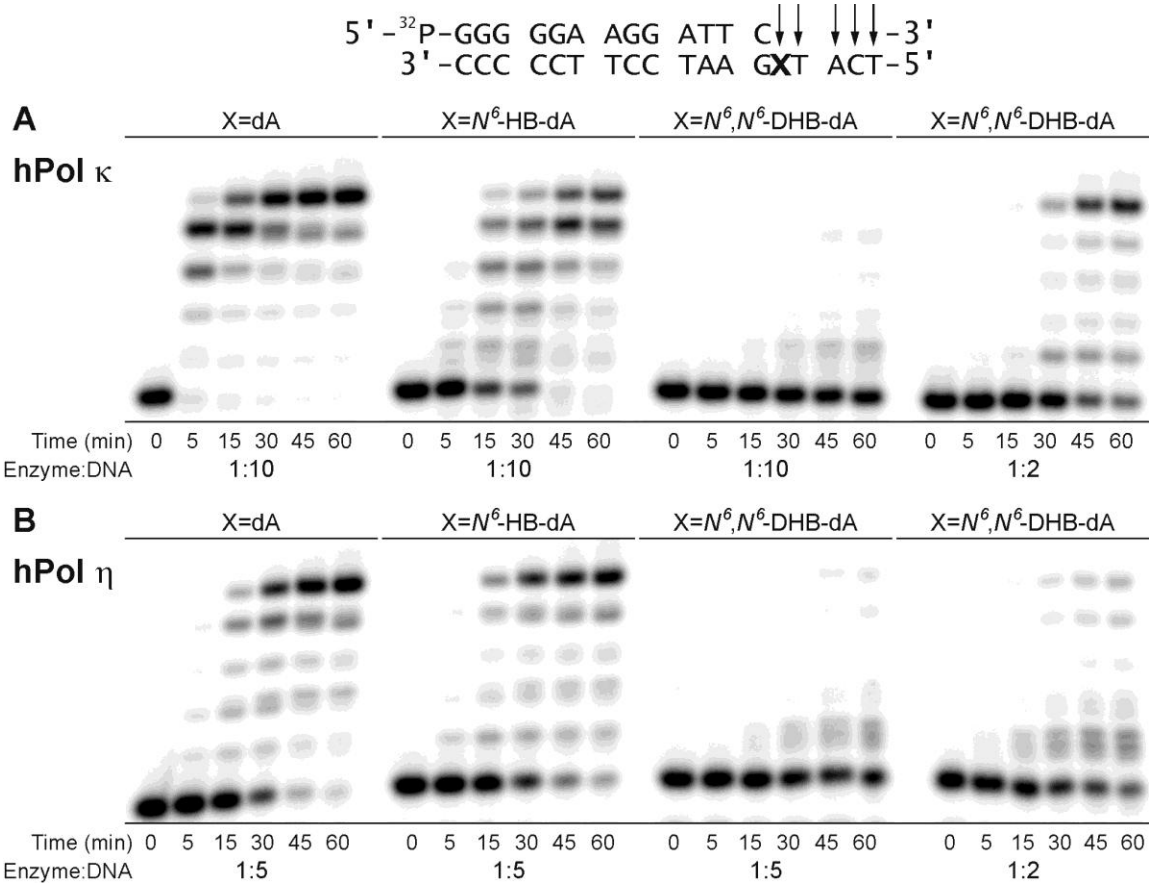

Figure 6.2 Primer extension (standing start) opposite dA, (*S*)-N^6-HB-dA or *(R,R)*-N^6,N^6-DHB-dA adduct by hPol *κ* and hPol *η*

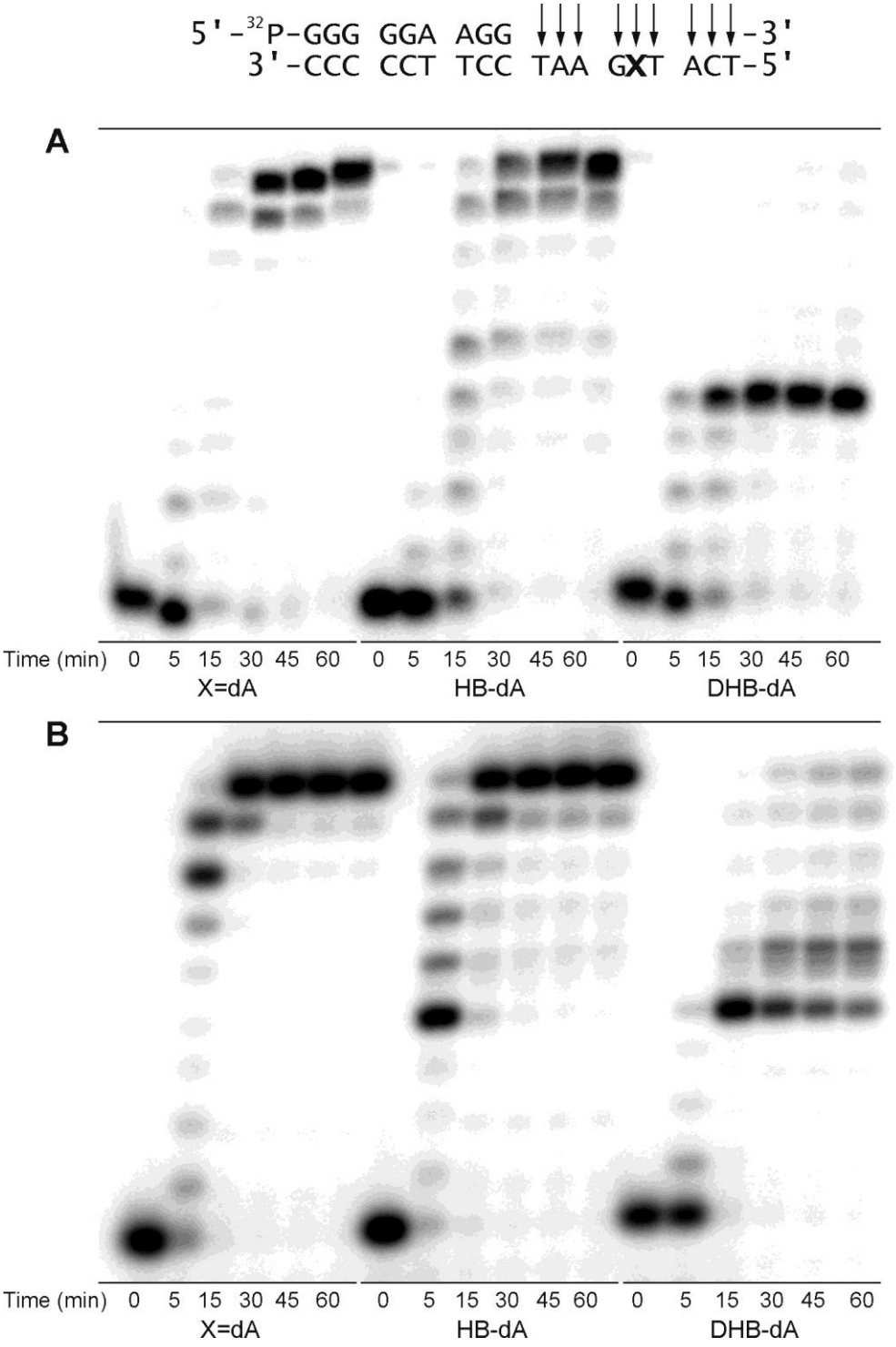

Figure 6.3 Primer extension (running start) opposite dA, (*S*)-N^6-HB-dA and *(R,R)*-N^6,N^6-DHB-dA adduct by hPol β and hPol κ.

6.3.2 Co-operativity and synergistic effects of TLS polymerases during replication past *(R,R)*-N^6,N^6-DHB-dA

To determine whether TLS polymerases can work cooperatively to bypass *(R,R)*-N^6,N^6-DHB-dA adducts, additional experiments were conducted with multiple enzymes. As shown in the right panel of Figure 6.1B, hPol ι incorporates a single nucleotide opposite *(R,R)*-N^6,N^6-DHB-dA, with no further primer extension. When the incomplete extension products from hPol ι reaction were incubated with hPol η, full extension to 18-mer products was observed (Figure 6.4). Similar results were obtained when hPol ι and hPol η were added simultaneously (Figure 6.5). As a negative control, parallel reactions were performed with hPol ι or hPol η separately and these were combined following protein inactivation. We found that the amount of 18-mer full extension products following dual enzyme incubation (12%) was significantly higher than in control reactions (2%) (Figure 6.5, compare lanes DHB-dA (iota+eta 1:1, 60 min) and Additive lane A4). While these observations provide preliminary evidence that hPol ι and hPol η can act synergistically to bypass *(R,R)*-N^6,N^6-DHB-dA lesions, further studies are needed incorporating additional protein factors such as proliferating cell nuclear antigen (PCNA), which can facilitate polymerase switching.

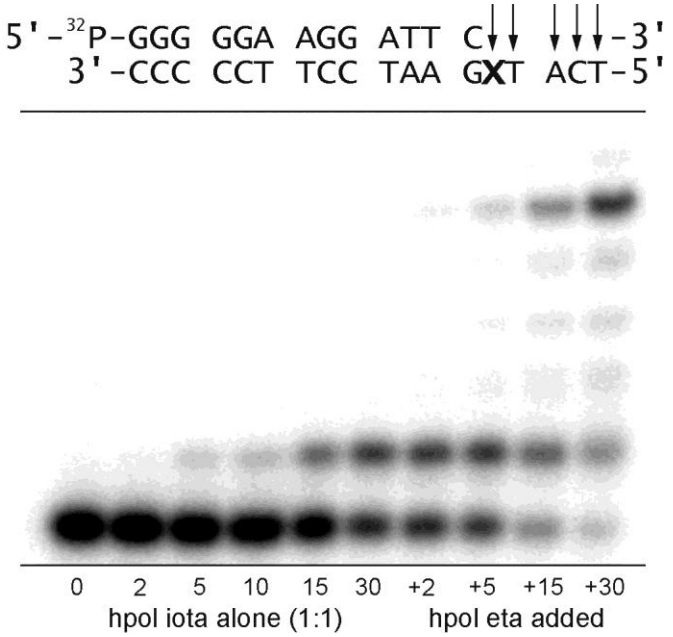

Figure 6.4 Cooperativity of human TLS polymerases *ι* and *η* during the bypass of *(R,R)*-N^6,N^6-DHB-dA lesion

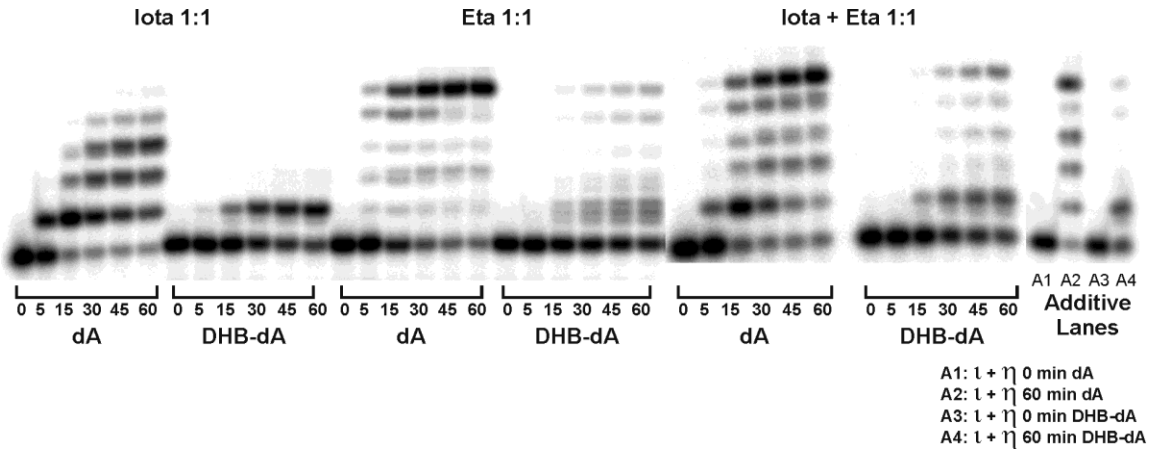

Figure 6.5 Synergistic effect of combination of TLS polymerases *ι* and *η* during the bypass of *(R,R)*-N^6,N^6-DHB-dA lesion

6.3.3 Steady-state kinetic analysis of incorporation of individual dNTPs opposite the lesions

To determine which nucleotides are incorporated opposite (*R,R*)-N^6,N^6-DHB-dA and *(S)*-N^6-HB-dA I by human DNA polymerases, single nucleotide insertion experiments were conducted in the presence of dAMP, dCMP, dGMP, or dTMP. We found that all four nucleotides were incorporated opposite *(S)*-N^6-HB-dA I and *(R,R)*-N^6,N^6-DHB-dA I by hPol η and hPol κ, although with different efficiency. In contrast, hPol ι incorporated only the correct base (dTMP) opposite both lesions, and hPol β incorporated dTMP opposite *(S)*-N^6-HB-dA, but was unable to insert any base opposite *(R,R)*-N^6,N^6-DHB-dA.

Additional single nucleotide insertion experiments were performed in the presence of increasing concentrations of each of individual dNTPs (0-800 μM) for specified time periods (0-180 min) in order to obtain steady-state kinetic parameters (k_{cat} and K_m) for nucleotide incorporation. The resulting data were used to calculate the catalytic specificity constants ($k_{cat}/K_{m)}$ and the misinsertion frequencies for nucleotide insertion (*f)* for each polymerase. The k_{cat}/K_m values can be used as a measure of insertion efficiency.

We found that hPol β was 19-fold less efficient at incorporating the correct base (dTMP) opposite *(S)*-N^6-HB-dA I as compared to unmodified dA (Table 6.1). No kinetic analysis was possible for dTMP incorporation opposite *(R,R)*-N^6,N^6-DHB-dA by this polymerase, as the product formation was not quantifiable. In the case of hPol ι, dTMP incorporation opposite *(S)*-N^6-HB-dA I and *(R,R)*-N^6,N^6-DHB-dA was 5- and 33- fold

less efficient than opposite native dA (positive control), respectively. As shown in Table 6.1, the k_{cat} values for these reactions were similar; but the K_m values were markedly increased in the presence of lesions (Table 6.1).

As expected, human pol κ incorporated primarily dTMP opposite unmodified dA, while dAMP and dGMP were incorporated 50-400 fold less efficiently (Table 6.1). For templates containing *(S)*-N^6-HB-dA I, hPol κ catalyzed the addition of the correct nucleobase (dTMP), although the efficiency of dTMP incorporation was 3 fold less than that opposite unmodified dA (positive control). The other three bases were incorporated 100 fold less efficiently (Table 6.1), suggesting that this adduct retains the ability to preferentially form Watson-Crick base pair with dT. In contrast, all four nucleotides were added opposite *(R,R)*-N^6,N^6-DHB-dA (T > C > A > G), with only ~1.5 more efficient dTMP insertion as compared to the other three bases (Table 6.1). dTMP incorporation opposite *(R,R)*-N^6,N^6-DHB-dA by hPol κ was ~450 fold less efficient than opposite dA (Table 6.1), indicating that hPol κ was less tolerant of *(R,R)*-N^6,N^6-DHB-dA modification.

Human TLS polymerase hPol η preferentially incorporated dTMP opposite unmodified dA (positive control) and *(S)*-N^6-HB-dA I adducts (Table 6.1). The efficiency of dTMP incorporation opposite *(S)*-N^6-HB-dA was 50 fold higher than that of dAMP or dCMP and ~200 fold higher than dGMP insertion (Table 6.1). The preference order of nucleotide insertion by hPol η opposite *(R,R)*-N^6,N^6-DHB-dA was G > T = A = C, with ~1.6 fold higher efficiency for dGMP insertion as compared to the other three bases. k_{cat}/K_m values for insertion of all four dNTPs opposite *(R,R)*-N^6,N^6-DHB-dA were

similar for both hPol η and hPol κ (Table 6.1). The efficiency of dTMP incorporation opposite *(R,R)*-N^6,N^6-DHB-dA by hPol η was ~800 fold less as compared to unmodified dA, indicative of a low tolerance of TLS polymerases for this lesion (Table 6.1). Overall, these results indicate that translesion synthesis by TLS polymerases is essentially error-free for *(S)*-N^6-HB-dA I and is highly error-prone for *(R,R)*-N^6,N^6-DHB-dA. Furthermore, *(R,R)*-N^6,N^6-DHB-dA bypass by all TLS polymerases studied was quite inefficient, suggesting that it blocks DNA replication.

Table 6.1 Steady-state kinetic parameters for single nucleotide incorporation opposite dA, (*S*)-N^6-HB-dA and *(R,R)*-N^6,N^6-DHB-dA

Polymerase	Template	dNTP	k_{cat} (min^{-1})	K_m (μM)	k_{cat}/K_m (μM^{-1} min^{-1})	*f*	*Fold decrease efficiency*
hPol *κ*	Da	T	5.72 ± 0.57	5.5 ± 1.8	1.04	1	1
		A	0.87 ± 0.05	354.6 ± 44.9	2.4 X 10^{-3}	2.4 X 10^{-3}	433
		G	4.27 ± 0.70	197.0 ± 18.1	0.02	0.02	52
	N^6-HB-dA	T	5.16 ± 0.46	13.7 ± 2.5	0.38	1	3
		A	0.83 ± 0.02	153.0 ± 11.5	5.4 X 10^{-3}	0.01	193
		G	0.97 ± 0.08	180.1 ± 34.6	5.4 X 10^{-3}	0.01	193
		C	0.08 ± 0.01	15.3 ± 7.6	5.5 X 10^{-3}	0.01	189
	N^6,N^6-DHB-dA	T	0.35 ± 0.04	152.8 ± 37.0	2.3 X 10^{-3}	1	452
		A	0.35 ± 0.03	285.7 ± 67.4	1.2 X 10^{-3}	0.53	867
		G	0.45 ± 0.06	454.6 ± 118.4	1.0 X 10^{-3}	0.43	1040
		C	0.29 ± 0.03	169.5 ± 37.7	1.7 X 10^{-3}	0.76	612
hPol *η*	dA	T	2.38 ± 0.19	1.8 ± 0.5	1.32	1	1
		A	0.60 ± 0.02	51.3 ± 7.0	0.01	8.8 X 10^{-3}	132
		G	0.52 ± 0.07	85.3 ± 27.3	6.0 X 10^{-3}	4.6 X 10^{-3}	220
	N^6-HB-dA	T	2.60 ± 0.19	30.9 ± 7.4	0.08	1	16
		A	0.15 ± 0.02	111.6 ± 31.3	1.4 X 10^{-3}	0.02	943
		G	0.07 ± 0.01	176.9 ± 35.6	0.4 X 10^{-3}	4.6 X 10^{-3}	3300
		C	0.25 ± 0.02	177.8 ± 30.2	1.4 X 10^{-3}	0.02	943
	N^6,N^6-DHB-dA	T	0.13 ± 0.02	78.6 ± 16.8	1.7 X 10^{-3}	1	776
		A	0.12 ± 0.01	72.0 ± 14.2	1.6 X 10^{-3}	0.98	825
		G	0.31 ± 0.02	114.7 ± 18.7	2.7 X 10^{-3}	1.64	489
		C	0.25 ± 0.02	140.2 ± 32.5	1.8 X 10^{-3}	1.06	733
hPol *ι*	dA	T	1.01 ± 0.03	21.1 ±1.8	0.05	1	1
	N^6-HB-dA	T	0.88 ± 0.06	83.0 ± 13.2	0.01	1	5
	N^6,N^6-DHB-dA	T	0.74 ± 0.08	480.6 ± 116.7	1.5 X 10^{-3}	1	33
hPol *β*	dA	T	2.59 ± 0.51	27.9 ± 7.1	0.09	1	1
	N^6-HB-dA	T	2.44 ± 0.40	510.6 ± 139.9	4.8 X 10^{-3}	1	19

6.3.4 LC-MS/MS analysis of primer extension products formed by hPol η and hPol κ

In order to confirm the results of primer extension and steady-state kinetic experiments conducted by gel electrophoresis and to uncover additional genetic changes not detectable by gel electrophoresis, the products of hPols κ and η mediated translesion synthesis past *(S)*-N^6-HB-dA I and *(R,R)*-N^6,N^6-DHB-dA were sequenced by HPLC-ESI-MS/MS. The capillary HPLC-ESI$^-$-MS/MS methodology previously reported by our laboratory was employed *(247)*. In brief, the primer employed for primer extension is constructed to contain a uracil residue 3 bases upstream from the lesion site. Following *in vitro* replication, the extended primer is cleaved with UDG/piperidine treatment to yield 5-, 6- or 7-mer products that can be readily sequenced by tandem mass spectrometry *(247)*. The relative abundance of each primer extension product is calculated by comparing their HPLC-MS peak areas to that of an internal standard, while the product identity is established by MS/MS sequencing as described previously *(247)*.

Primer extension reactions of *(S)*-N^6-HB-dA I template by hPol κ contained oligonucleotide fragments with *m/z* values of 825.1, 1078.7, 1086.2, 1090.7. MS/MS spectra have revealed that these products correspond to 5'-p TC**TTA**TGA-3', 5'-p TC**CA**TGA-3', 5'-p TC**TA**TGA-3' and 5'-p TC**AA**TGA-3', respectively. The error-free extension product 5'-p TC**TA**TGA-3' accounted for 82.5% of the total (Scheme 6.3). The relative contributions of other minor extension products 5'-p TC**TTA**TGA-3', 5'-p TC**CA**TGA-3', and 5'-p TC**AA**TGA-3' were 6, 3, and 8.5%, respectively (Scheme 6.3).

HPLC-ESI-MS/MS sequencing of primer extension products originating from hPol κ catalyzed replication of *(R,R)*-N^6,N^6-DHB-dA containing template resulted in a

complex mixture of products, including those at *m/z* 777.6, 922.1, 934.1, 942.1, 1078.7, 1086.2, 1090.7 and 1098.7, which correspond to 5'-p TC__TGA-3', 5'-p TC**C**_TGA-3', 5'-p TC**A**_TGA-3', 5'-p TC**G**_TGA-3', 5'-p TC**CA**TGA-3', 5'-p TC**TA**TGA-3', 5'-p TC**AA**TGA-3' and 5'-p TC**GA**TGA-3', respectively. HPLC-ESI-MS extracted ion chromatograms of these primer extension products are shown in Figure 6.6. The product of error-free extension, 5'-p TC**TA**TGA-3' accounted for only 37% of total extension products. The product formed by misinsertion of A opposite the lesion (5'-p TC**AA**TGA-3') accounted for 20% of the products (Scheme 6.3). Approximately 30% and 10% of total extension products corresponded to -1 and -2 deletions. 5'-p TC**A**_TGA-3' and 5'-p TC__TGA-3' were the major deletion products, corresponding to 18 and 9% of total products, respectively (Scheme 3). Complete results of primer extension products for both lesions in the presence of hPol κ are summarized in Scheme 6.3.

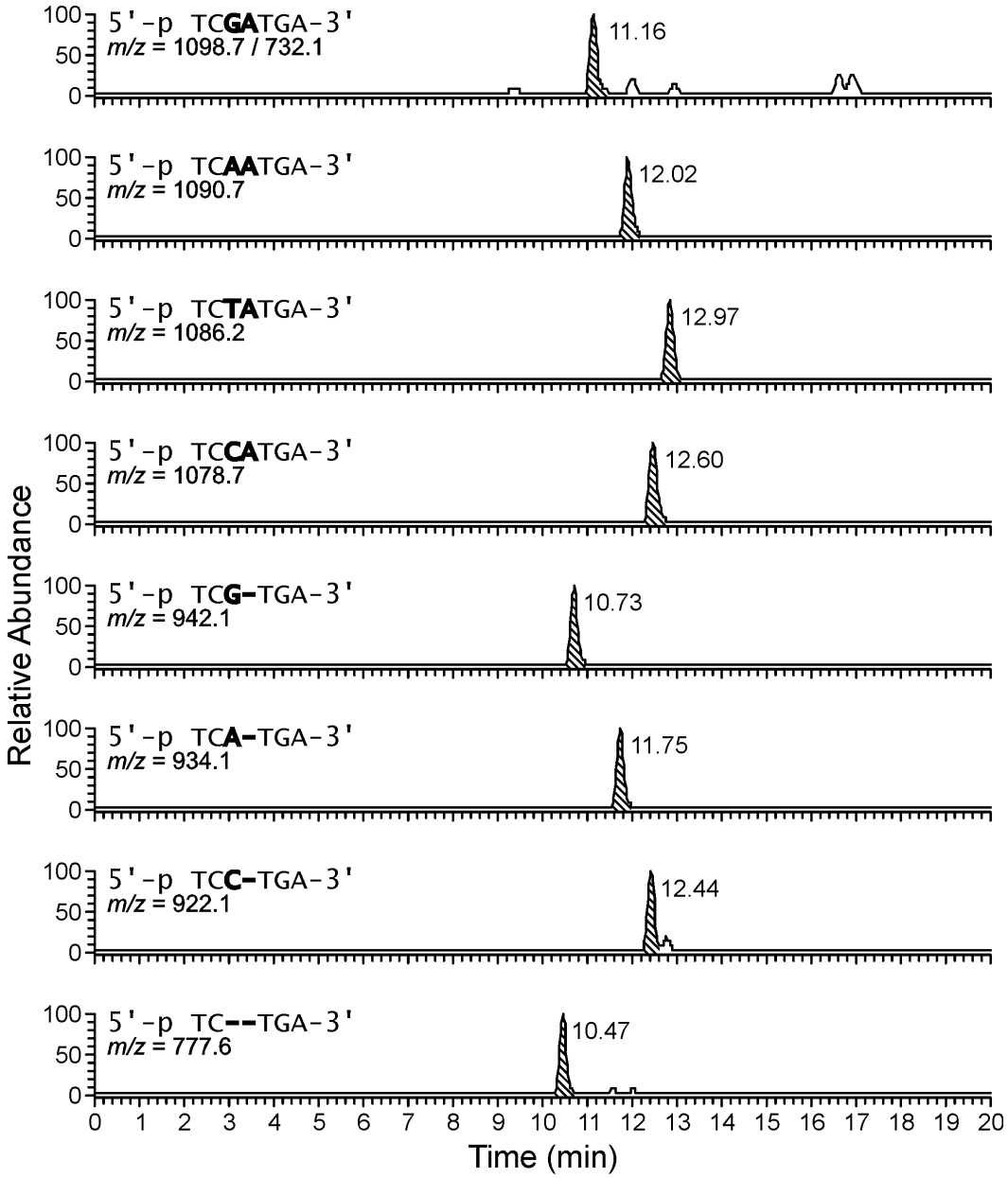

Figure 6.6 Extracted ion chromatograms of primer extension products opposite *(R,R)*-N^6,N^6-DHB-dA adduct template by hPol κ

Scheme 6.3 Summary of primer extension products opposite *(S)*-N^6-HB-dA and *(R,R)*-N^6,N^6-DHB-dA by hPol κ

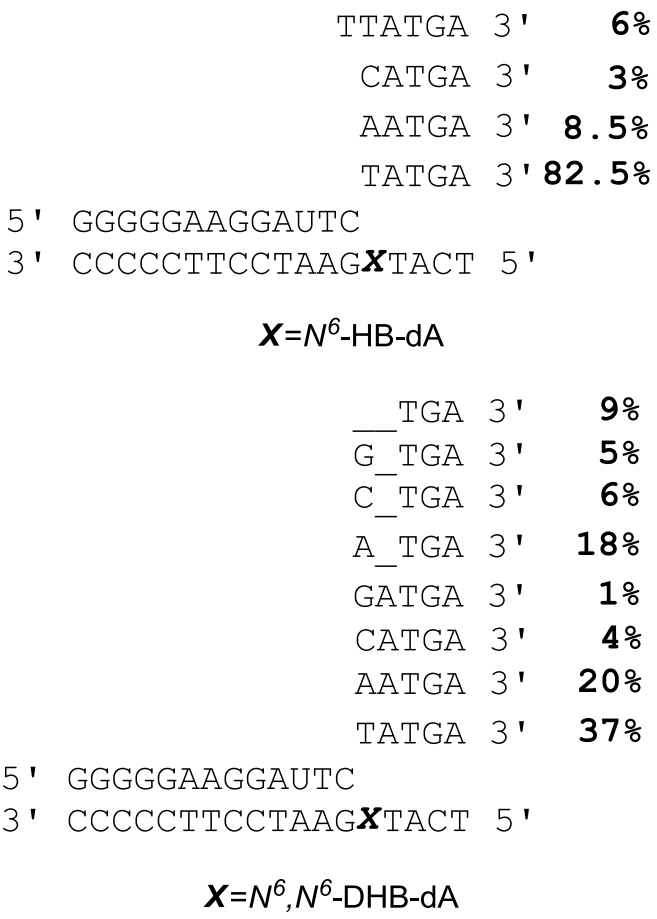

Parallel reactions were conducted for hPol η. We found that *in vitro* replication of *(S)*-N^6-HB-dA I containing template resulted in two main products: 5'-p TC**TA**TGA-3' (92%) and 5'-p TC**CA**TGA-3' (8%) (Scheme 6.4). In contrast, hPol η catalyzed bypass of *(R,R)*-N^6,N^6-DHB-dA generated the same 7 products which were also detected in the hPol κ reaction (Scheme 6.3). However, the relative contributions of these primer extension products were significantly different as compared to hPol κ reaction. The major product (5'-p TC**CA**TGA-3') was formed by misinsertion of C opposite *(R,R)*-N^6,N^6-DHB-dA (46%) (Scheme 6.4). Only 19% of the products were error-free (5'-p TC**TA**TGA-3'). Similar to hPol κ reaction, 20% of primer extension products were identified as 5'-p TC**AA**TGA-3'. Deletion products accounted for 15% of total products (Scheme 6.4).

The exact nucleotide sequence of each extension product was determined from their MS/MS spectra. Good sequence coverage of a-B and w ions was obtained to accurately identify the sequence of primer extension products. For example, MS/MS spectra of the product with *m/z* 1078.7 yielded ions at *m/z* 1059.3, 1276.3 (Figure 6.7B) which corresponds to a_4-B_4 ion and w_4 ion of 5'-p TC**CA**TGA-3', respectively. MS/MS spectra of the major primer extension products (5'-p TC**TA**TGA-3', 5'-p TC**AA**TGA-3', 5'-p TC**CA**TGA-3' and 5'-p TC**A**_TGA-3') are shown in Figure 6.7. Overall, the HPLC-ESI-MS/MS results (Schemes 6.3, 6.4) confirmed that polymerase bypass of *(S)*-N^6-HB-dA I is mainly error-free, while *(R,R)*-N^6,N^6-DHB-dA adducts are highly error-prone, resulting in A→G transitions, A→T transversions, A→C transversions, and deletions.

Scheme 6.4 Summary of primer extension products opposite *(S)*-N^6-HB-dA and *(R,R)*-N^6,N^6-DHB-dA by hPol η

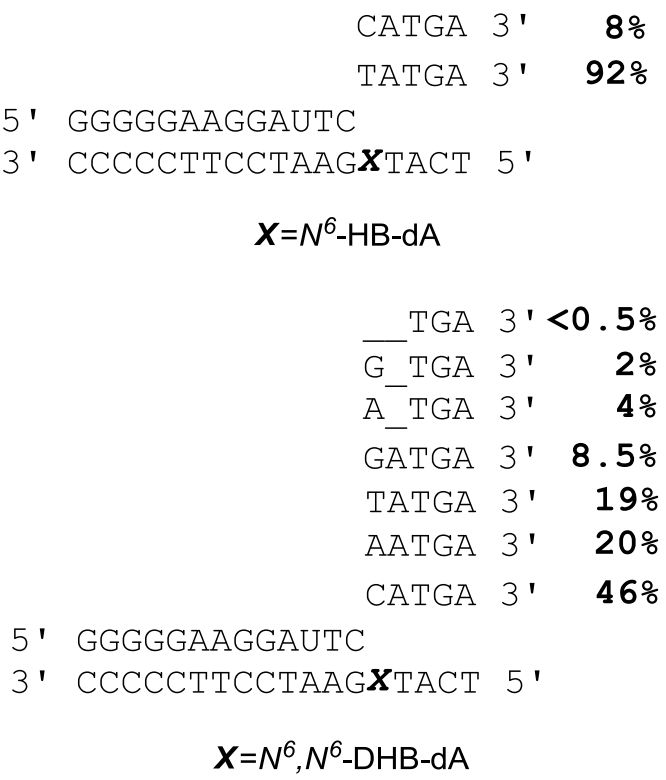

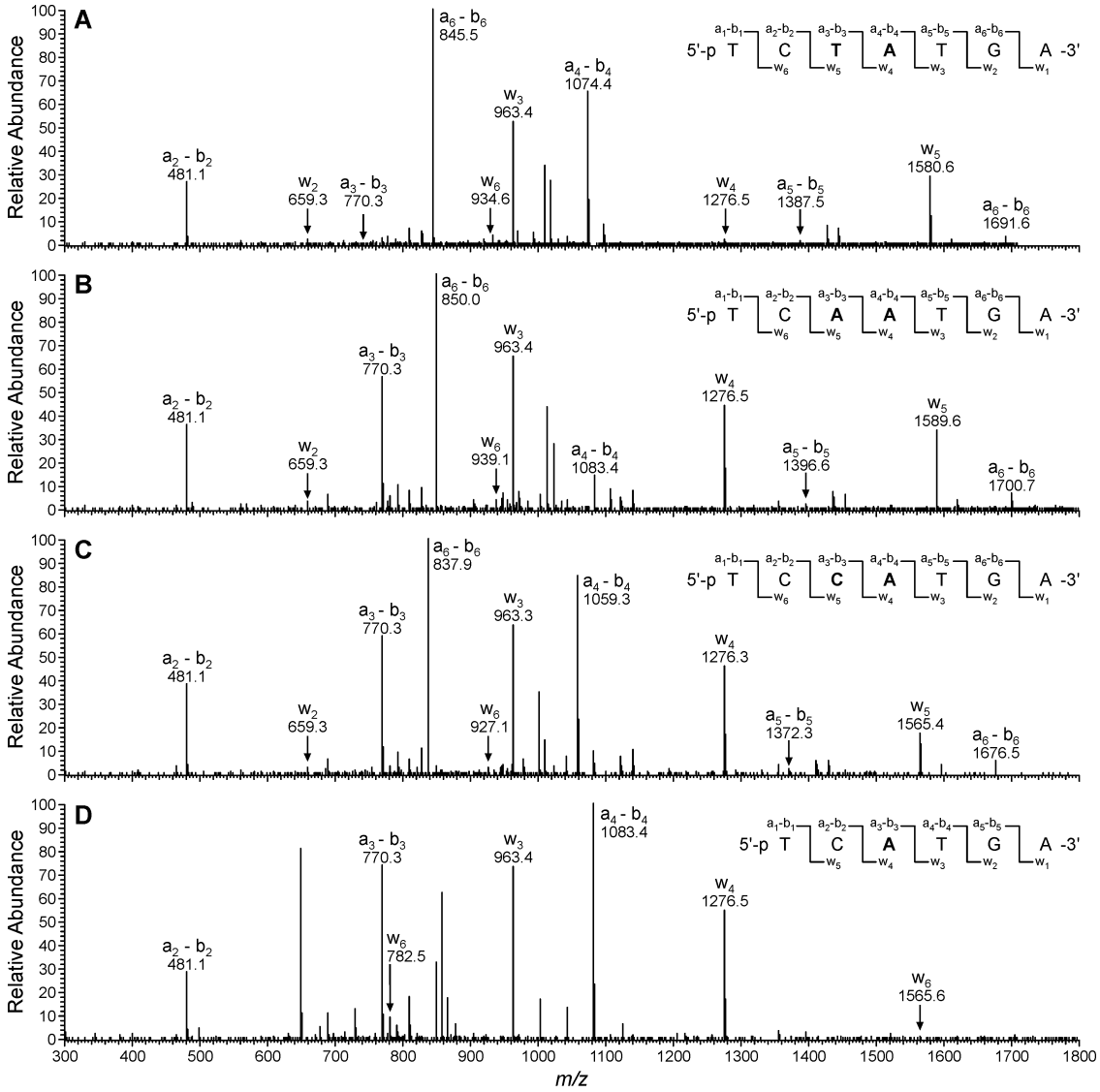

Figure 6.7 MS/MS spectra of the major products formed upon *in vitro* primer extension opposite *(R,R)*-N^6,N^6-DHB-dA by hPol κ and hPol η

6.4 Discussion

EB and DEB are carcinogenic metabolites formed upon cytochrome P450-mediated metabolic activation of BD *(16;248)*. Studies in human lymphoblastoid TK6 cells have revealed that EB and DEB induce mutations at the *hprt* and *tk* loci, with DEB being ~100 fold more mutagenic than EB *(34)*. EB treatment of Rat2 *laci* transgenic cells and human TK6 lymphoblasts resulted in an increased frequency of A → T transversions *(35)*. Additionally, A→C transversions were also observed in Rat2 *laci* transgenic cells *(35)*. EB induced A→T transversions and deletions in the lung of B6C3F1 *laci* transgenic female mice, while DEB induced A→T transversions and deletions at *hprt* locus in human TK6 lymphoblasts *(35;239)*. A high frequency of A→T and A→G mutations was observed in the bone marrow and spleen of B6C3F1 *laci* transgenic female mice exposed to BD *(35)*.

It has been previously reported that *bis*-N^6A-BD and *N1*-(1-hydroxy-3-buten-2-yl) deoxyinosine lesions induced A→G mutations *(179)*. In contrast, the identity of deoxyadenosine adducts responsible for A→T transversions has remained unknown. *In vitro* translesion synthesis experiments involving DEB-induced *(R,S)*-1,N^6-γ HMHP-dA adducts (Chapter V) showed that these adducts induced A→T, A→C transversions *(247)*. Another DEB-induced exocyclic dA lesion detected in our earlier study is N^6,N^6-DHB-dA *(48)*. Since in this adduct the exocyclic N^6 position of dA is blocked by pyrrolidine-3,4-diol moiety, it cannot participate in standard Watson-Crick hydrogen bonding with dT, thereby leading to potential mispairing. Similarly, the identity of EB-derived dA adducts that induce A→T transversions has not been established. EB can alkylate DNA

to form regioisomeric N^6-HB-dA I and N^6-HB-dA II adducts *in vitro* and *in vivo (42;52;182;183;246)*, but previous *in vitro* and *in vivo* replication studies have been limited to N^6-HB-dA II *(177)*. The mutagenic potential of N^6-HB-dA I has not been previously evaluated. In the present study, we conducted *in vitro* translesion synthesis studies on synthetic DNA templates containing (*S*)-N^6-HB-dA I and *(R,R)*-N^6,N^6-DHB-dA in the presence of human DNA polymerases *β*, *η*, *ι* and *κ*.

Standing-start and running-start primer extension studies showed that *(S)*-N^6-HB-dA I can be efficiently bypassed by human DNA polymerases *β*, *η*, *ι* and *κ* (Figures 6.1, 6.2, 6.3). Similar to our previous primer extension studies with *(R,S)*-1,N^6-*γ* HMHP-dA adduct *(247)*, *(R,R)*-N^6,N^6-DHB-dA also blocked DNA synthesis by hPol *β* (Figures 6.1A, 6.3A). hPol *ι* was able to insert a base opposite the lesion but didn't extend the primer further (Figure 6.1B). Standing-start primer extension studies of *(R,R)*-N^6,N^6-DHB-dA in the presence of hPols *κ* and *η* required 2.5 times higher enzyme concentration as compared to positive control or *(S)*-N^6-HB-dA I for the formation of fully extended 18-mer products (Figure 6.2). For running-start primer extension studies in the presence of hPol *κ* (Figure 6.3B) and hPol *η*, significant amounts of 18-mer were detected, but the major products were 13- and 14-mers. Furthermore, steady-state kinetics confirmed that the incorporation of dTMP opposite *(R,R)*-N^6,N^6-DHB-dA adduct by hPols *η* and *κ* is ~400-800 fold less efficient than opposite native dA (Table 6.1). Taken together these results suggested that the *(R,R)*-N^6,N^6-DHB-dA lesions significantly reduce the rate of DNA synthesis (Figure 6.3B). Similar decreases in efficiency (up to 1000-fold) were also reported for the incorporation of dTMP opposite 1,N^6-ethenodeoxyadenosine by hPol *κ*

(165). hPol ι inserted dTMP opposite *(R,R)*-N^6,N^6-DHB-dA with higher efficiency than hPols *η* and *κ* (Table 6.1), although it did not catalyze primer extension to the terminus. The presence of *(S)*-N^6-HB-dA I lesion also decreased the catalytic efficiency of nucleotide insertion but only by 3-16 fold similar to *(R,S)*-1,N^6-*γ* HMHP-dA lesions. All four bases were incorporated with similar frequencies opposite *(R,R)*-N^6,N^6-DHB-dA by hPols *η* and hPol *κ* (Table 6.1) indicating that this lesion is highly mutagenic. In comparison, incorrect bases (A and G) were incorporated with similar frequencies opposite *(R,S)*-1,N^6-*γ* HMHP-dA lesions along with the correct base T *(247)*. However, T was the most preferred base incorporated opposite *(S)*-N^6-HB-dA I indicating that these adducts are non-mutagenic.

The mutagenic ability of the lesions were further investigated by conducting primer extension studies and sequencing the primer extension products by a sensitive HPLC-ESI$^-$-MS/MS method previously employed by our laboratory *(247)*. HPLC-MS/MS primer extension studies opposite *(S)*-N^6-HB-dA I in the presence of hPols *η* and *κ* showed that the major product was 5'-p TC**TA**TGA-3' resulting from error-free replication (Schemes 6.3 and 6.4). HPLC-MS/MS results for *(S)*-N^6-HB-dA were in agreement with gel electrophoresis experiments (Table 6.1), indicating that the primer extension is mostly error-free. *In vitro* translesion synthesis experiments with N^6-HB-dA II, the regioisomer of N^6-HB-dA I (Scheme 6.1) have also showed that *E.Coli* polymerases were able to bypass the lesion efficiently. Additionally, T was the preferred base inserted opposite the N^6-HB-dA II *(177)*. *In vivo* studies further confirmed that N^6-

HB-dA II lesion was non-mutagenic. Similarly, our data with N^6-HB-dA I also indicate that this lesion is non-mutagenic.

HPLC-MS/MS sequencing of the extension products generated upon *in vitro* replication of *(R,R)*-N^6,N^6-DHB-dA-containing template by hPols η and κ were identified as 5'-p TC**C**ATGA-3', 5'-p TC**T**ATGA-3', 5'-p TC**A**ATGA-3' and 5'-p TC**G**ATGA-3' (Schemes 6.3 and 6.4). This confirmed our steady-state kinetic results that all four bases can be incorporated opposite *(R,R)*-N^6,N^6-DHB-dA. These events, if happen *in vivo*, would result in A→G, A→T and A→C mutations. Additionally significant amounts of -1 and -2 deletion products were observed in primer extension reactions opposite *(R,R)*-N^6,N^6-DHB-dA indicating that this adduct induces deletion mutations. In our earlier study with *(R,S)*-1,N^6-γ HMHP-dA (another DEB induced exocyclic dA adduct), we found that the adduct induces A→T, A→C mutations and deletions *(247)*. These results indicate that *(R,R)*-N^6,N^6-DHB-dA along with previously identified *(R,S)*-1,N^6-γ HMHP-dA are the BD induced deoxyadenosine adducts responsible for the induction of A→T, A→C, A→G mutations and deletion events.

In summary, our gel electrophoresis and HPLC-MS/MS primer extension studies indicate that the human DNA polymerases *β, η, κ* and *ι* are able to bypass *(S)*-N^6-HB-dA I, while only hPols *κ* and *η* can bypass *(R,R)*-N^6,N^6-DHB-dA adducts. The efficiency of incorporation of the correct nucleotide dTMP opposite BD-dA exocyclic lesions was *(S)*-N^6-HB-dA I ~ *(R,S)*1,N^6-γ HMHP-dA >> *(R,R)*-N^6,N^6-DHB-dA. Among the three adducts, *(S)*-N^6-HB-dA I is primarily non-mutagenic, probably because for this

monoadduct, there is still one N^6-hydrogen available for correct hydrogen bonding with dT (Scheme 6.5). *(R,R)*-N^6,N^6-DHB-dA is more mutagenic than *(R,S)*-1,N^6-γ HMHP-dA since all the four bases were incorporated opposite *(R,R)*-N^6,N^6-DHB-dA and the majority of the primer extension products were error-prone. Our results indicate that *(R,R)*-N^6,N^6-DHB-dA can primarily induce A→G, A→T mutations, deletions, and some A→C transversions, while *(S)*-N^6-HB-dA I is non-mutagenic and is unlikely to be responsible for the monoepoxide's mutagenic ability. While exact mechanism of mispairing of *(R,R)*-N^6,N^6-DHB-dA with all four bases requires additional NMR and crystallographic studies, we hypothesized that it might adopt a syn conformation around the glycosidic bond (Scheme 6.5) similar to *(R,S)*-1,N^6-γ HMHP-dA. Structural studies are currently in progress to investigate this extreme mutagenicity of *(R,R)*-N^6,N^6-DHB-dA.

Scheme 6.5 Proposed models for base pairing of *(S)*-N^6-HB-dA and *(R,R)*-N^6,N^6-DHB-dA with dT

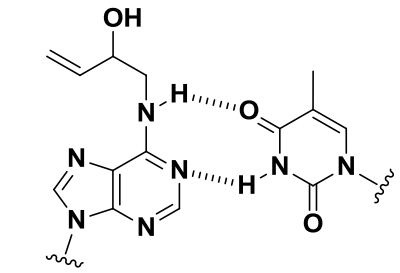

***N*^{6}-HB-dA (*anti*)** **dT (*anti*)**

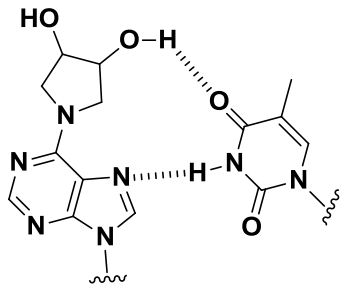

***N*^{6},*N*^{6}-DHB-dA (*syn*)** **dT (*anti*)**

VII. SUMMARY AND CONCLUSIONS

Lung cancer is the major type of cancer in the US, with an estimated mortality of 159,480 in 2013 *(2)*. Approximately 87% of these lung cancer deaths can be directly attributed to cigarette smoking *(2)*. The risk of lung cancer is significantly different among different ethnic and racial groups *(9;14)*. African American and Native Hawaiian smokers have a higher risk of lung cancer as compared to European American, Latin American and Japanese American smokers (Table 1.2) *(14)*. Although it has been hypothesized that these inter-ethnic differences in lung cancer risk are due to differences in carcinogen metabolism among the different ethnic groups *(9;14)*, very few studies have investigated such a possibility *(249)*. Among 70 other carcinogens present in cigarette smoke, 1,3-butadiene (BD) has a very high cancer risk index *(25)* and hence we chose to investigate whether there are ethnic differences in metabolism of BD.

BD is metabolically activated by CYP2E1 and CYP2A6 to form electrophilic metabolites, EB, HMVK, EBD, and DEB which can undergo detoxification by hydrolysis (via epoxide hydrolase) or glutathione conjugation (Scheme 1.1) *(27-30;189)*. The glutathione conjugates of EB, HMVK, EBD, and DEB can be further metabolically converted into mercapturic acids, MHBMA, DHBMA, THBMA and *bis*-BDMA, respectively, and excreted in urine (Scheme 1.1) *(31;93)*. If not detoxified, EB, EBD and DEB can alkylate nucleophilic sites of DNA to form covalent nucleobase adducts including mono adducts *(52;59)*, exocyclic adducts *(48;67)*, and DNA-DNA cross links *(46;64;68)*. These DNA adducts, if not repaired, can induce mutations in critical genes, ultimately leading to lung cancer *(7)*. Urinary metabolites can be used as biomarkers of

carcinogen activation and detoxification *in vivo (209)* and hence we hypothesized that differences in BD metabolism in the different ethnic/racial groups will be reflected in differences in the levels of the four urinary metabolites of BD, MHBMA, DHBMA, THBMA and *bis*-BDMA.

Among the BD-urinary metabolites, only MHBMA and DHBMA have been previously quantified in urine of rats and humans exposed to BD *(33;96;99;110)*. Although THBMA is formed from the most abundant BD-epoxide EBD, this metabolite has not been previously detected in humans, e.g. smokers and occupationally exposed workers. DEB, the most genotoxic BD-epoxide can potentially react with two glutathione molecules to form *bis*-glutathione conjugates *in vitro (94)*. We hypothesized that these *bis*-glutathione conjugates can be further modified to *bis*-mercapturic acids and excreted in urine as *bis*-BDMA. If detected *in vivo*, this urinary metabolite can be used as a specific biomarker of DEB. Hence, the initial goals of this thesis were to develop HPLC-ESI$^-$-MS/MS methods for the quantification of novel urinary metabolites of BD, THBMA and *bis*-BDMA *in vivo* and evaluate their potential as biomarkers of BD exposure and bioactivation.

A sensitive and specific stable isotope dilution HPLC-ESI$^-$-MS/MS method was developed for the quantification of THBMA in human urine (Chapter II). We applied this method for THBMA quantification in urine samples from smokers (N = 27) and nonsmokers (N = 19). Significant amounts of THBMA were detected in both smokers and non-smokers (Figure 2.6). Urinary THBMA concentrations in smokers (21.6 ± 10.2 ng/mg creatinine) were significantly higher than in non-smokers (13.7 ± 7.9 ng/mg

creatinine) ($p < 0.01$) (Figure 2.6). The presence of endogenous THBMA in samples from non-smokers might be due to environmental exposure to BD or because of an alternate endogenous source yet to be identified. Additionally, we also found that the THBMA levels decreased by ~45% after smoking cessation (Figure 2.7). Because higher levels of THBMA were present in smokers as compared to non-smokers and THBMA levels decreased after smoking cessation, we concluded that a significant amount of THBMA is directly formed from BD present in cigarette smoke. However, since THBMA is also present in urine of non-smokers, it might not be the best biomarker of smoking-mediated exposure to BD.

The second goal of this thesis was the development of a sensitive HPLC-ESI$^-$-MS/MS method for quantification of *bis*-BDMA in urine of rats exposed to BD, humans occupationally exposed to BD, and smokers. Significant amounts of *bis*-BDMA were detected in the urine of F344 rats exposed to 62.5 ppm or 200 ppm BD, while no *bis*-BDMA was detected in urine of rats exposed to filtered air (Figures 3.4 and 3.5). However, the urinary concentrations of *bis*-BDMA in occupationally exposed workers and smokers were below the LOD of our method (0.1 ng/ml) (Figure 3.7) confirming earlier reports of the inefficient formation of DEB in humans *(26;89)*. Additionally, the urinary concentrations of MHBMA, DHBMA and THBMA were also determined in rat and human urine samples. In rats, the relative contribution of individual urinary metabolites to total BD-mercapturic acids was DHBMA (47%)>THBMA (37%)>MHBMA (15%)>*bis*-BDMA (1%) (Figure 3.6A). However, in humans the metabolites were DHBMA (93%)>THBMA (5%)>MHBMA (2%)>*bis*-BDMA (<0.1%)

(Figure 3.6B). These results reveal significant interspecies differences in metabolism of BD between rats and humans. However, it should also be noted that the high percentage of DHBMA in humans might be due to the presence of an endogenous source. Furthermore, we observed gender differences in BD metabolism, with female rats excreting higher concentrations of *bis*-BDMA as compared to males (Figure 3.5 A). Since *bis*-BDMA was not detected in humans, it cannot be used as a biomarker in smokers to study the interethnic differences in lung cancer risk.

Our third goal was to develop a robust, high throughput HPLC-ESI$^-$-MS/MS method for quantification of MHBMA and DHBMA in human urine and apply the method for quantification of these metabolites in urine of smokers belonging to different ethnic groups. The levels of MHBMA decreased by >90% upon smoking cessation, therefore this metabolite can be considered as a specific biomarker of exposure to BD in cigarette smoke *(33)*. DHBMA, on the other hand is present in urine of both smokers and non-smokers, and the urinary DHBMA levels remain constant even after smoking cessation *(33)*. Metabolic ratio (MHBMA/MHBMA+DHBMA) has been widely used as an indicator of relative contribution of detoxification pathways (glutathione conjugation vs. epoxide hydrolysis) and hence can be used to study any inter-ethnic differences in BD metabolism *(85)*. Although, a number of HPLC-MS/MS methods for quantification of MHBMA and DHBMA in humans have been reported in literature (Table 1.5), none of the methods employ a 96 well plate SPE method amenable for multiple sample processing in large studies. Additionally, most of the methods use a relatively large volume of urine (>0.5 ml) which was not available for our studies (Table 1.5). We

developed and validated an Oasis HLB 96 well plate SPE method and a sensitive HPLC-ESI$^-$-MS/MS method (LOQ: MHBMA, 0.5 ng/ml; DHBMA, 10 ng/ml) (Table 4.1).

This new method was employed to quantify BD-urinary mercapturic acids in workers employed at a BD and SBR manufacturing facility in Czech Republic *(85)*. We found significantly higher amounts of MHBMA and DHBMA in urine of workers exposed to BD as compared to controls (Figure 4.1, Table 4.2). Additionally, we also found significantly higher amounts of THBMA in exposed workers as compared to controls (Figure 4.2, Table 4.2). In the exposed group, male workers excreted significantly higher amounts of MHBMA, DHBMA and THBMA as compared to controls (Table 4.2). These differences were observed probably because males were exposed to significantly higher concentrations of BD as compared to females (Table 4.2). Indeed, when the urinary concentrations were normalized to per unit dose of BD, only MHBMA formation was found to be significantly higher in males as compared to females (Table 4.2). We also found that there were no differences in MHBMA/MHBMA+DHBMA metabolic ratio between males and females (Table 4.2) suggesting that there are no gender differences in relative usage of BD detoxification pathways. A strong association was observed between BD exposure and urinary BD-mercapturic acids (Figure 4.4). Correlation studies also revealed a strong association between and among the three BD-urinary mercapturic acids (Figure 4.5, Table 4.3). Significant correlations were also found between each of BD-urinary mercapturic acids and BD-hemoglobin adducts (HB-Val and *pyr*-Val) (Figure 4.5, Table 4.3).

The new method was further applied to quantify MHBMA and DHBMA in urine of smokers of Native Hawaiian, Japanese American and European American descent (N=200 per group). We found that the mean urinary MHBMA concentrations (adjusted for age, sex and log nicotine equivalents) significantly differed among the three ethnic groups (p=0.0002) with the highest MHBMA amounts observed in European Americans (6.7 ng/mg creatinine), followed by Native Hawaiians (5.3 ng/mg creatinine) and the lowest in Japanese American smokers (4.3 ng/mg creatinine) (Table 4.4). However, it should be noted that the lung cancer risk is highest in Native Hawaiian smokers, intermediate in European American smokers and least in Japanese American smokers. Significant ethnic differences were observed in the MHBMA/MHBMA+DHBMA metabolic ratio (p = 0.0037) but not for DHBMA (p=0.15) (Table 4.4). These results provided preliminary evidence for the presence of inter-ethnic differences in BD metabolism. A larger study involving smokers from two ethnic groups, European-Americans (N=450) and African-Americans (N=450) was also completed. We found median MHBMA levels in European–American smokers (11.2 ng/mg creatinine) were significantly higher than in African-American smokers (8.9 ng/mg creatinine) (Table 4.5). In contrast, no significant ethnic differences were observed for urinary DHBMA concentration and metabolic ratio between the ethnic groups (Table 4.5). Additionally, genome-wide association study (GWAS) analysis revealed significant associations between single-nucleotide polymorphisms (SNPs) in chromosome 22 (22564172bp – 22735492 bp, nearby genes GSTT1, GSTT2, DDT and MIF) and MHBMA. GSTT1 is the major enzyme involved in the detoxification of EB (precursor to MHBMA). Overall,

the results from the two studies confirm our earlier hypothesis that there are significant differences in metabolism of BD among different ethnic groups (Tables 4.4 and 4.5). However, additional correlation analysis between genetic polymorphisms and urinary metabolites will need to be completed to identify specific genetic polymorphisms responsible for these differences. These results indicate that because of different frequency of genetic polymorphisms in carcinogen metabolizing genes among ethnic groups, there are measurable ethnic differences in metabolic activation and deactivation of carcinogens, ultimately leading to differences in susceptibility to lung cancer.

Among the four urinary BD metabolites investigated in this work, MHBMA is the most specific biomarker of BD. A strong association was found between MHBMA and BD exposure (Figure 4.4). Additionally, MHBMA concentrations were significantly different among the ethnic groups in two multi-ethnic cohort studies (Tables 4.4 and 4.5). In contrast, no significant ethnic differences were observed with DHBMA. Furthermore, DHBMA and THBMA were detected in significant amounts in non-smokers, probably due to their endogenous formation in humans. *bis*-BDMA would be an ideal biomarker of BD bioactivation to DEB, but unfortunately *bis*-BDMA concentrations in human urine were below the LOD of our method and hence cannot be used for human studies.

The second part of the thesis focuses on investigating the mutagenic ability of three BD-dA adducts (Scheme 1.4). The investigations of deoxyadenosine adducts are of special importance because BD, EB, and DEB induce a large number of A→T mutations and deletions *(35)*. Although polymerase bypass of some BD-dA lesions has been studied previously (Chart 1.3) *(177-181)*, the identity of specific lesions responsible for A→T

mutations remained to be determined. We have focused on three BD-dA adducts (Scheme 1.4) which have been observed *in vitro* (N^6-HB-dA, N^6,N^6-DHB-dA, 1,N^6-HMHP-dA) and *in vivo* (N^6-HB-dA and 1,N^6-HMHP-dA) *(48;52;67)*. 1,N^6-HMHP-dA lesions have been shown to persist in tissues of laboratory mice following exposure to BD *(185)*. Since N^6,N^6-DHB-dA and 1,N^6-HMHP-dA are exocyclic lesions that cannot form Watson-Crick pairs and are likely to block replicative DNA polymerases, we hypothesized that they are subject to bypass by translesion synthesis (TLS) polymerases, potentially leading to mutations because of the relatively low fidelity of these enzymes *(120;121;130)*. *In vitro* replication studies were conducted with synthetic 18-mer template strands generated by the post-oligomerization strategy developed in our laboratory *(186)*. Each template strand contained site-specific *(S)*-N^6-HB-dA, *(R,R)*-N^6,N^6-DHB-dA and *(R,S)*- 1,N^6-γ-HMHP-dA adducts (Schemes 5.2 and 6.2). Following annealing to a 13-mer primer with 3' terminus one base before the lesion (standing start conditions), primer extension was conducted in the presence of human polymerases *β, η, ι,* and *κ* .

We found that among the three lesions, *(S)*-N^6-HB-dA adducts was the least mutagenic and easiest to bypass. Human polymerases *β, η, ι,* and *κ* were able to bypass the lesion and extend the primer to the terminus (18-mer, except for hPol *ι* which formed a 16-mer) (Figures 6.1, 6.2). Steady-state kinetic experiments showed that T was the preferred base of incorporation opposite *(S)*-N^6-HB-dA (Table 6.1). Additionally, sequencing of primer extension products using HPLC-ESI-MS/MS confirmed that

primer extension opposite *(S)*-N^6-HB-dA was error-free, as the correct product (5'p-TCTATGA-3') accounted for > 80% of all products (Schemes 6.3 and 6.4).

In contrast, exocyclic 1,N^6-γ-HMHP-dA and N^6,N^6-DHB-dA adducts blocked replication and induced polymerase errors. Primer extension studies past *(R,S)*- 1,N^6-γ-HMHP-dA using gel electrophoresis showed that primer extension by hPol β was completely blocked by *(R,S)*- 1,N^6-γ-HMHP-dA (Figure 5.1 A). hPol ι was able to incorporate a base but could not extend the primer beyond that (Figure 5.1 B). Steady-state kinetic experiments confirmed that the presence of the lesion decreased the polymerization rates as indicated by low k_{cat}/K_m ratios for nucleotide incorporation opposite the lesions (Table 5.1). Importantly, A and G were incorporated with a high frequency opposite 1,N^6-γ-HMHP-dA. Further analysis of primer extension products by HPLC-ESI$^-$-MS/MS *(164)* revealed that nucleotide incorporation opposite *(R,S)*- 1,N^6-γ-HMHP-dA by hPol κ was highly mutagenic, producing only 18% of error-free product (5'p-TCTATGA-3') (Scheme 5.3A). The rest of the primer extensions products correspond to misincorporation of A, G opposite the lesion and -1, -2 deletion products (Schemes 5.3, 5.4 and 5.5, Chapter V). These results are consistent with the ability of DEB to induce A →T transversions and frameshift mutations *(35)*.

Similar to *(R,S)*- 1,N^6-γ-HMHP-dA lesions, *(R,R)*-N^6,N^6-DHB-dA lesions also blocked replication by non-TLS polymerase hPol β (Figure 6.1 A). hPol ι was able to incorporate only a base opposite *(R,R)*-N^6,N^6-DHB-dA lesion to form a 14-mer primer but was unable to extend further (Figure 6.1 B). hPols η and κ were unable to extend the primer at low enzyme:DNA concentration ratios, but were able to extend the primer

completely to the terminus at higher concentration ratios (Figure 6.2). Steady-state kinetic experiments revealed that all four bases were incorporated almost with identical frequencies opposite *(R,R)*-N^6,N^6-DHB-dA lesions by hPols η and κ (Table 6.1). Additionally, the k_{cat}/K_m for incorporation of nucleotide incorporation opposite this lesion was only ~ 0.002, reflecting a decreased tolerance of TLS polymerases for this lesion (Table 6.1). Primer extension studies with HPLC-MS/MS showed that >60% of the primer extension products opposite this lesion were error-prone (Schemes 6.3 and 6.4). Our results indicate that *(R,R)*-N^6,N^6-DHB-dA can induce A→G, A→T, A→C and deletion mutations (Schemes 6.3 and 6.4).

In summary, studies described in this thesis have identified two novel urinary metabolites of BD, THBMA and *bis*-BDMA (Scheme 1.1), which were subsequently detected in urine of BD-exposed laboratory animals (THBMA and *bis*-BDMA) and humans exposed to BD via smoking and/or occupational exposure (THBMA) (Figures 2.5, 3.4 and 4.2). Additionally, a high throughput, ultra-sensitive HPLC-ESI$^-$-MS/MS method was developed and successfully employed for the quantification of MHBMA and DHBMA in smokers belonging to different ethnic groups in two separate multi-ethnic cohort studies (Chapter IV). Significant ethnic differences in urinary concentrations of MHBMA were observed, with European American smokers excreting the highest levels, followed by African Americans and Native Hawaiians, and Japanese group excreting the lowest amounts of BD metabolites (Tables 4.4 and 4.5). To our knowledge, this study provides the first definitive evidence for ethnic differences in BD metabolism, which may contribute to the observed differences in lung cancer risk. Furthermore, we investigated

the mutagenic potential of three BD-dA adducts, *(S)*-N^6-HB-dA, *(R,R)*-N^6,N^6-DHB-dA and *(R,S)*- 1,N^6-γ-HMHP-dA. We found that while *(S)*-N^6-HB-dA lesions were non-mutagenic, *(R,R)*-N^6,N^6-DHB-dA and *(R,S)*- 1,N^6-γ-HMHP-dA produced high levels of base substitutions and frameshift mutations (Schemes 5.3, 5.4, 6.3, and 6.4) providing a likely mechanism for the induction of A→T transversions and deletion mutations in cells and animals exposed to BD and DEB.

VIII. FUTURE WORK

8.1 Quantification of *bis*-BDMA in rats and humans exposed to low concentrations of BD

As described in Chapter III, DEB-specific urinary biomarker *bis*-BDMA was detected in the urine of rats exposed to high doses of BD (62.5 ppm or 200 ppm) (Figure 3.4) but not in occupationally exposed workers (~1 ppm BD exposure) (Figure 3.7). Since humans are generally exposed to much lower doses of BD, it would be important to study the formation of *bis*-BDMA in urine of laboratory rats and mice exposed to 0.5, 1 or 1.5 ppm BD. Boysen et al. have detected the formation of DEB-specific hemoglobin adducts (*pyr*-Val) *(89)* in both control and exposed workers, therefore it is likely that *bis*-BDMA is formed in humans, albeit at much lower concentrations. Our current HPLC-ESI$^-$-MS/MS method with an LOD of 1 ng/ml was not sufficient to detect *bis*-BDMA in human urine. We attempted to develop a more sensitive capillary HPLC-ESI$^-$-MS/MS method with a Zorbax SB-C18 (0.5 X 100 mm, 5µ) column with an LOD of 0.1 ng/ml, but could not detect any *bis*-BDMA in exposed workers or smokers (Figure 3.7B).

To increase HPLC-ESI$^-$-MS/MS method sensitivity, the use of alternate SPE methods (e.g. Strata X-A) should be explored. Our preliminary studies suggest that this would improve SPE recovery for *bis*-BDMA, as well as decrease the interferences that cause ion suppression. Alternatively, use of accurate mass LTQ Orbitrap mass spectrometry might help decrease the baseline noise and further improve the sensitivity. The use of NanoLC LC-ESI$^-$-MS/MS will further improve sensitivity but the presence of high salts and interferences from urine matrix might be the deterrents. An offline HPLC

clean-up or consecutive SPE clean-ups (C18 and ion-exchange) followed by analysis by NanoLC LC-ESI$^-$-MS/MS might be an interesting methodology to explore.

8.2 DHB-Lysine as a novel urinary biomarker of DEB formation from BD

Since *bis*-BDMA, specific biomarker of DEB formation form BD, could not be detected in the urine of occupationally exposed workers or smokers (Figure 3.7), alternate DEB-specific biomarkers could be explored. DEB is known to react with N-terminal valine of hemoglobin to form exocyclic *pyr*-Val adducts (Scheme 1.2) *(89)*. We hypothesize that DEB can similarly alkylate side chain of amino acids (e.g. lysine) to form *N,N*-2,3-dihydroxybutan-1,4-diyl-lysine adducts (DHB-Lysine). These would be excreted in urine following proteolytic degradation of the affected proteins as small modified peptides or adducted Lysine. We attempted to synthesize authentic DHB-Lysine by reacting tBoc-Lysine with equimolar amounts of DEB in the presence of triethylamine and glacial acetic acid at 50 $^{\circ}$C for 7 days (Scheme 8.1) *(250)*. The formation of tBoc-DHB-Lysine (*m/z* 333) was confirmed by infusion into ion trap MS and the reaction mixture was fractionated by semi-preparative HPLC. The purified tBoc-DHB-Lysine was deprotected with 10% TFA, and DHB-Lysine was isolated by semi-preparative HPLC. The identity of the product was established by tandem mass spectrometry (Figure 8.1).

HPLC-ESI-MS/MS method development for DHB-Lysine in human urine is challenging because the extreme polarity of this modified amino acid. Initial attempts were made to increase the retention of this analyte on reverse phase HPLC in the presence of ion pairing agents such as perfluoroheptanoic acid. These methods need to be optimized further and applied to urine samples of laboratory rats exposed to BD by inhalation and occupationally exposed workers to investigate the formation of DHB-Lysine *in vivo*.

Scheme 8.1 Synthesis of DHB-Lysine

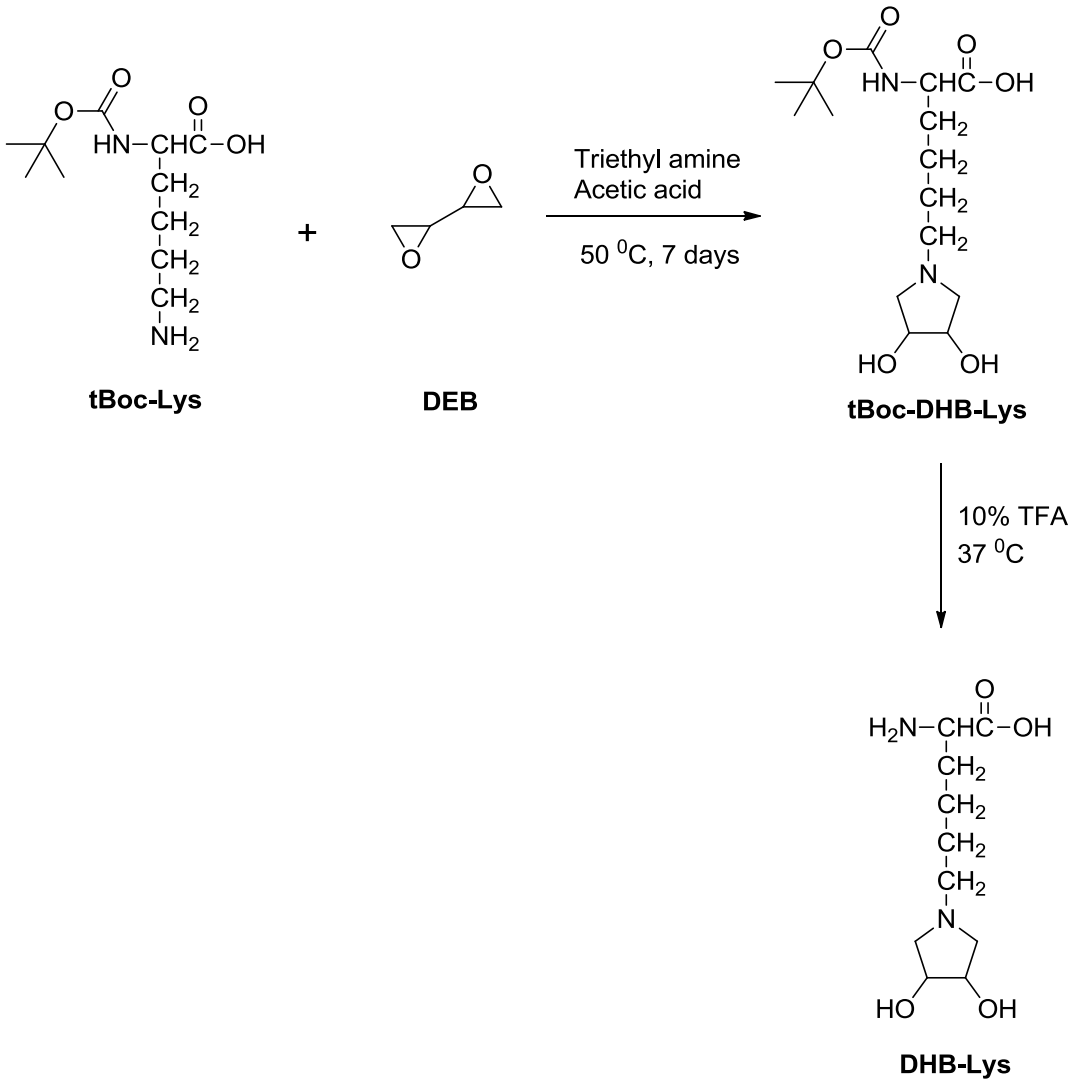

tBoc-Lys **DEB** **tBoc-DHB-Lys** **DHB-Lys**

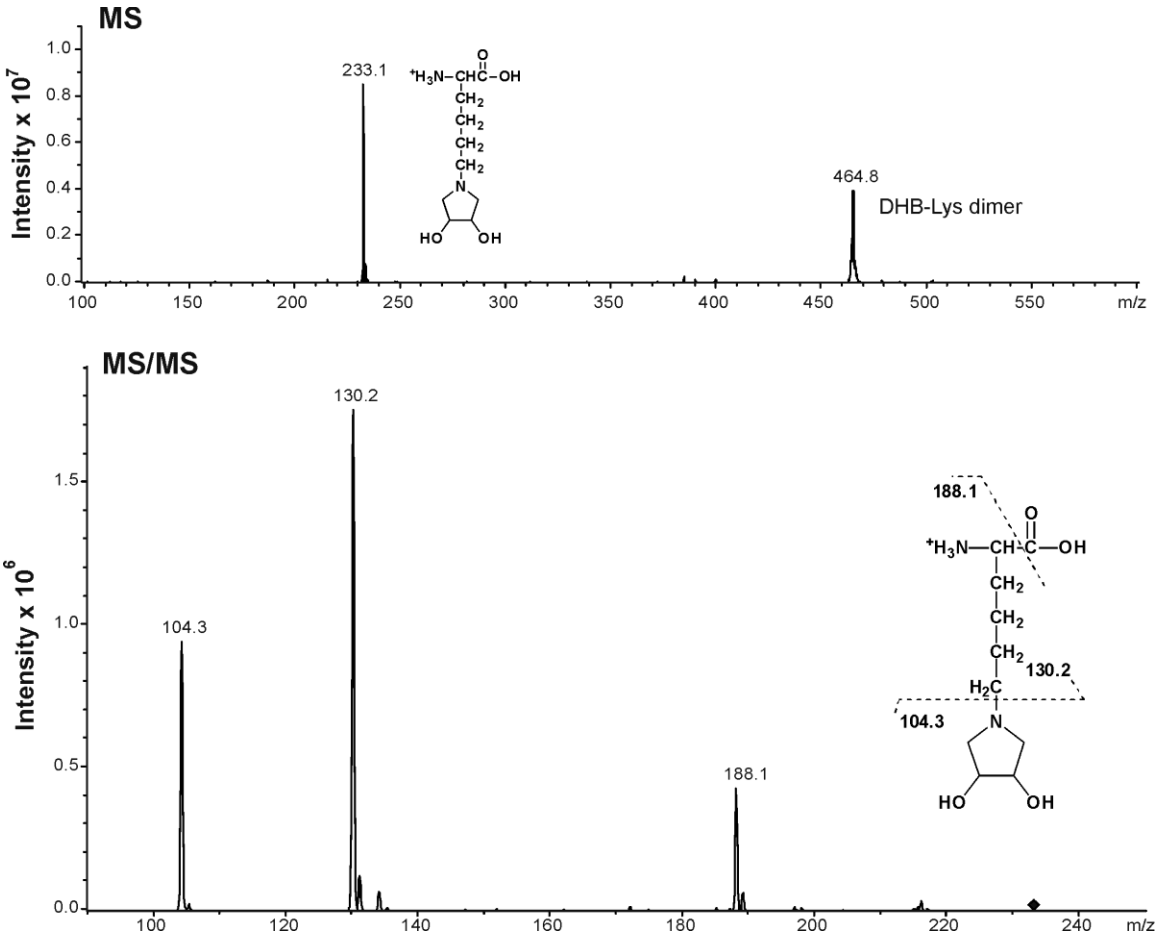

Figure 8.1 MS/MS spectrum of DHB-Lysine

8.3 Development of an HPLC-MS/MS method for simultaneous quantification of MHBMA, DHBMA and THBMA

In this thesis, an HPLC-MS/MS method for simultaneous quantification of MHBMA and DHBMA was developed (Chapter IV). THBMA was quantified by a separate HPLC-MS/MS method on a different HPLC column (Chapters II, IV). This was because the recoveries of THBMA with the Oasis HLB SPE method (used for MHBMA and DHBMA) are close to 0%. More recently, we have found that Isolute ENV+ cartridges offer >40% recoveries for all the three urinary metabolites of BD and can be used for simultaneous quantification of MHBMA, DHBMA and THBMA in human urine. Alternatively, Strata X-A columns also offer good recoveries of all the three analytes and need to be explored in the future.

The ability of the Diphenyl HPLC column (Agilent) currently only used for MHBMA and DHBMA) to retain THBMA needs to be evaluated. Alternate columns that retain polar compounds such as Synergi Polar-RP can be tested. If a HPLC-MS/MS method for simultaneous quantification of MHBMA, DHBMA and THBMA can be developed, it will be highly efficient as it would save sample, sample processing time, and MS analysis time. Such a method would be highly beneficial for future multi-ethnic cohort studies or animal studies with large number of samples as it will provide important information on formation of THBMA along with MHBMA and DHBMA.

8.4 Identifying the DHBMA and THBMA concentrations directly related to BD exposure

High concentrations of DHBMA and THBMA have been detected in the urine of non-smokers (Chapter II) *(33;206)*. It has been hypothesized that EB-diol, the common precursor to HMVK and EBD can be formed during the carbohydrate catabolism *(87)*. The portion of EB-diol that is formed from direct exposure to BD and subsequent detoxification to DHBMA and THBMA has not been assessed before. To differentiate the endogenous DHBMA and THBMA formation from that formed from BD exposure, the following experiment can be performed.

F344 rats can be exposed with 62.5 ppm $^{13}C_2$-1,3-butadiene for 2 weeks (6 h/day, 5 days/week). At the end of the exposure period, urine samples would be collected and then the urinary concentrations of $^{13}C_2$-DHBMA, $^{13}C_2$-THBMA along with DHBMA and THBMA can be determined by the stable isotope dilution HPLC-ESI$^-$-MS/MS methods described in Chapters II and IV. Comparison of $^{13}C_2$-DHBMA, $^{13}C_2$-THBMA with endogenous DHBMA and THBMA would provide information on the relative formation of these BD-mercapturic acids from BD exposure vs other endogenous sources.

8.5 Expanding multi-ethnic cohort study to different racial groups and correlation studies

Our preliminary results from a small multi-ethnic study (200 smokers per group) confirmed that there are significant differences in the MHBMA concentrations among Native Hawaiian, Japanese American and European American smokers (Table 4.4 in Chapter IV). Unfortunately, no significant association studies between the genetic polymorphisms and MHBMA concentrations were possible because of the low frequency of polymorphisms in a study population of 600 smokers.

In a larger multi-ethnic cohort study, we examined the differences in BD metabolism between African American and European American smokers (N=450 per group). We found that European American smokers excreted significantly higher concentrations of MHBMA as compared to African American smokers (Table 4.5 in Chapter IV). It will be interesting to expand this larger study to other ethnic groups, e.g. Native Hawaiian, Japanese American, and Latin American smokers (N=450 per group) so that the total study population would be ~2500 smokers. That would provide an opportunity to conduct GWAS between genetic polymorphisms and urinary BD-mercapturic acids to understand the genetic basis for differences in metabolism. Eventually, such a study could contribute to our understanding of the origins of ethnic differences in lung cancer risk. The proposed study design is summarized in Figure 8.2.

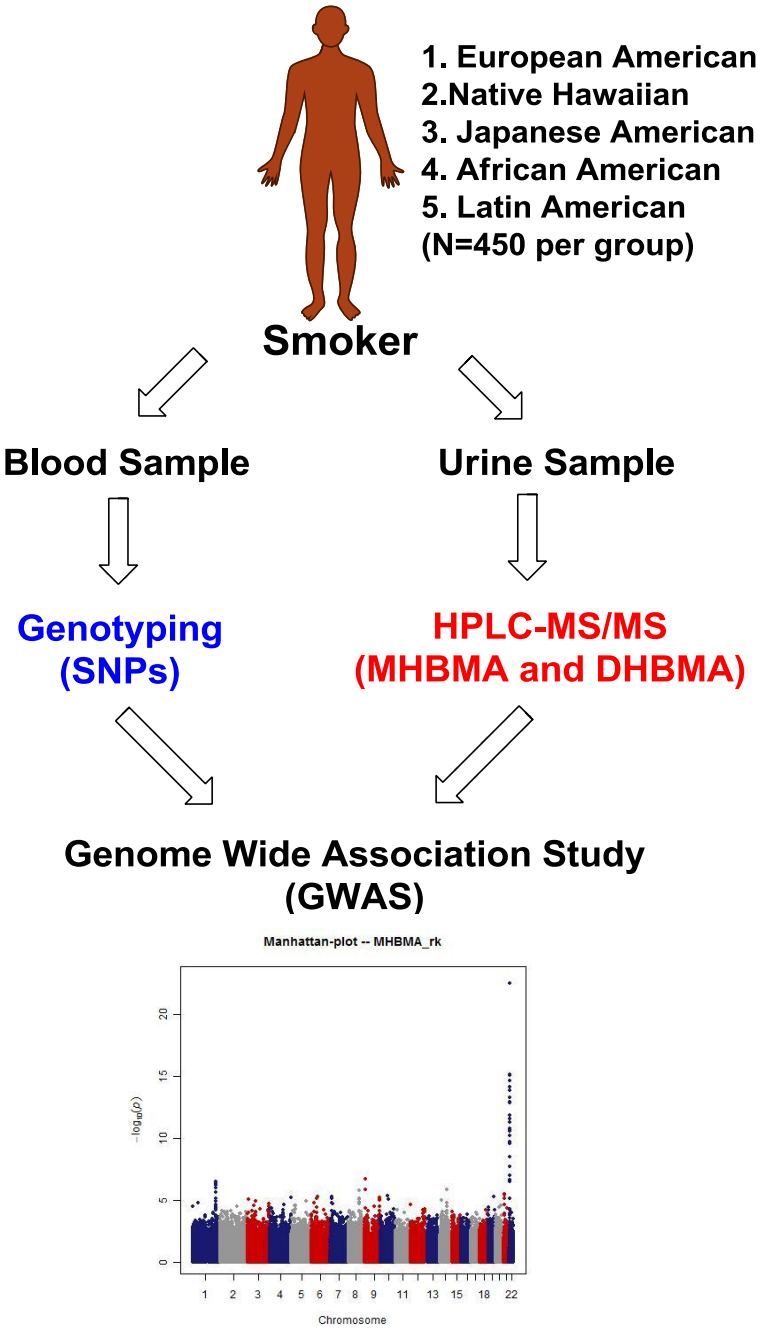

Figure 8.2 GWAS design for the multi-ethnic cohort study

8.6 Investigate the mutagenic ability of other BD-dA lesions and improve HPLC-MS/MS primer extension methodology

In the present thesis, the mutagenic ability of *(R,R)*-N^6,N^6-DHB-dA and *(R,S)*- 1,N^6-γ-HMHP-dA was evaluated (Chapters V and VI). It would be interesting to perform similar translesion synthesis studies for additional stereoisomers of the adducts, e.g. *(S,S)*-N^6,N^6-DHB-dA and *(R,R)*- 1,N^6-γ-HMHP-dA (Chart 8.1). The synthesis of oligonucleotide templates incorporating these adducts at site-specific positions has already been described by our group *(186)*. Additionally, we previously reported that 1,N^6-γ-HMHP-dA adducts undergo base-catalyzed Dimroth arrangement to form 1,N^6-α-HMHP-dA *(48)*. Since 1,N^6-γ-HMHP-dA adducts induce A→T mutations and deletions, translesion synthesis studies opposite 1,N^6-α-HMHP-dA adducts would be especially interesting.

Another potential area of improvement is the HPLC-MS/MS methodology for primer extension studies. In the present method, a 13 mer uracil containing primer is annealed to an 18 mer template containing the adduct, and the resulting primer-template complex is incubated in the presence of TLS polymerases and dNTPs. At the end of incubation, the primer is cleaved by UDG hydrolysis and piperidine treatment, and the primer extension products were directly injected onto the LC-MS. The disadvantage of the current method is the presence of interferences such as UDG and template which might result in suppression of primer extension products. Christov et al. have modified this methodology using a biotinylated primer/template duplex (Scheme 8.2) *(176)*. After the extension reaction, the biotinylated primer was separated from the other components by streptavidin capture and further subjected to UDG hydrolysis and piperidine treatment

(Scheme 8.2). This methodology offers superior clean-up of primer extension products and hence improves the detection of those primer extension products present at low levels. This methodology can be directly applied to translesion synthesis studies in our laboratory to further improve the sensitivity.

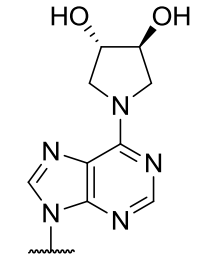

(S,S)-N^6-DHB-dA

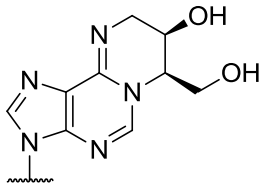

(R,R)-1,N^6-γ-HMHP-dA

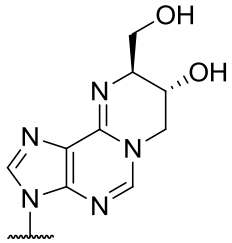

(S,R)-1,N^6-α-HMHP-dA

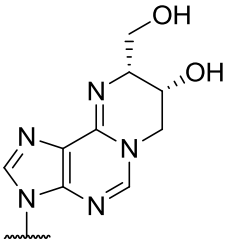

(R,R)-1,N^6-α-HMHP-dA

Chart 8.1 New BD-dA adducts of interest

Scheme 8.2 Improved method for HPLC-MS/MS primer extension studies

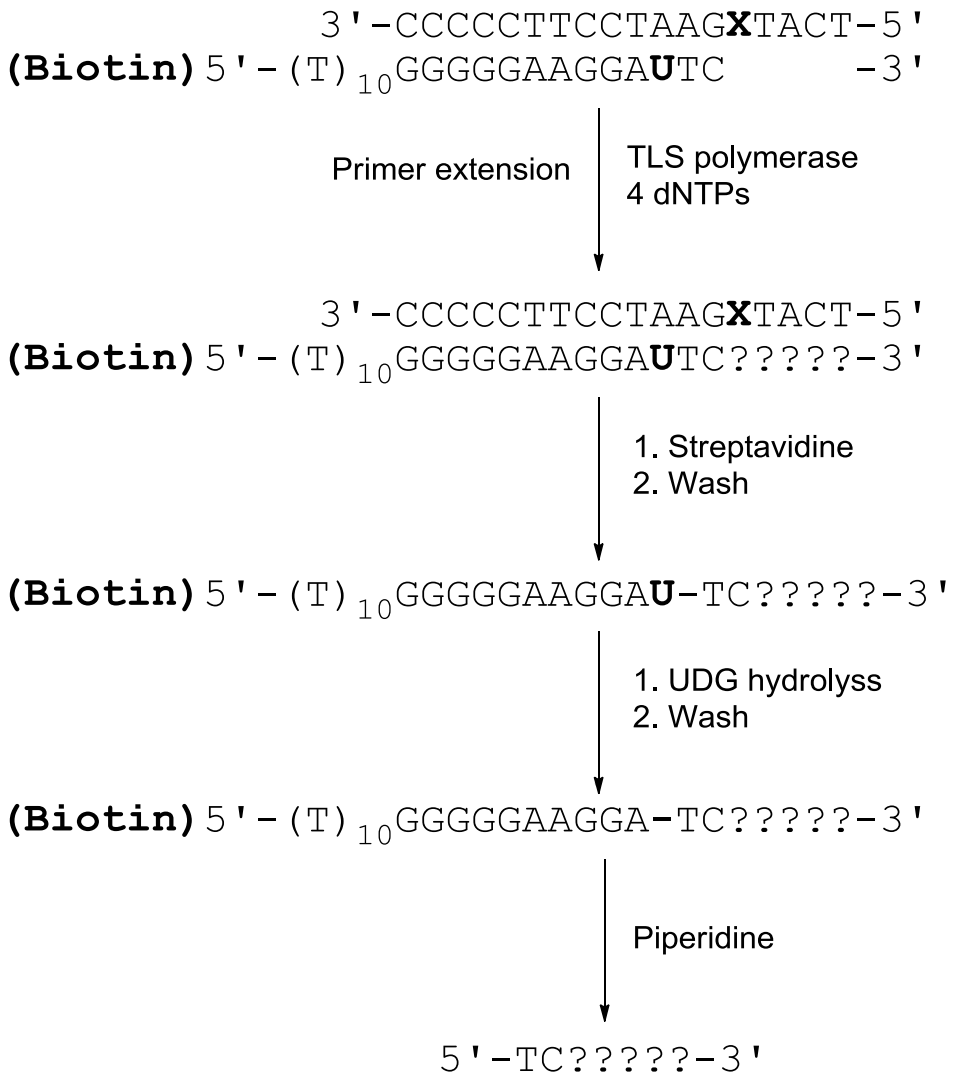

IX. BIBLIOGRAPHY

1. Jemal, A., Bray, F., Center, M. M., Ferlay, J., Ward, E., and Forman, D. (2011) Global cancer statistics. *CA Cancer J Clin.*, **61**, 69-90.

2. American Cancer Society (2013) Cancer Facts & Figures 2013. *http://www.cancer.org/acs/groups/content/@epidemiologysurveilance/documents/document/acspc-036845.pdf (Accessed May 1, 2013)*.

3. American Cancer Society (2013) Tobacco-Related Cancers Fact Sheet. *http://www.cancer.org/cancer/cancercauses/tobaccocancer/tobacco-related-cancer-fact-sheet (Accessed May 1, 2013)*.

4. International Agency for Research on Cancer (2012) A Review of Human Carcinogens: Personal Habits and Indoor Combustions. *IARC monographs on the evaluation of carcinogenic risks to humans*, **100 E**.

5. Hecht, S. S. (2003) Tobacco carcinogens, their biomarkers and tobacco-induced cancer. *Nat.Rev.Cancer*, **3**, 733-744.

6. Rendic, S. and Guengerich, F. P. (2012) Contributions of human enzymes in carcinogen metabolism. *Chem.Res.Toxicol.*, **25**, 1316-1383.

7. Hecht, S. S. (1999) Tobacco smoke carcinogens and lung cancer. *J Natl.Cancer Inst.*, **91**, 1194-1210.

8. Christmann, M., Tomicic, M. T., Roos, W. P., and Kaina, B. (2003) Mechanisms of human DNA repair: an update. *Toxicology*, **193**, 3-34.

9. Le Marchand, L., Wilkens, L. R., and Kolonel, L. N. (1992) Ethnic differences in the lung cancer risk associated with smoking. *Cancer Epidemiol.Biomarkers Prev.*, **1**, 103-107.

10. Hinds, M. W., Stemmermann, G. N., Yang, H. Y., Kolonel, L. N., Lee, J., and Wegner, E. (1981) Differences in lung cancer risk from smoking among Japanese, Chinese and Hawaiian women in Hawaii. *Int.J Cancer*, **27**, 297-302.

11. Schwartz, A. G. and Swanson, G. M. (1997) Lung carcinoma in African Americans and whites. A population-based study in metropolitan Detroit, Michigan. *Cancer*, **79**, 45-52.

12. Stellman, S. D., Takezaki, T., Wang, L., Chen, Y., Citron, M. L., Djordjevic, M. V., Harlap, S., Muscat, J. E., Neugut, A. I., Wynder, E. L., Ogawa, H., Tajima, K., and Aoki, K. (2001) Smoking and lung cancer risk in American and Japanese

men: an international case-control study. *Cancer Epidemiol.Biomarkers Prev.*, **10**, 1193-1199.

13. Stellman, S. D., Chen, Y., Muscat, J. E., Djordjevic, M. V., Richie, J. P., Jr., Lazarus, P., Thompson, S., Altorki, N., Berwick, M., Citron, M. L., Harlap, S., Kaur, T. B., Neugut, A. I., Olson, S., Travaline, J. M., Witorsch, P., and Zhang, Z. F. (2003) Lung cancer risk in white and black Americans. *Ann.Epidemiol.*, **13**, 294-302.

14. Haiman, C. A., Stram, D. O., Wilkens, L. R., Pike, M. C., Kolonel, L. N., Henderson, B. E., and Le Marchand, L. (2006) Ethnic and racial differences in the smoking-related risk of lung cancer. *N.Engl.J Med.*, **354**, 333-342.

15. National Cancer Institute.Bethesda, M. (2013) SEER Cancer Statistics Review 1975-2010. *http://seer.cancer.gov/statfacts/html/lungb.html (accessed August 18, 2013)*..

16. Himmelstein, M. W., Acquavella, J. F., Recio, L., Medinsky, M. A., and Bond, J. A. (1997) Toxicology and epidemiology of 1,3-butadiene. *Crit Rev.Toxicol.*, **27**, 1-108.

17. White, W. C. (2007) Butadiene production process overview. *Chem.Biol.Interact.*, **166**, 10-14.

18. National Toxicology Program (2011) 1,3-Butadiene. *Rep Carcinog.*, **12**, 75-77.

19. Brunnemann, K. D., Kagan, M. R., Cox, J. E., and Hoffmann, D. (1990) Analysis of 1,3-butadiene and other selected gas-phase components in cigarette mainstream and sidestream smoke by gas chromatography-mass selective detection. *Carcinogenesis*, **11**, 1863-1868.

20. Melnick, R. L., Huff, J., Chou, B. J., and Miller, R. A. (1990) Carcinogenicity of 1,3-butadiene in C57BL/6 x C3H F1 mice at low exposure concentrations. *Cancer Res.*, **50**, 6592-6599.

21. Owen, P. E., Glaister, J. R., Gaunt, I. F., and Pullinger, D. H. (1987) Inhalation toxicity studies with 1,3-butadiene. 3. Two year toxicity/carcinogenicity study in rats. *Am.Ind.Hyg.Assoc.J.*, **48**, 407-413.

22. Macaluso, M., Larson, R., Delzell, E., Sathiakumar, N., Hovinga, M., Julian, J., Muir, D., and Cole, P. (1996) Leukemia and cumulative exposure to butadiene, styrene and benzene among workers in the synthetic rubber industry. *Toxicology*, **113**, 190-202.

23. Delzell, E., Sathiakumar, N., Hovinga, M., Macaluso, M., Julian, J., Larson, R., Cole, P., and Muir, D. C. (1996) A follow-up study of synthetic rubber workers. *Toxicology*, **113**, 182-189.

24. Cheng, H., Sathiakumar, N., Graff, J., Matthews, R., and Delzell, E. (2007) 1,3-Butadiene and leukemia among synthetic rubber industry workers: exposure-response relationships. *Chem.Biol.Interact.*, **166**, 15-24.

25. Fowles, J. and Dybing, E. (2003) Application of toxicological risk assessment principles to the chemical constituents of cigarette smoke. *Tob.Control*, **12**, 424-430.

26. Swenberg, J. A., Bordeerat, N. K., Boysen, G., Carro, S., Georgieva, N. I., Nakamura, J., Troutman, J. M., Upton, P. B., Albertini, R. J., Vacek, P. M., Walker, V. E., Sram, R. J., Goggin, M., and Tretyakova, N. (2011) 1,3-Butadiene: Biomarkers and application to risk assessment. *Chem.Biol.Interact.*, **192**, 150-154.

27. Csanady, G. A., Guengerich, F. P., and Bond, J. A. (1992) Comparison of the biotransformation of 1,3-butadiene and its metabolite, butadiene monoepoxide, by hepatic and pulmonary tissues from humans, rats and mice. *Carcinogenesis*, **13**, 1143-1153.

28. Duescher, R. J. and Elfarra, A. A. (1994) Human liver microsomes are efficient catalysts of 1,3-butadiene oxidation: evidence for major roles by cytochromes P450 2A6 and 2E1. *Arch.Biochem.Biophys.*, **311**, 342-349.

29. Krause, R. J. and Elfarra, A. A. (1997) Oxidation of butadiene monoxide to meso- and (+/-)-diepoxybutane by cDNA-expressed human cytochrome P450s and by mouse, rat, and human liver microsomes: evidence for preferential hydration of meso-diepoxybutane in rat and human liver microsomes. *Arch.Biochem.Biophys.*, **337**, 176-184.

30. Krause, R. J., Sharer, J. E., and Elfarra, A. A. (1997) Epoxide hydrolase-dependent metabolism of butadiene monoxide to 3-butene-1,2-diol in mouse, rat, and human liver. *Drug Metab Dispos.*, **25**, 1013-1015.

31. van Sittert, N. J., Megens, H. J., Watson, W. P., and Boogaard, P. J. (2000) Biomarkers of exposure to 1,3-butadiene as a basis for cancer risk assessment. *Toxicol.Sci.*, **56**, 189-202.

32. Sprague, C. L. and Elfarra, A. A. (2004) Mercapturic acid urinary metabolites of 3-butene-1,2-diol as *in vivo* evidence for the formation of hydroxymethylvinyl ketone in mice and rats. *Chem.Res.Toxicol.*, **17**, 819-826.

33. Carmella, S. G., Chen, M., Han, S., Briggs, A., Jensen, J., Hatsukami, D. K., and Hecht, S. S. (2009) Effects of smoking cessation on eight urinary tobacco carcinogen and toxicant biomarkers. *Chem.Res.Toxicol.*, **22**, 734-741.

34. Cochrane, J. E. and Skopek, T. R. (1994) Mutagenicity of butadiene and its epoxide metabolites: I. Mutagenic potential of 1,2-epoxybutene, 1,2,3,4-diepoxybutane and 3,4-epoxy-1,2-butanediol in cultured human lymphoblasts. *Carcinogenesis*, **15**, 713-717.

35. Recio, L., Steen, A. M., Pluta, L. J., Meyer, K. G., and Saranko, C. J. (2001) Mutational spectrum of 1,3-butadiene and metabolites 1,2-epoxybutene and 1,2,3,4-diepoxybutane to assess mutagenic mechanisms. *Chem.Biol.Interact.*, **135-136**, 325-341.

36. Ma, H., Wood, T. G., Ammenheuser, M. M., Rosenblatt, J. I., and Ward, J. B., Jr. (2000) Molecular analysis of *hprt* mutant lymphocytes from 1, 3-butadiene-exposed workers. *Environ.Mol.Mutagen.*, **36**, 59-71.

37. Liu, S., Ao, L., Du, B., Zhou, Y., Yuan, J., Bai, Y., Zhou, Z., and Cao, J. (2008) *HPRT* mutations in lymphocytes from 1,3-butadiene-exposed workers in China. *Environ.Health Perspect.*, **116**, 203-208.

38. Hayes, R. B., Xi, L., Bechtold, W. E., Rothman, N., Yao, M., Henderson, R., Zhang, L., Smith, M. T., Zhang, D., Wiemels, J., Dosemeci, M., Yin, S., and O'Neill, J. P. (1996) *hprt* mutation frequency among workers exposed to 1,3-butadiene in China. *Toxicology*, **113**, 100-105.

39. Tates, A. D., van Dam, F. J., de Zwart, F. A., Darroudi, F., Natarajan, A. T., Rossner, P., Peterkova, K., Peltonen, K., Demopoulos, N. A., Stephanou, G., Vlachodimitropoulos, D., and Sram, R. J. (1996) Biological effect monitoring in industrial workers from the Czech Republic exposed to low levels of butadiene. *Toxicology*, **113**, 91-99.

40. Swenberg, J. A., Koc, H., Upton, P. B., Georgueva, N., Ranasinghe, A., Walker, V. E., and Henderson, R. (2001) Using DNA and hemoglobin adducts to improve the risk assessment of butadiene. *Chem.Biol.Interact.*, **135-136**, 387-403.

41. Citti, L., Gervasi, P. G., Turchi, G., Bellucci, G., and Bianchini, R. (1984) The reaction of 3,4-epoxy-1-butene with deoxyguanosine and DNA *in vitro*: synthesis and characterization of the main adducts. *Carcinogenesis*, **5**, 47-52.

42. Tretyakova, N., Lin, Y., Sangaiah, R., Upton, P. B., and Swenberg, J. A. (1997) Identification and quantitation of DNA adducts from calf thymus DNA exposed to 3,4-epoxy-1-butene. *Carcinogenesis*, **18**, 137-147.

43. Tretyakova, N. Y., Lin, Y. P., Upton, P. B., Sangaiah, R., and Swenberg, J. A. (1996) Macromolecular adducts of butadiene. *Toxicology*, **113**, 70-76.

44. Tretyakova, N. Y., Sangaiah, R., Yen, T. Y., and Swenberg, J. A. (1997) Synthesis, characterization, and *in vitro* quantitation of N-7-guanine adducts of diepoxybutane. *Chem.Res.Toxicol.*, **10**, 779-785.

45. Park, S. and Tretyakova, N. (2004) Structural characterization of the major DNA-DNA cross-link of 1,2,3,4-diepoxybutane. *Chem.Res.Toxicol.*, **17**, 129-136.

46. Park, S., Hodge, J., Anderson, C., and Tretyakova, N. (2004) Guanine-adenine DNA cross-linking by 1,2,3,4-diepoxybutane: potential basis for biological activity. *Chem.Res.Toxicol.*, **17**, 1638-1651.

47. Park, S., Anderson, C., Loeber, R., Seetharaman, M., Jones, R., and Tretyakova, N. (2005) Interstrand and intrastrand DNA-DNA cross-linking by 1,2,3,4-diepoxybutane: role of stereochemistry. *J Am Chem.Soc.*, **127**, 14355-14365.

48. Seneviratne, U., Antsypovich, S., Goggin, M., Dorr, D. Q., Guza, R., Moser, A., Thompson, C., York, D. M., and Tretyakova, N. (2010) Exocyclic deoxyadenosine adducts of 1,2,3,4-diepoxybutane: synthesis, structural elucidation, and mechanistic studies. *Chem.Res.Toxicol.*, **23**, 118-133.

49. Zhang, X. Y. and Elfarra, A. A. (2003) Identification and characterization of a series of nucleoside adducts formed by the reaction of 2'-deoxyguanosine and 1,2,3,4-diepoxybutane under physiological conditions. *Chem.Res.Toxicol.*, **16**, 1606-1615.

50. Zhang, X. Y. and Elfarra, A. A. (2004) Characterization of the reaction products of 2'-deoxyguanosine and 1,2,3,4-diepoxybutane after acid hydrolysis: formation of novel guanine and pyrimidine adducts. *Chem.Res.Toxicol.*, **17**, 521-528.

51. Zhang, X. Y. and Elfarra, A. A. (2005) Reaction of 1,2,3,4-diepoxybutane with 2'-deoxyguanosine: initial products and their stabilities and decomposition patterns under physiological conditions. *Chem.Res.Toxicol.*, **18**, 1316-1323.

52. Koivisto, P., Adler, I. D., Sorsa, M., and Peltonen, K. (1996) Inhalation exposure of rats and mice to 1,3-butadiene induces N6-adenine adducts of epoxybutene detected by ^{32}P-postlabeling and HPLC. *Environ.Health Perspect.*, **104 Suppl 3**, 655-657.

53. Koivisto, P., Sorsa, M., Pacchierotti, F., and Peltonen, K. (1997) 32P-postlabelling/HPLC assay reveals an enantioselective adduct formation in N7 guanine residues *in vivo* after 1,3-butadiene inhalation exposure. *Carcinogenesis*, **18**, 439-443.

54. Koivisto, P., Adler, I. D., Pacchierotti, F., and Peltonen, K. (1998) DNA adducts in mouse testis and lung after inhalation exposure to 1,3-butadiene. *Mutat.Res.*, **397**, 3-10.

55. Koivisto, P., Kilpelainen, I., Rasanen, I., Adler, I. D., Pacchierotti, F., and Peltonen, K. (1999) Butadiene diolepoxide- and diepoxybutane-derived DNA adducts at N7-guanine: a high occurrence of diolepoxide-derived adducts in mouse lung after 1,3-butadiene exposure. *Carcinogenesis*, **20**, 1253-1259.

56. Koivisto, P. and Peltonen, K. (2001) N7-guanine adducts of the epoxy metabolites of 1,3-butadiene in mice lung. *Chem.Biol.Interact.*, **135-136**, 363-372.

57. Zhao, C., Vodicka, P., Sram1 RJ, and Hemminki, K. (2000) Human DNA adducts of 1,3-butadiene, an important environmental carcinogen. *Carcinogenesis*, **21**, 107-111.

58. Zhao, C., Vodicka, P., Sram, R. J., and Hemminki, K. (2001) DNA adducts of 1,3-butadiene in humans: relationships to exposure, GST genotypes, single-strand breaks, and cytogenetic end points. *Environ.Mol.Mutagen.*, **37**, 226-230.

59. Tretyakova, N. Y., Chiang, S. Y., Walker, V. E., and Swenberg, J. A. (1998) Quantitative analysis of 1,3-butadiene-induced DNA adducts *in vivo* and *in vitro* using liquid chromatography electrospray ionization tandem mass spectrometry. *J Mass Spectrom*, **33**, 363-376.

60. Koc, H., Tretyakova, N. Y., Walker, V. E., Henderson, R. F., and Swenberg, J. A. (1999) Molecular dosimetry of N-7 guanine adduct formation in mice and rats exposed to 1,3-butadiene. *Chem.Res.Toxicol.*, **12**, 566-574.

61. Oe, T., Kambouris, S. J., Walker, V. E., Meng, Q., Recio, L., Wherli, S., Chaudhary, A. K., and Blair, I. A. (1999) Persistence of N7-(2,3,4-trihydroxybutyl)guanine adducts in the livers of mice and rats exposed to 1,3-butadiene. *Chem.Res.Toxicol.*, **12**, 247-257.

62. Booth, E. D., Kilgour, J. D., Robinson, S. A., and Watson, W. P. (2004) Dose responses for DNA adduct formation in tissues of rats and mice exposed by inhalation to low concentrations of 1,3-[2,3-[^{14}C]-butadiene. *Chem.Biol.Interact.*, **147**, 195-211.

63. Boogaard, P. J., de Kloe, K. P., Booth, E. D., and Watson, W. P. (2004) DNA adducts in rats and mice following exposure to [4-^{14}C]-1,2-epoxy-3-butene and to [2,3-^{14}C]-1,3-butadiene. *Chem.Biol.Interact.*, **148**, 69-92.

64. Goggin, M., Loeber, R., Park, S., Walker, V., Wickliffe, J., and Tretyakova, N. (2007) HPLC-ESI$^+$-MS/MS analysis of N7-guanine-N7-guanine DNA cross-links in tissues of mice exposed to 1,3-butadiene. *Chem.Res.Toxicol.*, **20**, 839-847.

65. Goggin, M., Anderson, C., Park, S., Swenberg, J., Walker, V., and Tretyakova, N. (2008) Quantitative high-performance liquid chromatography-electrospray ionization-tandem mass spectrometry analysis of the adenine-guanine cross-links of 1,2,3,4-diepoxybutane in tissues of butadiene-exposed B6C3F1 mice. *Chem.Res.Toxicol.*, **21**, 1163-1170.

66. Goggin, M., Swenberg, J. A., Walker, V. E., and Tretyakova, N. (2009) Molecular dosimetry of 1,2,3,4-diepoxybutane-induced DNA-DNA cross-links in B6C3F1 mice and F344 rats exposed to 1,3-butadiene by inhalation. *Cancer Res.*, **69**, 2479-2486.

67. Goggin, M., Seneviratne, U., Swenberg, J. A., Walker, V. E., and Tretyakova, N. (2010) Column switching HPLC-ESI$^+$-MS/MS methods for quantitative analysis of exocyclic dA adducts in the DNA of laboratory animals exposed to 1,3-butadiene. *Chem.Res.Toxicol.*, **23**, 808-812.

68. Sangaraju, D., Goggin, M., Walker, V., Swenberg, J., and Tretyakova, N. (2012) NanoHPLC-nanoESI$^+$-MS/MS quantitation of *bis*-N7-guanine DNA-DNA cross-links in tissues of B6C3F1 mice exposed to subppm levels of 1,3-butadiene. *Anal.Chem.*, **84**, 1732-1739.

69. Sangaraju, D., Villalta, P., Goggin, M., Agunsoye, M. O., Campbell, C., and Tretyakova, N. (2013) Capillary HPLC-Accurate Mass MS/MS Quantitation of N7-(2,3,4-Trihydroxybut-1-yl)-guanine Adducts of 1,3-Butadiene in Human Leukocyte DNA. *Chem.Res.Toxicol. (In Press)*.

70. Moll, T. S., Harms, A. C., and Elfarra, A. A. (2000) A comprehensive structural analysis of hemoglobin adducts formed after *in vitro* exposure of erythrocytes to butadiene monoxide. *Chem.Res.Toxicol.*, **13**, 1103-1113.

71. Basile, A., Ferranti, P., Pocsfalvi, G., Mamone, G., Miraglia, N., Caira, S., Ambrosi, L., Soleo, L., Sannolo, N., and Malorni, A. (2001) A novel approach for identification and measurement of hemoglobin adducts with 1,2,3,4-diepoxybutane by liquid chromatography/electrospray ionisation mass spectrometry and matrix-assisted laser desorption/ionisation tandem mass spectrometry. *Rapid Commun.Mass Spectrom*, **15**, 527-540.

72. Lindh, C. H., Kristiansson, M. H., Berg-Andersson, U. A., and Cohen, A. S. (2005) Characterization of adducts formed between human serum albumin and the butadiene metabolite epoxybutanediol. *Rapid Commun.Mass Spectrom*, **19**, 2488-2496.

73. Boysen, G., Georgieva, N. I., Upton, P. B., Walker, V. E., and Swenberg, J. A. (2007) N-terminal globin adducts as biomarkers for formation of butadiene derived epoxides. *Chem.Biol.Interact.*, **166**, 84-92.

74. Osterman-Golkar, S., Kautiainen, A., Bergmark, E., Hakansson, K., and Maki-Paakkanen, J. (1991) Hemoglobin adducts and urinary mercapturic acids in rats as biological indicators of butadiene exposure. *Chem.Biol.Interact.*, **80**, 291-302.

75. Perez, H. L., Lahdetie, J., Landin, H., Kilpelainen, I., Koivisto, P., Peltonen, K., and Osterman-Golkar, S. (1997) Haemoglobin adducts of epoxybutanediol from exposure to 1,3-butadiene or butadiene epoxides. *Chem.Biol.Interact.*, **105**, 181-198.

76. Kautiainen, A., Fred, C., Rydberg, P., and Tornqvist, M. (2000) A liquid chromatography tandem mass spectrometric method for *in vivo* dose monitoring of diepoxybutane, a metabolite of butadiene. *Rapid Commun.Mass Spectrom*, **14**, 1848-1853.

77. Boysen, G., Georgieva, N. I., Upton, P. B., Jayaraj, K., Li, Y., Walker, V. E., and Swenberg, J. A. (2004) Analysis of diepoxide-specific cyclic N-terminal globin adducts in mice and rats after inhalation exposure to 1,3-butadiene. *Cancer Res.*, **64**, 8517-8520.

78. Osterman-Golkar, S. M., Bond, J. A., Ward, J. B., Jr., and Legator, M. S. (1993) Use of haemoglobin adducts for biomonitoring exposure to 1,3-butadiene. *IARC Sci.Publ.*,127-134.

79. Fred, C., Kautiainen, A., Athanassiadis, I., and Tornqvist, M. (2004) Hemoglobin adduct levels in rat and mouse treated with 1,2:3,4-diepoxybutane. *Chem.Res.Toxicol.*, **17**, 785-794.

80. Swenberg, J. A., Christova-Gueorguieva, N. I., Upton, P. B., Ranasinghe, A., Scheller, N., Wu, K. Y., Yen, T. Y., and Hayes, R. (2000) 1,3-butadiene: cancer, mutations, and adducts. Part V: Hemoglobin adducts as biomarkers of 1,3-butadiene exposure and metabolism. *Res.Rep.Health Eff.Inst.*,191-210.

81. Hayes, R. B., Zhang, L., Swenberg, J. A., Yin, S. N., Xi, L., Wiencke, J., Bechtold, W. E., Yao, M., Rothman, N., Haas, R., O'Neill, J. P., Wiemels, J., Dosemeci, M., Li, G., and Smith, M. T. (2001) Markers for carcinogenicity among butadiene-polymer workers in China. *Chem.Biol.Interact.*, **135-136**, 455-464.

82. Albertini, R. J., Sram, R. J., Vacek, P. M., Lynch, J., Wright, M., Nicklas, J. A., Boogaard, P. J., Henderson, R. F., Swenberg, J. A., Tates, A. D., and Ward, J. B.,

Jr. (2001) Biomarkers for assessing occupational exposures to 1,3-butadiene. *Chem.Biol.Interact.*, **135-136**, 429-453.

83. Albertini, R. J., Sram, R. J., Vacek, P. M., Lynch, J., Nicklas, J. A., van Sittert, N. J., Boogaard, P. J., Henderson, R. F., Swenberg, J. A., Tates, A. D., Ward, J. B., Jr., Wright, M., Ammenheuser, M. M., Binkova, B., Blackwell, W., de Zwart, F. A., Krako, D., Krone, J., Megens, H., Musilova, P., Rajska, G., Ranasinghe, A., Rosenblatt, J. I., Rossner, P., Rubes, J., Sullivan, L., Upton, P., and Zwinderman, A. H. (2003) Biomarkers in Czech workers exposed to 1,3-butadiene: a transitional epidemiologic study. *Res.Rep.Health Eff.Inst.*,1-141.

84. Vacek, P. M., Albertini, R. J., Sram, R. J., Upton, P., and Swenberg, J. A. (2010) Hemoglobin adducts in 1,3-butadiene exposed Czech workers: female-male comparisons. *Chem.Biol.Interact.*, **188**, 668-676.

85. Albertini, R. J., Sram, R. J., Vacek, P. M., Lynch, J., Rossner, P., Nicklas, J. A., McDonald, J. D., Boysen, G., Georgieva, N., and Swenberg, J. A. (2007) Molecular epidemiological studies in 1,3-butadiene exposed Czech workers: female-male comparisons. *Chem.Biol.Interact.*, **166**, 63-77.

86. Begemann, P., Upton, P. B., Ranasinghe, A., Swenberg, J. A., Soleo, L., Vimercati, L., Gelormini, A., Fustinoni, S., Zwirner-Baier, I., and Neumann, H. G. (2001) Hemoglobin adducts as biomarkers of 1,3-butadiene in occupationally low exposed Italian workers and a few diesel-exposed miners. *Chem.Biol.Interact.*, **135-136**, 675-678.

87. Fustinoni, S., Soleo, L., Warholm, M., Begemann, P., Rannug, A., Neumann, H. G., Swenberg, J. A., Vimercati, L., and Colombi, A. (2002) Influence of metabolic genotypes on biomarkers of exposure to 1,3-butadiene in humans. *Cancer Epidemiol.Biomarkers Prev.*, **11**, 1082-1090.

88. Georgieva, N. I., Boysen, G., Bordeerat, N., Walker, V. E., and Swenberg, J. A. (2010) Exposure-response of 1,2:3,4-diepoxybutane-specific N-terminal valine adducts in mice and rats after inhalation exposure to 1,3-butadiene. *Toxicol.Sci.*, **115**, 322-329.

89. Boysen, G., Georgieva, N. I., Bordeerat, N. K., Sram, R. J., Vacek, P., Albertini, R. J., and Swenberg, J. A. (2012) Formation of 1,2:3,4-diepoxybutane-specific hemoglobin adducts in 1,3-butadiene exposed workers. *Toxicol.Sci.*, **125**, 30-40.

90. Sabourin, P. J., Burka, L. T., Bechtold, W. E., Dahl, A. R., Hoover, M. D., Chang, I. Y., and Henderson, R. F. (1992) Species differences in urinary butadiene metabolites; identification of 1,2-dihydroxy-4-(N-acetylcysteinyl)butane, a novel metabolite of butadiene. *Carcinogenesis*, **13**, 1633-1638.

91. Bechtold, W. E., Strunk, M. R., Chang, I. Y., Ward, J. B., Jr., and Henderson, R. F. (1994) Species differences in urinary butadiene metabolites: comparisons of metabolite ratios between mice, rats, and humans. *Toxicol.Appl.Pharmacol.*, **127**, 44-49.

92. Nauhaus, S. K., Fennell, T. R., Asgharian, B., Bond, J. A., and Sumner, S. C. (1996) Characterization of urinary metabolites from Sprague-Dawley rats and B6C3F1 mice exposed to [1,2,3,4-13C]butadiene. *Chem.Res.Toxicol.*, **9**, 764-773.

93. Richardson, K. A., Peters, M. M., Wong, B. A., Megens, R. H., van Elburg, P. A., Booth, E. D., Boogaard, P. J., Bond, J. A., Medinsky, M. A., Watson, W. P., and van Sittert, N. J. (1999) Quantitative and qualitative differences in the metabolism of 14C-1,3-butadiene in rats and mice: relevance to cancer susceptibility. *Toxicol.Sci.*, **49**, 186-201.

94. Boogaard, P. J., Sumner, S. C., and Bond, J. A. (1996) Glutathione conjugation of 1,2:3,4- diepoxybutane in human liver and rat and mouse liver and lung *in vitro*. *Toxicol.Appl.Pharmacol.*, **136**, 307-316.

95. Boogaard, P. J., van Sittert, N. J., and Megens, H. J. (2001) Urinary metabolites and haemoglobin adducts as biomarkers of exposure to 1,3-butadiene: a basis for 1,3-butadiene cancer risk assessment. *Chem.Biol.Interact.*, **135-136**, 695-701.

96. Urban, M., Gilch, G., Schepers, G., van Miert, E., and Scherer, G. (2003) Determination of the major mercapturic acids of 1,3-butadiene in human and rat urine using liquid chromatography with tandem mass spectrometry. *J Chromatogr.B Analyt.Technol.Biomed.Life Sci.*, **796**, 131-140.

97. McDonald, J. D., Bechtold, W. E., Krone, J. R., Blackwell, W. B., Kracko, D. A., and Henderson, R. F. (2004) Analysis of butadiene urinary metabolites by liquid chromatography-triple quadrupole mass spectrometry. *J Anal.Toxicol.*, **28**, 168-173.

98. Fustinoni, S., Perbellini, L., Soleo, L., Manno, M., and Foa, V. (2004) Biological monitoring in occupational exposure to low levels of 1,3-butadiene. *Toxicol.Lett.*, **149**, 353-360.

99. Sapkota, A., Halden, R. U., Dominici, F., Groopman, J. D., and Buckley, T. J. (2006) Urinary biomarkers of 1,3-butadiene in environmental settings using liquid chromatography isotope dilution tandem mass spectrometry. *Chem.Biol.Interact.*, **160**, 70-79.

100. Navasumrit, P., Arayasiri, M., Hiang, O. M., Leechawengwongs, M., Promvijit, J., Choonvisase, S., Chantchaemsai, S., Nakngam, N., Mahidol, C., and

Ruchirawat, M. (2008) Potential health effects of exposure to carcinogenic compounds in incense smoke in temple workers. *Chem.Biol.Interact.*, **173**, 19-31.

101. Arayasiri, M., Mahidol, C., Navasumrit, P., Autrup, H., and Ruchirawat, M. (2010) Biomonitoring of benzene and 1,3-butadiene exposure and early biological effects in traffic policemen. *Sci.Total Environ.*, **408**, 4855-4862.

102. Schettgen, T., Musiol, A., Alt, A., Ochsmann, E., and Kraus, T. (2009) A method for the quantification of biomarkers of exposure to acrylonitrile and 1,3-butadiene in human urine by column-switching liquid chromatography-tandem mass spectrometry. *Anal.Bioanal.Chem.*, **393**, 969-981.

103. Yuan, J. M., Gao, Y. T., Wang, R., Chen, M., Carmella, S. G., and Hecht, S. S. (2012) Urinary levels of volatile organic carcinogen and toxicant biomarkers in relation to lung cancer development in smokers. *Carcinogenesis*, **33**, 804-809.

104. Ding, Y. S., Blount, B. C., Valentin-Blasini, L., Applewhite, H. S., Xia, Y., Watson, C. H., and Ashley, D. L. (2009) Simultaneous determination of six mercapturic acid metabolites of volatile organic compounds in human urine. *Chem.Res.Toxicol.*, **22**, 1018-1025.

105. Roethig, H. J., Munjal, S., Feng, S., Liang, Q., Sarkar, M., Walk, R. A., and Mendes, P. E. (2009) Population estimates for biomarkers of exposure to cigarette smoke in adult U.S. cigarette smokers. *Nicotine.Tob.Res.*, **11**, 1216-1225.

106. Sarkar, M., Muhammad-Kah, R., Liang, Q., Kapur, S., Feng, S., and Roethig, H. (2013) Evaluation of spot urine as an alternative to 24h urine collection for determination of biomarkers of exposure to cigarette smoke in adult smokers. *Environ.Toxicol.Pharmacol.*, **36**, 108-114.

107. Eckert, E., Drexler, H., and Goen, T. (2010) Determination of six hydroxyalkyl mercapturic acids in human urine using hydrophilic interaction liquid chromatography with tandem mass spectrometry (HILIC-ESI-MS/MS). *J Chromatogr.B Analyt.Technol.Biomed.Life Sci.*, **878**, 2506-2514.

108. Eckert, E., Schmid, K., Schaller, B., Hiddemann-Koca, K., Drexler, H., and Goen, T. (2011) Mercapturic acids as metabolites of alkylating substances in urine samples of German inhabitants. *Int.J Hyg.Environ.Health*, **214**, 196-204.

109. Eckert, E., Leng, G., Gries, W., and Goen, T. (2013) Excretion of mercapturic acids in human urine after occupational exposure to 2-chloroprene. *Arch.Toxicol.*.

110. Sterz, K., Scherer, G., Krumsiek, J., Theis, F. J., and Ecker, J. (2012) Identification and quantification of 1-hydroxybutene-2-yl mercapturic acid in human urine by. *Chem.Res.Toxicol.*, **25**, 1565-1567.

111. Sharer, J. E., Duescher, R. J., and Elfarra, A. A. (1992) Species and tissue differences in the microsomal oxidation of 1,3-butadiene and the glutathione conjugation of butadiene monoxide in mice and rats. Possible role in 1,3-butadiene-induced toxicity. *Drug Metab Dispos.*, **20**, 658-664.

112. Seaton, M. J., Follansbee, M. H., and Bond, J. A. (1995) Oxidation of 1,2-epoxy-3-butene to 1,2:3,4-diepoxybutane by cDNA-expressed human cytochromes P450 2E1 and 3A4 and human, mouse and rat liver microsomes. *Carcinogenesis*, **16**, 2287-2293.

113. Henderson, R. F., Thornton-Manning, J. R., Bechtold, W. E., and Dahl, A. R. (1996) Metabolism of 1,3-butadiene: species differences. *Toxicology*, **113**, 17-22.

114. Thornton-Manning, J. R., Dahl, A. R., Bechtold, W. E., Griffith, W. C., Jr., and Henderson, R. F. (1997) Comparison of the disposition of butadiene epoxides in Sprague-Dawley rats and B6C3F1 mice following a single and repeated exposures to 1,3-butadiene via inhalation. *Toxicology*, **123**, 125-134.

115. Thornton-Manning, J. R., Dahl, A. R., Bechtold, W. E., and Henderson, R. F. (1996) Gender and species differences in the metabolism of 1,3-butadiene to butadiene monoepoxide and butadiene diepoxide in rodents following low-level inhalation exposures. *Toxicology*, **113**, 322-325.

116. Thornton-Manning, J. R., Dahl, A. R., Bechtold, W. E., Griffith, W. C., Jr., Pei, L., and Henderson, R. F. (1995) Gender differences in the metabolism of 1,3-butadiene in Sprague-Dawley rats following a low level inhalation exposure. *Carcinogenesis*, **16**, 2875-2878.

117. Filser, J. G., Hutzler, C., Meischner, V., Veereshwarayya, V., and Csanady, G. A. (2007) Metabolism of 1,3-butadiene to toxicologically relevant metabolites in single-exposed mice and rats. *Chem.Biol.Interact.*, **166**, 93-103.

118. Friedberg, E. C. (2003) DNA damage and repair. *Nature*, **421**, 436-440.

119. Sancar, A., Lindsey-Boltz, L. A., Unsal-Kacmaz, K., and Linn, S. (2004) Molecular mechanisms of mammalian DNA repair and the DNA damage checkpoints. *Annu.Rev.Biochem.*, **73**, 39-85.

120. Prakash, S., Johnson, R. E., and Prakash, L. (2005) Eukaryotic translesion synthesis DNA polymerases: specificity of structure and function. *Annu.Rev.Biochem.*, **74**, 317-353.

121. Waters, L. S., Minesinger, B. K., Wiltrout, M. E., D'Souza, S., Woodruff, R. V., and Walker, G. C. (2009) Eukaryotic translesion polymerases and their roles and regulation in DNA damage tolerance. *Microbiol.Mol.Biol.Rev.*, **73**, 134-154.

122. Lehmann, A. R., Niimi, A., Ogi, T., Brown, S., Sabbioneda, S., Wing, J. F., Kannouche, P. L., and Green, C. M. (2007) Translesion synthesis: Y-family polymerases and the polymerase switch. *DNA Repair (Amst)*, **6**, 891-899.

123. Yang, W. (2005) Portraits of a Y-family DNA polymerase. *FEBS Lett.*, **579**, 868-872.

124. Yang, W. and Woodgate, R. (2007) What a difference a decade makes: insights into translesion DNA synthesis. *Proc.Natl.Acad.Sci.U.S.A*, **104**, 15591-15598.

125. Ling, H., Boudsocq, F., Woodgate, R., and Yang, W. (2001) Crystal structure of a Y-family DNA polymerase in action: a mechanism for error-prone and lesion-bypass replication. *Cell*, **107**, 91-102.

126. Trincao, J., Johnson, R. E., Escalante, C. R., Prakash, S., Prakash, L., and Aggarwal, A. K. (2001) Structure of the catalytic core of *S. cerevisiae* DNA polymerase eta: implications for translesion DNA synthesis. *Mol.Cell*, **8**, 417-426.

127. Goodman, M. F. (2002) Error-prone repair DNA polymerases in prokaryotes and eukaryotes. *Annu.Rev.Biochem.*, **71**, 17-50.

128. Kunkel, T. A. (2004) DNA replication fidelity. *J Biol.Chem.*, **279**, 16895-16898.

129. Sale, J. E., Lehmann, A. R., and Woodgate, R. (2012) Y-family DNA polymerases and their role in tolerance of cellular DNA damage. *Nat.Rev.Mol.Cell Biol.*, **13**, 141-152.

130. McCulloch, S. D. and Kunkel, T. A. (2008) The fidelity of DNA synthesis by eukaryotic replicative and translesion synthesis polymerases. *Cell Res.*, **18**, 148-161.

131. Grotjahn, L., Frank, R., and Blocker, H. (1982) Ultrafast sequencing of oligodeoxyribonucleotides by FAB-mass spectrometry. *Nucleic Acids Res.*, **10**, 4671-4678.

132. Grotjahn, L., Bl+¦cker, H., and Frank, R. (1985) Mass spectroscopic sequence analysis of oligonucleotides. *Biol.Mass Spectrom.*, **12**, 514-524.

133. McNeal, C. J., Narang, S. A., Macfarlane, R. D., Hsiung, H. M., and Brousseau, R. (1980) Sequence determination of protected oligodeoxyribonucleotides containing phosphotriester linkages by californium-252 plasma desorption mass spectrometry. *Proc.Natl.Acad.Sci.U.S.A*, **77**, 735-739.

134. McNeal, C. J., Ogilvie, K. K., Theriault, N. Y., and Nemer, M. J. (1982) A new method for sequencing fully protected oligonucleotides using californium-252

plasma desorption mass spectrometry. 1. Negative ions of dinucleoside monophosphates. *J.Am.Chem.Soc.*, **104**, 972-975.

135. Cerny, R. L., Gross, M. L., and Grotjahn, L. (1986) Fast atom bombardment combined with tandem mass spectrometry for the study of dinucleotides. *Anal.Biochem.*, **156**, 424-435.

136. Cerny, R. L., Tomer, K. B., Gross, M. L., and Grotjahn, L. (1987) Fast atom bombardment combined with tandem mass spectrometry for determining structures of small oligonucleotides. *Anal.Biochem.*, **165**, 175-182.

137. Wang, Z., Wan, K. X., Ramanathan, R., Taylor, J. S., and Gross, M. L. (1998) Structure and fragmentation mechanisms of isomeric T-rich oligodeoxynucleotides: a comparison of four tandem mass spectrometric methods. *J.Am.Soc.Mass Spectrom.*, **9**, 683-691.

138. Nordhoff, E., Ingendoh, A., Cramer, R., Overberg, A., Stahl, B., Karas, M., Hillenkamp, F., and Crain, P. F. (1992) Matrix-assisted laser desorption/ionization mass spectrometry of nucleic acids with wavelengths in the ultraviolet and infrared. *Rapid Commun.Mass Spectrom.*, **6**, 771-776.

139. Nordhoff, E., Karas, M., Cramer, R., Hahner, S., Hillenkamp, F., Kirpekar, F., Lezius, A., Muth, J., Meier, C., and Engels, J. W. (1995) Direct mass spectrometric sequencing of low-picomole amounts of oligodeoxynucleotides with up to 21 bases by matrix-assisted laser desorption/ionization mass spectrometry. *J.Mass Spectrom.*, **30**, 99-112.

140. Stemmler, E. A., Buchanan, M. V., Hurst, G. B., and Hettich, R. L. (1995) Analysis of modified oligonucleotides by matrix-assisted laser desorption/ionization Fourier transform mass spectrometry. *Anal.Chem.*, **67**, 2924-2930.

141. Hettich, R. and Buchanan, M. (1991) Structural Characterization of Normal and Modified Oligonucleotides by Matrix-assisted Laser Desorption Fourier Transform Mass Spectrometry. *Journal of The American Society for Mass Spectrometry*, **2**, 402-412.

142. Juhasz, P., Roskey, M. T., Smirnov, I. P., Haff, L. A., Vestal, M. L., and Martin, S. A. (1996) Applications of delayed extraction matrix-assisted laser desorption ionization time-of-flight mass spectrometry to oligonucleotide analysis. *Anal.Chem.*, **68**, 941-946.

143. Talbo, G. and Mann, M. (1996) Aspects of the sequencing of carbohydrates and oligonucleotides by matrix-assisted laser desorption/ionization post-source decay. *Rapid Commun.Mass Spectrom.*, **10**, 100-103.

144. Spengler, B. (1997) Post-source decay analysis in matrix-assisted laser desorption/ionization mass spectrometry of biomolecules. *J.Mass Spectrom.*, **32**, 1019-1036.

145. Hagan, N. A., Smith, C. A., Antoine, M. D., Lin, J. S., Feldman, A. B., and Demirev, P. A. (2012) Enhanced in-source fragmentation in MALDI-TOF-MS of oligonucleotides using 1,5-diaminonapthalene. *J.Am.Soc.Mass Spectrom.*, **23**, 773-777.

146. McLuckey, S. A., Van Berkel, G. J., and Glish, G. L. (1992) Tandem Mass Spectrometry of Small, Multiply Charged Oligonucleotides. *J.Am.Soc.Mass Spectrom.* **3**, 60-70.

147. Jacobson, K. B., Arlinghaus, H. F., Buchanan, M. V., Chen, C. H., Glish, G. L., Hettich, R. L., and McLuckey, S. A. (1991) Applications of mass spectrometry to DNA sequencing. *Genet.Anal.Tech.Appl.*, **8**, 223-229.

148. Little, D. P., Chorush, R. A., Speir, J. P., Senko, M. W., Kelleher, N. L., and McLafferty, F. W. (1994) Rapid Sequencing of Oligonucleotides by High-Resolution Mass Spectrometry. *J.Am.Chem.Soc.*, **116**, 4893-4897.

149. Ni, J., Pomerantz, C., Rozenski, J., Zhang, Y., and McCloskey, J. A. (1996) Interpretation of oligonucleotide mass spectra for determination of sequence using electrospray ionization and tandem mass spectrometry. *Anal.Chem.*, **68**, 1989-1999.

150. Owens, D. R., Bothner, B., Phung, Q., Harris, K., and Siuzdak, G. (1998) Aspects of oligonucleotide and peptide sequencing with MALDI and electrospray mass spectrometry. *Bioorg.Med.Chem.*, **6**, 1547-1554.

151. Barry, J. P., Vouros, P., Van Schepdael, A., and Law, S. J. (1995) Mass and sequence verification of modified oligonucleotides using electrospray tandem mass spectrometry. *J.Mass Spectrom.*, **30**, 993-1006.

152. Schurch, S., Tromp, J. M., and Monn, S. T. (2007) Mass spectrometry of oligonucleotides. *Nucleosides Nucleotides Nucleic Acids*, **26**, 1629-1633.

153. Murray, K. K. (1996) DNA sequencing by mass spectrometry. *J Mass Spectrom*, **31**, 1203-1215.

154. Rozenski, J., Crain, P. F., and McCloskey, J. A. (1999) The RNA Modification Database: 1999 update. *Nucleic Acids Res.*, **27**, 196-197.

155. Rozenski, J. and McCloskey, J. A. (2002) SOS: a simple interactive program for ab initio oligonucleotide sequencing by mass spectrometry. *J Am Soc.Mass Spectrom*, **13**, 200-203.

156. Oberacher, H., Wellenzohn, B., and Huber, C. G. (2002) Comparative sequencing of nucleic acids by liquid chromatography-tandem mass spectrometry. *Anal.Chem.*, **74**, 211-218.

157. Oberacher, H., Mayr, B. M., and Huber, C. G. (2004) Automated de novo sequencing of nucleic acids by liquid chromatography-tandem mass spectrometry. *J Am Soc.Mass Spectrom*, **15**, 32-42.

158. Oberacher, H. and Pitterl, F. (2011) Tandem mass spectrometric de novo sequencing of oligonucleotides using simulated annealing for stochastic optimization. *Int.J.Mass Spectrom.*, **304**, 124-129.

159. Tretyakova, N., Villalta, P. W., and Kotapati, S. (2013) Mass spectrometry of structurally modified DNA. *Chem.Rev.*, **113**, 2395-2436.

160. Choi, J. Y., Zang, H., Angel, K. C., Kozekov, I. D., Goodenough, A. K., Rizzo, C. J., and Guengerich, F. P. (2006) Translesion synthesis across 1,N^2-ethenoguanine by human DNA polymerases. *Chem.Res.Toxicol.*, **19**, 879-886.

161. Christov, P. P., Petrova, K. V., Shanmugam, G., Kozekov, I. D., Kozekova, A., Guengerich, F. P., Stone, M. P., and Rizzo, C. J. (2010) Comparison of the *in vitro* replication of the *7*-(2-oxoheptyl)-1,N^2-etheno-2'-deoxyguanosine and 1,N^2-etheno-2'-deoxyguanosine lesions by *Sulfolobus solfataricus* P2 DNA polymerase IV (Dpo4). *Chem.Res.Toxicol.*, **23**, 1330-1341.

162. Maddukuri, L., Eoff, R. L., Choi, J. Y., Rizzo, C. J., Guengerich, F. P., and Marnett, L. J. (2010) *In vitro* bypass of the major malondialdehyde- and base propenal-derived DNA adduct by human Y-family DNA polymerases kappa, iota, and Rev1. *Biochemistry*, **49**, 8415-8424.

163. Stover, J. S., Chowdhury, G., Zang, H., Guengerich, F. P., and Rizzo, C. J. (2006) Translesion synthesis past the C8- and N^2-deoxyguanosine adducts of the dietary mutagen 2-Amino-3-methylimidazo[4,5-*f*]quinoline in the *Nar*I recognition sequence by prokaryotic DNA polymerases. *Chem.Res.Toxicol.*, **19**, 1506-1517.

164. Zang, H., Goodenough, A. K., Choi, J. Y., Irimia, A., Loukachevitch, L. V., Kozekov, I. D., Angel, K. C., Rizzo, C. J., Egli, M., and Guengerich, F. P. (2005) DNA adduct bypass polymerization by Sulfolobus solfataricus DNA polymerase Dpo4: analysis and crystal structures of multiple base pair substitution and frameshift products with the adduct 1,N^2-ethenoguanine. *J.Biol.Chem.*, **280**, 29750-29764.

165. Levine, R. L., Miller, H., Grollman, A., Ohashi, E., Ohmori, H., Masutani, C., Hanaoka, F., and Moriya, M. (2001) Translesion DNA synthesis catalyzed by human pol eta and pol kappa across 1,N^6-ethenodeoxyadenosine. *J Biol.Chem.*, **276**, 18717-18721.

166. Vaisman, A., Masutani, C., Hanaoka, F., and Chaney, S. G. (2000) Efficient translesion replication past oxaliplatin and cisplatin GpG adducts by human DNA polymerase eta. *Biochemistry*, **39**, 4575-4580.

167. Fischhaber, P. L., Gerlach, V. L., Feaver, W. J., Hatahet, Z., Wallace, S. S., and Friedberg, E. C. (2002) Human DNA polymerase kappa bypasses and extends beyond thymine glycols during translesion synthesis *in vitro*, preferentially incorporating correct nucleotides. *J Biol.Chem.*, **277**, 37604-37611.

168. Stafford, J. B., Eoff, R. L., Kozekova, A., Rizzo, C. J., Guengerich, F. P., and Marnett, L. J. (2009) Translesion DNA synthesis by human DNA polymerase eta on templates containing a pyrimidopurinone deoxyguanosine adduct, 3-(2'-deoxy-β-D-*erythro*-pentofuranosyl)pyrimido-[1,2-*a*]purin-10(3*H*)-one. *Biochemistry*, **48**, 471-480.

169. Zang, H., Irimia, A., Choi, J. Y., Angel, K. C., Loukachevitch, L. V., Egli, M., and Guengerich, F. P. (2006) Efficient and high fidelity incorporation of dCTP opposite 7,8-dihydro-8-oxodeoxyguanosine by Sulfolobus solfataricus DNA polymerase Dpo4. *J.Biol.Chem.*, **281**, 2358-2372.

170. Eoff, R. L., Irimia, A., Angel, K. C., Egli, M., and Guengerich, F. P. (2007) Hydrogen bonding of 7,8-dihydro-8-oxodeoxyguanosine with a charged residue in the little finger domain determines miscoding events in Sulfolobus solfataricus DNA polymerase Dpo4. *J.Biol.Chem.*, **282**, 19831-19843.

171. Eoff, R. L., Angel, K. C., Egli, M., and Guengerich, F. P. (2007) Molecular basis of selectivity of nucleoside triphosphate incorporation opposite O^6-benzylguanine by sulfolobus solfataricus DNA polymerase Dpo4: steady-state and pre-steady-state kinetics and x-ray crystallography of correct and incorrect pairing. *J.Biol.Chem.*, **282**, 13573-13584.

172. Choi, J. Y., Chowdhury, G., Zang, H., Angel, K. C., Vu, C. C., Peterson, L. A., and Guengerich, F. P. (2006) Translesion synthesis across O^6-alkylguanine DNA adducts by recombinant human DNA polymerases. *J.Biol.Chem.*, **281**, 38244-38256.

173. Eoff, R. L., Irimia, A., Egli, M., and Guengerich, F. P. (2007) Sulfolobus solfataricus DNA polymerase Dpo4 is partially inhibited by "wobble" pairing between O^6-methylguanine and cytosine, but accurate bypass is preferred. *J.Biol.Chem.*, **282**, 1456-1467.

174. Zhang, H., Eoff, R. L., Kozekov, I. D., Rizzo, C. J., Egli, M., and Guengerich, F. P. (2009) Versatility of Y-family Sulfolobus solfataricus DNA polymerase Dpo4 in translesion synthesis past bulky N^2-alkylguanine adducts. *J.Biol.Chem.*, **284**, 3563-3576.

175. Zang, H., Chowdhury, G., Angel, K. C., Harris, T. M., and Guengerich, F. P. (2006) Translesion synthesis across polycyclic aromatic hydrocarbon diol epoxide adducts of deoxyadenosine by Sulfolobus solfataricus DNA polymerase Dpo4. *Chem.Res.Toxicol.*, **19**, 859-867.

176. Christov, P. P., Angel, K. C., Guengerich, F. P., and Rizzo, C. J. (2009) Replication past the N^5-methyl-formamidopyrimidine lesion of deoxyguanosine by DNA polymerases and an improved procedure for sequence analysis of *in vitro* bypass products by mass spectrometry. *Chem.Res.Toxicol.*, **22**, 1086-1095.

177. Carmical, J. R., Nechev, L. V., Harris, C. M., Harris, T. M., and Lloyd, R. S. (2000) Mutagenic potential of adenine N^6 adducts of monoepoxide and diolepoxide derivatives of butadiene. *Environ.Mol.Mutagen.*, **35**, 48-56.

178. Carmical, J. R., Zhang, M., Nechev, L., Harris, C. M., Harris, T. M., and Lloyd, R. S. (2000) Mutagenic potential of guanine N^2 adducts of butadiene mono- and diolepoxide. *Chem.Res.Toxicol.*, **13**, 18-25.

179. Kanuri, M., Nechev, L. V., Tamura, P. J., Harris, C. M., Harris, T. M., and Lloyd, R. S. (2002) Mutagenic spectrum of butadiene-derived *N*1-deoxyinosine adducts and N^6,N^6-deoxyadenosine intrastrand cross-links in mammalian cells. *Chem.Res.Toxicol.*, **15**, 1572-1580.

180. Fernandes, P. H., Hackfeld, L. C., Kozekov, I. D., Hodge, R. P., and Lloyd, R. S. (2006) Synthesis and mutagenesis of the butadiene-derived *N*3 2'-deoxyuridine adducts. *Chem.Res.Toxicol.*, **19**, 968-976.

181. Carmical, J. R., Kowalczyk, A., Zou, Y., Van Houten, B., Nechev, L. V., Harris, C. M., Harris, T. M., and Lloyd, R. S. (2000) Butadiene-induced intrastrand DNA cross-links: a possible role in deletion mutagenesis. *J.Biol.Chem.*, **275**, 19482-19489.

182. Koivisto, P., Kostiainen, R., Kilpelainen, I., Steinby, K., and Peltonen, K. (1995) Preparation, characterization and ^{32}P-postlabeling of butadiene monoepoxide N^6-adenine adducts. *Carcinogenesis*, **16**, 2999-3007.

183. Koivisto, P., Adler, I. D., Pacchierotti, F., and Peltonen, K. (1998) Regio and stereospecific DNA adduct formation in mouse lung at N^6 and N7 position of adenine and guanine after 1,3 butadiene inhalation exposure. *Biomarkers*, **3**, 385-397.

184. Dorr, D. Q., Murphy, K., and Tretyakova, N. (2007) Synthesis of DNA oligodeoxynucleotides containing structurally defined N^6-(2-hydroxy-3-buten-1-yl)-adenine adducts of 3,4-epoxy-1-butene. *Chem.Biol.Interact.*, **166**, 104-111.

185. Goggin, M., Sangaraju, D., Walker, V. E., Wickliffe, J., Swenberg, J. A., and Tretyakova, N. (2011) Persistence and repair of bifunctional DNA adducts in tissues of laboratory animals exposed to 1,3-butadiene by inhalation. *Chem.Res.Toxicol.*, **24**, 809-817.

186. Seneviratne, U., Antsypovich, S., Dorr, D. Q., Dissanayake, T., Kotapati, S., and Tretyakova, N. (2010) DNA Oligomers Containing Site-Specific and Stereospecific Exocyclic Deoxyadenosine Adducts of 1,2,3,4-Diepoxybutane: Synthesis, Characterization, and Effects on DNA Structure. *Chem.Res.Toxicol.*, **23**, 1556-1567.

187. Sathiakumar, N., Graff, J., Macaluso, M., Maldonado, G., Matthews, R., and Delzell, E. (2005) An updated study of mortality among North American synthetic rubber industry workers. *Occup.Environ.Med.*, **62**, 822-829.

188. Kirman, C. R., Albertini, R. A., and Gargas, M. L. (2010) 1,3-Butadiene: III. Assessing carcinogenic modes of action. *Crit Rev.Toxicol.*, **40 Suppl 1**, 74-92.

189. Malvoisin, E. and Roberfroid, M. (1982) Hepatic microsomal metabolism of 1,3-butadiene. *Xenobiotica*, **12**, 137-144.

190. Elfarra, A. A., Krause, R. J., and Selzer, R. R. (1996) Biochemistry of 1,3-butadiene metabolism and its relevance to 1,3-butadiene-induced carcinogenicity. *Toxicology*, **113**, 23-30.

191. Bolt, H. M. and Jelitto, B. (1996) Biological formation of the 1,3-butadiene DNA adducts 7-*N*-(2-hydroxy-3-buten-1-yl)guanine, 7-*N*-(1-hydroxy-3-buten-2-yl)guanine and 7-*N*-(2,3,4-trihydroxy-butyl)guanine. *Toxicology*, **113**, 328-330.

192. Loeber, R., Rajesh, M., Fang, Q., Pegg, A. E., and Tretyakova, N. (2006) Cross-linking of the human DNA repair protein O6-alkylguanine DNA alkyltransferase to DNA in the presence of 1,2,3,4-diepoxybutane. *Chem.Res.Toxicol.*, **19**, 645-654.

193. Michaelson-Richie, E. D., Loeber, R. L., Codreanu, S. G., Ming, X., Liebler, D. C., Campbell, C., and Tretyakova, N. Y. (2010) DNA-protein cross-linking by 1,2,3,4-diepoxybutane. *J Proteome.Res.*, **9**, 4356-4367.

194. Jelitto, B., Vangala, R. R., and Laib, R. J. (1989) Species differences in DNA damage by butadiene: role of diepoxybutane. *Arch.Toxicol.Suppl.*, **13**, 246-249.

195. Henderson, R. F., Barr, E. B., Belinsky, S. A., Benson, J. M., Hahn, F. F., and Menache, M. G. (2000) 1,3-butadiene: cancer, mutations, and adducts. Part I: Carcinogenicity of 1,2,3,4-diepoxybutane. *Res.Rep.Health Eff.Inst.*,11-43.

196. Swenberg, J. A., Boysen, G., Georgieva, N., Bird, M. G., and Lewis, R. J. (2007) Future directions in butadiene risk assessment and the role of cross-species internal dosimetry. *Chem.Biol.Interact.*, **166**, 78-83.

197. Thornton-Manning, J. R., Dahl, A. R., Bechtold, W. E., Griffith, W. C., Jr., and Henderson, R. F. (1995) Disposition of butadiene monoepoxide and butadiene diepoxide in various tissues of rats and mice following a low-level inhalation exposure to 1,3-butadiene. *Carcinogenesis*, **16**, 1723-1731.

198. Boettcher, M. I. and Angerer, J. (2005) Determination of the major mercapturic acids of acrylamide and glycidamide in human urine by LC-ESI-MS/MS. *J.Chromatogr.B Analyt.Technol.Biomed.Life Sci.*, **824**, 283-294.

199. Almeida, A. M., Castel-Branco, M. M., and Falcao, A. C. (2002) Linear regression for calibration lines revisited: weighting schemes for bioanalytical methods. *J Chromatogr.B Analyt.Technol.Biomed.Life Sci.*, **774**, 215-222.

200. Baweja, R. (1987) Application of reversed-phase high-performance liquid-Chromatography for the separation of deuterium and hydrogen analogs of aromatic-hydrocarbons. *Analytica Chimica Acta*, **192**, 345-348.

201. Urban, M., Kavvadias, D., Riedel, K., Scherer, G., and Tricker, A. R. (2006) Urinary mercapturic acids and a hemoglobin adduct for the dosimetry of acrylamide exposure in smokers and nonsmokers. *Inhal.Toxicol.*, **18**, 831-839.

202. Mascher, D. G., Mascher, H. J., Scherer, G., and Schmid, E. R. (2001) High-performance liquid chromatographic-tandem mass spectrometric determination of 3-hydroxypropylmercapturic acid in human urine. *J.Chromatogr.B Biomed.Sci.Appl.*, **750**, 163-169.

203. Schettgen, T., Musiol, A., and Kraus, T. (2008) Simultaneous determination of mercapturic acids derived from ethylene oxide (HEMA), propylene oxide (2-HPMA), acrolein (3-HPMA), acrylamide (AAMA) and N,N-dimethylformamide (AMCC) in human urine using liquid chromatography/tandem mass spectrometry. *Rapid Commun.Mass Spectrom.*, **22**, 2629-2638.

204. Richardson, K. A., Peters, M. M., Megens, R. H., van Elburg, P. A., Golding, B. T., Boogaard, P. J., Watson, W. P., and van Sittert, N. J. (1998) Identification of novel metabolites of butadiene monoepoxide in rats and mice. *Chem.Res.Toxicol.*, **11**, 1543-1555.

205. Tretyakova, N., Sangaiah, R., Yen, T. Y., Gold, A., and Swenberg, J. A. (1997) Adenine adducts with diepoxybutane: isolation and analysis in exposed calf thymus DNA. *Chem.Res.Toxicol.*, **10**, 1171-1179.

206. Kotapati, S., Matter, B. A., Grant, A. L., and Tretyakova, N. Y. (2011) Quantitative analysis of trihydroxybutyl mercapturic acid, a urinary metabolite of 1,3-butadiene, in humans. *Chem.Res.Toxicol.*, **24**, 1516-1526.

207. Sasiadek, M., Norppa, H., and Sorsa, M. (1991) 1,3-Butadiene and its epoxides induce sister-chromatid exchanges in human lymphocytes *in vitro*. *Mutat.Res.*, **261**, 117-121.

208. Kligerman, A. D., DeMarini, D. M., Doerr, C. L., Hanley, N. M., Milholland, V. S., and Tennant, A. H. (1999) Comparison of cytogenetic effects of 3,4-epoxy-1-butene and 1,2:3, 4-diepoxybutane in mouse, rat and human lymphocytes following *in vitro* G0 exposures. *Mutat.Res.*, **439**, 13-23.

209. Hecht, S. S. (2002) Human urinary carcinogen metabolites: biomarkers for investigating tobacco and cancer. *Carcinogenesis*, **23**, 907-922.

210. Dekant, W., Vamvakas, S., Henschler, D., and Anders, M. W. (1988) Enzymatic conjugation of hexachloro-1,3-butadiene with glutathione. Formation of 1-(glutathion-S-yl)-1,2,3,4,4-pentachlorobuta-1,3-diene and 1,4-bis(glutathion-S-yl)-1,2,3,4-tetrachlorobuta-1,3-diene. *Drug Metab Dispos.*, **16**, 701-706.

211. Liebler, D. C., Meredith, M. J., and Guengerich, F. P. (1985) Formation of glutathione conjugates by reactive metabolites of vinylidene chloride in microsomes and isolated hepatocytes. *Cancer Res.*, **45**, 186-193.

212. Wheeler, J. B., Stourman, N. V., Armstrong, R. N., and Guengerich, F. P. (2001) Conjugation of haloalkanes by bacterial and mammalian glutathione transferases: mono- and vicinal dihaloethanes. *Chem.Res.Toxicol.*, **14**, 1107-1117.

213. Thornton-Manning, J. R., Dahl, A. R., Allen, M. L., Bechtold, W. E., Griffith, W. C., Jr., and Henderson, R. F. (1998) Disposition of butadiene epoxides in Sprague-Dawley rats following exposures to 8000 ppm 1,3-butadiene: comparisons with tissue epoxide concentrations following low-level exposures. *Toxicol.Sci.*, **41**, 167-173.

214. Kultz, D. (2003) Evolution of the cellular stress proteome: from monophyletic origin to ubiquitous function. *J Exp.Biol.*, **206**, 3119-3124.

215. Kultz, D. (2005) Molecular and evolutionary basis of the cellular stress response. *Annu.Rev.Physiol*, **67**, 225-257.

216. Schmiederer, M., Knutson, E., Muganda, P., and Albrecht, T. (2005) Acute exposure of human lung cells to 1,3-butadiene diepoxide results in G1 and G2 cell cycle arrest. *Environ.Mol.Mutagen.*, **45**, 354-364.

217. Koturbash, I., Scherhag, A., Sorrentino, J., Sexton, K., Bodnar, W., Tryndyak, V., Latendresse, J. R., Swenberg, J. A., Beland, F. A., Pogribny, I. P., and Rusyn, I. (2011) Epigenetic alterations in liver of C57BL/6J mice after short-term inhalational exposure to 1,3-butadiene. *Environ.Health Perspect.*, **119**, 635-640.

218. Yadavilli, S. and Muganda, P. M. (2004) Diepoxybutane induces caspase and p53-mediated apoptosis in human lymphoblasts. *Toxicol.Appl.Pharmacol.*, **195**, 154-165.

219. Le Marchand, L., Sivaraman, L., Pierce, L., Seifried, A., Lum, A., Wilkens, L. R., and Lau, A. F. (1998) Associations of CYP1A1, GSTM1, and CYP2E1 polymorphisms with lung cancer suggest cell type specificities to tobacco carcinogens. *Cancer Res.*, **58**, 4858-4863.

220. Bernardini, S., Hirvonen, A., Pelin, K., and Norppa, H. (1998) Induction of sister chromatid exchange by 1,2-epoxy-3-butene in cultured human lymphocytes: influence of GSTT1 genotype. *Carcinogenesis*, **19**, 377-380.

221. De Bont, R. and van Larebeke, N. (2004) Endogenous DNA damage in humans: a review of quantitative data. *Mutagenesis*, **19**, 169-185.

222. Prakash, S. and Prakash, L. (2002) Translesion DNA synthesis in eukaryotes: a one- or two-polymerase affair. *Genes Dev.*, **16**, 1872-1883.

223. Friedberg, E. C., Lehmann, A. R., and Fuchs, R. P. (2005) Trading places: how do DNA polymerases switch during translesion DNA synthesis? *Mol.Cell*, **18**, 499-505.

224. Woodgate, R. (1999) A plethora of lesion-replicating DNA polymerases. *Genes Dev.*, **13**, 2191-2195.

225. Ohmori, H., Friedberg, E. C., Fuchs, R. P., Goodman, M. F., Hanaoka, F., Hinkle, D., Kunkel, T. A., Lawrence, C. W., Livneh, Z., Nohmi, T., Prakash, L., Prakash, S., Todo, T., Walker, G. C., Wang, Z., and Woodgate, R. (2001) The Y-family of DNA polymerases. *Mol.Cell*, **8**, 7-8.

226. Burgers, P. M., Koonin, E. V., Bruford, E., Blanco, L., Burtis, K. C., Christman, M. F., Copeland, W. C., Friedberg, E. C., Hanaoka, F., Hinkle, D. C., Lawrence, C. W., Nakanishi, M., Ohmori, H., Prakash, L., Prakash, S., Reynaud, C. A., Sugino, A., Todo, T., Wang, Z., Weill, J. C., and Woodgate, R. (2001) Eukaryotic

DNA polymerases: proposal for a revised nomenclature. *J.Biol.Chem.*, **276**, 43487-43490.

227. Boudsocq, F., Iwai, S., Hanaoka, F., and Woodgate, R. (2001) *Sulfolobus solfataricus* P2 DNA polymerase IV (Dpo4): an archaeal DinB-like DNA polymerase with lesion-bypass properties akin to eukaryotic poleta. *Nucleic Acids Res.*, **29**, 4607-4616.

228. Plosky, B. S. and Woodgate, R. (2004) Switching from high-fidelity replicases to low-fidelity lesion-bypass polymerases. *Curr.Opin.Genet.Dev.*, **14**, 113-119.

229. Nair, D. T., Johnson, R. E., Prakash, L., Prakash, S., and Aggarwal, A. K. (2006) Hoogsteen base pair formation promotes synthesis opposite the 1,N^6-ethenodeoxyadenosine lesion by human DNA polymerase ι. *Nat.Struct.Mol.Biol.*, **13**, 619-625.

230. Cochrane, J. E. and Skopek, T. R. (1994) Mutagenicity of butadiene and its epoxide metabolites: II. Mutational spectra of butadiene, 1,2-epoxybutene and diepoxybutane at the hprt locus in splenic T cells from exposed B6C3F1 mice. *Carcinogenesis*, **15**, 719-723.

231. Pence, M. G., Choi, J.-Y., Egli, M., and Guengerich, F. P. (2010) Structural basis for proficient incorporation of dTTP opposite O^6-methylguanine by human DNA polymerase ι. *J.Biol.Chem.*, **285**, 40666-40672.

232. Pence, M. G., Blans, P., Zink, C. N., Fishbein, J. C., and Perrino, F. W. (2011) Bypass of N^2-ethylguanine by human DNA polymerase κ. *DNA Repair (Amst)*, **10**, 56-64.

233. Choi, J.-Y. and Guengerich, F. P. (2005) Adduct size limits efficient and error-free bypass across bulky N^2-guanine DNA lesions by human DNA polymerase η. *J.Mol.Biol.*, **352**, 72-90.

234. Fiala, K. A., Brown, J. A., Ling, H., Kshetry, A. K., Zhang, J., Taylor, J. S., Yang, W., and Suo, Z. (2007) Mechanism of template-independent nucleotide incorporation catalyzed by a template-dependent DNA polymerase. *J.Mol.Biol.*, **365**, 590-602.

235. Pence, M. G., Blans, P., Zink, C. N., Hollis, T., Fishbein, J. C., and Perrino, F. W. (2009) Lesion bypass of N^2-ethylguanine by human DNA polymerase ι. *J.Biol.Chem.*, **284**, 1732-1740.

236. Johnson, R. E., Washington, M. T., Haracska, L., Prakash, S., and Prakash, L. (2000) Eukaryotic polymerases ι and ζ act sequentially to bypass DNA lesions. *Nature*, **406**, 1015-1019.

237. Tissier, A., McDonald, J. P., Frank, E. G., and Woodgate, R. (2000) pol ι, a remarkably error-prone human DNA polymerase. *Genes Dev.*, **14**, 1642-1650.

238. Zhang, Y., Yuan, F., Wu, X., and Wang, Z. (2000) Preferential incorporation of G opposite template T by the low-fidelity human DNA polymerase ι. *Mol.Cell Biol.*, **20**, 7099-7108.

239. Steen, A. M., Meyer, K. G., and Recio, L. (1997) Analysis of hprt mutations occurring in human TK6 lymphoblastoid cells following exposure to 1,2,3,4-diepoxybutane. *Mutagenesis*, **12**, 61-67.

240. Eoff, R. L., Stafford, J. B., Szekely, J., Rizzo, C. J., Egli, M., Guengerich, F. P., and Marnett, L. J. (2009) Structural and functional analysis of Sulfolobus solfataricus Y-family DNA polymerase Dpo4-catalyzed bypass of the malondialdehyde-deoxyguanosine adduct. *Biochemistry*, **48**, 7079-7088.

241. Perrino, F. W., Blans, P., Harvey, S., Gelhaus, S. L., McGrath, C., Akman, S. A., Jenkins, G. S., LaCourse, W. R., and Fishbein, J. C. (2003) The N^2-ethylguanine and the O^6-ethyl- and O^6-methylguanine lesions in DNA: contrasting responses from the "bypass" DNA polymerase η and the replicative DNA polymerase α. *Chem.Res.Toxicol.*, **16**, 1616-1623.

242. Hecht, S. S. (2006) Cigarette smoking: cancer risks, carcinogens, and mechanisms. *Langenbecks Arch.Surg.*, **391**, 603-613.

243. Lehmann, A. R. (2005) Replication of damaged DNA by translesion synthesis in human cells. *FEBS Lett.*, **579**, 873-876.

244. Ahrendt, S. A., Decker, P. A., Alawi, E. A., Zhu Yr, Y. R., Sanchez-Cespedes, M., Yang, S. C., Haasler, G. B., Kajdacsy-Balla, A., Demeure, M. J., and Sidransky, D. (2001) Cigarette smoking is strongly associated with mutation of the K-ras gene in patients with primary adenocarcinoma of the lung. *Cancer*, **92**, 1525-1530.

245. Hollstein, M., Sidransky, D., Vogelstein, B., and Harris, C. C. (1991) p53 mutations in human cancers. *Science*, **253**, 49-53.

246. Selzer, R. R. and Elfarra, A. A. (1999) *In vitro* reactions of butadiene monoxide with single- and double-stranded DNA: characterization and quantitation of several purine and pyrimidine adducts. *Carcinogenesis*, **20**, 285-292.

247. Kotapati, S., Maddukuri, L., Wickramaratne, S., Seneviratne, U., Goggin, M., Pence, M. G., Villalta, P., Guengerich, F. P., Marnett, L., and Tretyakova, N. (2012) Translesion synthesis across 1,N^6-(2-hydroxy-3-hydroxymethylpropan-1,3-diyl)-2'-deoxyadenosine (1,N^6-γ-HMHP-dA) adducts by human and archebacterial DNA polymerases. *J Biol.Chem.*, **287**, 38800-38811.

248. Kirman, C. R., Albertini, R. J., Sweeney, L. M., and Gargas, M. L. (2010) 1,3-Butadiene: I. Review of metabolism and the implications to human health risk assessment. *Crit Rev.Toxicol.*, **40 Suppl 1**, 1-11.

249. Derby, K. S., Cuthrell, K., Caberto, C., Carmella, S. G., Franke, A. A., Hecht, S. S., Murphy, S. E., and Le Marchand, L. (2008) Nicotine metabolism in three ethnic/racial groups with different risks of lung cancer. *Cancer Epidemiol.Biomarkers Prev.*, **17**, 3526-3535.

250. Jayaraj, K., Georgieva, N. I., Gold, A., Sangaiah, R., Koc, H., Klapper, D. G., Ball, L. M., Reddy, A. P., and Swenberg, J. A. (2003) Synthesis and characterization of peptides containing a cyclic Val adduct of diepoxybutane, a possible biomarker of human exposure to butadiene. *Chem.Res.Toxicol.*, **16**, 637-643.